



UNIVERSIDADE FEDERAL DO AMAZONAS

PRÓ-REITORIA DE PESQUISA E PÓS-GRADUAÇÃO



REDE DE BIODIVERSIDADE E BIOTECNOLOGIA DA AMAZÔNIA LEGAL

**INVESTIGAÇÃO QUÍMICA E BIOLÓGICA DE *Penicillium*  
ENDOFITICOS PRODUTORES DE ALCALÓIDES E DE  
MOLÉCULAS COM POTENCIAL BIOTECNOLÓGICO**

FRANCINALDO ARAUJO DA SILVA FILHO

**MANAUS - AM**

**2021**

FRANCINALDO ARAUJO DA SILVA FILHO

**INVESTIGAÇÃO QUÍMICA E BIOLÓGICA DE *Penicillium*  
ENDOFITICOS PRODUTORES DE ALCALÓIDES E DE  
MOLÉCULAS COM POTENCIAL BIOTECNOLÓGICO**

Tese apresentada ao Programa de Pós-Graduação – BIONORTE da Universidade Federal do Amazonas – UFAM, como parte dos requisitos para obtenção do Título de Doutor na área de Biodiversidade e Biotecnologia, área de Concentração Biotecnologia.

**Orientadora:** Profa. Dra. Antonia Queiroz Lima de Souza (FCA/UFAM)

**Co-Orientador:** Prof. Dr. Afonso Duarte Leão de Souza (DQ/UFAM)

Colaborador: Felipe Moura Araujo da Silva (DQ/UFAM)

**MANAUS - AM**

**2021**

### Ficha Catalográfica

Ficha catalográfica elaborada automaticamente de acordo com os dados fornecidos pelo(a) autor(a).

S586i Silva Filho, Francinaldo Araujo da  
Investigação química e biológica de penicillium endofíticos  
produtores de alcalóides e de moléculas com potencial  
biotecnológico / Francinaldo Araujo da Silva Filho . 2021  
170 f.: il.; 31 cm.

Orientadora: Antonia Queiroz Lima de Souza  
Coorientador: Afonso Duarte Leão de Souza  
Tese (Doutorado em Biodiversidade e Biotecnologia da Rede  
Bionorte) - Universidade Federal do Amazonas.

1. Fungos. 2. Metabolitos secundários. 3. Produtos naturais. 4.  
Taxonomia. I. Souza, Antonia Queiroz Lima de. II. Universidade  
Federal do Amazonas III. Título

FRANCINALDO ARAÚJO DA SILVA FILHO

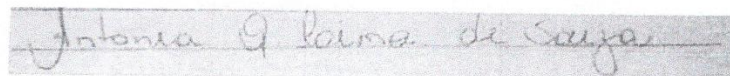
INVESTIGAÇÃO QUÍMICA E BIOLÓGICA DE PENICILLIUM ENDOFÍTICOS  
PRODUTORES DE ALCALÓIDES E DE MOLÉCULAS COM POTENCIAL  
BIOTECNOLÓGICO

Tese apresentada ao Curso de Doutorado do Programa de Pós-Graduação em Biodiversidade e Biotecnologia da Rede de Biodiversidade e Biotecnologia da Amazônia Legal, na Universidade do Estado do Amazonas, como requisito para obtenção do título de Doutor em Biodiversidade e Conservação.

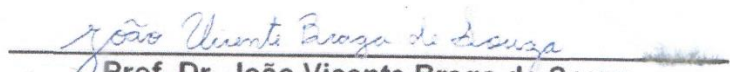
Orientador (a): **Profa. Dra. Antonia Queiroz Lima de Souza (FCA/UFAM)**

Coorientador: **Prof. Dr. Afonso Duarte Leão de Souza (DQ/UFAM)**

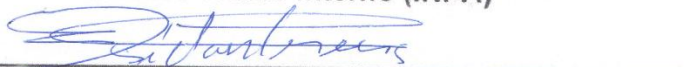
Banca Examinadora:



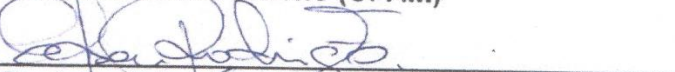
**Profa. Dra. Antonia Queiroz Lima de Souza**  
**Presidente (FCA/UFAM)**



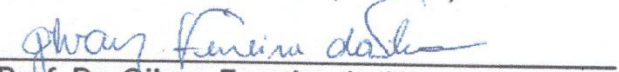
**Prof. Dr. João Vicente Braga de Souza**  
**Membro Titular Interno (INPA)**



**Prof. Dr. José Odair**  
**Membro Titular Interno (UFAM)**



**Prof. Dr. Edson Rodrigues Filho**  
**Membro Titular Externo (UFSCar)**



**Prof. Dr. Gilvan Ferreira da Silva**  
**Membro Titular Externo (EMBRAPA)**

MANAUS-AMAZONAS

Junho/2021

## **AGRADECIMENTOS**

A Deus, por guiar meus passos mesmo em momentos de pouca fé, pelas bençãos concedidas e pelas dificuldades superadas;

À minha família, em especial aos meus pais Luisa e Francinaldo (*in memoriam*), e o meu irmão Gunther pelo amor, educação e apoio dedicados. Tudo isso e todos os momentos vividos nessa etapa da vida só fizeram sentido por causa da existência de vocês. Também à minha cunhada-irmã querida Fernanda Luzeiro por tudo;

Ao meu irmão Felipe Moura Araujo da Silva, talvez o maior tutor que tive na vida e o maior influenciador para eu ter entrado na pesquisa. Sem você eu provavelmente não teria chegado até aqui, muito obrigado por tudo!

À minha namorada Pammela Riker. Seu apoio, companheirismo, respeito, incentivo, entre tantas outras coisas me fizeram mais forte e me deram coragem nos momentos de dificuldade. Você foi e é essencial pra mim!

À minha orientadora Profª Drª. Antonia Queiroz Lima de Souza e meu co-orientador Prof. Dr. Afonso Duarte Leão de Souza, pela amizade, convívio, paciência, apoio, confiança e conhecimentos transmitidos. Cada conversa contribuiu enormemente para a minha formação acadêmica e como pessoa, muito obrigado!

Aos colegas do Laboratório de Bioensaios e Microbiologia (LaBMicrA) da Central Analítica da UFAM em especial para Gabriel, Adriana, Sandro, Paulo Henrique, Débora, Ana Paula, Ketlen, Marjory, Ruan, Luan, Alzira, Marta, Paulo, Rachid, Sarah e Rafael, pelo companheirismo, pelos momentos de auxílio principalmente na dificuldade, cumplicidade vividos ao longo do percurso e momentos de descontração.

Aos professores da Rede de Biodiversidade e Biotecnologia da Amazônia Legal e a coordenação (PPG- BIONORTE).

À CAPES, pela bolsa de estudos concedida e pelo projeto Pró-Amazônia, Nº 047/2012.

A todos que de alguma forma contribuíram para a realização deste trabalho.

## RESUMO

A Amazônia possui uma das biodiversidades mais ricas do planeta, e apesar disso, pouco conhecemos da mesma, o que torna de extrema importância novos estudos voltados para o conhecimento de novas espécies na região. Os fungos, dentre eles, os endofíticos já se mostraram como promissora fonte de compostos bioativos como potencial fármacos. Um dos gêneros mais promissores quanto à produção de metabólitos secundários é o *Penicillium*, que já vem sendo amplamente utilizado em diversos ramos industriais devido a sua alta produção de metabólitos e pela rapidez de crescimento, com isso, este trabalho buscou contribuir com dados relevantes sobre a morfologia, biologia molecular e produção de metabólitos secundários de microrganismos endofíticos do gênero *Penicillium* de plantas medicinais da Amazônia. No capítulo I, podemos observar o histórico sobre o gênero *Penicillium* bem como as ferramentas utilizadas para estudá-lo taxonomicamente, um breve estado da arte. O capítulo II, apresenta o estudo polifásico realizado com 29 linhagens de *Penicillium* isolados como endofítos de diferentes plantas medicinais da Amazônia Brasileira. Foi possível identificar os 29 isolados, sendo sete espécies diferentes de *Penicillium* e um espécie de *Talaromyces*, e agrupar as linhagens por espécie. Esta análise, juntamente com o perfil químico de metabolitos secundários e a morfologia, ajudou a entender a relação das linhagens por filogenia, bem como a influência que as plantas hospedeiras têm tanto em nível químico quanto molecular. Por fim, este capítulo mostrou a necessidade das três técnicas combinadas como método eficaz para identificar espécies próximas do gênero *Penicillium*. O capítulo III apresenta o estudo químico realizado com 25 destas linhagens do gênero *Penicillium*, demonstrando o potencial de várias linhagens endofíticas de *Penicillium* de plantas medicinais da Amazônia como produtoras de alcalóides, incluindo *P. paxilli*, *P. rubens* e *P. oxalicum*. Além disso, a abordagem proposta baseada no perfil químico por ESI-MS em combinação com a análise de PCA forneceu uma estratégia simples e eficaz para discriminar isolados de *Penicillium* capazes de produzir diferentes tipos de alcalóides com potencial biotecnológico. No capítulo IV foi realizado o estudo *in silico* e sugere que a paxilina e seus compostos relacionados podem desempenhar um papel fundamental como inibidores de proteínas para *Sars-CoV-2* e o vírus 2 da dengue. Vale ressaltar que essas abordagens são importantes do ponto de vista da saúde pública para ambas as doenças e como referência para o potencial biotecnológico de fungos endofíticos da Amazônia Brasileira que temos investigado.

## ABSTRACT

The Amazon region has one of the richest biodiversities on the planet, and in spite of that, we know little about it, which makes new studies focused on the knowledge of new species in the region extremely important. Fungi, among them, endophytes, have already shown to be a promising source of bioactive compounds as potential drugs. One of the most promising genera for the production of secondary metabolites is *Penicillium*, which has already been widely used in several industrial sectors due to its high production of metabolites and the rapid growth, with this, this work sought to contribute with relevant data on the morphology, molecular biology and production of secondary metabolites of endophytic microorganisms from medicinal plants in the Amazon of the genus *Penicillium*. In chapter I, we can observe the history of the genus as well as the tools used to study it taxonomically. Chapter II presents the polyphasic study carried out with 29 species of *Penicillium* from LabMicra work collection. With the molecular data, it was possible to identify all 29 strains, seven different species of *Penicillium* and one species of *Talaromyces*, and group the strains by species. This analysis, together with the chemical profile and morphology, helped to understand the relationship of the strains, as well as the influence that the host plant has at both chemical and molecular levels. Finally, this chapter showed that all three techniques combined proved to be an effective method for identifying even species close to the genus *Penicillium*. Chapter III presents the chemical study carried out with 25 species of *Penicillium*, demonstrating the potential of several endophytic strains from plants in the Amazon as producers of alkaloids, including *P. paxilli*, *P. rubens* and *P. oxalicum*. In addition, the proposed approach based on the chemical profile by ESI-MS in combination with PCA analysis provided a simple and effective strategy to discriminate strains of *Penicillium* capable of producing different types of alkaloids with biotechnological potential. Chapter IV suggested that paxilline and their related compounds can play a key role as inhibitors of important nonstructural proteins (nsp) for SARS-CoV-2 and dengue viruses. Obviously, further researches are necessary to certify the docking results reported here, as well as the adequate application of these substances against COVID-19 and dengue fever. Overall, this work contributed with the knowledge of the endophytic strains of the genus *Penicillium* from Amazon and showed its potential as secondary metabolites producers.

## LISTA DE FIGURAS

### CAPÍTULO I

**Figura 1-**Ocorrência de espécies de *Penicillium* no mundo de acordo com o Gbif.org.....30

**Figura 2-**Padrões de ramificação dos conidióforos observados em *Penicillium*. A - Conidióforos com fiálides solitárias; B - Monoverticilado; C - Divaricato; D e E - Biverticilado; F - Terveticilado; G - Poliverticilado.....31

**Figura 3-**Estrutura da penicilina isolada pro Fleming.....34

### CAPÍTULO II

**Figure 1-**Morphology of the fungi *Penicillium adametzii*, strain 46. A = PDA front, B = CYA front, C = ISP2 front, D = PDA back, E = CYA back, F = ISP2 back, G= Micromorphology (100x).....54

**Figure 2-**Morphology of the fungi *Penicillium adametzii*, strain 180. A = PDA front, B = CYA front, C = ISP2 front, D = PDA back, E = CYA back, F = ISP2 back, G= Micromorphology(400x). .....54

**Figure 3-**Morphology of the fungi *Penicillium citrinum*, strain 409. A = PDA front, B = CYA front, C = ISP2 front, D = PDA back, E = CYA back, F = ISP2 back, G= Micromorphology(200x). .....55

**Figure 4-**Morphology of the fungi *Penicillium citrinum*, strain 414. A = PDA front, B = CYA front, C = ISP2 front, D = PDA back, E = CYA back, F = ISP2 back, G= Micromorphology(200x). .....55

**Figure 5-**Morphology of the fungi *Penicillium citrinum*, strain 457. A = PDA front, B = CYA front, C = ISP2 front, D = PDA back, E = CYA back, F = ISP2 back, G= Micromorphology(1000x).....55

**Figure 6-**Morphology of the fungi *Penicillium glabrum*, strain 38. A = PDA front, B = CYA front, C = ISP2 front, D = PDA back, E = CYA back, F = ISP2 back, G= Micromorphology(400x).....56

<b>Figure 7</b> -Morphology of the fungi <i>Penicillium glabrum</i> , strain 404. A = PDA front, B = CYA front, C = ISP2 front, D = PDA back, E = CYA back, F = ISP2 back, G= Micromorphology(100x) .....	56
<b>Figure 8</b> -Morphology of the fungi <i>Penicillium glabrum</i> , strain 408. A = PDA front, B = CYA front, C = ISP2 front, D = PDA back, E = CYA back, F = ISP2 back, G= Micromorphology(100x) .....	57
<b>Figure 9</b> -Morphology of the fungi <i>Penicillium oxalicum</i> , strain 64. A = PDA front, B = CYA front, C = ISP2 front, D = PDA back, E = CYA back, F = ISP2 back, G= Micromorphology(100x) .....	58
<b>Figure 10</b> -Morphology of the fungi <i>Penicillium oxalicum</i> , strain 71. A = PDA front, B = CYA front, C = ISP2 front, D = PDA back, E = CYA back, F = ISP2 back, G= Micromorphology(100x) .....	58
<b>Figure 11</b> -Morphology of the fungi <i>Penicillium oxalicum</i> , strain 143. A = PDA front, B = CYA front, C = ISP2 front, D = PDA back, E = CYA back, F = ISP2 back, G= Micromorphology(400x) .....	58
<b>Figure 12</b> -Morphology of the fungi <i>Penicillium oxalicum</i> , strain 149. A = PDA front, B = CYA front, C = ISP2 front, D = PDA back, E = CYA back, F = ISP2 back, G= Micromorphology(400x) .....	59
<b>Figure 13</b> -Morphology of the fungi <i>Penicillium oxalicum</i> , strain 407. A = PDA front, B = CYA front, C = ISP2 front, D = PDA back, E = CYA back, F = ISP2 back, G= Micromorphology(100x) .....	59
<b>Figure 14</b> -Morphology of the fungi <i>Penicillium paxilli</i> , strain 48. A = PDA front, B = CYA front, C = ISP2 front, D = PDA back, E = CYA back, F = ISP2 back, G= Micromorphology(200x) .....	60
<b>Figure 15</b> -Morphology of the fungi <i>Penicillium paxilli</i> , strain 52. A = PDA front, B = CYA front, C = ISP2 front, D = PDA back, E = CYA back, F = ISP2 back, G= Micromorphology(200x) .....	60

<b>Figure 16</b> -Morphology of the fungi <i>Penicillium paxilli</i> , strain 56. A = PDA front, B = CYA front, C = ISP2 front, D = PDA back, E = CYA back, F = ISP2 back, G= Micromorphology(400x) .....	60
<b>Figure 17</b> -Morphology of the fungi <i>Penicillium paxilli</i> , strain 153. A = PDA front, B = CYA front, C = ISP2 front, D = PDA back, E = CYA back, F = ISP2 back, G= Micromorphology(200x) .....	61
<b>Figure 18</b> -Morphology of the fungi <i>Penicillium paxilli</i> , strain 307. A = PDA front, B = CYA front, C = ISP2 front, D = PDA back, E = CYA back, F = ISP2 back, G= Micromorphology(400x) .....	61
<b>Figure 19</b> -Morphology of the fungi <i>Penicillium rubens</i> , strain 135. A = PDA front, B = CYA front, C = ISP2 front, D = PDA back, E = CYA back, F = ISP2 back, G= Micromorphology(400x) .....	62
<b>Figure 20</b> -Morphology of the fungi <i>Penicillium rubens</i> , strain 154. A = PDA front, B = CYA front, C = ISP2 front, D = PDA back, E = CYA back, F = ISP2 back, G= Micromorphology(400x) .....	62
<b>Figure 21</b> -Morphology of the fungi <i>Penicillium rubens</i> , strain 155. A = PDA front, B = CYA front, C = ISP2 front, D = PDA back, E = CYA back, F = ISP2 back, G= Micromorphology(400x) .....	63
<b>Figure 22</b> -Morphology of the fungi <i>Penicillium rubens</i> , strain 392. A = PDA front, B = CYA front, C = ISP2 front, D = PDA back, E = CYA back, F = ISP2 back, G= Micromorphology (200x).....	63
<b>Figure 23</b> -Morphology of the fungi <i>Penicillium rubens</i> , strain 401. A = PDA front, B = CYA front, C = ISP2 front, D = PDA back, E = CYA back, F = ISP2 back, G= Micromorphology(100x) .....	63
<b>Figure 24</b> -Morphology of the fungi <i>Penicillium rubens</i> , strain 403. A = PDA front, B = CYA front, C = ISP2 front, D = PDA back, E = CYA back, F = ISP2 back, G= Micromorphology(100x) .....	64

<b>Figure 25</b> -Morphology of the fungi <i>Penicillium rubens</i> , strain 433. A = PDA front, B = CYA front, C = ISP2 front, D = PDA back, E = CYA back, F = ISP2 back, G= Micromorphology(400x).....	64
<b>Figure 26</b> -Morphology of the fungi <i>Talaromyces versatilis</i> , strain 391. A = PDA front, B = CYA front, C = ISP2 front, D = PDA back, E = CYA back, F = ISP2 back, G= Micromorphology(1000x).....	65
<b>Figure 27</b> -Morphology of the fungi <i>Talaromyces versatilis</i> , strain 395. A = PDA front, B = CYA front, C = ISP2 front, D = PDA back, E = CYA back, F = ISP2 back, G= Micromorphology(1000x).....	65
<b>Figure 28</b> -Morphology of the fungi <i>Talaromyces versatilis</i> , strain 396. A = PDA front, B = CYA front, C = ISP2 front, D = PDA back, E = CYA back, F = ISP2 back, G= Micromorphology(200x).....	65
<b>Figure 29</b> -Morphology of the fungi <i>Penicillium sumatraense</i> , strain 415. A = PDA front, B = CYA front, C = ISP2 front, D = PDA back, E = CYA back, F = ISP2 back, G= Micromorphology(400x).....	66
<b>Figure 30</b> -Molecular Phylogenetic analysis by Maximum Parsimony (MP) method of the <i>Penicillium</i> strains.....	70
<b>Figure 31</b> -Dendrogram obtained with the HCA analysis of the profile of metabolites produced by <i>Penicillium</i> strains in CYA medium.....	72
<b>Figure 32</b> -Dendrogram obtained with the HCA analysis of the profile of metabolites produced by <i>Penicillium</i> strains in ISP2 medium.....	73
<b>Figure 33</b> -Dendrogram obtained with the HCA analysis of the profile of metabolites produced by <i>Penicillium</i> strains in PDA médium.....	73
<b>CAPÍTULO III</b>	
<b>Figure 1</b> -PCA score plots (A and B) and biplot of scores and loadings (C) generated from the crude extract ESI-MS data from twenty-five endophytic <i>Penicillium</i> strains from Amazon medicinal plants (A-Y).....	91

**Figure 2**-ESI-MS/MS spectra (positive mode) of the ion at  $m/z$  390 (A), 420 (B), 448 (C), 436 (D), and 404 (E), present in the crude extracts of *Penicillium* strains.....92

**Figure 3**-Isolated and identified compounds from the *Penicillium* strains present in groups I (1), III (2-4) and IV (5).....93

## MATERIAL SUPLEMENTAR – CAPÍTULO III

**Figure S1**-ESI-MS spectrum (positive mode) of the crude extract from GhcR3 2.2 (A).....101

**Figure S2**-ESI-MS spectrum (positive mode) of the crude extract from PbR2 2.2 (B).....101

**Figure S3**-ESI-MS spectrum (positive mode) of the crude extract from GhcR1 1.1a (C).....102

**Figure S4**-ESI-MS spectrum (positive mode) of the crude extract from GhcC1 1.2c (D).....102

**Figure S5**-ESI-MS spectrum (positive mode) of the crude extract from StspC2 1.2c (E).....103

**Figure S6**-ESI-MS spectrum (positive mode) of the crude extract from GhR1 2.1 (F).....103

**Figure S7**-ESI-MS spectrum (positive mode) of the crude extract from VrF1 2.2(G).....103

**Figure S8**-ESI-MS spectrum (positive mode) of the crude extract from AspC2 2.2 (H).....104

**Figure S9**-ESI-MS spectrum (positive mode) of the crude extract from AnspG1 2.2 (I).....104

**Figure S10**-ESI-MS spectrum (positive mode) of the crude extract from GhcR1 1.1b (J).....105

<b>Figure S11</b> -ESI-MS spectrum (positive mode) of the crude extract from AnspG1 2.3b (K).....	105
<b>Figure S12</b> -ESI-MS spectrum (positive mode) of the crude extract from VrF2 2.3 (L).....	106
<b>Figure S13</b> -ESI-MS spectrum (positive mode) of the crude extract from VrC2 2.1c (M).....	106
<b>Figure S14</b> -ESI-MS spectrum (positive mode) of the crude extract from GhG2 2.1 (N).....	107
<b>Figure S15</b> -ESI-MS spectrum (positive mode) of the crude extract from AnspG1 2.3a (O).....	107
<b>Figure S16</b> -ESI-MS spectrum (positive mode) of the crude extract from AnspC2 3.1 (P).....	108
<b>Figure S17</b> -ESI-MS spectrum (positive mode) of the crude extract from GhR1 2.1a (Q).....	108
<b>Figure S18</b> -ESI-MS spectrum (positive mode) of the crude extract from GhcG3 2.2 (R).....	109
<b>Figure S19</b> -ESI-MS spectrum (positive mode) of the crude extract from GhR2 1.2b (S).....	109
<b>Figure S20</b> -ESI-MS spectrum (positive mode) of the crude extract from VrC2 1.2 (T).....	110
<b>Figure S21</b> -ESI-MS spectrum (positive mode) of the crude extract from AnspcG1 3.3 (U).....	110
<b>Figure S22</b> -ESI-MS spectrum (positive mode) of the crude extract from GhcR3 2.2 (V).....	111
<b>Figure S23</b> -ESI-MS spectrum (positive mode) of the crude extract from GhG3 2.2c (W).....	111

<b>Figure S24</b> -ESI-MS spectrum (positive mode) of the crude extract from EjC3 2.1a (X).....	112
<b>Figure S25</b> -ESI-MS spectrum (positive mode) of the crude extract from GhcC2 2.2a (Y).....	112
<b>Figure S26</b> -ESI-MS/MS spectrum (positive mode) of the ion at <i>m/z</i> 390 present in the crude extract of GhcR3 2.2 (V).....	112
<b>Figure S27</b> -ESI-MS/MS spectrum (positive mode) of the ion at <i>m/z</i> 420 present in the crude extract of GhcR3 2.2 (V).....	113
<b>Figure S28</b> -ESI-MS/MS spectrum (positive mode) of the ion at <i>m/z</i> 448 present in the crude extract of VrC2 2.1c (M).....	113
<b>Figure S29</b> -ESI-MS/MS spectrum (positive mode) of the ion at <i>m/z</i> 436 present in the crude extract of AnspG1 2.3a (O).....	114
<b>Figure S30</b> -ESI-MS/MS spectrum (positive mode) of the ion at <i>m/z</i> 404 present in the crude extract of GhcR3 2.2 (V).....	114
<b>Figure S31</b> -APCI-MS spectrum (positive mode) of the paxillin (1).....	115
<b>Figure S32</b> - <sup>1</sup> H NMR spectrum (500 MHz, MeOD) of the paxilline (1).....	115
<b>Figure S33</b> - <sup>13</sup> C NMR spectrum (125 MHz, MeOD) of the paxilline (1).....	116
<b>Figure S34</b> - <sup>1</sup> H- <sup>13</sup> C correlations observed by HSQC for the paxilline (1).....	116
<b>Figure S35</b> - <sup>1</sup> H- <sup>13</sup> C correlations observed by HMBC for the paxilline (1).....	116
<b>Figure S36</b> -APCI-MS spectrum (positive mode) of the glandicoline B (2).....	117
<b>Figure S37</b> - <sup>1</sup> H NMR spectrum (500 MHz, MeOD) of the glandicoline B (2).....	117
<b>Figure S38</b> - <sup>1</sup> H- <sup>13</sup> C correlations observed by HSQC for glandicoline B (2).....	118
<b>Figure S39</b> - <sup>1</sup> H- <sup>13</sup> C correlations observed by HMBC for glandicoline B (2).....	118

## CAPÍTULO IV

<b>Figure 1</b> -Chemical structures of alkaloids previously reported in Amazon Penicillium strains and their related compounds.....	127
<b>Figure 2</b> -Main interactions observed for the top-scored inhibitors of SARS-CoV-2 Mpro by docking analysis.....	129
<b>Figure 3</b> -Main interactions observed for the top-scored inhibitors of SARS-CoV-2 RdRp by docking analysis.....	132
<b>Figure 4</b> -Main interactions observed for the top-scored inhibitors of DENV-2 protease by docking analysis.....	133
<b>Figure 5</b> -Main interactions observed for the top-scored inhibitors of DENV-2 RdRp by docking analysis.....	134
<b>Figure 6</b> - Main interactions observed for the top-scored inhibitors of DENV-2 MTase by docking analysis .....	135
<b>MATERIAL SUPLEMENTAR – CAPÍTULO IV</b>	
<b>Figure S1</b> - Main interactions observed between X77 and SARS-CoV-2 Mpro by docking analysis.....	144
<b>Figure S2</b> -Main interactions observed between paxiline and SARS-CoV-2 Mpro by docking analysis.....	144
<b>Figure S3</b> -Main interactions observed between PCM6 and SARS-CoV-2 Mpro by docking analysis.....	145
<b>Figure S4</b> -Main interactions observed between 13-desoxy-paxilline and SARS-CoV-2 Mpro by docking analysis.....	145
<b>Figure S5</b> -Main interactions observed between paspaline and SARS-CoV-2 Mpro by docking analysis.....	146
<b>Figure S6</b> -Main interactions observed between roquefortine C and SARS-CoV-2 Mpro by docking analysis.....	146
<b>Figure S7</b> - Main interactions observed between roquefortine D and SARS-CoV-2 Mpro by docking analysis.....	147

<b>Figure S8</b> -Main interactions observed between oxaline and SARS-CoV-2 Mpro by docking analysis.....	147
<b>Figure S9</b> -Main interactions observed between glandicoline A and SARS-CoV-2 Mpro by docking analysis.....	148
<b>Figure S10</b> -Main interactions observed between meleagrine and SARS-CoV-2 Mpro by docking analysis.....	148
<b>Figure S11</b> -Main interactions observed between glandicoline B and SARS-CoV-2 Mpro by docking analysis.....	149
<b>Figure S12</b> -Main interactions observed between paspaline and SARS-CoV-2 RdRp by docking analysis.....	149
<b>Figure S13</b> -Main interactions observed between 13-desoxy-paxilline and SARS-CoV-2 RdRp by docking analysis.....	150
<b>Figure S14</b> -Main interactions observed between paxilline and SARS-CoV-2 RdRp by docking analysis.....	150
<b>Figure S15</b> -Main interactions observed between PCM6 and SARS-CoV-2 RdRp by docking analysis.....	151
<b>Figure S16</b> -Main interactions observed between roquefortine C and SARS-CoV-2 RdRp by docking analysis.....	151
<b>Figure S17</b> -Main interactions observed between glandicoline A and SARS-CoV-2 RdRp by docking analysis.....	152
<b>Figure S18</b> - Main interactions observed between roquefortine D and SARS-CoV-2 RdRp by docking analysis.....	152
<b>Figure S19</b> -Main interactions observed between meleagrine and SARS-CoV-2 RdRp by docking analysis.....	153
<b>Figure S20</b> -Main interactions observed between glandicoline B and SARS-CoV-2 RdRp by docking analysis.....	153

<b>Figure S21</b> -Main interactions observed between oxaline and SARS-CoV-2 RdRp by docking analysis.....	154
<b>Figure S22</b> -Main interactions observed between PCM6 and DENV2 NS2B-NS3 protease by docking analysis.....	154
<b>Figure S23</b> -Main interactions observed between 13-desoxy-paxilline and DENV2 NS2B-NS3 protease by docking analysis.....	155
<b>Figure S24</b> -Main interactions observed between paxilline and DENV2 NS2B-NS3 protease by docking analysis.....	155
<b>Figure S25</b> -Main interactions observed between paspaline and DENV2 NS2B-NS3 protease by docking analysis.....	156
<b>Figure S26</b> -Main interactions observed between glandicoline B and DENV2 NS2B-NS3 protease by docking analysis.....	156
<b>Figure S27</b> -Main interactions observed between roquefortine C and DENV2 NS2B-NS3 protease by docking analysis.....	157
<b>Figure S28</b> -Main interactions observed between glandicoline A and DENV2 NS2B-NS3 protease by docking analysis.....	157
<b>Figure S29</b> - Main interactions observed between roquefortine D and DENV2 NS2B-NS3 protease by docking analysis.....	158
<b>Figure S30</b> -Main interactions observed between meleagrine and DENV2 NS2B-NS3 protease by docking analysis.....	158
<b>Figure S31</b> -Main interactions observed between oxaline and DENV2 NS2B-NS3 protease by docking analysis.....	159
<b>Figure S32</b> -Main interactions observed between 13-desoxy-paxilline and DENV2 RdRp by docking analysis.....	159
<b>Figure S33</b> -Main interactions observed between paxilline and DENV2 RdRp by docking analysis.....	160

<b>Figure S34</b> -Main interactions observed between paspaline and DENV2 RdRp by docking analysis.....	160
<b>Figure S35</b> -Main interactions observed between glandicoline B and DENV2 RdRp by docking analysis.....	161
<b>Figure S36</b> - Main interactions observed between roquefortine D and DENV2 RdRp by docking analysis.....	161
<b>Figure S37</b> -Main interactions observed between PCM6 and DENV2 RdRp by docking analysis.....	162
<b>Figure S38</b> -Main interactions observed between roquefortine C and DENV2 RdRp by docking analysis.....	162
<b>Figure S39</b> -Main interactions observed between glandicoline A and DENV2 RdRp by docking analysis.....	163
<b>Figure S40</b> -Main interactions observed between meleagrine and DENV2 RdRp by docking analysis.....	163
<b>Figure S41</b> -Main interactions observed between oxaline and DENV2 RdRp by docking analysis.....	164
<b>Figure S42</b> -Main interactions observed between SAH and DENV2 methyltransferase by docking analysis.....	164
<b>Figure S43</b> - Main interactions observed between 13-desoxy-paxilline and DENV2 MTase by docking analysis.....	165
<b>Figure S44</b> -Main interactions observed between paxilline and DENV2 MTase by docking analysis.....	165
<b>Figure S45</b> -Main interactions observed between PCM6 and DENV2 MTase by docking analysis.....	166
<b>Figure S46</b> -Main interactions observed between paspaline and DENV2 MTase by docking analysis.....	166

<b>Figure S47</b> -Main interactions observed between roquefortine C and DENV2 MTase by docking analysis.....	167
<b>Figure S48</b> -Main interactions observed between glandicoline B and DENV2 MTase by docking analysis.....	167
<b>Figure S49</b> -Main interactions observed between glandicoline A and DENV2 MTase by docking analysis.....	168
<b>Figure S50</b> - Main interactions observed between roquefortine D and DENV2 MTase by docking analysis .....	168
<b>Figure S51</b> -Main interactions observed between meleagrine and DENV2 MTase by docking analysis.....	169
<b>Figure S52</b> -Main interactions observed between oxaline and DENV2 MTase by docking analysis.....	169

## LISTA DE TABELAS

### CAPÍTULO I

**Tabela 1**-Primers usados para amplificação e sequenciamento de *Penicillium*.....33

**Tabela 2**-Alguns metabólitos secundários isolados de espécies do gênero *Penicillium*  
.....34

### CAPÍTULO II

**Table 1**-Selected *Penicillium* strains from the work collection of the LabMicra/UFAM  
.....53

**Table 2**-Molecular identification based on the ITS region of endophytic *Penicillium*  
strains by BLASTn from NCBI.....68

### CAPÍTULO III

**Table 1**-Endophytic *Penicillium* strains subjected to alkaloidal screening.....85

**Table 2**-Species identification of nine *Penicillium* endophytic strains by molecular  
approach with NCBI's BLASTn information.....94

### MATERIAL SUPLEMENTAR – CAPÍTULO III

**Table 1S**-Assignment of 1H and 13C NMR data for the paxilline (1).....118

**Table 2S**-Assignment of 1H and 13C NMR data for the glandicoline B (2).....119

### CAPÍTULO IV

**Table 1**-Docking analysis data for previously reported Amazon *Penicillium* alkaloids and  
their related compounds.....130

## SUMÁRIO GERAL

<b>1. INTRODUÇÃO GERAL.....</b>	22
<b>2. CAPÍTULO I (Revisão bibliográfica) - Gênero <i>Penicillium</i>: Biodiversidade, potencial químico e biotecnológico.....</b>	27
<b>3. OBJETIVOS.....</b>	43
3.1 Objetivo geral.....	43
3.2 Objetivos específicos.....	43
<b>4. APRESENTAÇÃO DOS CAPÍTULOS.....</b>	44
<b>5. CAPÍTULO II-Identificação polifásica de <i>Penicillium spp.</i> endofíticas da Amazônia.....</b>	45
<b>6. CAPÍTULO III (Artigo publicado) -Triagem de isolados de <i>Penicillium</i> endofítico de plantas da Amazônia produtoras de alcalóide por espectrometria de massa de ionização por eletrospray (ESI-MS) e análise de componente principal (PCA).....</b>	80
<b>7. CAPÍTULO IV- Alcalóides de linhagens de <i>Penicillium</i> da Amazônia como potenciais inibidores das enzimas alvo de SARS-CoV-2 e DENV-2.....</b>	120
<b>8. CONCLUSÕES GERAIS.....</b>	170

## 1. INTRODUÇÃO GERAL

A Amazônia possui uma das biodiversidades mais ricas do planeta, diversidade esta que desperta o interesse na busca por novas moléculas com potencial farmacológico. A procura por novos produtos com potencial biotecnológico pela indústria farmacêutica vem crescendo ao decorrer dos anos, sendo os produtos naturais considerados promissores para o desenvolvimento de novos fármacos (HARVEY, 2000). Esta pesquisa tem levado a descoberta de fármacos com um papel de extrema importância no tratamento de doenças humanas (BUTLER; ROBERTSON; COOPER, 2014). Por exemplo, das 175 moléculas pequenas registradas de 1940 a 2014 para o tratamento de câncer, 85 (49%) são produtos naturais ou derivados com modificação semi-sintética. Além disso, uma boa parcela dos fármacos utilizados para o tratamento das mais diversas doenças são de origem natural (NEWMAN; CRAGG, 2020).

Dentre as diversas fontes naturais produtoras de compostos bioativos, destacam-se os fungos. Os fungos estão amplamente distribuídos em todo o planeta, integrando os ciclos biogeoquímicos de todos os ecossistemas (BRANCO, 2019). Eles compreendem uma grande variedade de espécies, cerca de 3,8 milhões, distribuídas principalmente em ambientes como solo, água, e associados a plantas e outros organismos (HAWKSWORTH; LUCKING, 2017). Estes seres constituem um dos grupos menos explorados do ponto de vista químico (VISAGIE et al., 2014). Os fungos constituem uma fonte rica de fármacos e moléculas de potencial biotecnológico, incluindo já comprovados: antibióticos, antioxidantes, antitumorais, agentes imunossupressores, entre outros (NEWMAN; CRAGG; SNADER, 2000; ALY et al., 2010; KOZLOVSKY; ZHELIFONOVA; ANTIPOVA, 2013; QIAN et al., 2013). Aproximadamente 42% dos produtos naturais biologicamente ativos são obtidos de fungos (HAUTBERGUE et al., 2017).

Quando os fungos são associados ao interior das plantas, são conhecidos como endofíticos, e vivem nos espaços inter e intracelular desses indivíduos por pelo menos um período de seu ciclo de vida (PETRINI, 1991). Alguns destes fungos se destacam por ter a capacidade de mimetizar compostos da planta hospedeira criando assim uma grande diversidade química e potencial para compostos bioativos (ZHANG; SONG; TAN, 2006; GUO et al., 2008; GUNATILAKA, 2012; QIAN et al., 2013). Metabólitos secundários de fungos endofíticos tem se mostrado uma fonte promissora de novos fármacos, como

exemplos, os alcalóides taxol e vincristina, são considerados potentes agentes anticancerígenos (STROBEL et al., 1996; GUO et al., 2006). No entanto, os endófitos de florestas tropicais e subtropicais do mundo, ainda são pouco estudados quanto a sua biodiversidade e o seu potencial biotecnológico (ARORA; RAMAWAT, 2017), principalmente se considerarmos os poucos grupos que trabalham com química de microrganismos no mundo e na Amazônia.

Um dos gêneros mais promissores quanto à produção de metabólitos secundários é o *Penicillium*, que já vem sendo amplamente utilizado em diversos ramos industriais devido a sua alta produção de metabólitos e pela rapidez de crescimento (VISAGIE et al., 2014). Também é tido como uma fonte promissora de compostos bioativos, como polifenóis, policetídeos e alcaloides (BRINGAMANN et al., 2005; MARINHO et al., 2005; LU et al., 2010;). Em estudos recentes com microrganismos amazônicos, os alcaloides glandicolina B e um dicetopiperazinico, isolados de *Penicillium* e *Gliocladium*, respectivamente, demonstraram potencial citotóxico e antibacteriano (KOOLEN et al., 2012a, 2012b). A prospecção de compostos bioativos ou novas moléculas de microrganismos é uma tarefa importante e complexa, que geralmente exige técnicas analíticas modernas com alta sensibilidade e seletividade, como a baseada em espectrometria de massa (MS) (CONVINGTON et al., 2017) e ensaios biológicos. Nos últimos anos, essas abordagens bioguiadas e associadas com MS têm se mostrado uma estratégia poderosa para a triagem e identificação de compostos bioativos em espécies de plantas e microrganismos, bem como abordagens quimiotaxonômicas, quando combinadas com ferramentas quimiométricas (SILVA et al., 2016). Onde, por exemplo, duas novas espécies de *Penicillium* (*P. tulipae* e *P. radicícola*) foram descobertas com auxílio de perfis químicos por MS com comparação as espécies já descritas (OVERY; FRISVAD, 2003). Sendo assim, tendo em vista a necessidade atual de identificar organismos amazônicos promissores na produção de novos princípios ativos, e visando o conhecimento sobre as linhagens de microrganismos acessadas nesta pesquisa, seja pelo perfil químico e genômico, seja pela identificação morfológica e molecular e pelos ensaios biológicos, este trabalho buscou contribuir com dados relevantes sobre a produção de metabólitos secundários de microrganismos endofíticos de plantas medicinais da Amazônia do gênero *Penicillium* e seu potencial biotecnológico.

## REFERÊNCIAS

- ARORA, J.; RAMAWAT, K. An introduction to endophytes. In: Endophytes: Biology and Biotechnology; Springer: Berlin, Germany, 2017; pp. 1–23.
- ALY, A. H.; DEBBAB, A.; KJER, J.; PROKSCH, P. Fungal endophytes from higher plants: A prolific source of phytochemicals and other bioactive natural products. **Fungal Diversity**, v. 41, p. 1–16, 2010.
- BRANCO, S. Fungal diversity from communities to genes. **Fung. Biology. Rev.** v. 33 p. 225–237, 2019
- BRINGMANN, G.; LANG, G.; GULDER, T. A. M.; TSURUTA, H.; MUHLBACHER, J.; MAKSIMENKA, K.; STEFFENS, S.; SCHAUMANN, K.; STOHR, R.; WIESE, J.; IMHOFF, J. F.; PEROVIC-OTTSTADT, S.; BOREIKO, O.; MULLER, W. E. G. The first sorbicillinoid alkaloids, the antileukemic sorbicillactones A and B, from a sponge-derived *Penicillium chrysogenum* strain. **Tetrahedron**. V. 61, p. 7252-7265, 2005
- BORGES, W.; BORGES, K.; BONATO, P.; SAID, S.; PUPO, M.; Endophytic fungi: natural products, enzymes and biotransformation reactions. **Current Organic Chemistry**, v. 13, p. 1137, 2009
- BUTLER, M. S.; ROBERTSON, A. A. B.; COOPER, M. A. Natural product and natural product derived drugs in clinical trials. **Nat. Prod. Rep.**, v. 31, n. 11, p. 1612–1661, 2014.
- COVINGTON, B. C., MCLEAN, J. A. & BACHMANN, B. O. Comparative mass spectrometry-based metabolomics strategies for the investigation of microbial secondary metabolites. **Nat. Prod. Rep.** 34, p. 6–24, 2017.
- GUO, B. H.; WANG, Y. C.; ZHOU, X. W.; HU, K.; TAN, F.; MIAO, Z. Q.; TANG, K. X. An endophytic taxol-producing fungus BT2 isolated from *Taxus chinensis* var. mairei. **African Journal of Biotechnology**, v. 5, n. May, p. 875–877, 2006.
- GUO, B.; WANG, Y.; SUN, X.; TANG, K. Bioactive Natural Products from Endophytes : A Review 1. v. 44, n. 2, p. 6838, 2008.
- GUNATILAKA, A. A. L. Natural Products from Plant-associated Microorganisms: Distribution, Structural Diversity, Bioactivity, and Implications of Their Occurrence. **J Nat Prod**, v. 69, n. 3, p. 509–526, 2012.
- HARVEY, A. Strategies for discovering drugs from previously unexplored natural products. **Drug Discovery Today**, v. 5, n. 7, p. 294–300, 2000.
- HAUTBERGUE, T.; PUEL, O.; TADRIST, S.; MENEGHETTI, L.; PÉAN, M.; DELAFORGE, M.; DEBRAUWER, L.; OSWALD, I. P.; JAMIN, E. L. Evidencing 98 secondary metabolites of *Penicillium verrucosum* using substrate isotopic labeling and high-resolution mass spectrometry. **Journal of Chromatography B: Analytical Technologies in the Biomedical and Life Sciences**, v. 1071, p. 29–43, 2017
- HAWKSWORTH, D. L.; LUCKING, R. Fungal diversity revisited: 2.2 € to 3.8 million species. **Microbiol. Spectr.** V. 5, p. 1-17, 2017

KOOLEN, H. H. F.; SOARES, E. R.; DA SILVA, F. M. A.; DE ALMEIDA, R. A.; DE SOUZA, A. D. L.; DE MEDEIROS, L. S.; FILHO, E. R.; DE SOUZA, A. Q. L. An antimicrobial alkaloid and other metabolites produced by *Penicillium* sp. an endophytic fungus isolated from *Mauritia flexuosa* L. F. **Quimica Nova**, v. 35, n. 4, p. 771–774, 2012a.

KOOLEN, H. H. F.; SOARES, E. R.; DA SILVA, F. M. A.; DE SOUZA, A. Q. L.; DE MEDEIROS, L. S.; FILHO, E. R.; DE ALMEIDA, R. A.; RIBEIRO, I. A.; DO Ó PESSOA, C.; DE MORAIS, M. O.; DA COSTA, P. M.; DE SOUZA, A. D. L. An antimicrobial diketopiperazine alkaloid and co-metabolites from an endophytic strain of *Gliocladium* isolated from *Strychnos* cf. *toxifera*. **Natural Product Research**, v. 26, n. 21, p. 2013–2019, 2012b.

KOZLOVSKY, A. G.; ZHELIFONOVA, V. P.; ANTIPOVA, T. V. Biologically active metabolites of *Penicillium* fungi. **Signpost Open Access Journal of Organic and Biomolecular Chemistry**, v. 01, p. 11–21, 2013.

LU, Z.; ZHU, H.; FU, P.; WANG, Y.; ZHANG, Z.; LIN, H.; LIU, P.; ZHUANG, Y.; HONG, K.; ZHU, W. Cytotoxic polyphenols from the marine-derived fungus *Penicillium expansum*. **J. Nat. Prod.** V. 73, p. 911–914, 2010

MARINHO, A. M. R.; RODRIGUES-FILHO, E.; MOITINHO, M. D. L. R.; SANTOS, L. S. Biologically active polyketides produced by *Penicillium janthinellum* isolated as an endophytic fungus from fruits of *Melia azedarach*. **J. Braz. Chem. Soc.** V. 16, p. 280–283, 2005

NEWMAN, D. J.; CRAGG, G. M. Natural products as sources of new drugs over the nearly four decades from 01/1981 to 09/2019. **Journal of Natural Products**, v. 83, n. 3, p. 770–803, 2020.

NEWMAN, D. J.; CRAGG, G. M.; SNADER, K. M. The influence of natural products upon drug discovery. **Natural Product Reports**, v. 17, n. 3, p. 215–234, 2000.

NIELSEN, K. F.; SMEDSGAARD, J. Fungal metabolite screening: Database of 474 mycotoxins and fungal metabolites for dereplication by standardised liquid chromatography-UV-mass spectrometry methodology. **J. Chromatogr. A.** v. 1002, p. 111–136, 2003

OVERY, D. P.; FRISVAD, J. C. New *Penicillium* Species Associated with Bulbs and Root Vegetables. **Systematic and Applied Microbiology**, v. 26, n. 4, p. 631–639, 2003.

PETRINI, O. Fungal endophytes of tree leaves. IN: ANDREWS, J., S. HIRANO (EDS) **Microbial Ecology of Leaves**. Springer Verlag, Nova Iorque, 1991, p. 179–197.

QIAN, Y.; YU, H.; HE, D.; YANG, H.; WANG, W.; WAN, X.; WANG, L. Biosynthesis of silver nanoparticles by the endophytic fungus *Epicoccum nigrum* and their activity against pathogenic fungi. **Bioprocess and Biosystems Engineering**, v. 36, n. 11, p. 1613–1619, 2013.

SILVA, F. M. A.; SILVA-FILHO, F. A.; LIMA, B. R.; ALMEIDA, R. A.; SOARES, E. R.; KOOLEN, H. H. F.; SOUZA, A. D. L.; PINHEIRO, M. L. B. Chemotaxonomy of the Amazonian *Unonopsis* species based on leaf alkaloid fingerprint direct infusion ESI-MS

and chemometric analysis. **Journal of the brazilian chemical society**. V. 27, p. 599-604, 2016.

STROBEL, G.; HESS, W.; FORD, E.; SIDHU, R.; YANG, X. Taxol from fungal endophytes and the issue of biodiversity. **Journal of Industrial Microbiology & Biotechnology**, v. 17, n. 5–6, p. 417–423, 1996.

VISAGIE, C. M.; HOUBRAKEN, J.; FRISVAD, J. C.; HONG, S. B.; KLAASSEN, C. H. W.; PERRONE, G.; SEIFERT, K. A.; VARGA, J.; YAGUCHI, T.; SAMSON, R. A. Identification and nomenclature of the genus *Penicillium*. **Studies in Mycology**, v. 78, n. 1, p. 343–371, 2014.

ZHANG, H. W.; SONG, Y. C.; TAN, R. X. Biology and chemistry of endophytes. **Natural Product Reports**, v. 23, n. 5, p. 753–771, 2006.

## 2. CAPITULO I

### REVISÃO BIBLIOGRÁFICA

**Gênero *Penicillium*: Biodiversidade, potencial químico e biotecnológico<sup>1</sup>**

---

<sup>1</sup>Este capítulo está na forma de artigo e deverá ser traduzido e submetido para publicação na revista FEMS Microbiology Reviews (ISSN: 1574-6976)

## Gênero *Penicillium*: Biodiversidade, potencial químico e biotecnológico

Francinaldo Araujo da Silva Filho, Felipe Moura Araujo da Silva, Afonso Duarte Leão de Souza,  
Antonia Queiroz Lima de Souza

Submetido XX/XX/20XX – Aceito XX/XX/20XX – Publicado on-line XX/XX/20XX

### **Resumo**

Os fungos do gênero *Penicillium* são diversos e ocorrem em todo o mundo. Suas espécies desempenham papéis importantes em diversas áreas, como por exemplo, na indústria de alimentos e na farmacêutica. O gênero atualmente contém 483 espécies aceitas e dezenas mais que estão em revisão pela comissão do Código Internacional de Nomenclatura para algas, fungos e plantas. O gênero *Penicillium* pode ser encontrado em praticamente todos os ecossistemas, sendo: aquático, em solo, como endófitos, como simbóticos de algas, de insetos e etc. O gênero apresenta um grande arsenal enzimático que ajuda às espécies pertencentes a este gênero a se adaptarem aos diversos tipos de clima, condição de nutrientes e a todos os tipos de estresse do meio ambiente onde estão crescendo. Com isso, as espécies deste gênero acabam sendo uma fonte promissora de metabólitos secundários, produzidos frente a diferentes ambientes como uma resposta adaptativa. Espécies desse gênero têm sido descritas como produtoras de diversos compostos bioativos, como a Oxalina que é um anticâncer já comercializado e obtido de *P. oxalicum*, o que torna a química do gênero ainda mais atrativa para novas pesquisas.

**Palavras-chave:** Fungo, Metabólito secundário, Produto natural, Alimentos.

### **Abstract**

*Penicillium* is a diverse genus that occurs worldwide and its species play important roles in several areas, such as in the food industry. The genus currently contains 483 species accepted and dozens more to be accepted that are under review by the International Code of Nomenclature commission for algae, fungi and plants. The genus *Penicillium* can be found in practically all ecosystems, being: Aquatic, in soil, endophytic, as decomposers and etc. Thus, the genus has a large enzymatic arsenal that helps species belonging to this genus to proliferate in different types of climate, nutrient conditions and all types of stress in the environment where it is growing. Thus, species of the genus *Penicillium* end up being a promising source of secondary metabolites, which they produce to survive certain environments. Species of this genus have been described as producers of several bioactive compounds, such as Oxaline, which is an anticancer already commercialized and obtained from *Penicillium oxalicum*, which makes the chemistry of the genus even more attractive for new research.

**Keywords:** Fungi, Secondary metabolite, Natural product

## 1. Introdução

O *Penicillium* é bem conhecido e um dos gêneros de fungos mais comuns, ocorrendo em uma ampla gama de habitats, do solo à vegetação, água e ar, ambientes internos e diversos produtos alimentícios. Tem uma distribuição mundial e um grande impacto econômico em diversas áreas (Frisvad and Samson 2004). Sua principal função na natureza é a decomposição de matérias orgânicas, onde as espécies causam podridões devastadoras como patógenos pré e pós-colheita em plantações (Samson et al., 2010), bem como produz uma gama diversificada de micotoxinas (Frisvad et al. 2004b). Algumas espécies também têm impactos positivos, como na indústria de alimentos com algumas espécies para a produção de queijos especiais, como Camembert, ou Roquefort (Nelson, 1970; Karahadian et al., 1985; Giraud et al., 2010). Seu potencial degradativo resultou na espécie sendo utilizada para a produção de novas enzimas, tendo participação nas indústrias têxtil e alimentícia (Adsul et al., 2007; Terrasan et al., 2010). Seu maior impacto, porém, é a produção de penicilina, um antibiótico que revolucionou as abordagens médicas para o tratamento de doenças bacterianas. (Visagie et al., 2016). Com a descoberta da penicilina por Fleming (1929) se despertou os olhares de diversos pesquisadores para a química do gênero, e desde então diversas pesquisas vêm sendo realizadas para a produção de metabólitos secundários.

## 2. Metodologia

Para a elaboração do presente trabalho foram consultados os seguintes sítios de busca de bancos de dados: Pubmed, Scielo, ScienceDirect e Web of Science buscando todas as publicações até o ano de 2021. As palavras-chaves utilizadas foram: “*Penicillium*” associada com as palavras “secondary metabolite”, “nomenclature”, “natural product”, “occurrence” e “molecular biology”.

## 3. Revisão bibliográfica

### 3.1 O gênero *Penicillium*

O nome *Penicillium* foi proposto pela primeira vez por Link em 1809, e é derivado de *penicillus*, que significa "pincel". Diversos trabalhos começaram a ser reportados sobre o gênero no século 19, entretanto Dierckx, em 1901, introduziu um sistema de classificação, incluindo os subgêneros *Biverticillium*, *Aspergilloides* e *Eupenicillium* (Visagie et al., 2014). Em 1949, Thom e Raper publicaram um trabalho chamado “Manual

of the Penicillia”, que foi uma das mais importantes contribuições para o conhecimento desse gênero. Nela, classificaram 137 espécies de *Penicillium* (a partir da colônia e ramificações dos conidióforos) em 12 seções, 18 subseções e quatro subgêneros (Pitt et al., 1979). Em 1980, Pitt realizou uma pesquisa que introduziu novos nomes, chegando a 150 espécies aceitas e designou neótipos de muitas espécies, separou *EuPenicillium* de *Penicillium* (seção) e subdividiu 31 antigos gêneros em séries, resultando em quatro subgêneros, 10 seções e 21 em séries (Houbraken and Samson, 2011; Visagie et al., 2014). Com o advindo das técnicas moleculares a partir dos anos 90, mais espécies foram aceitas no gênero, quando Pitt, em 2000 atualizou o número de espécies do gênero para 225 (Pitt et al., 2000). O gênero *Penicillium* pertence ao filo Ascomycota, classe Eutiomycetes, ordem Eurotiales e à família *Aspergillaceae*. É um gênero grande e atualmente é composto por 483 espécies aceitas (Houbraken et al., 2020).

O gênero *Penicillium* pode ser encontrado em todos os tipos de ambiente e condições, como: aquático, em solo, como endofítico e etc. (Visagie et al., 2014). Segundo o site The Global Biodiversity Information Facility (Gbif) que rastreia todas as publicações e banco de dados dos organismos existem 34,349 registro de *Penicillium*, mas apenas 18,681 coordenadas já foram registradas no mundo todo (Figura 1), tendo maior concentração de registros na Austrália, oeste europeu e Américas.

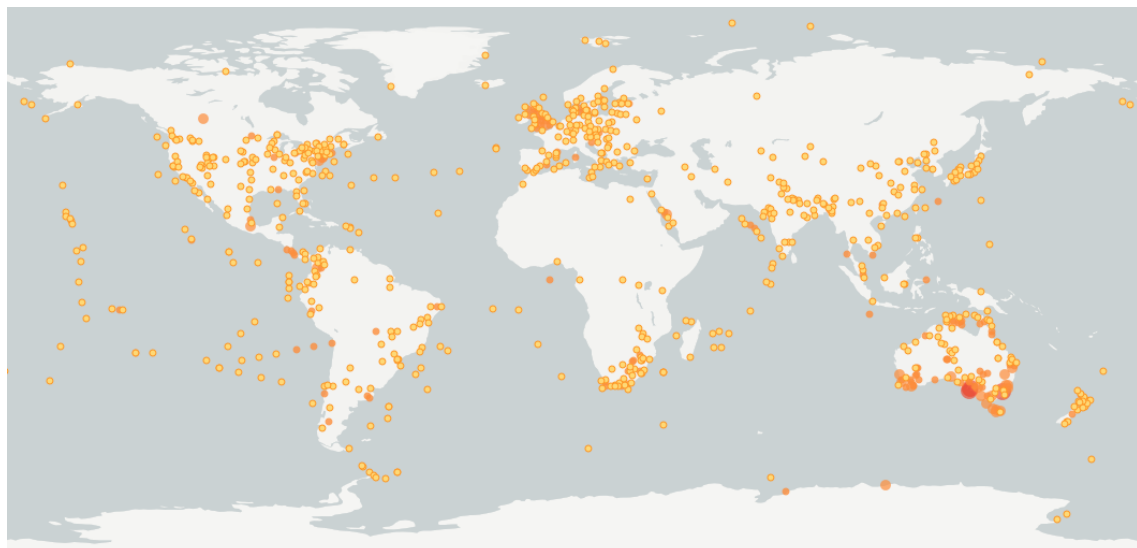


**Figura 1.** Ocorrência de espécies de *Penicillium* no mundo de acordo com o Gbif.org (acessado em 05/05/2021).

### 3.2 Identificação do Gênero *Penicillium*

#### 3.2.1 Identificação micromorfologica do gênero *Penicillium*

O gênero *Penicillium* é caracterizado pela produção de conídios em cadeias a partir de verticilos das fiálides (Pitt et al., 2000). As espécies monoverticiladas de *Penicillium* foram classificadas no subgênero *Aspergilloides*, as espécies biverticiladas foram classificadas no subgênero *Furcatum*. As espécies biverticiladas, que demonstravam um arranjo regular, com as métuas localizadas, terminalmente, à estirpe, foram classificadas no subgênero *Biverticillium* (Visagie et al., 2014). A observação das estruturas microscópicas, tais como: hifa hialina ou demácia, septada ou cenocítica, forma, disposição e formação dos esporos, são suficientes, em geral, para a identificação dos *Penicillium*. A morfologia microscópica é melhor visualizada com a técnica de microcultivo que preserva a disposição original dos esporos sobre as hifas e mantém íntegras certas estruturas formadoras de esporos (Pitt et al., 1979).

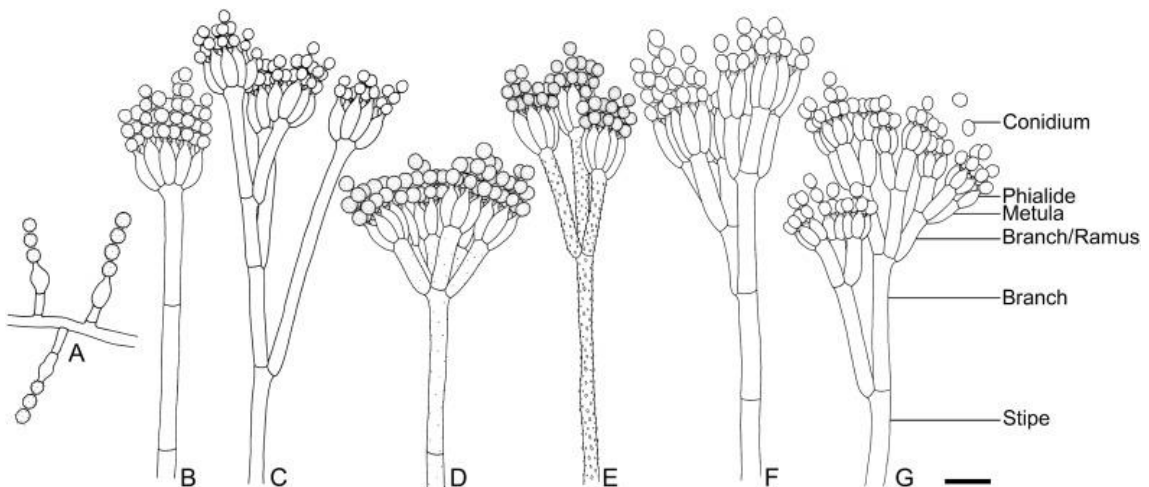


**Figura 2.** Padrões de ramificação dos conidióforos observados em *Penicillium*. A - Conidióforos com fiálides solitárias; B - Monoverticilado; C - Divaricato; D e E - Biverticilado; F - Terveticilado; G - Poliverticilado. Fonte: (VISAGIE et al., 2014)

### 3.2.2 Identificação macromorfológica do gênero *Penicillium*

A morfologia é a arquitetura física por meio da qual um organismo funciona e se adapta ao seu ambiente, mas alguns aspectos podem variar ou ser induzidos por variáveis presentes. Como resultado, as linhagens caracterizadas em um laboratório podem parecer diferentes quando cultivadas em outro devido a diferenças sutis em nutrientes, temperatura, iluminação ou umidade (Visagie et al., 2014). Isso às vezes torna as comparações entre diferentes estudos muito difíceis. Esses efeitos podem ser minimizados usando técnicas de trabalho estritamente padronizadas para a preparação do meio, técnica de inoculação e condições de cultivo (Samson e Pitt 1985, Okuda 1994, Okuda et al. 2000). As colônias de *Penicillium*, do ponto de vista macroscópico, começam

brancas. Então, e dependendo da espécie e de outros fatores, começam a adquirir cores como verde, verde-azulado ou cinza, isso vai depender dos nutrientes que compõem o meio de cultura em que estes fungos foram cultivados (Visagie et al., 2014). Os meios Czapek Yeast Autolysate Agar (CYA) e Malt Extract Agar (MEA) são os recomendados na literatura para identificação macromorfológica de *Penicillium* (Houbraken et al., 2011). Para cores de conídios consistentes, a adição de sulfato de zinco e sulfato de cobre como oligoelementos (1 g ZnSO<sub>4</sub>.7H<sub>2</sub>O e 0,5 g CuSO<sub>4</sub>.5H<sub>2</sub>O em 100 ml de água destilada) é de extrema importância porque esses metais variam amplamente na água usada em diferentes locais e são essenciais para a produção de pigmentos (Visagie et al., 2016).

Para incubadoras de bancada, as placas não precisam ser incubadas em caixas ou sacos, a menos que haja uma forte corrente de ar na incubadora. Todos os meios são incubados à temperatura padrão de 26 °C por 7 d. É crucial que as temperaturas sejam cuidadosamente verificadas, pois pequenas diferenças de temperatura têm um grande impacto sobre crescimento da colônia (Pitt et al., 2000). Após 7 d, os diâmetros da colônia são medidos na parte mais larga desta. Características importantes usadas para descrever *Penicillium* incluem a textura da colônia, grau de esporulação, a cor de conídios, a abundância, textura e cor dos micélios, a presença e cores de pigmentos solúveis e exsudatos, cores do dorso da colônia e grau de crescimento. (Visagie et al., 2014).

### 3.2.3 Identificação molecular do gênero *Penicillium*

Existem espécies em que os corpos de frutificação são estruturas morfológicamente muito complexas, dificultando uma caracterização em que seja possível separar os mais próximos. Além disso, algumas estruturas reprodutivas se apresentam apenas em uma pequena parte do ciclo de vida do fungo, tornando difícil a utilização desse caráter fenotípico (El-Enshasy et al., 2006; Krimitzas et al., 2013). A análise filogenética das características variáveis do DNA, atualmente, é a técnica mais viável utilizada para reconhecer as espécies de acordo com sua evolução. Como uma ferramenta integrada à abordagem morfológica, a filogenia tem auxiliado nas questões taxonômicas, delimitando as espécies que são muito próximas (Bauer et al., 2015; Jayasiri et al., 2015). A identificação das espécies de qualquer eucarioto se faz possível com uso de uma sequência de DNA e um banco de dados de referências (Visagie et al., 2014). As regiões Internal Transcribed Space (ITS) do rDNA foram aceitas como padrão para a

identificação de fungos. São regiões de escolha para análises filogenética principalmente porque para a maioria das espécies estudadas, possui similaridade em grande parte dos casos devido ao alto grau de preservação evolutiva, o que garante confiabilidade nos dados para comparação. Além disso, essa região evolui a taxas diferentes produzindo assim dados informativos importantes para a análise (Schoch et al., 2012; Washburne et al., 2018). Porém, as regiões *ITS* possuem algumas limitações, assim, genes codificadores de proteínas como as RNA polimerases (RPB1 e RPB2), β-tubulina e calmodulina têm provado serem bons marcadores para o reconhecimento das espécies de *Penicillium* (Visagie et al., 2014). As regiões e os primers correspondentes podem ser observados a seguir (Tabela 1).

Tabela 1. Primers usados para amplificação e sequenciamento de *Penicillium*.

Locus	Nome do primer	Direção	Sequencia do primer (5'-3')	Referencia
Internal Transcribed Spacer (Its)	ITS 1	Foward	TCC GTA GGT GAA CCT GCG G	White et al., 1990
	ITS 4	Reverse	TCC TCC GCT TAT TGA TAT GC	White et al., 1990
β-tubulina (BenA)	Bt2a	Foward	GGT AAC CAA ATC GGT GCT GCT TTC	Glass and Donaldson, 1995
	Bt2b	Reverse	ACC CTC AGT GTA GTG ACC CTT GGC	Glass and Donaldson, 1995
Calmodulina (CaM)	CMD5	Foward	CCG AGT ACA AGG ARG CCT TC	Hong et al., 2006
	CMD6	Reverse	CCG ATR GAG GTC ATR ACG TGG	Hong et al., 2006
	CF1	Foward	GCC GAC TCT TTG ACY GAR GAR	Peterson et al., 2005
	CF4	Reverse	TTT YTG CAT CAT RAG YTG GAC	Peterson et al., 2005
RNA polymerase II (RPB2)	5F	Foward	GAY GAY MGW GAT CAY TTY GG	Liu et al., 1999
	7CR	Reverse	CCC ATR GCT TGY TTR CCC AT	Liu et al., 1999
	5Feur	Foward	GAY GAY CGK GAY CAY TTC GG	Houbraken et al., 2012
	7CReur	Reverse	CCC ATR GCY TGY TTR CCC AT	Houbraken et al., 2012

Como a identificação, com base apenas em características morfológicas, não possibilita diferenciar as espécies com precisão, quando se trata de subgêneros muito

próximos associada a carência de taxonomistas especialistas para cada gênero, técnicas bioquímicas e moleculares, atualmente, são as mais utilizadas para tal finalidade e no estudo de diversidade de populações (Krimitzas et al., 2013). As técnicas moleculares fornecem um bom número de características viáveis para a taxonomia de fungos, que tem um papel fundamental no reconhecimento das espécies fúngicas (Geiser et al., 2007). É importante considerar que, para uma identificação mais precisa, é necessária a combinação destas técnicas moleculares com as características morfológicas, fisiológicas e químicas, que é conhecida como identificação polifásica (Houbraken and Samson, 2011; Visagie et al., 2014).

### 3.3 A química do gênero *Penicillium*

Desde a descoberta da penicilina (Figura 3) por Fleming (1929), espécies de *Penicillium* têm sido prospectadas quanto à produção de metabólitos secundários com potencial bioativo, incluindo substâncias antimicrobianas (Gao et al., 2011), antifúngicas, imunossupressores e também micotoxinas potentes (Andersen et al., 2004; Jin et al., 2016). A Tabela 2 mostra alguns metabólitos secundários isolados de espécies do gênero *Penicillium*.

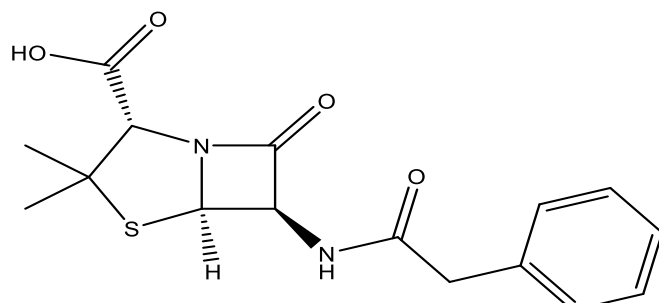


**Figura 3.** Estrutura da penicilina isolada pro Fleming.

**Tabela 1.** Metabólitos secundários isolados de espécies do gênero *Penicillium*.

Espécie	Metabólito	Peso molecular	Atividade biológica	Referência
<i>Penicillium Chrysogenum</i>	Conidiogenona B	286	Antimicrobiana	(Gao et al., 2011)
<i>P.vulpinum</i>	Patulina	154	Anticancer, micotoxina	(Monteillier et al., 2018)
<i>P. roqueforti</i>	Ácido penicílico Roquefortina A,	170, 298, 389, 391,	Micotoxinas	(Müller and Amend, 1997;

	C, D, E, F, G e H	457, 419, 517 e 487		Rabha and Jha, 2018)
<i>P. charlesii</i>	Ácido carólico	182	NR	(Torsten and Per, 1980)
<i>Penicillium</i> sp.	Chrysogine	190	Anticancer e antimicrobiana	(Yunianto et al., 2014)
<i>P. expansum</i>	Xantocilina e Meleagrina	288 e 433	Antibiótica e Anticancer	(Kozlovsky et al., 2004; Yunianto et al., 2014)
<i>P. viridicatum</i>	Ocratoxina A, Viridicatina e Viridicatol	403, 237 e 253	Micotoxina, Antitumoral	(Frisvad et al., 2004; Heguy et al., 1998)
<i>P. citrinum</i>	Citrinina	250	Micotoxina	(Rabha and Jha, 2018)
<i>P. waksmanii</i>	Agroclavina, Quinocitrininas A e B, Epoxyagroclavina	238, NR, 254	Antibiotica, Antimicrobiana, Antitumoral e Neurotrópica	(Rabha and Jha, 2018; Kozlovsky et al., 2013)
<i>P. aurantiumgriseum</i>	Aurantioclavina	226	Citotóxica	(Zhi et al., 2007)
<i>P. thomii</i>	Zosteropenilina	273	Anticancer	(Afiyatullov et al., 2017)
<i>P. hirsutum</i>	Glandicolina A e B	403, 419	Antimicrobiana	(Overy et al., 2005; Koolen et al., 2012)
<i>P. piscarium</i>	Piscarininas A e B	NR	Antitumoral	(Rabha and Jha, 2018)
<i>P. rugulosum</i>	Puberulinas A e B	371 e 387	Antitumoral	(KOZLOVSKY et al., 2013)
<i>P. camemberti</i>	Ácido Ciclopiazônico	336	Micotoxina	(Bars, 1979)
<i>P. griseofulvum</i>	Griseofulvina	352	Antimicrobiana	(Rabha and Jha, 2018)
<i>P. commune</i>	Piroclavina	240	NR	(Frisvad et al., 2004)
<i>P. janczewskii</i>	Costaclavina	240	NR	(Zhelifonova et al., 2010)
<i>P. lanosum</i>	Fumiquinazolina s A e B	445	Antitumoral	(Hwang et al., 2016)
<i>P. janczewskii</i>	Penitrem A	634	Inseticida	(Herbert, 2003)
<i>P. janthinellum</i>	Janthitrem B	585	Inseticida	(Herbert, 2003)
<i>P. atrovenetum</i>	Ácido 3-nitropropiônico	119	NR	(Herbert, 2003)

<i>P. paxilli</i>	Paxilina	435	Toxina tremorgênica	(Springer et al., 1975)
<i>P. oxalicum</i>	Penioxalamina A, Oxalina	447, 447	Citotóxica, Anticancer	(Hu et al., 2014)

Legenda: NR – Não reportado

Os extrolitos são produzidos pelo micélio e estruturas esporulantes de espécies de *Penicillium*, e exsudatos, pigmentos difusíveis, e as cores reversas também são misturas de metabólitos secundários. Estudos de perfis extrolitos foram muito úteis para desvendar alguns conceitos morfológicos de espécies antes do sequenciamento de DNA. A identificação de espécies desconhecidas usando extrólitos é possível para laboratórios químicos bem equipados. A melhor maneira de usar extrolitos como meios de identificação é extraír e separar por HPLC e, em seguida, identificar parcial ou totalmente o maior número de metabólitos secundários possível, geralmente usando tecnologia baseada em espectrometria de massas (Frisvad et al. 2008). Os meios usados para identificação, especialmente CYA e YES, são ideais para a produção da maioria dos principais extrólitos em *Penicillium*. Uma produção satisfatória de metabólitos secundários depende muito do meio em que os fungos são cultivados, mas uma regra geral é que quanto mais complexo um meio, mais diversidade química os fungos exibirão. Os meios contendo grandes quantidades de sacarose e glicose junto com extrato de levedura ou extrato de malte e minerais adicionados e metais traço, geralmente fornecem a produção de metabólitos mais variada e as concentrações mais altas de compostos. Os “plugs” de ágar com o fungo crescido são extraídos com uma mistura de diclorometano, acetato de etila e metanol. Os metabólitos extraídos podem então ser analisados usando técnicas avançadas de separação e detecção, por exemplo, cromatografia líquida de alta precisão e espectrometria de massa de alta resolução (Klitgaard et al. 2014). Às vezes, apenas alguns extrolitos são necessários para confirmar a identidade de um isolado de *Penicillium*. Se um isolado produz griseofulvina e roquefortina C, só pode ser *P. coprophilum*, *P. griseofulvum* ou *P. sclerotigenum* e se o isolado também produz ácido ciclopiazônico, só pode ser *P. griseofulvum* (Frisvad e Samson, 2004). Identificação fundamentada puramente em metabólitos secundários não é ainda possível para todas as espécies de *Penicillium*, mas bancos de dados futuros poderão ser desenvolvidos para permitir que este método seja usado para identificação de todas as espécies do gênero.

#### 4. Considerações finais

Nesta revisão foram abordados temas referentes ao gênero *Penicillium*, focando-se na identificação das espécies do mesmo, a importância química do gênero e biodiversidade registrada no Banco mundial de informações sobre a biodiversidade. Destacando a diversidade intraespecífica do gênero como excelente e reconhecido produtor de metabólitos secundários com diversas atividades biológicas já descritas.

#### REFERENCIAS

- AFIYATULLOV, S. S.; LESHCHENKO, E. V.; BERDYSHEV, D. V.; SOBOLEVSKAYA, M. P.; ANTONOV, A. S.; DENISENKO, V. A.; POPOV, R. S.; PIVKIN, M. V.; UDOVENKO, A. A.; PISLYAGIN, E. A.; VON AMSBERG, G.; DYSHLOVOY, S. A. Article zosteropenillines: Polyketides from the marine-derived fungus *Penicillium thomii*. **Marine Drugs**, v. 15, n. 2, 2017.
- ADSUL, M. G.; BASTAWDE, K. B.; VARMA, A. J.; et al. Strain improvement of *Penicillium janthinellum* NCIM 1171 for increased cellulase production. **Bioresource Technology**, v. 98, p. 1467–1473, 2007.
- ANDERSEN, B.; SMEDSGAARD, J.; FRISVAD, J. C. *Penicillium expansum*: Consistent Production of Patulin, Chaetoglobosins, and Other Secondary Metabolites in Culture and Their Natural Occurrence in Fruit Products. **Journal of Agricultural and Food Chemistry**, v. 52, n. 8, p. 2421–2428, 2004.
- BARS, J. Le. Cyclopiazonic acid production by *Penicillium camemberti* Thom and Cyclopiazonic Acid Production by *Penicillium camemberti* Thom and Natural Occurrence of This Mycotoxin in Cheese. v. 38, n. 6, p. 1052–1055, 1979.
- BAUER, R.; GARNICA, S.; OBERWINKLER, F.; RIESS, K.; WEISS, M.; BEGEROW, D. Entorrhizomycota: A new fungal phylum reveals new perspectives on the evolution of Fungi. **PLoS ONE**, v. 10, n. 7, 2015.
- EL-ENSHASY, H. Process characteristics, products, and applications. In: Bioprocessing for Value-Added Products from Renewable Resources. YANG, S. 1 ed. Elsevier Science. Novembro, 2006.
- FRISVAD, J. C.; ANDERSEN, B.; THRANE, U. The use of secondary metabolite profiling in fungal taxonomy. **Mycological Research**, v. 112, p. 231–240, 2008.

FRISVAD, J. C.; SAMSON, R. A. Polyphasic taxonomy of *Penicillium* subgenus *Penicillium*. A guide to identification of food and air-borne terverticillate Penicillia and their mycotoxins. **Studies in Mycology**, v. 49, p. 1–174, 2004.

FRISVAD, J. C.; SMEDSGAARD, J.; LARSEN, T. O.; et al. Mycotoxins, drugs and other extrolites produced by species in *Penicillium* subgenus *Penicillium*. **Studies in Mycology**, v. 49, p. 201–241, 2004b.

GAO, S. S.; LI, X. M.; LI, C. S.; PROKSCH, P.; WANG, B. G. Penicisteroids A and B, antifungal and cytotoxic polyoxygenated steroids from the marine alga-derived endophytic fungus *Penicillium chrysogenum* QEN-24S. **Bioorganic and Medicinal Chemistry Letters**, v. 21, n. 10, p. 2894–2897, 2011.

GBIF: The Global Biodiversity Information Facility (2021) Available from: <https://www.gbif.org/occurrence/map?q=Penicillium>. Accessed: 20/04/2021.

GLASS, N. L.; DONALDSON, G. C. Development of premier sets designed for use with the PCR to amplify conserved genes from filamentous Ascomycetes. **Applied and Environmental Microbiology** v. 61, p. 1323–1330, 1995.

GEISER, D. M.; KLICH, M. A.; FRISVAD, J. C.; PETERSON, S. W.; VARGA, J.; SAMSON, R. A. The current status of species recognition and identification in *Aspergillus*. **Studies in Mycology**, v. 59, p. 1–10, 2007.

GIRAUD, F.; GIRAUD, T.; AGUILETA, G.; FOURNIER, E.; SAMSON, R.; CRUAUD, C.; LACOSTE, S.; ROPARS, J.; TELLIER, A.; DUPONT, J. Microsatellite loci to recognize species for the cheese starter and contaminating strains associated with cheese manufacturing. **International Journal of Food Microbiology**, v. 137, p. 204–213, 2010.

HEGUY, A.; CAI, P.; MEYN, P.; HOUCK, D.; RUSSO, S.; MICHITSCH, R.; PEARCE, C.; KATZ, B.; BRINGMANN, G.; FEINEIS, D.; TAYLOR, D.; TYMS, A. Isolation and Characterization of the Fungal Metabolite 3-O-Methylviridicatin as an Inhibitor of Tumour Necrosis Factor -Induced Human Immunodeficiency Virus Replication. **Antiviral Chemistry and Chemotherapy**, v. 9, n. 2, p. 149–155, 1998.

HERBERT, R. B. The biosynthesis of plant alkaloids and nitrogenous microbial metabolites. **Natural Product Reports**, v. 20, n. 5, p. 494–508, 2003.

Hong, S-B.; Cho, H-S.; Shin, H-D.; et al. Novel Neosartorya species isolated from soil in Korea. **International Journal of Systematic and Evolutionary Microbiology** v. 56, p. 477–486, 2006.

HOUBRAKEN, J.; SAMSON, R. A. Phylogeny of *Penicillium* and the segregation of Trichocomaceae into three families. **Studies in Mycology**, v. 70, p. 1–51, 2011.

HOUBRAKEN, J.; SPIERENBURG, H.; FRISVAD, J. C. *Rasamonia*, a new genus comprising thermotolerant and hermophilic *Talaromyces* and *Geosmithia* species. **Antonie van Leeuwenhoek** v. 101, p. 403–421, 2012.

HOUBRAKEN, J., KOCSUBÉ, S., VISAGIE, C. M., YILMAZ, N., WANG, X. C., MEIJER, M., KRAAK, B., HUBKA, V., BEN SCH, K., SAMSON, R. A., & FRISVAD, J. C. Classification of *Aspergillus*, *Penicillium*, *Talaromyces* and related genera (*Eurotiales*): An overview of families, genera, subgenera, sections, series and species. **Studies in mycology**, v. 95, p. 5–169. 2020.

HU, X. L.; BIAN, X. Q.; WU, X.; LI, J. Y.; HUA, H. M.; PEI, Y. H.; HAN, A. H.; BAI, J. Penioxalamine A, a novel prenylated spiro-oxindole alkaloid from *Penicillium oxalicum* TW01-1. **Tetrahedron Letters**, v. 55, n. 29, p. 3864–3867, 2014.

HWANG, I. H.; CHE, Y.; SWENSON, D. C.; GLOER, J. B.; WICKLOW, D. T.; PETERSON, S. W.; DOWD, P. F. Haenaminde and fumiquinazoline analogs from a fungicolous isolate of *Penicillium lanosum*. **Journal of Antibiotics**, v. 69, n. 8, p. 631–636, 2016.

JAYASIRI, S. C.; HYDE, K. D.; ARIYAWANSA, H. A.; BHAT, J.; BUYCK, B.; CAI, L.; DAI, Y. C.; ABD-ELSALAM, K. A.; ERTZ, D.; HIDAYAT, I.; JEWON, R.; JONES, E. B. G.; et al. The Faces of Fungi database: fungal names linked with morphology, phylogeny and human impacts. **Fungal Diversity**, v. 74, n. 1, p. 3–18, 2015.

JIN, Z. Muscarine, imidazole, oxazole and thiazole alkaloids. **Natural Product Reports**, v. 33, n. 11, p. 1268–1317, 2016.

KARAHADIAN, C.; JOSEPHSON, D. B.; LINDSAY, R. C. Volatile compounds from *Penicillium* sp. contributing musty-earthy notes to Brie and Camembert cheese flavors. **Journal of Agricultural and Food Chemistry**, v. 33, p. 339–343, 1985

KLITGAARD, A.; IVERSEN, A.; ANDERSEN, MR.; et al. Aggressive dereplication using UHPLC-DAD-QTOF – screening extracts for up to 3000 fungal secondary metabolites. **Analytical and Bioanalytical Chemistry**, v. 406, p. 1933–1943, 2014.

KOOLEN, H. H. F.; SOARES, E. R.; DA SILVA, F. M. A.; DE ALMEIDA, R. A.; DE SOUZA, A. D. L.; DE MEDEIROS, L. S.; FILHO, E. R.; DE SOUZA, A. Q. L. An antimicrobial alkaloid and other metabolites produced by *Penicillium* sp. an endophytic fungus isolated from *Mauritia flexuosa* L. F. **Quimica Nova**, v. 35, n. 4, p. 771–774, 2012.

KOZLOVSKY, A. G.; ZHELIFONOVA, V. P.; ANTIPOVA, T. V.; ADANIN, V. M.; NOVIKOVA, N. D.; DESHEVAYA, E. A.; SCHLEGEL, B.; DAHSE, H. M.; GOLLMIK, F.; GRAFE, U. *Penicillium expansum*, a resident fungal strain of the orbital complex Mir, producing xanthocillin X and questiomycin A. **Applied Biochemistry and Microbiology**, v. 40, n. 3, p. 291–295, 2004.

KOZLOVSKY, A. G.; ZHELIFONOVA, V. P.; ANTIPOVA, T. V. Biologically active metabolites of *Penicillium* fungi. **Signpost Open Access Journal of Organic and Biomolecular Chemistry**, v. 01, p. 11–21, 2013.

KRIMITZAS, A.; PYRRI, I.; KOUVELIS, V.; KAPSANAKI-GOTSI, E.; TYPAS, M. A phylogenetic analysis of greek isolates of *Aspergillus* species based on morphology and nuclear and mitochondrial gene sequences. **Hindawi Publishing Corporation BioMed Research International**, v. 2013, p. 18, 2013.

LIU, Y. J.; WHELEN, S.; HALL, B. D. Phylogenetic relationships among ascomycetes: evidence from an RNA polymerase II subunit. **Molecular Biology and Evolution** v. 16, p. 1799–1808, 1999.

MONTEILLIER, A.; ALLARD, P. M.; GINDRO, K.; WOLFENDER, J. L.; CUENDET, M. Lung cancer chemopreventive activity of patulin isolated from *Penicillium vulpinum*. **Molecules**, v. 23, n. 3, p. 1–12, 2018.

MÜLLER, H. M.; AMEND, R. Formation and disappearance of mycophenolic acid, patulin, penicillic acid and PR toxin in maize silage inoculated with *Penicillium roqueforti*. **Archives of Animal Nutrition**, v. 50, n. 3, p. 213–225, 1997.

NELSON, J. H. Production of blue cheese flavor via submerged fermentation by *Penicillium roqueforti*. **Journal of Agricultural and Food Chemistry**, v. 18, p. 567–569, 1970

OVERY, D. P.; NIELSEN, K. F.; SMEDSGAARD, J. Roquefortine/oxaline biosynthesis pathway metabolites in *Penicillium* ser. *Corymbifera*: In planta production and implications for competitive fitness. **Journal of Chemical Ecology**, v. 31, n. 10, p. 2373–2390, 2005.

PETERSON, S. W.; VEJA, F.; POSADA, F.; et al. *Penicillium coffeae*, a new endophytic species isolated from a coffee plant and its phylogenetic relationship to *P. fellutanum*, *P. thiersii* and *P. brocae* based on parsimony analysis of ulitlocus DNA sequences. **Mycologia** v. 97, p. 659–666, 2005.

PITT, J. **The genus Penicillium**. Londres: Academic Press, 1979.

PITT, J. I.; SAMSON, R. A.; FRISVAD, J. C. List of accepted species and their synonyms in the family Trichocomaceae. In: Integration of modern taxonomic methods for *Penicillium* and *Aspergillus* classification (SAMSON RA, PITT JI eds). Harwood Academic Publishers, Amsterdam: 9–79, 2000.

RABHA, J.; JHA, D. K. **Metabolic Diversity of *Penicillium***. 1 ed. Elsevier B.V., 2018.

SAMSON, R. A.; HOUBREAKEN, J.; THRANE, U.; FRISVAD, J. C.; ANDERSEN, B. Food and indoor fungi. 2 ed. CBS KNAW Biodiversity Center, Utrecht, Netherlands, 2010

SCHOCH, C. L.; SEIFERT, K. A.; HUHNDORF, S.; ROBERT, V.; SPOUGE, J. L.; LEVESQUE, C. A.; CHEN, W.; BOLCHACOVA, E.; VOIGT, K.; CROUS, P. W.; MILLER, A. N.; et al. Nuclear Ribosomal Internal Transcribed Spacer (ITS) region as a universal DNA barcode marker for Fungi. **Proceedings of the National Academy of Sciences**, v. 109, n. 16, p. 6241–6246, 2012.

SPRINGER, J. P.; CLARDY, J.; WELLS, J. M.; COLE, R. J.; KIRKSEY, J. W. The structure of paxilline, a tremorgenic metabolite of *Penicillium paxilli* bainier. **Tetrahedron Letters**, v. 16, n. 30, p. 2531–2534, 1975.

TERRASAN, C. R. F.; TEMER, B.; DUARTE, M. C. T.; et al. Production of xylanolytic enzymes by *Penicillium janczewskii*. **iORESOURCE Technology**, v. 101, p. 4139–4143, 2010.

TORSTEN, R.; PER, M. B. Aspects of the Biosynthesis of Carolic and Carlosic Acids in *Penicillium charlesii*. A <sup>13</sup>C NMR Study. **Acta Chemica Scandinavica B**, v. 34, p. 653–659, 1980.

VISAGIE, C. M.; HOUBREAKEN, J.; FRISVAD, J. C.; HONG, S. B.; KLAASSEN, C. H. W.; PERRONE, G.; SEIFERT, K. A.; VARGA, J.; YAGUCHI, T.; SAMSON, R. A. Identification and nomenclature of the genus *Penicillium*. **Studies in Mycology**, v. 78, n. 1, p. 343–371, 2014.

VISAGIE, C. M.; RENAUD, J. B.; BURGESS, K. M. N.; MALLOCH, D. W.; CLARK, D.; KETCH, L.; URB, M.; ASSABGUI, R.; SUMARAH, M. W.; SEIFERT, K. A. Fifteen new species of *Penicillium*. **Persoonia**, v. 36, p. 247–280, 2016.

WASHBURNE, A. D.; MORTON, J. T.; SANDERS, J.; MCDONALD, D.; ZHU, Q.; OLIVERIO, A. M.; KNIGHT, R. Methods for phylogenetic analysis of microbiome. **Nature Microbiology**, v. 3, n. 6, p. 652–661, 2018.

WHITE, T. J.; BRUNS, T.; LEE, S.; et al. Amplification and direct sequencing of fungal ribosomal RNA genes for phylogenetics. In: PCR protocols: a guide to methods and

applications (INNIS, M. A.; GELFAND, D. H.; SHINSKY, T. J.; WHITE, T. J.; (eds). Academic Press Inc, New York: p. 315–322, 1990.

YUNIANTO, P.; RUSMAN, Y.; SAEPUDIN, E.; SUWARSO, W. P.; SUMARYONO, W. Alkaloid (meleagrine and chrysogine) from endophytic fungi (*Penicillium* sp.) of *Annona squamosa* L.Pakistan. **Journal of Biological Sciences**, 2014.

ZHELIFONOVA, V. P.; ANTIPOVA, T. V.; KOZLOVSKY, a. G. Secondary metabolites in taxonomy of the *Penicillium* fungi. **Microbiology**, v. 79, n. 3, p. 277–286, 2010.

ZHI, H. X.; FANG, Y.; DU, L.; ZHU, T.; DUAN, L.; CHEN, J.; GU, Q. Q.; ZHU, W. M. Aurantiomides A-C, quinazoline alkaloids from the sponge-derived fungus *Penicillium aurantiogriseum* SP0-19. **Journal of Natural Products**, v. 70, n. 5, p. 853–855, 2007.

### **3. OBJETIVOS**

#### **3.1 Objetivo geral**

Identificar linhagens endofíticas amazônicas de *Penicillium* capazes de produzir substâncias com potencial farmacológico e/ou biotecnológico bem como investigar o potencial químico e biológico.

#### **3.2 Objetivos específicos**

- 1) Selecionar linhagens endofíticas de *Penicillium* isolados de planta medicinais da Amazônia promissoras quanto à produção de alcalóides e/ou de moléculas de valor biotecnológico;
- 2) Identificar por aspectos morfológicos e por biologia molecular as linhagens fúngicas selecionadas;
- 3) Analisar os perfís químicos e genômicos das linhagens de *Penicillium* endofíticos selecionados;
- 4) Isolar e caracterizar das linhagens selecionadas alcalóides e outras substâncias de valor biotecnológico;
- 5) Avaliar por *docking* molecular as atividades das moléculas isoladas e caracterizadas frente aos alvos dos vírus: do dengue tipo 2, bem como o da *Sars-CoV-2*.

## 4. APRESENTAÇÃO DOS CAPÍTULOS

O desenvolvimento destas se estendeu na introdução, na revisão e em 3 capítulos, onde são mencionados os materiais, as metodologias, os resultados e a discussão, de acordo com a apresentação abaixo, e as revistas às quais estão sendo enviadas:

**4.1 Capítulo II:** “Polyphasic Identification of Endophytic *Penicillium* spp. from Amazon” Este capítulo está formatado na forma de artigo e será enviado para à revista *Fungal Diversity* (ISSN 1560-2745).

**4.2 Capítulo III:** “Screening of Alkaloid-Producing Endophytic *Penicillium* strains from Amazon Medicinal Plants by Electrospray Ionization Mass Spectrometry (ESI-MS) and Principal Component Analysis (PCA)” Este capítulo está formatado na forma de artigo, o qual foi submetido à revista *Brazilian Journal of Chemical Society* (ISSN 1678-4790) em 21 de janeiro de 2021 e aceito em 13 de abril de 2021.

**4.3 Capítulo IV:** “Alkaloids from Amazon *Penicillium* strains as potential inhibitors of SARS-CoV-2 and DENV-2 target enzymes” Este capítulo está formatado na forma de artigo e será enviado para à revista *Brazilian Journal of Chemical Society* (ISSN 1678-4790).

## 5. CAPITULO II

### Identificação polifásica de *Penicillium* spp. endofíticas da Amazônia<sup>3</sup>

Francinaldo Araujo da Silva-Filho, Felipe Moura Araujo da Silva, Gilvan Ferreira da Silva, Jeferson Chagas da Cruz, Sarah Raquel Silveira da Silva, Afonso Duarte Leão de Souza, Antonia Queiroz Lima de Souza

Este capítulo apresenta o estudo polifásico realizado com espécies endofíticas do gênero *Penicillium* da coleção de trabalho do Laboratório de Bioensaios e Microrganismos da Amazonia (LabMicra). 29 isolados foram reativados a fim de estudar a Biodiversidade, suas morfologias, a região ITS 1-4 do rDNA e o perfil de metabólitos secundários. Com os dados moleculares, foi possível identificar todos os 29 isolados, sendo sete espécies de *Penicillium* e uma espécie de *Talaromyces*. Isso corroborou na interpretação morfológica. Também foi possível ver a perspectiva evolutiva das linhagens executando uma árvore filogenética com o método de Máxima Parcimônia. Esta análise, juntamente com o perfil químico, ajudou a entender a relação dos isolados bem como a influência que a planta hospedeira tem tanto em nível químico quanto molecular. Por fim, este trabalho mostrou que todas as três técnicas combinadas provaram ser uma metodologia mais eficaz para identificar espécies cripticas do gênero *Penicillium*.

---

<sup>3</sup>Este capítulo está na forma de artigo, formatado no modelo da revista e será submetido para publicação na Fungal Diversity (ISSN 1560-2745)

## Polyphasic identification of endophytic *Penicillium* spp. from Amazon

Francinaldo Araujo da Silva-Filho<sup>1</sup>, Felipe Moura Araujo da Silva<sup>3</sup>, Gilvan Ferreira da Silva<sup>6</sup>, Jeferson Chagas da Cruz<sup>6</sup>, Sarah Raquel Silveira da Silva<sup>1</sup>, Afonso Duarte Leão de Souza<sup>1,3,4</sup>, Antonia Queiroz Lima de Souza<sup>1,2, 3,5\*</sup>

<sup>1</sup>Programa de Pós-Graduação da Rede Bionorte – Escola Superior de Ciências da Saúde da Universidade do Estado do Amazonas, 69.000-000, Manaus, AM, Brazil

<sup>3</sup>Central Analítica - Centro de Apoio Multidisciplinar (CAM), Universidade Federal do Amazonas (UFAM), 69077-000, Manaus, AM, Brazil

<sup>4</sup>Departamento de Química (ICE), Universidade Federal do Amazonas, 69077-000, Manaus, AM, Brazil

<sup>5</sup>Faculdade de Ciências Agrárias (FCA), Universidade Federal do Amazonas, 69077-000, Manaus, AM, Brazil

<sup>6</sup>Embrapa Amazônia Ocidental, Empresa Brasileira de Pesquisa Agropecuária (EMBRAPA) Manaus, AM, Brazil

### **\*Corresponding author:**

Antonia Queiroz Lima de Souza, E-mail address: antoniaqueiroz@ufam.edu.br

## Abstract

*Penicillium* is a diverse genus that occurs worldwide and its species play important roles in several areas. The genus *Penicillium* can be found in practically all ecosystems, being: Aquatic, in soil, endophytic, as decomposers and etc. Due to the great variability of the genus, and the large number of species described, the *Penicillium* taxonomy based only on morphology becomes quite complex. This difficulty makes it necessary to search for new tools in order to complement and validate the identification. Thus, the objective of the present work was to carry out a research of the diversity of the genera *Penicillium* in the Amazon region utilizing a poliphasic approach. 29 endophytic strains of *Penicillium* were cultivated in order to study its morphology, molecular biology and chemical compounds. With the molecular data, it was possible to identify all 29 strains, being 7 different species of *Penicillium* and 1 species of *Talaromyces*, and group the strains by species. This helped with the morphological interpretation. It was also possible to see the evolutionary perspective of the strains by running a phylogenetic tree with Maximum Parsimony method. This analysis, together with the chemical profiling helped to understand the relation of the strains as well as the influence that the host plant has both in chemical and molecular level. Lastly, this work showed that all three techniques combined proved to be an effective method to identify even close species from the genus *Penicillium*.

**Keywords:** Taxonomy, Chemical profiling, Macromorphology, *Penicillium* strains, Phylogeny, HCA

## Introduction

Studies have estimated the existence of at least 2.2–3.8 million fungal species on Earth, from which only around 10% have been isolated and described (Hawksworth 2017). Brazil is a country of world prominence when it comes to biodiversity. Holder of one of the largest biodiversities in the world is home to millions of species of plants, animals and microorganisms distributed in different biomes (Valli and Bolzani, 2016). However, little is known about its biological potential and its possible use in biotechnology, which increases the importance of research in the discovery of new microbial processes and products.

*Penicillium* is a diverse genus that occurs worldwide and its species play important roles in several areas. The genus *Penicillium* can be found in practically all ecosystems, being: Aquatic, in soil, endophytic, as decomposers, etc. (Pitt and Hocking 1997). Ecologically, species of the genus *Penicillium* are extremely important in nature, as they actively participate in biogeochemical cycles, acting in the decomposition of organic matter (Visagie et al. 2014). Due to its high metabolic competence, they are not very nutritionally demanding, tolerating a immense variety of physical and physical-chemical conditions, such as temperature, water and pH (Visagie et al. 2016). It is precisely this high tolerance for extreme conditions that gives them the ability to grow in any environment they provide from the very beginning, from minimum amounts of mineral salts to the most complex carbon sources (Onions and Brady 1987). *Penicillium* is not only found in large numbers, but are also major contributors to the total micro fungal diversity in plants. In a review of *Penicillium* species diversity in plants surveys from around the world, Christensen et al., (2000) found that, on average, *Penicillium* spp. account for 21% of the total fungi isolated, with the highest number found in Syria (reaching 49%) and the lowest in a legume crop from India (3%).

The genus *Penicillium* belongs to the phylum Ascomycota, class Eutiomycetes, order Eurotiales and to the family *Aspergillaceae*. It is a large genus and currently consists of 483 accepted species (Houbraken et al. 2020). *Penicillium* fungi are used as a model in several basic research studies. In addition to the relevant environmental importance in the cycling of organic matter, *Penicillium* species have a wide biotechnological potential, being widely used for the production of enzymes for industrial, environmental, pharmaceutical, among others purposes. (Bon et al., 2008).

Due to the great variability of the genus, and the large number of species described, the *Penicillium* taxonomy based on morphology becomes quite complex. This difficulty makes it necessary to search for new tools in order to complement and validate the identification. Among them are molecular biology, which together with the morphology and biochemistry data, characterize a taxonomy polyphasic (Frisvad et al. 2008; Santos et al. 2009). The survey of the diversity of microorganisms in a region that is still poorly studied, with preserved vegetation, may result in the discovery of species not yet described, important from an environmental and economic point of view, promising to be used in biotechnological processes. Thus, the objective of the present work was to carry out a research of the diversity of the genera *Penicillium* in the LabMicra work collection with strains isolated from the Amazon region utilizing a poliphasic approach.

## **Materials and methods**

### **Fungal cultivation**

The 29 strains previously isolated from Amazon medicinal plants and deposited in the work collection of the Amazon Bioassay and Microorganism Laboratory from Amazon Federal University (LabMicrA/UFAM) and has the access to genetic heritage registered at Sistema Nacional de Gestão do Patrimônio Genético e do Conhecimento Tradicional

Associado (SisGen) under the code No. AD64E07 were grown in Petri dishes containing ISP2 (10 g corn starch, 4 g yeast extract, 10 g malt, 4 g dextrose, 20 g agar for every 1 L of distilled water), Potato Dextrose Agar (PDA) (20 g dextrose, 15 g agar, 200 g of potato for every 1 L of distilled water) and CYA (30 g cane sugar, 2 g sodium nitrate, 1 g monopotassium phosphate, 0.5 g magnesium sulfate, 0.5 g potassium chloride, 0.01 g iron sulfate for every 1 L of distilled water) medium with a central inoculum, for 10 days at a temperature of 26° C, generating 87 petri dishes (29 per medium) and 1 Control for each medium, totalizing 90 plates.

### **Morphologic analysis**

The characterization and morphological identification of the strains were carried out with macroscopic characteristics (colony color, mycelium color, presence or absence of exudate, color of the reverse, presence or absence of soluble pigmentation) and microscopic, all according to Visagie et al. (2016).

### **Micro-scale extracts preparation**

After the cultivation period described above and the observation of all 90 Petri dishes, three plugs of 6 mm diameter were removed from each plate, transferred to 5 cm test tubes, and extracted for 24 h with 2 mL of a solution containing 3:2:1 ethyl acetate/dichloromethane/methanol, with 1% formic acid. The solvent was then filtered through a small piece of cottonand concentrated, yielding around 1 mg of extract in general for all samples according to Smedsgaard (1997).

### **Chemotaxonomy analysis**

The micro-scale extracts were resuspended in methanol (HPLC grade), creating the stock solutions (1 mg/mL). Aliquots (5 µL) of the stock solutions were further diluted to 5 µg/mL and analyzed by direct infusion into the mass spectrometers. An ion-trap mass spectrometer, model LCQ Fleet (Thermo Scientific, San Jose, CA, USA), equipped with

electrospray ionization (ESI) interface and running in the positive ion mode was used to perform ESI-MS and a triple quadrupole mass spectrometer, model TSQ Quantum Access (Thermo Scientific, San Jose, CA, USA) to perform ESI-MS/MS analyses. Samples were directly infused into the ion source through the instrument syringe pump (10 $\mu$ L/min). MS analytical conditions: spray voltage, 5 kV; sheath gas, 10 arbitrary unit (arb); auxiliary gas, 5 arb; sweep gas, 0 arb; capillary temp, 200° C; capillary voltage, 40 V; tube lens, 115 V; mass range, *m/z* 150 to 1000. Argon was used as collision gas, and the ESI-MS/MS spectra were obtained using collision energies ranging from 25 to 30 eV. For the Hierarchical cluster analysis (HCA), the relative ion intensity obtained by ESI-MS from *m/z* 150 to 1000 (850 variables) was analyzed through Chemoface™ program.

### **Molecular biology analysis**

The identification of the *Penicillium* strains was confirmed by sequencing of the fungus *Internal Transcribed Space-1 (ITS)* and *ITS-2 rDNA* and compared with sequences from the GenBank. 10  $\mu$ L of the strains spore suspension concentrated in 30x10<sup>8</sup>cels/mL was incubated on 50 mL potato dextrose (PD), medium in a 125 mL Erlenmeyer and stirred for 36 h (120 rpm) at 26° C temperature. The mycelium was separated from the medium by filtration and crushed with silica gel and then proceeded to extraction. The genomic DNA was extracted by a Zymo Research Quick-DNA™ Fungal/Bacterial Miniprep Kit using its own protocol with some adaptations, using 50  $\mu$ L of the DNA Dilution Buffer instead of protocol's 100  $\mu$ L and using longer centrifugation times on all steps. After the extraction, the DNA was sequenced using a model 3500 GeneticAnalyzer (Applied Biosystems, Foster city, CA, USA). The consensus sequence was obtained using the program DNA Baser Assembly and all the data was then analyzed using Mega7 and processed using National Center for Biotechnology Information's (NCBI) Nucleotide Basic Local Alignment Search Tool (BLASTn) tool. The MP tree was obtained using the

Subtree-Pruning-Regrafting (SPR) algorithm, with search level 1 in which the initial trees were obtained by the random addition of sequences (10 replicates).

## Results and Discussion

### Morphological analysis

Morphology is the physical architecture through which an organism functions in and adapts to its environment, but some aspects may vary or be induced by specific cues in the immediate environment. As a result, strains characterized in one laboratory might look different when grown in another because of subtle differences in nutrients, temperature, lighting or humidity (Visagie et al., 2014). This sometimes makes comparisons between different studies very difficult. These effects can be minimized using strictly standardized working techniques for medium preparation, inoculation technique and cultivations conditions (Samson and Pitt 1985, Okuda 1994, Okuda et al. 2000). This part of the work was done with CYA, which is the default medium for morphology of the *Penicillium* genera in the literature (Visagie et al. 2014) and two other media, ISP2 which is used for the production of antibiotics in actinomycetes and which is being used more recently together with the oat media by LabMicrA to increase the variability of the isolated endophytes and is extremely rich in carbon and nitrogen sources and PDA which is common in the isolation of endophytes but don't have the minerals present in CYA. After observing the plates and with the molecular data, all fungi from the same species were grouped to better understand the effect of the medium on strains isolated from different places (Table 1). All plates can be observed in Figures 1-29.

**Table 1.** Selected *Penicillium* strains from the work collection of the LabMicrA/UFAM.

Strain number (Nº)	Code in the collection	Host plant	Part of the plant (isolated)
38	<i>AnspC2 3.1</i>	<i>Annona</i> sp.	Stems
46	<i>AnspcG3 1.2c</i>	<i>Annona</i> sp.	Twig bark
48	<i>AnspcG1 3.3</i>	<i>Annona</i> sp.	Twig bark
52	<i>AspC2 2.2</i>	<i>Annona</i> sp.	Stems
56	<i>AnspG1 2.2</i>	<i>Annona</i> sp.	Twig
64	<i>VrF1 2.2</i>	<i>Victoria amazonica</i>	Leaf
71	<i>VrC2 1.2</i>	<i>V. amazonica</i>	Stems
135	<i>PbR2 2.2</i>	<i>Mauritia flexuosa</i>	Root
143	<i>VrC2 2.1c</i>	<i>V. amazonica</i>	Stems
149	<i>VrF2 2.3</i>	<i>Vi. amazonica</i>	Leaf
153	<i>AnspG1 2.3a</i>	<i>Annona</i> sp.	Twig
154	<i>AnspC2 2.1</i>	<i>Annona</i> sp.	Stems
155	<i>AnspG1 2.3b</i>	<i>Annona</i> sp.	Twig
180	<i>StspC2 1.2c</i>	<i>Strychnos</i> sp.	Stems
307	<i>EjC3 2.1a</i>	<i>Piper peltata</i>	Stems
391	<i>GhR1 2.1</i>	<i>Gustavia elliptica</i>	Root
392	<i>GhG2 2.1</i>	<i>G. elliptica</i>	Twig
395	<i>GhC2 2.2a</i>	<i>G. elliptica</i>	Stems
396	<i>GhR1 2.1a</i>	<i>G. elliptica</i>	Root
401	<i>GhcR3 2.2</i>	<i>G. elliptica</i>	Root bark
403	<i>GhcR3 2.2</i>	<i>G. elliptica</i>	Root bark
404	<i>GhG3 1.1</i>	<i>G. elliptica</i>	Twig
407	<i>GhG3 2.2c</i>	<i>G. elliptica</i>	Twig
408	<i>GhR2 1.2b</i>	<i>G. elliptica</i>	Root
409	<i>GhcC2 2.2a</i>	<i>G. elliptica</i>	Stems root
414	<i>GhcC1 1.2c</i>	<i>G. elliptica</i>	Stems root
415	<i>GhcR1 1.1a</i>	<i>G. elliptica</i>	Root bark
433	<i>GhcR1 1.1b</i>	<i>G. elliptica</i>	Root bark
457	<i>GhcG3 2.2</i>	<i>G. elliptica</i>	Twig bark

**Group 1 - *Penicillium adametzii***

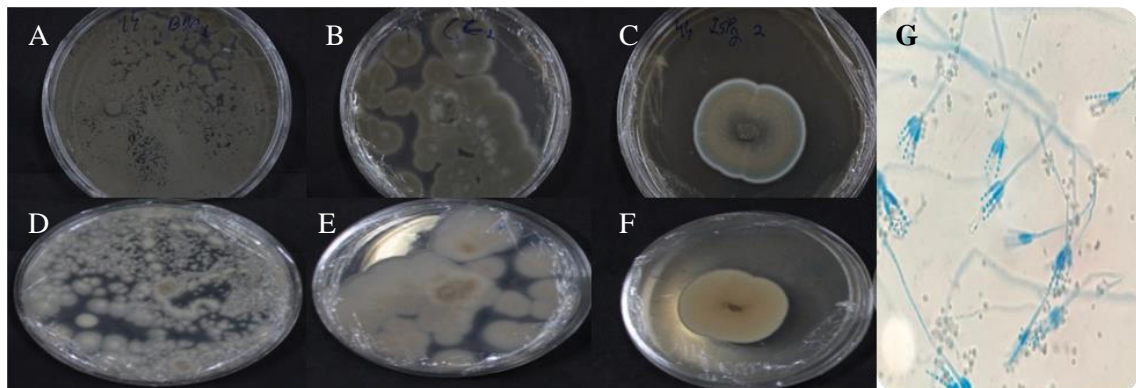


**Figure 1.** Morphology of the fungi *Penicillium adametzii*, strain 46. A = PDA front, B = CYA front, C = ISP2 front, D = PDA back, E = CYA back, F = ISP2 back, G = Micromorphology in PDA (100x).

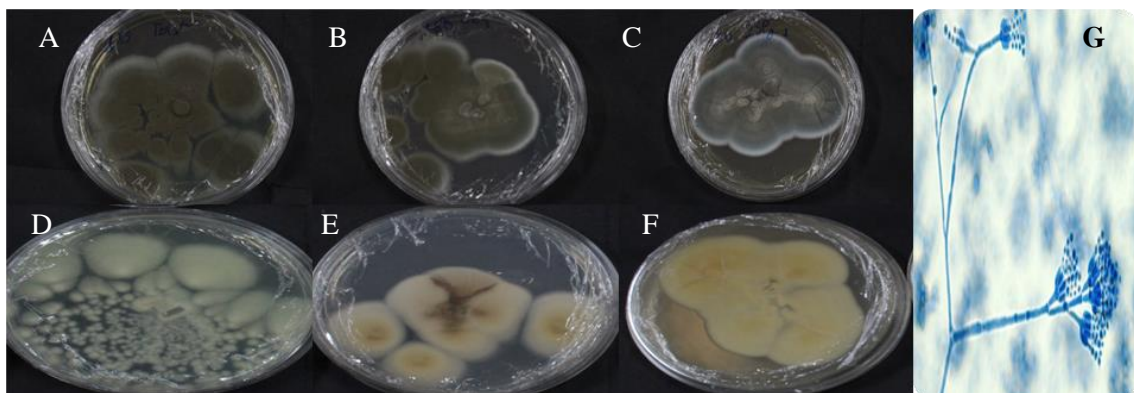


**Figure 2.** Morphology of the fungi *Penicillium adametzii*, strain 180. A = PDA front, B = CYA front, C = ISP2 front, D = PDA back, E = CYA back, F = ISP2 back, G= Micromorphology in PDA (400x).

The strains from the fungi *P. adametzii* (Figures 2 and 3) presented a dark green color in the PDA and CYA media, with a slightly brown color in the central part of the mycelium and with greenish and white edges. The texture of the colony varied from powdery in PDA to velvety in the ISP2 medium. The reverse side presents cream coloring in the PDA medium, a slightly orange tone with brown in the strain 180 in the CYA medium and an more present orange tone in the ISP2 medium. The CYA medium characteristics is in accord with the literature (Houbraken et al., 2020).

**Group 2 - *Penicillium citrinum***

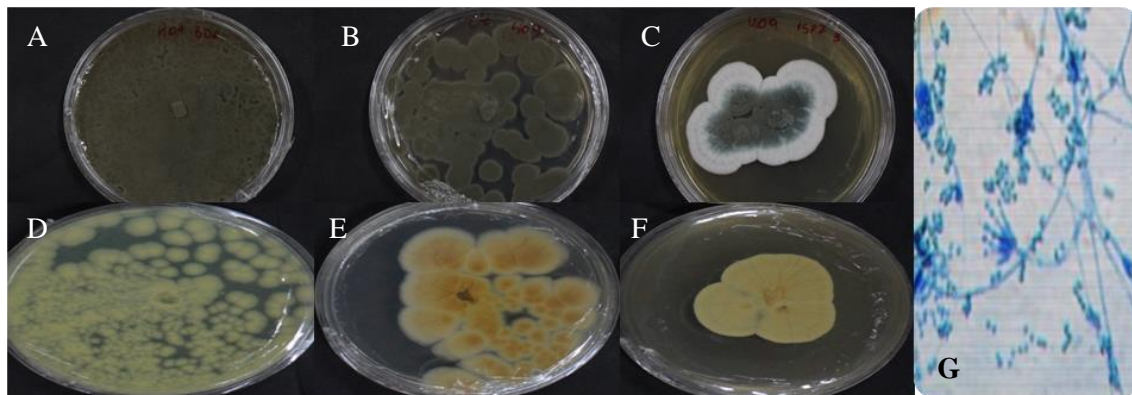


**Figure 3.** Morphology of the fungi *Penicillium citrinum*, strain 409. A = PDA front, B = CYA front, C = ISP2 front, D = PDA back, E = CYA back, F = ISP2 back, G = Micromorphology in PDA (200x).

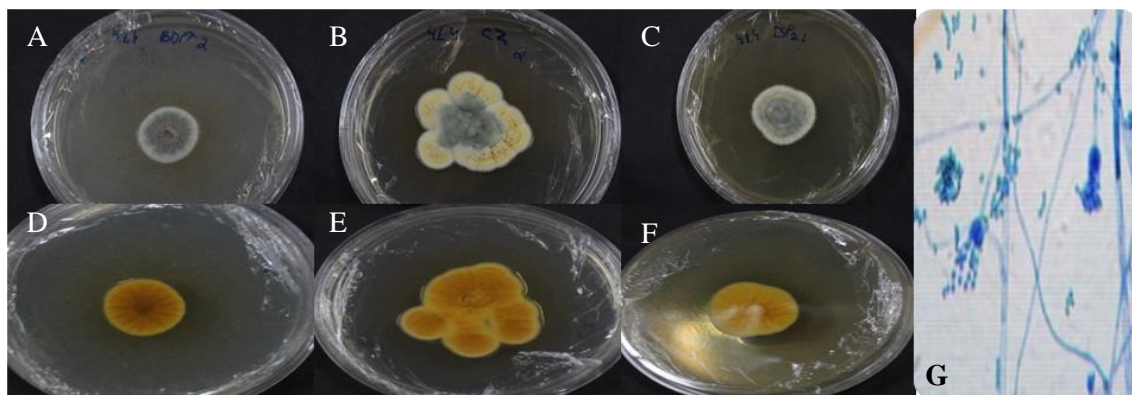


**Figure 4.** Morphology of the fungi *Penicillium citrinum*, strain 414. A = PDA front, B = CYA front, C = ISP2 front, D = PDA back, E = CYA back, F = ISP2 back, G = Micromorphology in PDA (200x).

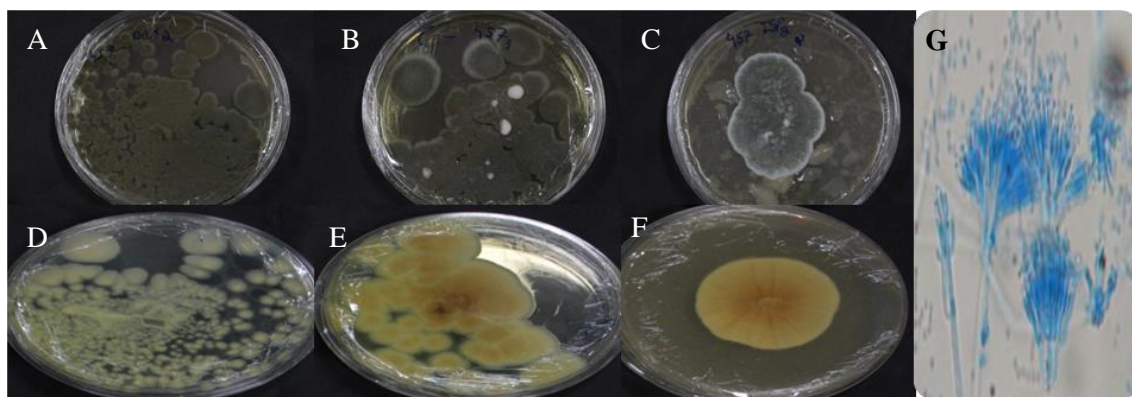


**Figure 5.** Morphology of the fungi *Penicillium citrinum*, strain 457. A = PDA front, B = CYA front, C = ISP2 front, D = PDA back, E = CYA back, F = ISP2 back, G= Micromorphology in PDA (1000x).

The strains *P. citrinum* (Figures 4-6) presented a green color in all media, with the exception of strain 414 in CYA media, that showed tones of orange in the edges, the colonies had rough textures in all media. The back has orange coloring in all media. It was possible to observe diffuse pigmentation present in orange coloring, around the mycelium. This variations of green to orange colors has already been described in the literature for this species (Houbraken et al., 2010).

### Group 3 - *Penicillium glabrum*

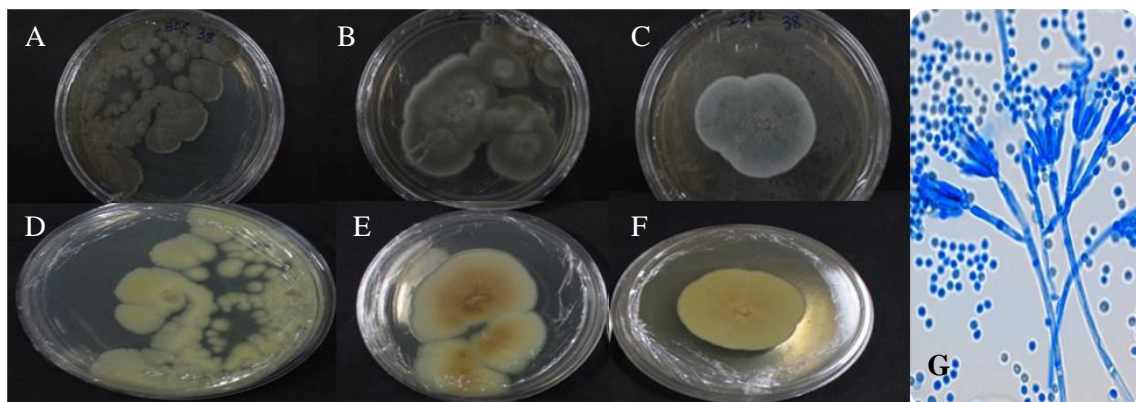


**Figure 6.** Morphology of the fungi *Penicillium glabrum*, strain 38. A = PDA front, B = CYA front, C = ISP2 front, D = PDA back, E = CYA back, F = ISP2 back, G = Micromorphology in PDA (400x).

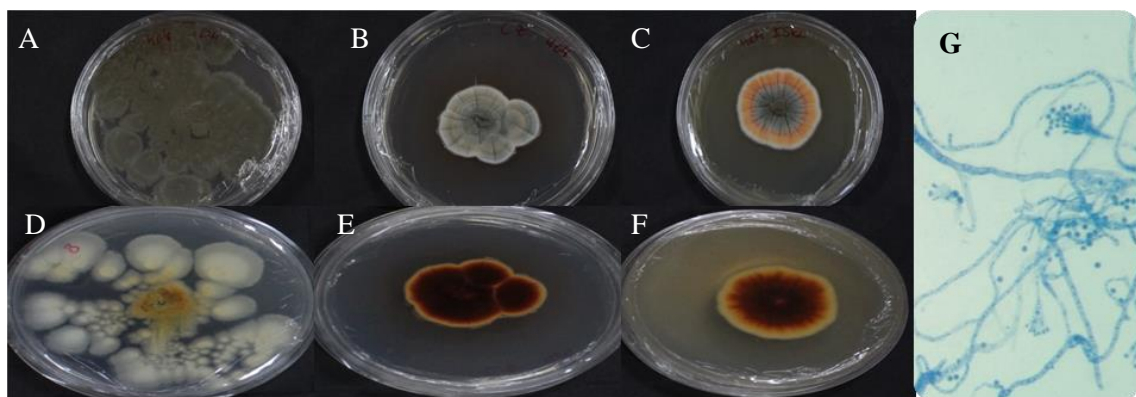


**Figure 7.** Morphology of the fungi *Penicillium glabrum*, strain 404. A = PDA front, B = CYA front, C = ISP2 front, D = PDA back, E = CYA back, F = ISP2 back, G= Micromorphology in PDA (100x).

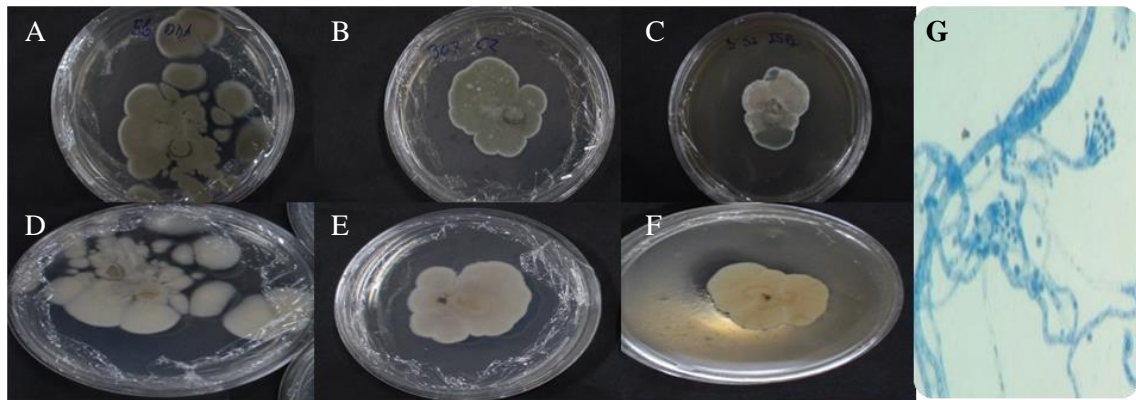


**Figure 8.** Morphology of the fungi *Penicillium glabrum*, strain 408. A = PDA front, B = CYA front, C = ISP2 front, D = PDA back, E = CYA back, F = ISP2 back, G = Micromorphology in PDA (100x).

The strains of *P. glabrum* (Figures 7-9) showed a greenish color in all cultivated media, with white borders more apparent in the ISP2 medium, which is common in the genus *Penicillium*. The texture of the colony varies from powdery to velvety in PDA and ISP2 respectively. The back of the colony is mostly cream colored in the PDA medium and cream in the CYA and ISP2 media. The strain 404 differed from the others, as it presented an orange tone in the ISP2 and CYA media, with a strong orange color in the back. Apart from this, the other characteristics had already been described for this species by Nevarez et al., (2009).

**Group 4 - *Penicillium oxalicum***

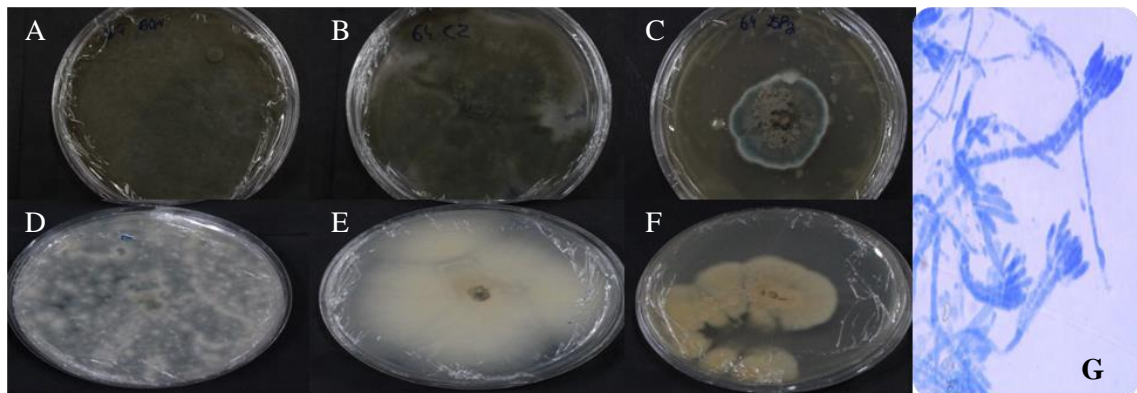


**Figure 9.** Morphology of the fungi *Penicillium oxalicum*, strain 64. A = PDA front, B = CYA front, C = ISP2 front, D = PDA back, E = CYA back, F = ISP2 back, G = Micromorphology in PDA (100x).

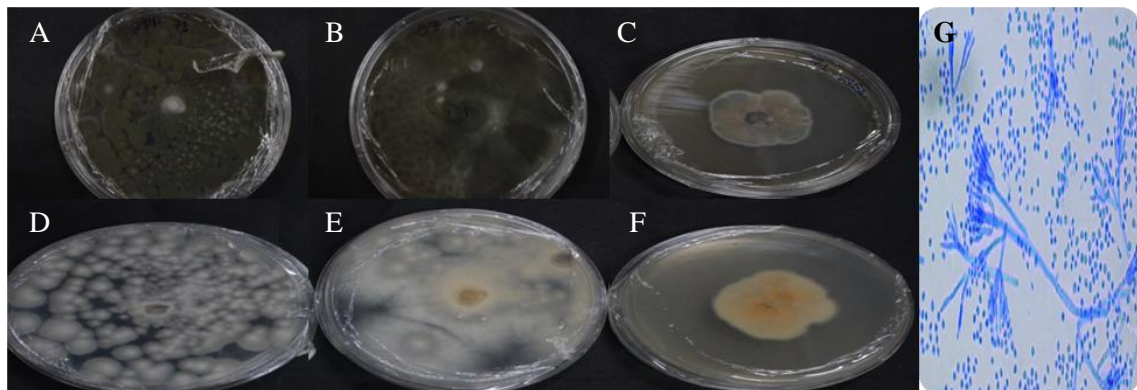


**Figure 10.** Morphology of the fungi *Penicillium oxalicum*, strain 71. A = PDA front, B = CYA front, C = ISP2 front, D = PDA back, E = CYA back, F = ISP2 back, G = Micromorphology in PDA (100x).

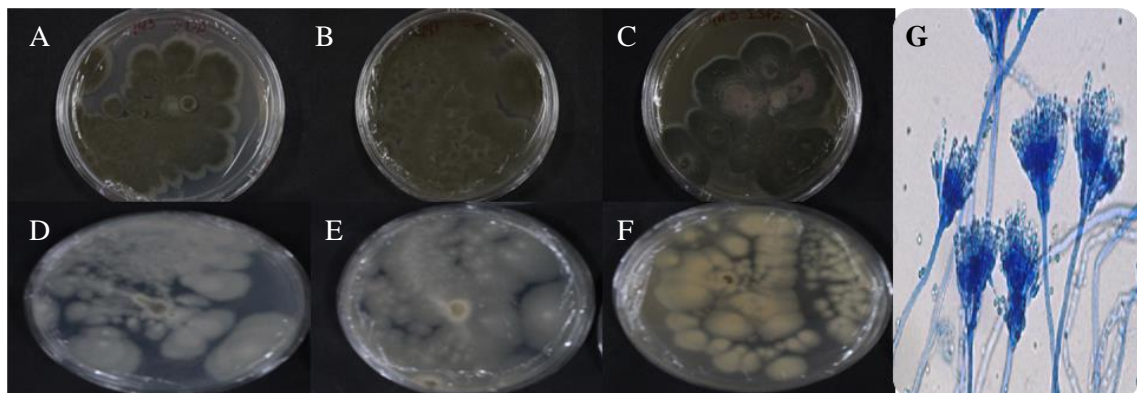


**Figure 11.** Morphology of the fungi *Penicillium oxalicum*, strain 143. A = PDA front, B = CYA front, C = ISP2 front, D = PDA back, E = CYA back, F = ISP2 back, G = Micromorphology in PDA (400x).

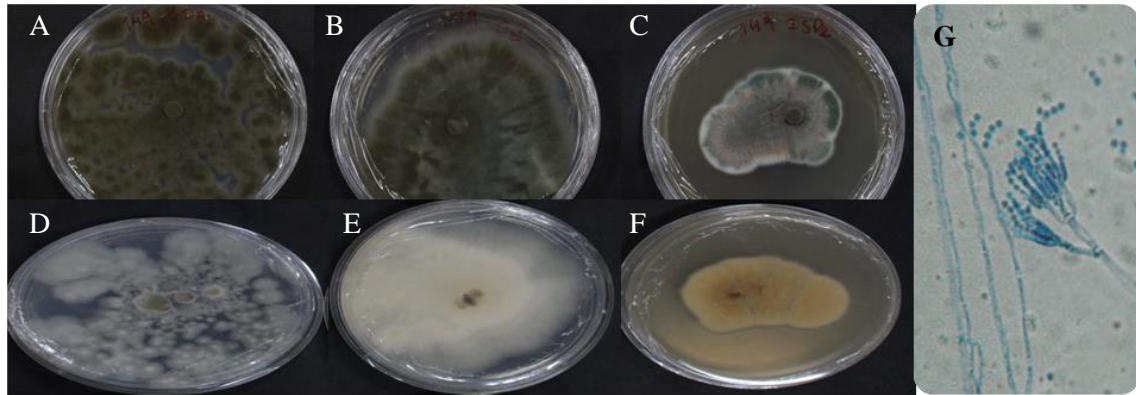


**Figure 12.** Morphology of the fungi *Penicillium oxalicum*, strain 149. A = PDA front, B = CYA front, C = ISP2 front, D = PDA back, E = CYA back, F = ISP2 back, G = Micromorphology in PDA (400x).

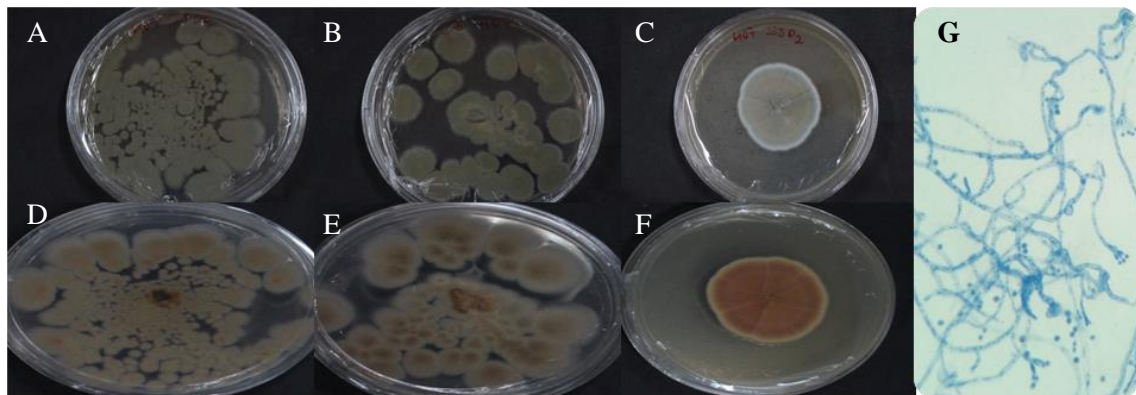


**Figure 13.** Morphology of the fungi *Penicillium oxalicum*, strain 407. A = PDA front, B = CYA front, C = ISP2 front, D = PDA back, E = CYA back, F = ISP2 back, G = Micromorphology in PDA (100x).

The strains of *P. oxalicum* (Figures 10-14) showed a dark green color in the PDA and CYA media, growing very quickly. In ISP2, on the other hand, it presented a green color with characteristic white edges, showing some parts with a slight brown tone. The texture of the colonies was powdery in PDA, cottony in CYA and velvety in ISP2. The back was white and cream in PDA and CYA, and brown in ISP2. Wasn't possible to identify apparent diffuse pigments. Strain 407 showed the brown color in all medias on

the verse. The morphology described is in accord to the literature for this specie (Zhao et al., 2010).

#### **Group 5 - *Penicillium paxilli***

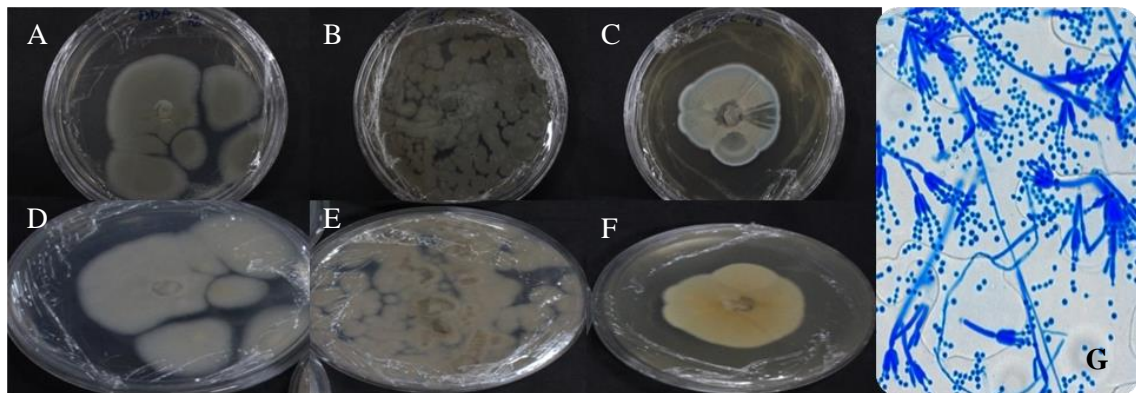


**Figure 14.** Morphology of the fungi *Penicillium paxilli*, strain 48. A = PDA front, B = CYA front, C = ISP2 front, D = PDA back, E = CYA back, F = ISP2 back, G = Micromorphology in PDA (200x).

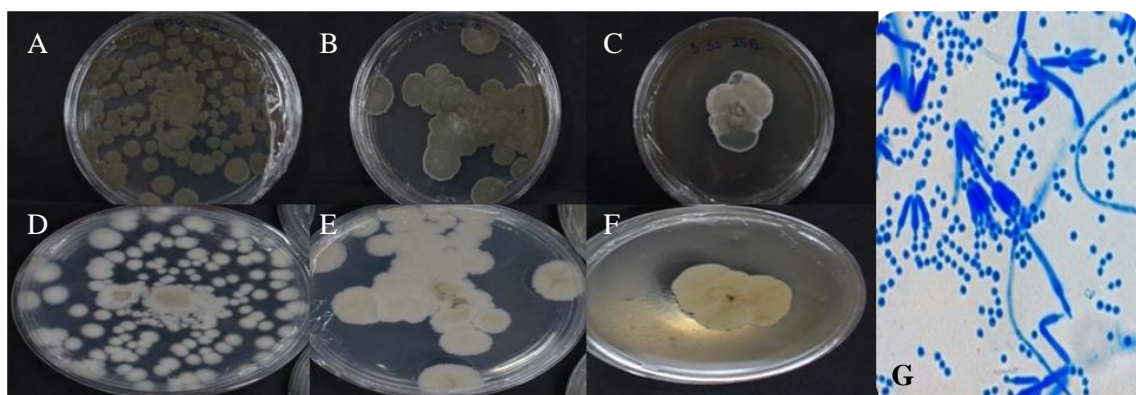


**Figure 15.** Morphology of the fungi *Penicillium paxilli*, strain 52. A = PDA front, B = CYA front, C = ISP2 front, D = PDA back, E = CYA back, F = ISP2 back, G = Micromorphology in PDA (200x).

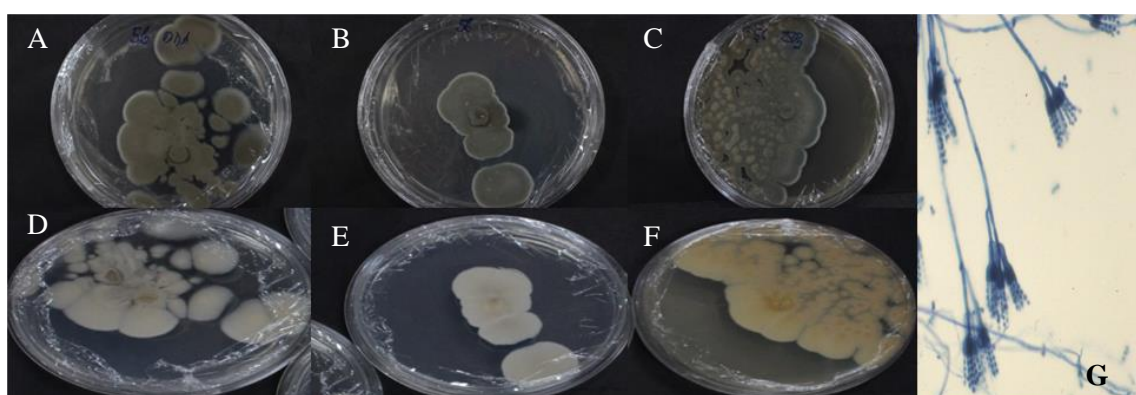


**Figure 16.** Morphology of the fungi *Penicillium paxilli*, strain 56. A = PDA front, B = CYA front, C = ISP2 front, D = PDA back, E = CYA back, F = ISP2 back, G = Micromorphology in PDA (400x).

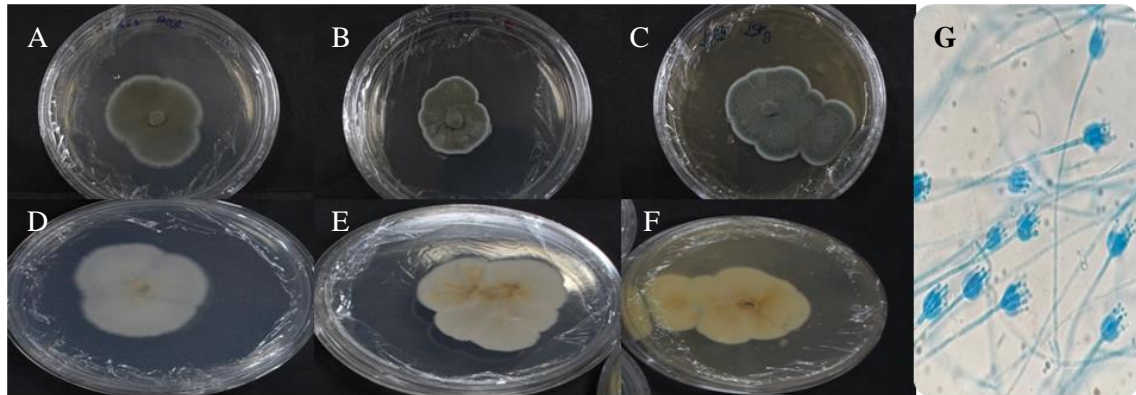


**Figure 17.** Morphology of the fungi *Penicillium paxilli*, strain 153. A = PDA front, B = CYA front, C = ISP2 front, D = PDA back, E = CYA back, F = ISP2 back, G = Micromorphology in PDA (200x).

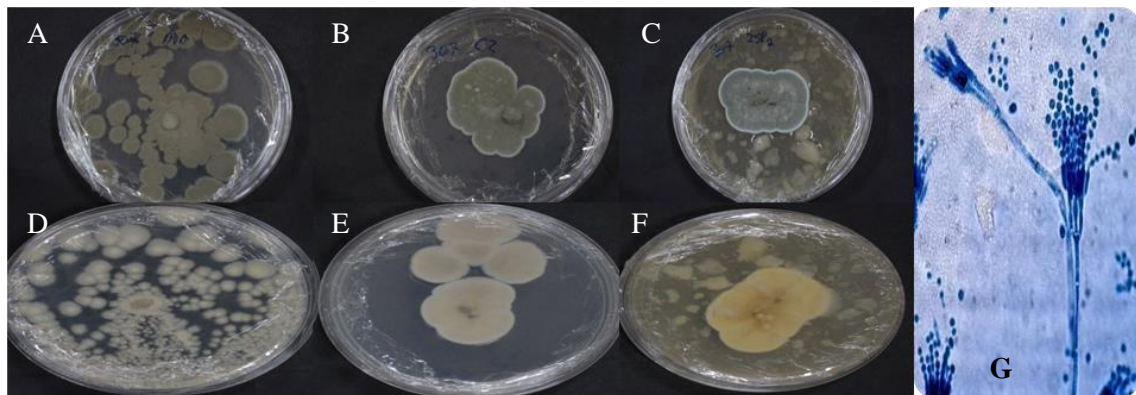


**Figure 18.** Morphology of the fungi *Penicillium paxilli*, strain 307. A = PDA front, B = CYA front, C = ISP2 front, D = PDA back, E = CYA back, F = ISP2 back, G = Micromorphology in PDA (400x).

The strains of *P. paxilli* (Figures 15-19) showed green color with a slight brown tone in the PDA and CYA media. In the ISP2 medium, something peculiar was observed, the mycelium presented it self in a segmented way, in light green and dark green with white edges. This suggests that the ISP2 medium, for this strain, can induce both types of reproduction due to the nutritional components of the medium as suggested by Visagie

et. al (2014). The texture of the colonies was velvety for all. The coloring of the back was white to cream in PDA and CYA media and orange in the ISP2 media. Wasn't possible to identify apparent diffuse pigments.

#### **Group 6 - *Penicillium rubens***

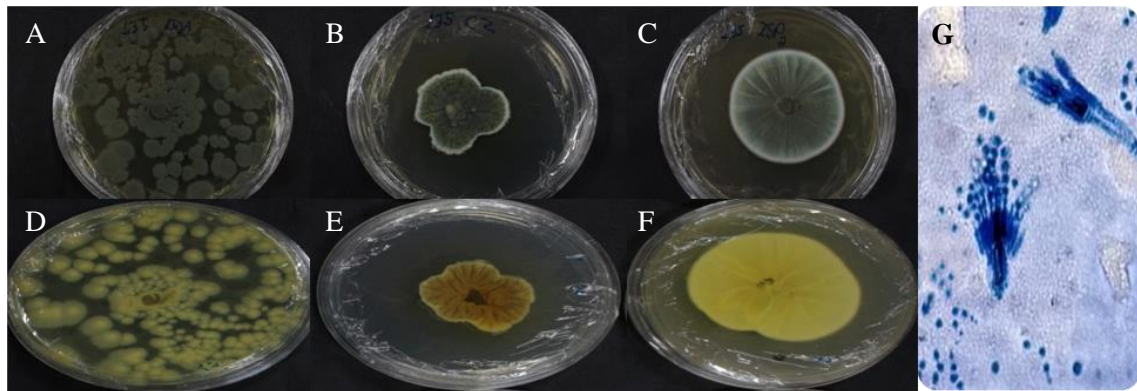


**Figure 19.** Morphology of the fungi *Penicillium rubens*, strain 135. A = PDA front, B = CYA front, C = ISP2 front, D = PDA back, E = CYA back, F = ISP2 back, G = Micromorphology in PDA (400x).

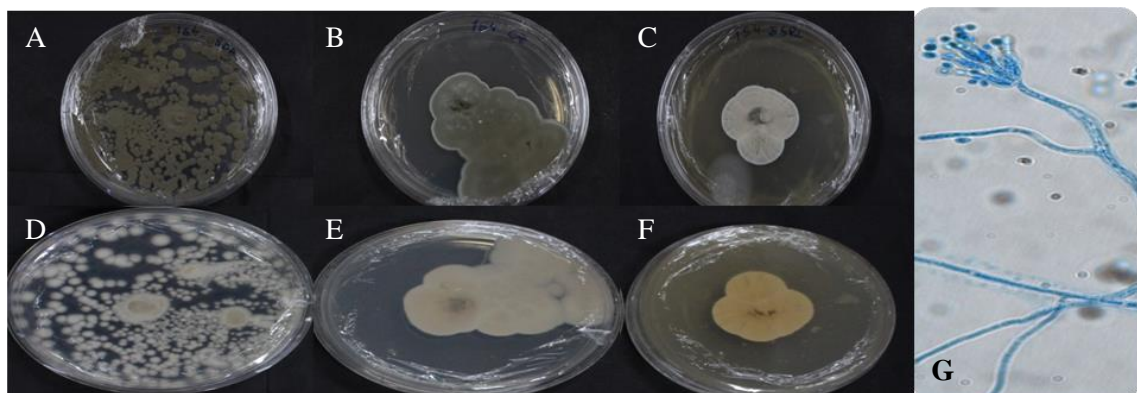


**Figure 20.** Morphology of the fungi *Penicillium rubens*, strain 154. A = PDA front, B = CYA front, C = ISP2 front, D = PDA back, E = CYA back, F = ISP2 back, G = Micromorphology in PDA (400x).

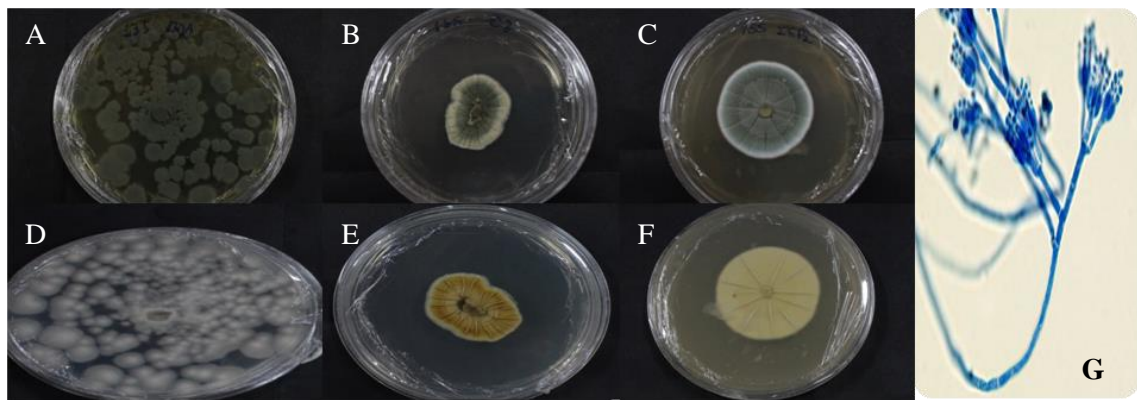


**Figure 21.** Morphology of the fungi *Penicillium rubens*, strain 155. A = PDA front, B = CYA front, C = ISP2 front, D = PDA back, E = CYA back, F = ISP2 back, G = Micromorphology in PDA (400x).

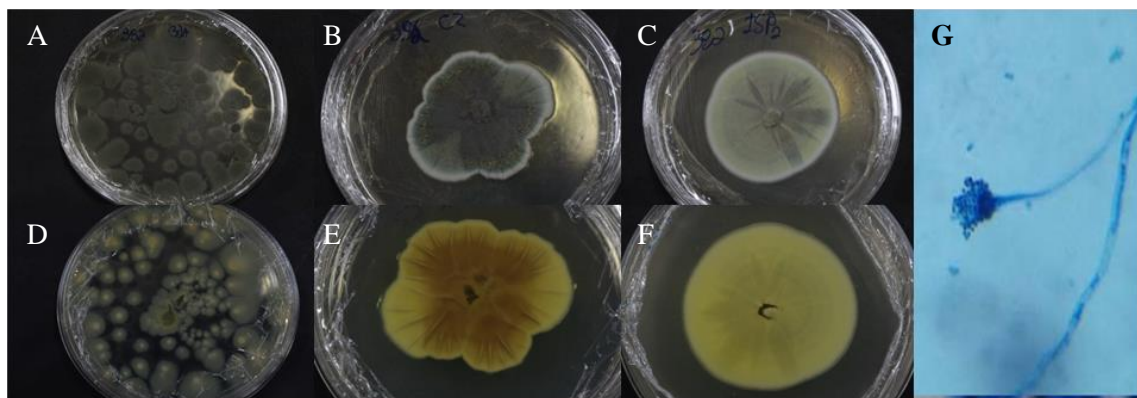


**Figure 22.** Morphology of the fungi *Penicillium rubens*, strain 392. A = PDA front, B = CYA front, C = ISP2 front, D = PDA back, E = CYA back, F = ISP2 back, G = Micromorphology in PDA (200x).

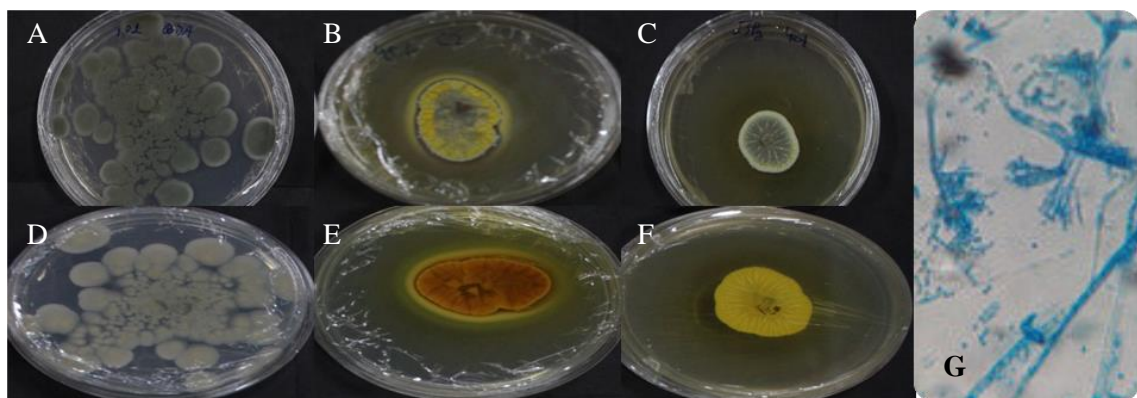


**Figure 23.** Morphology of the fungi *Penicillium rubens*, strain 401. A = PDA front, B = CYA front, C = ISP2 front, D = PDA back, E = CYA back, F = ISP2 back, G = Micromorphology in PDA (100x).

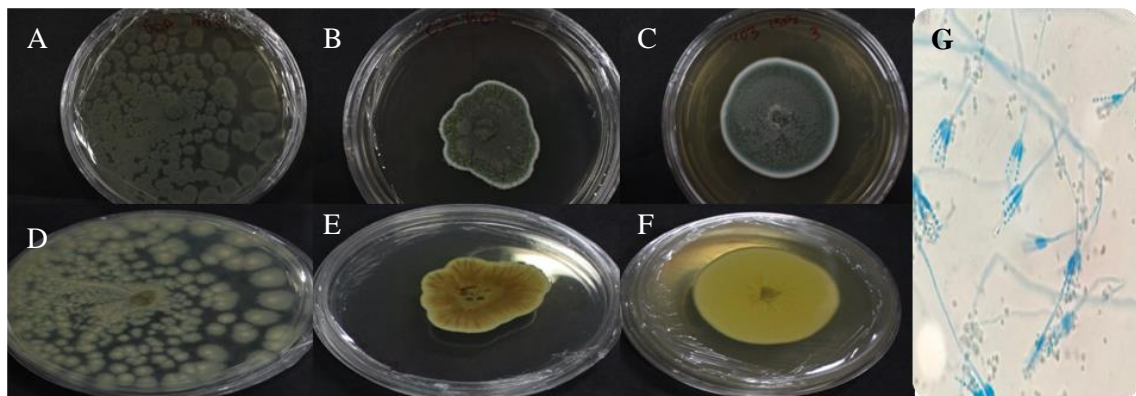


**Figure 24.** Morphology of the fungi *Penicillium rubens*, strain 403. A = PDA front, B = CYA front, C = ISP2 front, D = PDA back, E = CYA back, F = ISP2 back, G = Micromorphology in PDA (100x).

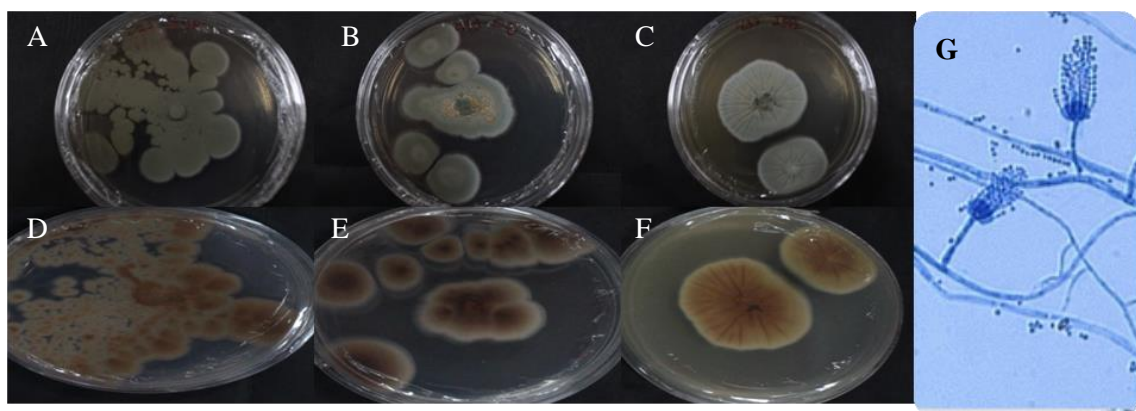


**Figure 25.** Morphology of the fungi *Penicillium rubens*, strain 433. A = PDA front, B = CYA front, C = ISP2 front, D = PDA back, E = CYA back, F = ISP2 back, G = Micromorphology in PDA (400x).

Strains of *P. rubens* (Figures 20-26) showed a greenish color with white borders characteristic of *Penicillium*. The texture of the colonies was velvety in PDA and ISP2, and was rough in the CYA medium for all strains. The back had a yellowish and orange color for the PDA and ISP2 media, and a brown color for CYA. It was possible to observe diffuse yellow pigment in all media for all strains. Strain 433 was the one different from the others, as it has a more dark brownish color on the verse. This species was previously known as a type of *P. chrysogenum* capable of producing penicillin, but Houbraeken et al., (2020) merged both groups (*P. chrysogenum* and *P. rubens*) under the name of *P. rubens*.

This species is commonly isolated as endophytes but can also be found in soil and food.

It is also common in temperate and subtropical regions.

**Group 7 - *Talaromyces versatilis***

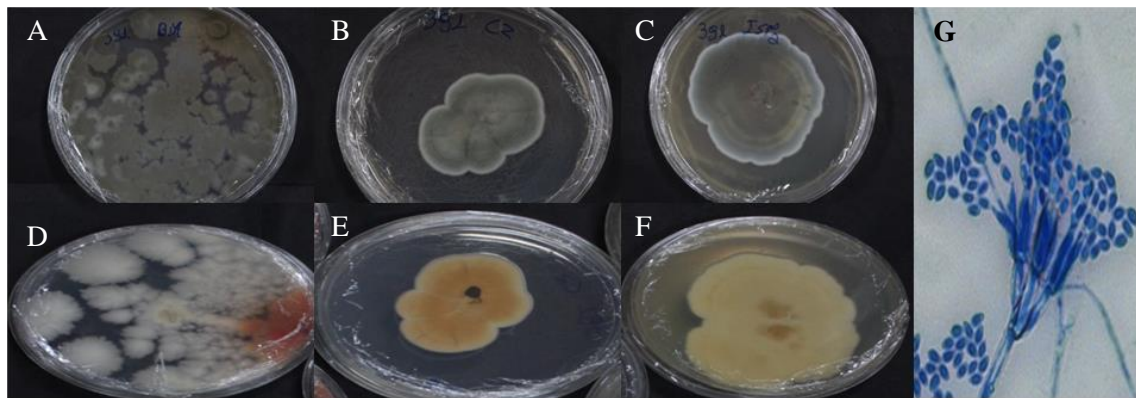


**Figure 26.** Morphology of the fungi *Talaromyces versatilis*, strain 391. A = PDA front, B = CYA front, C = ISP2 front, D = PDA back, E = CYA back, F = ISP2 back, G = Micromorphology in PDA (1000x).

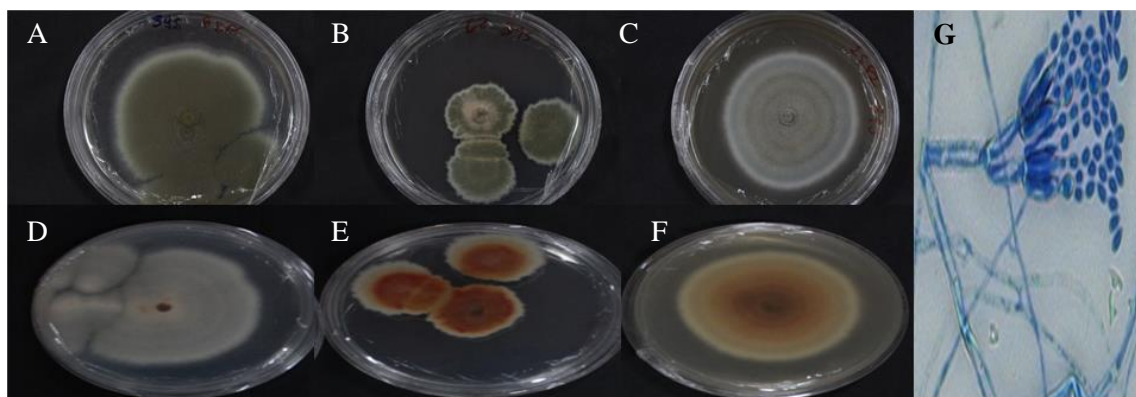


**Figure 27.** Morphology of the fungi *Talaromyces versatilis*, strain 395. A = PDA front, B = CYA front, C = ISP2 front, D = PDA back, E = CYA back, F = ISP2 back, G = Micromorphology in PDA (1000x).

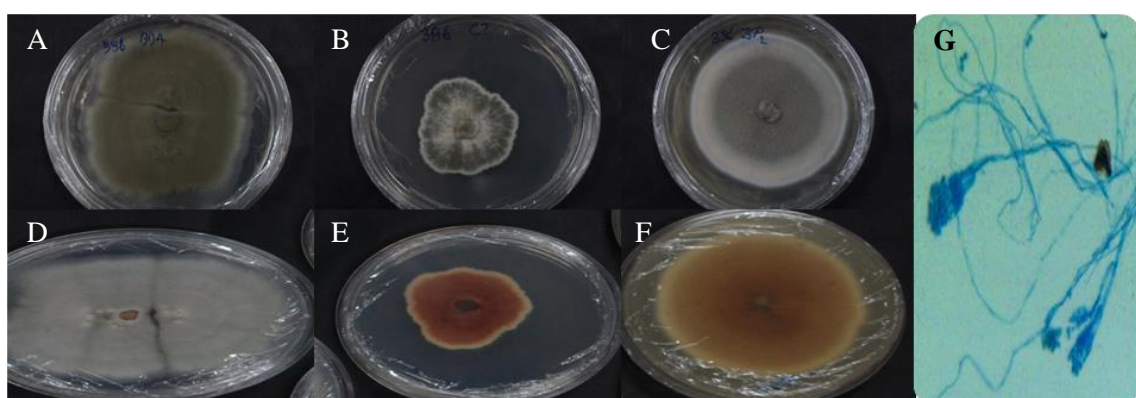


**Figure 28.** Morphology of the fungi *Talaromyces versatilis*, strain 396. A = PDA front, B = CYA front, C = ISP2 front, D = PDA back, E = CYA back, F = ISP2 back, G= Micromorphology in PDA (200x).

The strains 391, 395 and 396 (Figures 27-29) were identified as *Talaromyces versatilis* by molecular analysis. This genus is known to be the sexual morph of the genus *Penicillium* and they are close macromorphologically (Houbraken et al., 2020). The strains presented green color with white edges in the PDA medium and in a lighter shade in the ISP2 medium. In the CYA media, it presented green color with some points in a light pink shade. The colonies from the strain 391 showed velvety textures in the PDA and ISP2 media, being slightly rough in the CYA media. Strains 395 and 396 showed cottony texture in all media. The back had a crem color in the PDA medium and a strong orange in the Czapek medium, an orange that is repeated but more mildly in the ISP2 medium. It was possible to observe red diffuse pigment present in strains 395 and 396, this was already described in other species of the genus in the literature (Frisvad et al., 2013).

#### Group 8 - *Penicillium sumatraense*

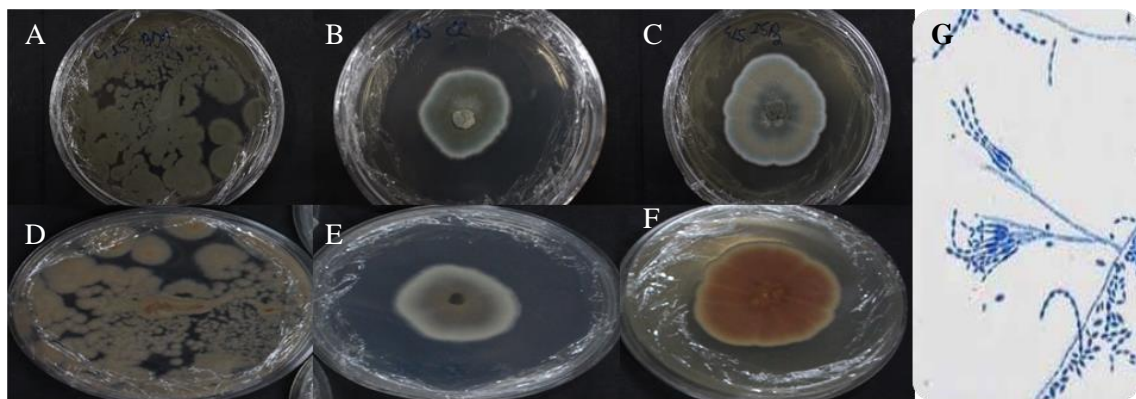


**Figure 29.** Morphology of the fungi *Penicillium sumatraense*, strain 415. A = PDA front, B = CYA front, C = ISP2 front, D = PDA back, E = CYA back, F = ISP2 back, G = Micromorphology in PDA (400x).

The strain 415 was the only one identified as *P. sumatraense* and it showed a green color in all media, while having more brownish shade on the ISP2 media. The texture of the colony was velvety in all media. The back of the colony presented a strong brown color in ISP2, while having a more mild brownish tone in PDA, and it presented a bronish with cream color in the CYA medium, same as described by Visagie et al., (2014).

Overall, for all the groups, it was possible to notice that the PDA and CYA media are really close in terms of inducing colors macromorphologically in *Penicillium*. Despite being close, it was observed that the CYA media had a richest display of the color spectrum, possibly by the minerals present in the media as supported by Visagie et al., (2014), this can prove to be very useful to help identify morphologically close species. On the other hand, the ISP2 media proved to have a different influence compared to the others, displaying totally different mycelium color sets, and several segmented mycelium probably inducing the sexual reproduction of some the species of *Penicillium*, this is likely to be happening as described by Dyer and Gorman (2011) and needs to be studied further.

### **Molecular analysis**

The rate of identification of the decoded nucleotide sequences of the strains in relation to the more similar ones deposited in the NCBI genomic bank, allowed the confirmation of those belonging to the genus *Penicillium* and indicate some belonging to the genus *Talaromyces* as discussed futher (Table 2).

**Table 2.** Molecular identification based on the *ITS* region of endophytic *Penicillium* strains by BLASTN from NCBI.

Strain	Specie	Max score	Total score	Query cover	E value	Percent identity	Accession
<b>46</b>	<i>P. adametzii</i>	1016	1016	99%	0	98.95%	KF313079.1
<b>180</b>	<i>P. adametzii</i>	881	881	100%	0	98.99%	JN714932.1
<b>409</b>	<i>P. citrinum</i>	1040	1156	100%	0	98.26%	MT597828.1
<b>414</b>	<i>P. citrinum</i>	881	881	98%	0	99.59%	MN634465.1
<b>457</b>	<i>P. citrinum</i>	1026	1026	100%	0	100%	MN879404.1
<b>38</b>	<i>P. glabrum</i>	1051	1198	100%	0	99.31%	JN180489.1
<b>404</b>	<i>P. glabrum</i>	1026	1026	96%	0	99.83%	MK387974.1
<b>408</b>	<i>P. glabrum</i>	1044	1044	99%	0	99.65%	JN180489.1
<b>64</b>	<i>P. oxalicum</i>	761	761	100%	0	98.61	MH367526.1
<b>71</b>	<i>P. oxalicum</i>	952	952	98%	0	99.81%	MN121543.1
<b>143</b>	<i>P. oxalicum</i>	979	979	100%	0	100%	MT588795.1
<b>149</b>	<i>P. oxalicum</i>	911	911	99%	0	99.80%	MH367526.1
<b>407</b>	<i>P. oxalicum</i>	948	948	100%	0	98.88%	MF186029.1
<b>48</b>	<i>P. paxilli</i>	898	898	100%	0	99.01%	MK120566.1
<b>52</b>	<i>P. paxilli</i>	990	1165	99%	0	100%	JN617709.1
<b>56</b>	<i>P. paxilli</i>	817	817	99%	0	98.49%	FJ884122.1
<b>153</b>	<i>P. paxilli</i>	979	979	100%	0	100%	MH856391.1
<b>307</b>	<i>P. paxilli</i>	924	924	98%	0	99.22%	JN851050.1
<b>135</b>	<i>P. rubens</i>	977	1082	100%	0	100%	LC325162.1
<b>154</b>	<i>P. rubens</i>	1005	1280	96%	0	98.11%	MH745129.1

<b>155</b>	<i>P. rubens</i>	846	846	100%	0	96.86%	MK140686.1
<b>392</b>	<i>P. rubens</i>	1042	1042	99%	0	100%	MT558923.1
<b>401</b>	<i>P. rubens</i>	970	970	100%	0	100%	MN604092.1
<b>403</b>	<i>P. rubens</i>	1195	1517	100%	0	98.12%	KU216703.1
<b>433</b>	<i>P. rubens</i>	1214	1576	100%	0	98.28	KU216703.1
<b>415</b>	<i>P. sumatraense</i>	1000	1000	100%	0	100%	MH171490.1
<b>391</b>	<i>T. versatilis</i>	1053	1169	99%	0	99.83%	MN431395.1
<b>395</b>	<i>T. versatilis</i>	1048	1048	100%	0	99.65	MN431395.1
<b>396</b>	<i>T. versatilis</i>	970	970	99%	0	99.62%	MK837960.1

The identification by molecular biology using the ITS-1 and ITS-2 regions of the rDNA, revealed the presence of seven distinct species of the genus *Penicillium*, with greater frequency of *P. rubens* with seven strains, *P. oxalicum* with five strains and *P. paxilli* with five strains. The majority of the sequences showed identity percentual above 98% when compared with the sequence deposited in the Genbank. The only exception was the strain 155, identified as *P. rubens*, with 96%. Also three strains were identified as *T. versatilis*.

The data set of the sequences from the *ITS-1* and *ITS-2* regions after being analyzed by the statistical method of Maximum Parsimony (MP), generated a consensus tree that explains the phylogenetic relationships between the strains studied (Figure 30), an *Aspergillus niger* was used as outgroup (OG).

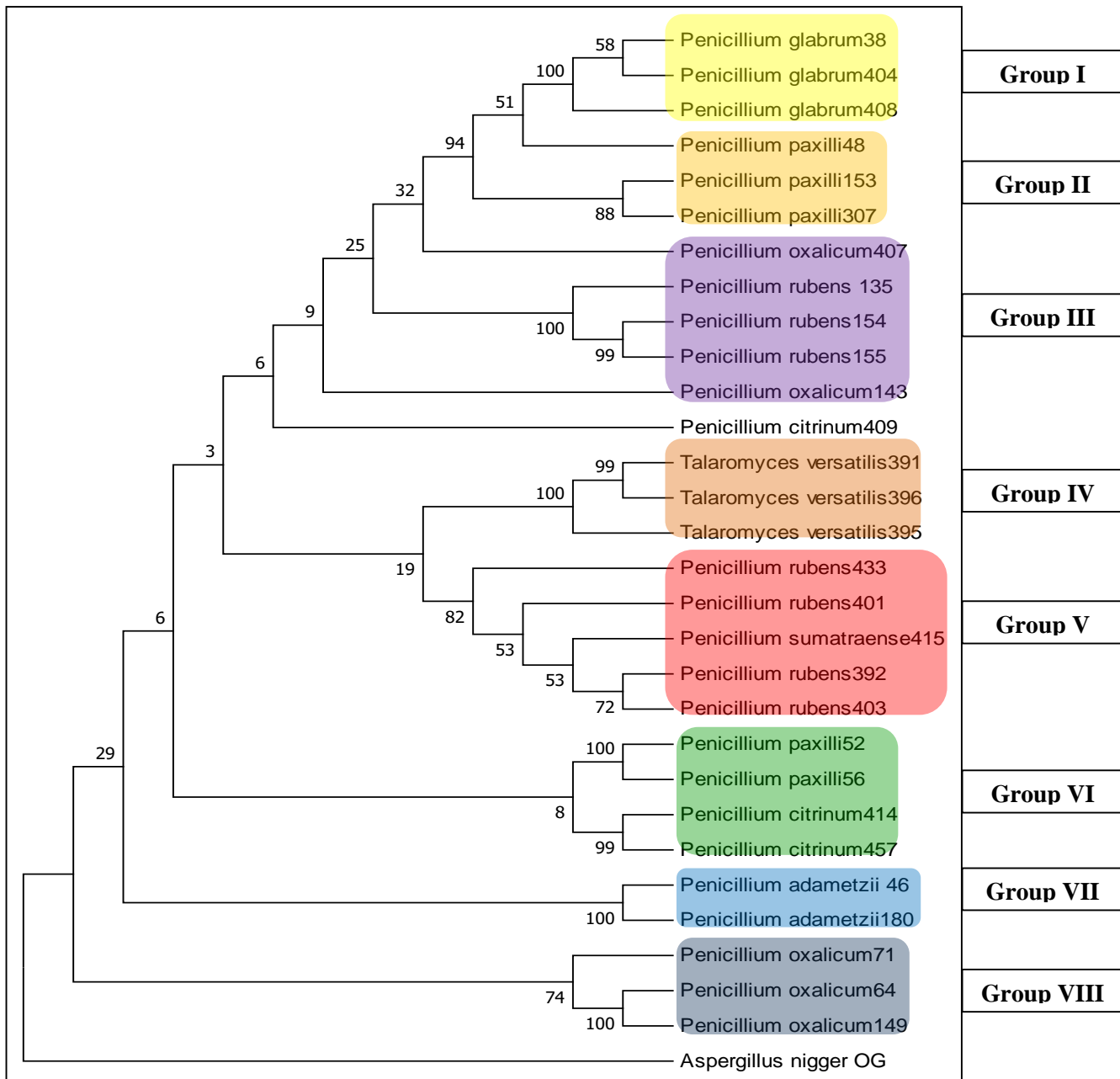


**Figure 30.** Molecular Phylogenetic Analysis by Maximum Parsimony (MP) method of the *Penicillium* Endophytic Amazonian strains from plants medicinal.

The most parsimonious tree had a length equal to 5543. The consistency index, retention index and composite index was 0.27, 0.45 and 0.12 respectively for all sites and parsimony-informative sites. The percentage of replicate trees in which the associated taxa clustered together in the bootstrap test (1000 replicates) are shown next to the branches. The results illustrated in the phylogenetic tree from the analysis by MP indicated the existence of five distinct clades.

In general, it was possible to group most strains of the same species, showing the efficiency of the analysis to separate the 7 different species of *Penicillium* as well as the 3 species of *Talaromyces* into 8 distinct groups. The significant genetic differences of the species registered in the phylogenetic tree, allow us to infer that the information from the ITS-1 and ITS-2 regions, using appropriate statistical tools, can efficiently separate the species of the genus *Penicillium*.

Strains from *P. rubens*, seems to be grouping according to the host, as all strains from group IV and V were found in *Annona* sp. and *G. elliptica* respectively. This may suggest that the host had an effect on the DNA of this strains. This is already reported as possible in the literature for fungi and can happen both ways, with the fungi influencing the host as well (Borah *et al.* 2018; Varga and Soulsbury, 2019) The opposite happens to the *P. paxilli* in groups II and VI, which had the same host but didn't grouped together.

The molecular taxonomy of *Penicillium* may become more robust and reliable using more than one region of the genome for the search in the database. The use of the *ITS* region despite being the most used and reliable, it is not the only one used for this purpose (Houbraken *et al.* 2016). Currently, *β-tubulin*, *Calmodulin* and *RNA Polymerase II second largest subunit (RPB2)* genes, have been useful for more accurate confirmation of molecular identification, and to evaluate the genetic diversity of fungi of the genus. (Glass & Donaldson, 1995; Liu *et al.*, 1999; Hong *et al.*, 2006; Visagie *et al.*, 2014). This is because the use of other regions conserved DNA increases the points of similarities between samples of the same and different species and, therefore, improve the results of the analysis.

Also, it is necessary to understand that genetic knowledge available in a database, such as Genbank, is formed through the sequences that are deposited over time (Benson *et al.*, 2016). Thus, the construction of the genetic profile knowledge of a diverse group such as *Penicillium*, goes through a process of improvement, expressed by the increase in the number of deposited

sequences, which it may even lead to the perception of data deposited with inaccuracies. We believe to be contributing, among other things, to the improvement of the knowledge of species of this genus, by depositing new sequences.

### Chemotaxonomic analysis

When analysing the MS data obtained for all three media, it was possible to observe that these samples are complex matrixes. The direct infusion ESI positive mass spectra of the *Penicillium* strains crude extracts from  $m/z$  150 to 1000 (850 variables) displayed several base peak ions with even mass, suggesting the presence of alkaloids in a large portion of the samples. Besides base peak, several other ions were observed, which can help grouping this strains in the HCA analysis. The analysis was carried out without pre treatments and running Principal Component Analysis (PCA) before HCA, using 10 principal components for each media (Figures 31-33).

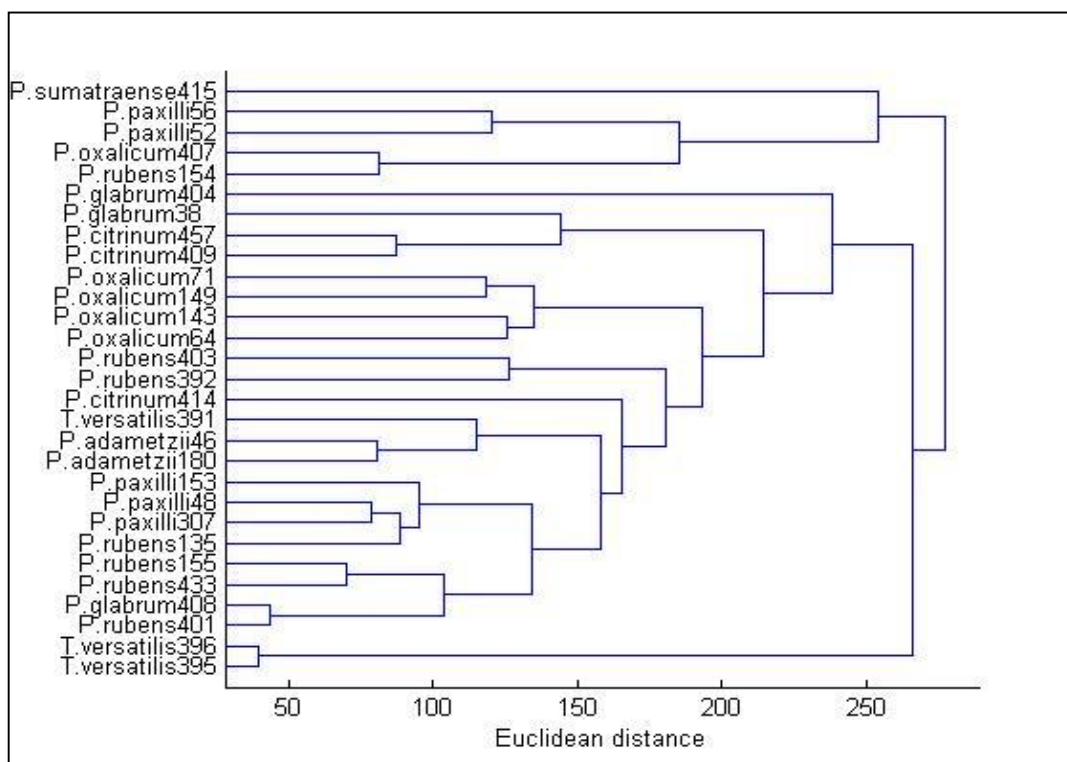


**Figure 31.** Dendrogram obtained with the HCA analysis of the profile of metabolites produced by *Penicillium* strains in CYA medium.

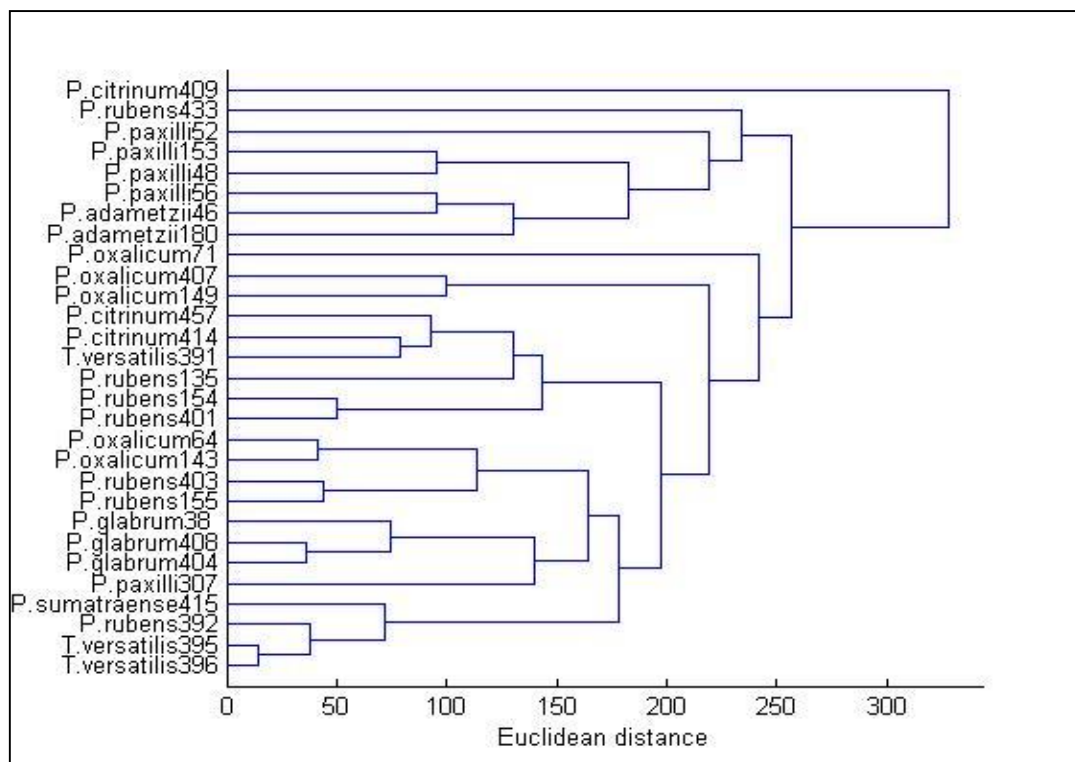


**Figure 32.** Dendrogram obtained with the HCA analysis of the profile of metabolites produced by *Penicillium* strains in ISP2 medium.

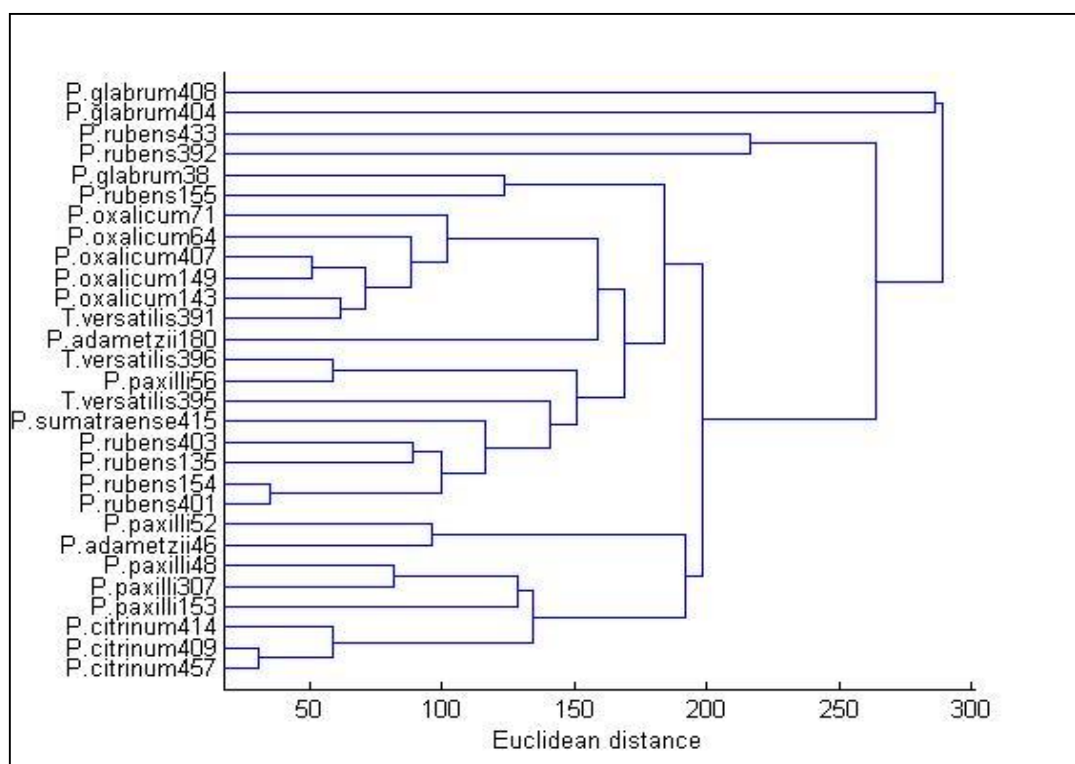


**Figure 33.** Dendrogram obtained with the HCA analysis of the profile of metabolites produced by *Penicillium* strains in PDA medium.

Different from the molecular analysis, the chemotaxonomic analysis seems to group the strains based on species a lot more, even from different hosts as supported by Frisvad et al. (1990). This can happen as some species produce key metabolites that helps distinguish them. For example, *P. rubens* tend to produce metabolites from the roquefortine pathway, *P. paxilli* produces paxilline and derivatives and *P. oxalicum* produces oxaline (Silva-Filho et al., 2021). It was very clear that this metabolites can and should vary according to the media, but overall it was also possible to group most strains of the same species, independent of the media utilized, showing the efficiency of the technique when using standardized procedures.

Together with the molecular identification, the chemical profile of metabolites secondary is a trustable tool for identification of *Penicillium* because it uses a large number of variables (Frisvad and Samson 2004; Ramos-Pereira et al., 2019). Despite the need to improve the approach to the study of the chemical profiles of species of *Penicillium*, whose cultivation variables are difficult to standardize, it is clear the viability of the technique for taxonomy. In addition to the cultivation, the different parameters of ionization and analysis must be optimized for the obtaining reproducible spectra that lead to the greatest number of ions detected.

## Conclusion

This analysis showed that not only the host but the medium can influence directly in the fungi. However, as shown in this work, this influence may vary depending on the species of the genus. Also, it was possible to observe the integration of morphological, molecular and chemical analysis as a effective method to identify species of the genus *Penicillium*.

### **Acknowledgements**

The authors are grateful to Central Analítica (UFAM) for all analysis, and Coordenação de Aperfeiçoamento de Pessoal de Nível Superior (CAPES) Conselho Nacional de Desenvolvimento Científico e Tecnológico (CNPQ), Financiadora de Estudos e Projetos (FINEP) and, Fundação de Amparo à Pesquisa do Estado do Amazonas (FAPEAM) for financial support.

## References

- Benson DA, Cavanaugh M, Clark K, Karsch-Mizrachi I, Lipman DJ, Ostell J, Sayers EW (2016) GenBank. *Nucleic Acid Research*. 45:37-42.
- Bon EPS, Ferrara MA, Corvo ML (2008) Enzimas em Biotecnologia Produção, aplicações e Mercado. Rio de Janeiro, Editora Interciência. ch. 5.
- Borah N, Albarouki E, Schirawski J (2018) Comparative Methods for Molecular Determination of Host-Specificity Factors in Plant-Pathogenic Fungi. *Int J Mol Sci*. 19:863.
- Christensen M, Frisvad JC, Tuthill DE (2000) *Penicillium* species diversity in soil and some taxonomic and ecological notes. In: Samson RA, Pitt JI (Ed.). Integration of Modern Taxonomic Methods for *Penicillium* and *Aspergillus* Classification. London: Harwood Academic Publishers. p. 309-321.
- Dyer PS, Gorman CMO (2011) A fungal sexual revolution: *Aspergillus* and *Penicillium* show the way. *Current Opinion in Microbiology*. 14:649-654.
- Frisvad JC, Filtenborg O (1990) Secondary Metabolites as Consistent Criteria in *Penicillium* Taxonomy and a Synoptic Key to *Penicillium* Subgenus *Penicillium*. In: Samson RA, Pitt JI (eds) Modern Concepts in *Penicillium* and *Aspergillus* Classification. NATO ASI Series (Series A: Life Sciences), vol 185. Springer, Boston, MA.
- Frisvad JC, Samson RA (2004) Polyphasic taxonomy of *Penicillium* subgenus *Penicillium*: A guide to identification of food and air-borne terverticillate Penicillia and their mycotoxins. *Studies in Micology*. 49:1-174.
- Frisvad, JC, Andersen B, Thrane U (2008) The use of secondary metabolite profiling in fungal taxonomy. *Mycological Research*. 112:231–240.
- Frisvad JC, Yilmaz N, Thrane U, Rasmussen KB, Houbraken J, et al. (2013) *Talaromyces atroroseus*, a New Species Efficiently Producing Industrially Relevant Red Pigments. *PLoS ONE*. 8: e84102.
- Glass NL, Donaldson GC (1995) development of premier sets designed for use with de PCR to amplify conserved genes from filamentous *Ascomycetes*. *Applied and Environmental Microbiology*. 61:1323-1330.

Hawksworth DL, Lücking R (2017) Fungal diversity revisited: 2.2 to 3.8 million species. *Microbiology Spectrum*. 5:1-17.

Hong SB, Cho HS, Shin HD et al., (2006) Novel *Neosartorya* species isolated from the soil in Korea. *International Journal of Systematic and Evolutionary Microbiology*. 56:477-486.

Houbraken J, Frisvad JC, Samson RA (2010) Taxonomy of *Penicillium citrinum* and related species. *Fungal Diversity*. 44:117–133.

Houbraken J, Samson RA, Yilmaz N (2016) Taxonomy of *Aspergillus*, *Penicillium* and *Talaromyces* and its significance for biotechnology in *Aspergillus* and *Penicillium* in the post-genomic era. Caister Academic Press, Wymondham, pp.1-15.

Houbraken J, Kocsubé S, Visagie CM, Yilmaz N, Wang XC, Meijer M, Kraak B, Hubka V, Samson RA, Frisvad JC (2020) Classification of *Aspergillus*, *Penicillium*, *Talaromyces* and related genera (Eurotiales): An overview of families, genera, subgenera, sections, series and species. *Studies in micology*. 95:5–169.

Liu YJ, Whelen S, Hall BD (1999) Phylogenetic relationships among *ascomycetes*: evidence from an RNA polymerase II subunit. *Molecular Biology and Evolution*. 16:1799-1808.

Nevarez L, Vasseur V, Le Madec A, Le Bras MA, Coroller L, Leguérinel I, Barbier G (2009) Physiological traits of *Penicillium glabrum* strain LCP 08.5568, a filamentous fungus isolated from bottled aromatised mineral water. *International Journal of Food Microbiology*. 130:166-171.

Okuda T (1994) Variation in colony characteristics of *Penicillium* strains resulting from minor variations in culture conditions. *Mycologia*. 86:259-262.

Okuda T, Klich MA, Seifert KA, et al. (2000) Media and incubation effect on morphological characteristics of *Penicillium* and *Aspergillus* in Samson RA, Pitt JI (Eds.), *Integration of modern taxonomic methods for Penicillium and Aspergillus classification*, Harwood Academic Publishers, Amsterdam, pp. 83-99.

- Onions AHS, Brady BL (1987). Taxonomy of *Penicillium* and *Acremonium*. In: Peberdy JF (Ed.) Biotechnology Handbooks 1 *Penicillium* and *Acremonium*. New York and London, Plenum Press. p. 1-36.
- Pitt JI, Hocking AD (1997) Fungi and food spoilage. 2nd ed. London: Blackie Academic and Professional. 540 p.
- Ramos-Pereira J, Mareze J, Patrinou E, Santos JA, López-Díaz TM (2019) Polyphasic identification of *Penicillium* spp. isolated from Spanish semi-hard ripened cheeses. *Food Microbiology*. 84:103253.
- Samson RA, Pitt JI (1985) General recommendations Samson RA, Pitt JI (Eds.), Advances in *Penicillium* and *Aspergillus* systematics. Plenum Press, London, pp. 455-460.
- Santos C, Paterson RRM, Venâncio A, Lima N (2009) Filamentous fungal characterizations by matrix-assisted laser desorption/ionization time-of-flight mass spectrometry. *Journal of Applied Microbiology*. 108: 375-385.
- Silva-Filho FA, Souza MMM, Rezende GO, Silva FMA, Cruz JC, Silva GF, Souza ADL, Souza AQL (2021) Screening of alkaloid-producing *Penicillium* strains for biotechnological applications by electrospray ionization mass spectrometry (ESI-MS) and principal component analysis (PCA). *Journal of Brazilian Chemical Society*.
- Smedsgaard, J (1997) Micro-scale extraction procedure for standardization screening of fungal metabolite production in cultures. *Journal of Chromatography A* 760:264-270.
- Tsang CC, Tang JYM, Lau SKP, Woo PCY (2018) Taxonomy and evolution of *Aspergillus*, *Penicillium* and *Talaromyces* in theomics era – Past, present and future. *Computational and Structural Biotechnology Journal*. 16:197-210.
- Valli M, Young MC, Bolzani VS (2016) A Beleza Invisível da Biodiversidade: O Táxon Rubiaceae. *Revista Virtual de Química*. 8:296-310.
- Varga S, Soulsbury CD (2019) Arbuscular mycorrhizal fungi change host plant DNA methylation systemically. *Plant Biol (Stuttg)*. 21:278-283.
- Visagie CM, Houbraken J, Frisvad JC, Hong SB, Klaassen CHW, Perrone G, Seifert KA, Varga J, Yaguchi T, Samson RA (2014) Identification and nomenclature of the genus

*Penicillium. Studies in Mycology.* 78:343–371.

Visagie CM, Renaud JB, Burgess KMN, Malloch DW, Clark D, Ketch L, Urb M, Assabgui R, Sumarah MW, Seifert KA (2016) Fifteen new species of *Penicillium*. *Persoonia*.36:247–280.

Zhao RB, Bao HY, Liu YX (2010) Isolation and Characterization of *Penicillium oxalicum* ZHJ6 for Biodegradation of Methamidophos. *Agricultural Sciences in China*. 9:695-703.

## 6. CAPÍTULO III

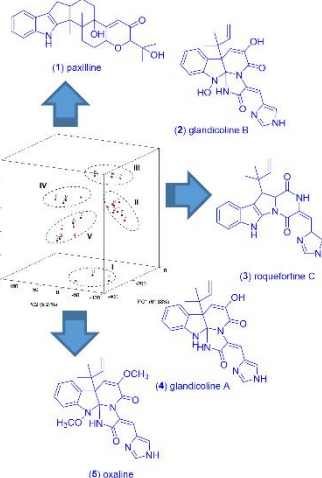
### Triagem de Cepas de *Penicillium* endofítico de plantas da Amazônia produtoras de alcalóide por espectrometria de massa de ionização por eletrospray (ESI-MS) e análise de componente principal (PCA)<sup>2</sup>

Francinaldo Araujo da Silva Filho, Marjory Michely Martins de Souza, Gabriel de Oliveira Rezende, Felipe Moura Araujo da Silva, Jeferson Chagas da Cruz, Gilvan Ferreira da Silva, Afonso Duarte Leão de Souza, Antonia Queiroz Lima de Souza

Este capítulo apresenta o estudo químico realizado com 25 espécimes do gênero *Penicillium* da coleção de trabalho do Laboratório de Bioensaios e Microrganismos da Amazônia da Universidade Federal do Amazonas (LabMicrA/UFAM). O trabalho se trata de uma triagem dos fungos por métodos espectrométricos afim de se prospectar espécies produtoras de metabólitos secundários com potencial bioativo. O presente trabalho demonstrou o potencial de várias cepas endofíticas de *Penicillium* de plantas medicinais da Amazônia como produtoras de alcalóides, incluindo *P. paxilli*, *P. rubens* e *P. oxalicum*, bem como descreveu o isolamento de 2 alcalóides e a identificação de 5 alcalóides, sendo 4 da rota das roquefortinas e um alcaloide dicetopiperazinico com diversas atividades já descritas. Além disso, a abordagem proposta fundamentada no perfil químico por ESI-MS em combinação com a análise de PCA forneceu uma estratégia simples e eficaz para discriminar cepas de *Penicillium* capazes de produzir diferentes tipos de alcalóides com potencial biotecnológico.

---

<sup>2</sup>Artigo submetido à revista *Journal of Brazilian Chemical Society* (ISSN 0887-2333) em Janeiro de 2021 e aceito para publicação em Abril de 2021.

**Graphical Abstract (GA)****GA Figure:****Penicillium strains**

**GA Text:** The ESI-MS and PCA analysis provided a simple and effective approach to screening alkaloid-producing endophytic *Penicillium* strains from Amazon medicinal plants.

**Screening of Alkaloid-Producing Endophytic *Penicillium* strains from Amazon Medicinal Plants by Electrospray Ionization Mass Spectrometry (ESI-MS) and Principal Component Analysis (PCA)**

**Francinaldo Araujo da Silva-Filho,<sup>a</sup> Marjory Michely Martins de Souza,<sup>b</sup> Gabriel de Oliveira Rezende,<sup>b</sup> Felipe Moura Araujo da Silva,<sup>c</sup> Jeferson Chagas da Cruz,<sup>d</sup> Gilvan Ferreira da Silva,<sup>d</sup> Afonso Duarte Leão de Souza,<sup>a,c,e</sup>and Antonia Queiroz Lima de Souza<sup>a,b,c,f,\*</sup>**

<sup>a</sup>*Programa de Pós-Graduação da Rede Bionorte, Universidade Federal do Amazonas (UFAM), 69077-000, Manaus, AM, Brazil*

<sup>b</sup>*Programa de Pós-Graduação Em Biotecnologia e Recursos Naturais, Escola Superior de Ciências da Saúde, Universidade do Estado do Amazonas (UEA), 69.000-000, Manaus, AM, Brazil*

<sup>c</sup>*Central Analítica - Centro de Apoio Multidisciplinar (CAM), Universidade Federal do Amazonas (UFAM), 69077-000, Manaus, AM, Brazil*

<sup>d</sup>*Embrapa Amazônia Ocidental, Empresa Brasileira de Pesquisa Agropecuária (EMBRAPA) Manaus, AM, Brazil*

<sup>e</sup>*Departamento de Química (ICE), Universidade Federal do Amazonas (UFAM), 69077-000, Manaus, AM, Brazil*

<sup>f</sup>*Faculdade de Ciências Agrárias (FCA), Universidade Federal do Amazonas (UFAM), 69077-000, Manaus, AM, Brazil*

\*antoniaqueiroz@ufam.edu.br

**Abstract**

The genus *Penicillium* is among the most promising alkaloid-producing fungal and therefore plays an important role in terms of producing molecules with biotechnological potential. Thus, in order to identify alkaloid-producing fungi, 25 endophytic *Penicillium* strains previously isolated from Amazon medicinal plants were subject to an integrative approach based on direct infusion positive electrospray ionization mass spectrometry (ESI-MS) and principal component analysis (PCA). The multivariate analysis pointed paxiline (**1**), glandicoline B (**2**), roquefortine C (**3**), and oxaline (**5**) as responsible for the segregation of three promising alkaloid-producing groups, been these groups constituted for *P. chrysogenum*, *P. oxalicum*, *P. paxilli*, and *P. rubens* strains. These alkaloids and the glandicoline A (**4**) were tentatively identified by multiple-stage mass spectrometry. In addition, compounds **1** and **2** were isolated and confirmed by using 1D and 2D NMR spectroscopy. Overall, the chemical profile analysis by ESI-MS along with PCA provided a simple and effective approach to screening alkaloid-producing *Penicillium* strains for biotechnological applications.

**Keywords:** glandicoline, paxilline, *Penicillium oxalicum*, *Penicillium paxilli*, *Penicillium rubens*, oxaline

## Introduction

Fungi are widely distributed throughout the planet integrating the biogeological cycles of all ecosystems.<sup>1</sup> They comprise a wide variety of species, around 3.8 million, distributed mainly on environments such as in soil, water, and associated with plants and others organisms.<sup>2</sup> When associated with plants they are known as endophytics, and live in the inter and intracellular spaces of this individual for at least a period of their life cycle.<sup>3</sup> Usually, they have a symbiotic association with the plants that protect and provide nutrients to the endophyte, which, in turn, benefit the host through the control of pathogens as well as in the absorption of nutrients and the production of phytohormones.<sup>4</sup> Thus, endophytes not only provide advantages to the host but also are sources of new metabolites with diverse biological activities.<sup>5</sup> Among these endophytes, some genus as *Aspergillus*, *Trichoderma*, *Fusarium*, and *Penicillium* stand out in terms of producing molecules with several biotechnological potentials, such as antibiotics, antioxidants, and antitumoral agents.<sup>6-9</sup>

Since the discovery of the penicillin in 1929, the genus *Penicillium*, which is composed by approximately 354 known species,<sup>10</sup> has been described as a promising source of bioactive compounds, such as polyphenols, polyketides, and alkaloids.<sup>11-13</sup> Alkaloids produced by *Penicillium* has been showed potential to biotechnological applications, been their antimicrobial, antiviral, and anticancer activities previously described.<sup>14-18</sup>

The prospection of bioactive compounds or new molecules from microorganisms is an important and complex task, which usually demands modern analytical techniques with high sensitivity and selectivity, such as that based on mass spectrometry (MS).<sup>19,20</sup> In the recent years, these mass spectrometry-based approaches has been proved to be a powerful strategy for the screening and identification of bioactive compounds in plant

and microorganism species as well as to chemotaxonomic approaches, when combined with chemometric tools.<sup>21-23</sup> Thus, in this study, 25 endophytic *Penicillium* strains previously isolated from Amazon medicinal plants were screened for alkaloid-producing by an integrative approach based on direct infusion positive electrospray ionization mass spectrometry (ESI-MS) and principal component analysis (PCA) analysis.

## Experimental

### Fungal cultivation and micro-scale metabolites extraction

The 25 strains previously isolated from Brazilian medicinal plants are deposited in the work collection of the Amazon Bioassay and Microorganism Laboratory from Amazon Federal University (LabMicra/UFAM) and has the access to genetic heritage registered at Sistema Nacional de Gestão do Patrimônio Genético e do Conhecimento Tradicional Associado (SisGen) under the code No. AD64E07 (Table 1). They were grown in Petri dishes containing ISP2 medium (10 g corn starch, 4 g yeast extract, 10 g malt, 4 g dextrose, and 20 g agar for every 1 L of distilled water) for 10 days at 26° C.

**Table 1.** Endophytic *Penicillium* strains subjected to alkaloidal screening.

Strains ID	ID in the Work Collection	Host (Plant)	Part of The Plant
A	<i>GhcR3 2.2 (401)</i>	<i>Gustavia elliptica</i>	Root bark
B	<i>PbR2 2.2 (135)</i>	<i>Mauritia flexuosa</i>	Root
C	<i>GhcR1 1.1a (415)</i>	<i>G. elliptica</i>	Root bark
D	<i>GhcC1 1.2c (414)</i>	<i>G. elliptica</i>	Stem bark
E	<i>StspC2 1.2c (180)</i>	<i>Strychnos</i> sp.	Stem
F	<i>GhR1 2.1 (391)</i>	<i>G. elliptica</i>	Root
G	<i>VrF1 2.2 (64)</i>	<i>Victoria amazonica</i>	Leaf
H	<i>AspC2 2.2 (52)</i>	<i>Annona</i> sp.	Stem
I	<i>AnspG1 2.2 (56)</i>	<i>Annona</i> sp.	Twig
J	<i>GhcR1 1.1b (433)</i>	<i>G. elliptica</i>	Root bark
K	<i>AnspG1 2.3b (155)</i>	<i>Annona</i> sp.	Twig
L	<i>VrF2 2.3 (149)</i>	<i>V. amazonica</i>	Leaf
M	<i>VrC2 2.1c (143)</i>	<i>V. amazonica</i>	Stem

N	<i>GhG2 2.1</i> (392)	<i>G. elliptica</i>	Twig
O	<i>AnspG1 2.3a</i> (153)	<i>Annona</i> sp.	Twig
P	<i>AnspC2 3.1</i> (38)	<i>Annona</i> sp.	Stem
Q	<i>GhR1 2.1a</i> (396)	<i>G. elliptica</i>	Root
R	<i>GhcG3 2.2</i> (457)	<i>G. elliptica</i>	Twig bark
S	<i>GhR2 1.2b</i> (408)	<i>G. elliptica</i>	Root
T	<i>VrC2 1.2</i> (71)	<i>V. amazonica</i>	Stem
U	<i>AnspcG1 3.3</i> (48)	<i>Annona</i> sp.	Twig bark
V	<i>GhcR3 2.2</i> (403)	<i>G. elliptica</i>	Root bark
W	<i>GhG3 2.2c</i> (407)	<i>G. elliptica</i>	Twig
X	<i>EjC3 2.1a</i> (307)	<i>Piper peltata</i>	Stem
Y	<i>GhcC2 2.2a</i> (409)	<i>G. elliptica</i>	Stem bark

After the cultivation period, three plugs of 6 mm diameter were removed from each plate and transferred to 5 cm test tubes and extracted for 24 h with 2 mL of a solution containing 3:2:1 ethyl acetate/dichloromethane/methanol, with 1% formic acid.<sup>24</sup> The solvent was then filtered through a small piece of cotton and concentrated, yielding around 1 mg of extract in general for all samples.

#### Fungal cultivation and large-scale metabolites extraction

For the fungal metabolic production, two strains with even peaks in their mass-spectra profiles, *P. paxilli* (**O**) and *P. rubens* (**V**), were cultivated in preparative scale, using 60 Erlenmeyer flasks of 1 L containing 300 mL of ISP2 liquid medium each. The cultivation was made at 26° C in static mode for 23 days. pH and glucose was measured in the beginning of the cultivation and in the end. After the cultivation period, the crude fermentation broth was separated from the mycelium by vacuum filtration. Extraction of the fermentation broth (18 L) was performed with ethyl acetate (3 x 500 mL),<sup>25</sup> providing the organic phase that was concentrated, yielding 1.3 g of crude extract for the *P. paxilli* and 1.9 g for the *P. rubens*. Both extracts were stored at 4 °C.

#### ESI-MS and PCA analysis

The micro-scale extracts were resuspended in methanol (HPLC grade), creating the stock solutions ( $1 \text{ mg mL}^{-1}$ ). Aliquots ( $5 \mu\text{L}$ ) of the stock solutions were further diluted to  $5 \mu\text{g mL}^{-1}$  and analyzed by direct infusion into the mass spectrometers. An ion-trap mass spectrometer, model LCQ Fleet (Thermo Scientific, San Jose, CA, USA), equipped with electrospray ionization (ESI) interface and running in the positive ion mode was used to perform ESI-MS and a triple quadrupole mass spectrometer, model TSQ Quantum Access (Thermo Scientific, San Jose, CA, USA) to perform ESI-MS/MS analyses. Samples were directly infused into the ion source through the instrument syringe pump ( $10 \mu\text{L min}^{-1}$ ). MS analytical conditions: spray voltage, 5 kV; sheath gas, 10 arbitrary unit (arb); auxiliary gas, 5 arb; sweep gas, 0 arb; capillary temp,  $200^\circ \text{ C}$ ; capillary voltage, 40 V; tube lens, 115 V; mass range,  $m/z$  150 to 1000. Argon was used as collision gas, and the ESI-MS/MS spectra were obtained using collision energies ranging from 25 to 30 eV. For the principal component analysis (PCA), initially, the relative ion intensity obtained by ESI-MS from  $m/z$  150 to 1000 (850 variables) was analyzed through Chemoface<sup>TM</sup> program.<sup>21,22</sup> In order to highlight only the alkaloid-producing strains groups, a new PCA analysis was performed based only in the relative intensity of even ions (426 variables).

### Alkaloids isolation

*P. paxilli* crude extract (1.3 g) was subjected to silica gel column chromatography (CC) with increasing gradient of polarity: hexane-ethyl acetate (70:30, 30:70, and 0:100, v/v), ethyl acetate-methanol (80:20 and 0:100, v/v), affording 5 fractions (50 mL each). Fraction 2 (PP.F2) (97 mg) was subjected to C18 CC eluted with water-methanol (50:50 to 0:100, v/v), giving 5 fractions (50 mL each). Then, the fractions 3 (PP.F2.3, 18 mg) and 4 (PP.F2.4, 10 mg) were pooled into a new fraction (PP.F2.3-4, 28 mg) according to MS analysis. PP.F2.3-4 was submitted to a semi-preparative Shimadzu HPLC, model

UFLC (Shimadzu, Columbia, MD, USA), using water (A) and methanol (B) as mobile phases. The gradient elution was as follows: 0-10 min, 70-100% B (v/v) and 10-25 min, 100% B at a flow rate of 3.4 mL min<sup>-1</sup>. A C18 column (250 mm × 10 mm, 5 m) was employed on the fractionation and the UV channels at 280 and 232 nm were monitored. A single injection was carried onto the column in DMSO (150 µL), yielding compound **1** (13 mg) as an amorphous white solid.

Similarly, *P. rubens* crude extract (1.9 g) was subjected to C18 CC eluted with water-methanol (70:30, 30:70, and 0:100, v/v), affording 3 fractions (50 mL each). Fraction 2 (PR.F2) (470 mg) was subjected to C18 CC and eluted with water-methanol (60:40, 40:60, and 0:100, v/v), giving 3 fractions (50 mL each). Then, fraction 2 (PR.F2-2) (80 mg) was subjected to over C18 CC and eluted with water-methanol (50:50 and 0:100, v/v), giving 2 fractions (50 mL each). Finally, fraction 1 (PR.F2-2-1) (30 mg) was submitted to a semi-preparative HPLC, model UFLC (Shimadzu, Columbia, MD, USA), using water (A) and methanol (B) as mobile phases. The gradient elution was as follows: 0-45 min, 45-59% B (v/v), 45-50 min, 59-100% B (v/v), and 50-70 min, 100% B (v/v) at a flow rate of 3.4 mL min<sup>-1</sup>. The same C18 column above was employed on the fractionation and the UV channels at 240 and 300 nm were monitored. A single injection was carried onto the column in DMSO (150 µL), which afforded compound **2** (5 mg) as an amorphous yellow solid.

### NMR analysis

The one-dimensional (1D) and two-dimensional (2D) nuclear magnetic resonance (NMR) analysis were performed with an AVANCE III HD 500 NMR spectrometer (Bruker, Billerica, MA, USA), operating at 11.75 T, observing <sup>1</sup>H at 500.13 and <sup>13</sup>C at 125.76 MHz. Deuterated methanol (MeOD) (Cambridge Isotope, Tewksbury, MA, USA)

was used as solvent. All chemical shifts ( $\delta$ ) are given in ppm relative to the solvent signal, and the coupling constants ( $J$ ) are given in Hz.

#### Microorganism identification

The identification of the alkaloid-producing *Penicillium* strains was confirmed by sequencing of the fungus internal transcribed space-1 (*ITS*) and *ITS-2 rDNA* and compared with sequences from the GenBank. 10  $\mu$ L of the strains spore suspension concentrated in  $30 \times 10^8$  cells  $mL^{-1}$  was incubated on 50 mL potato dextrose (PD), medium in a 125 mL Erlenmeyer and stirred for 36 h (120 rpm) at 26° C temperature. The mycelium was separated from the medium by filtration and crushed with silica gel and then preceded to extraction. The genomic DNA was extracted by a Zymo Research Quick-DNA™ Fungal/Bacterial Miniprep Kit using its own protocol with some adaptations, using 50  $\mu$ L of the DNA Dilution Buffer instead of protocol's 100  $\mu$ L and using longer centrifugation times on all steps. After the extraction, the DNA was sequenced using a model 3500 Genetic Analyzer (Applied Biosystems, Foster city, CA, USA). All the data was then analyzed and processed using National Center for Biotechnology Information's (NCBI) Nucleotide Basic Local Alignment Search Tool (BLASTn) tool (Table 2).

#### Results and Discussion

The direct infusion ESI positive mass spectra of the *Penicillium* strains crude extracts from  $m/z$  150 to 1000 displayed several base peak ions in the range of 400-800 Da (Figures S1 to S25), such as  $m/z$  420, 448, and 458, suggesting the presence of alkaloids in a large portion of the samples. This proposal was based on previous studies with fungal alkaloids containing an odd number of nitrogen atoms, such as indole

alkaloids, where protonation process provides products with even  $m/z$  values.<sup>26-28</sup> Besides base peak, several other ions were observed, indicating these samples as complex matrixes. In the first PCA score plot (Figure 1A), based on the relative intensity of  $m/z$  150 to 1000 (850 variables), five main groups (group I-V) were observed, being group I formed by three strains, group II by eight strains, group III by three strains, group IV by four strains and group V by seven strains. On the other hand, the second PCA score plot (Figure 1B), based on only the relative intensity of even ions (426 variables), highlighted the groups I, III, and IV as discrete alkaloid-producing groups. The groups II and V became together in this graph, revealing to be similar in the production of alkaloids. In fact, the strains of these groups have shown low intense even ions, revealing to be poor alkaloid producers, at least in the grown conditions used.

According to the PCA biplot (PC2xPC3) of scores and loadings (Figure 1C), the ions at  $m/z$  390, 420, 448, and 458 were the main responsible for the segregation of the groups I, III, and IV. The MS/MS spectra of some of these ions (Figure 2) revealed key fragmentations (losses of 68 or 69 Da) previously described for prenylated alkaloids, such as roquefortine and related compounds.<sup>17,26</sup>

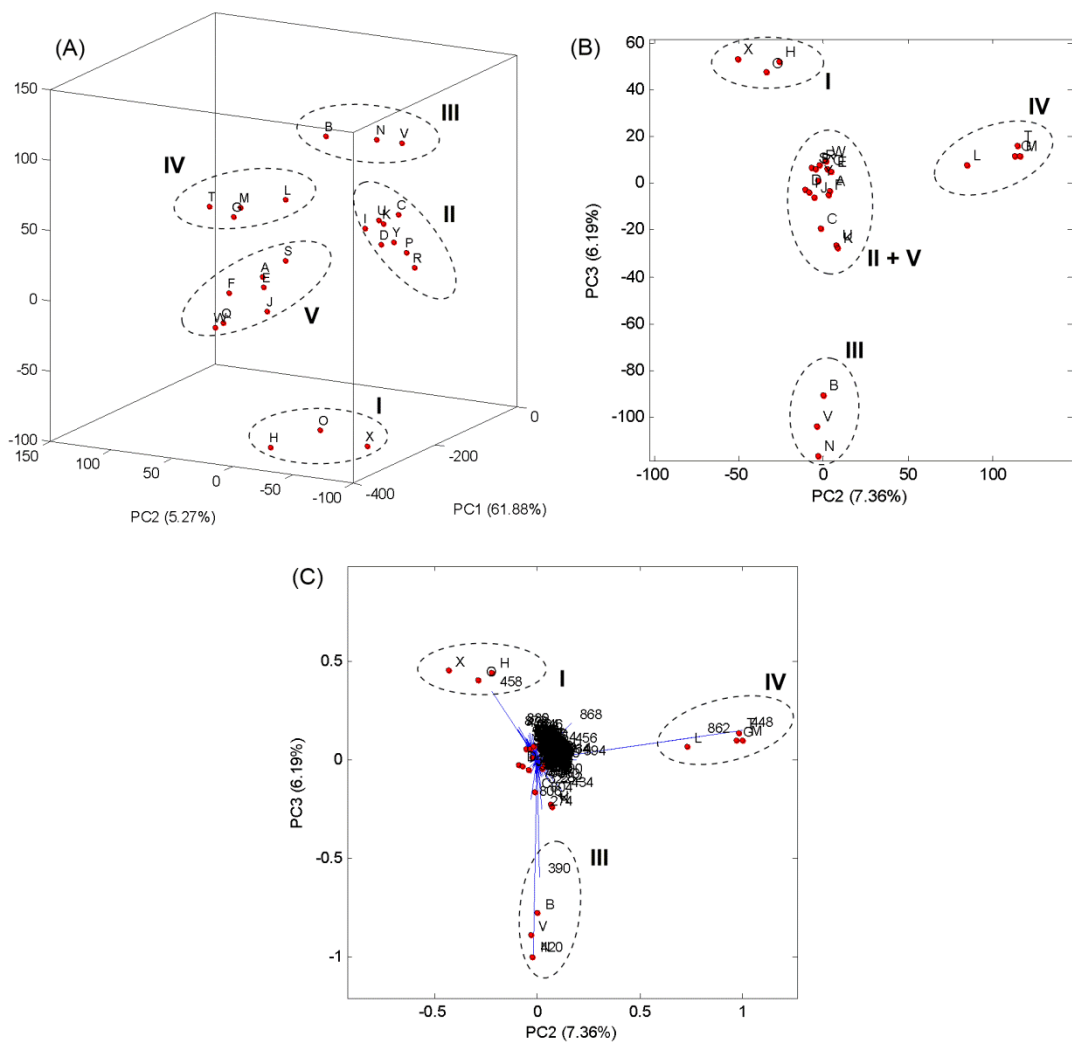


**Figure 1.** PCA score plots (A and B) and biplot of scores and loadings (C) generated from the crude extract ESI-MS data from twenty-five endophytic *Penicillium* strains from Amazon medicinal plants (A-Y).

The MS/MS spectrum of the ion at  $m/z$  390 (Figure 2A) displayed besides the initial loss of the prenyl group (-68 Da,  $m/z$  390 → 322), a base peak at  $m/z$  193, which is in accordance with the structure of roquefortine C (**3**) (Figure 3).<sup>26</sup> The MS/MS spectrum of the ion at  $m/z$  420 (Figure 2B) also displayed the initial loss of the prenyl group (-69 Da,  $m/z$  420 → 351), as well as a base peak at  $m/z$  289, being this fragmentation consistent with the structure of glandicoline B (**2**) (Figure 3).<sup>17</sup> Moreover, the MS/MS spectrum of the ion at  $m/z$  448 (Figure 2C) displayed an initial loss of a methoxyl group (-31 Da,  $m/z$

$448 \rightarrow 417$ ), followed by a loss of a prenyl group (-69 Da,  $417 \rightarrow 348$ ), which is in accordance with the structure of the alkaloid oxaline (**5**) (Figure 3).<sup>27</sup> On the other hand, the MS/MS spectrum of the ion at  $m/z$  458 do not generate fragments, even increasing the collision energy. Since this phenomenon is recurrent for sodium adduct molecular ions,<sup>28</sup> the sodium mass was taken into consideration, and the correspondent protonated ion at  $m/z$  436 was submitted to MS/MS analysis. Thus, the MS/MS spectrum of the ion at  $m/z$  436 (Figure 2D) presented a base peak at  $m/z$  130 and a less intense ion at  $m/z$  182, being this fragmentation consistent with the structure of paxilline (**1**) (Figure 3).<sup>28</sup> Paxilline (**1**), as well as glandicoline B (**2**), were also confirmed by a comparison of their NMR data (Figures S32 to S39, Tables 1S and 2S) with those reported in the literature.<sup>17,30,32</sup>

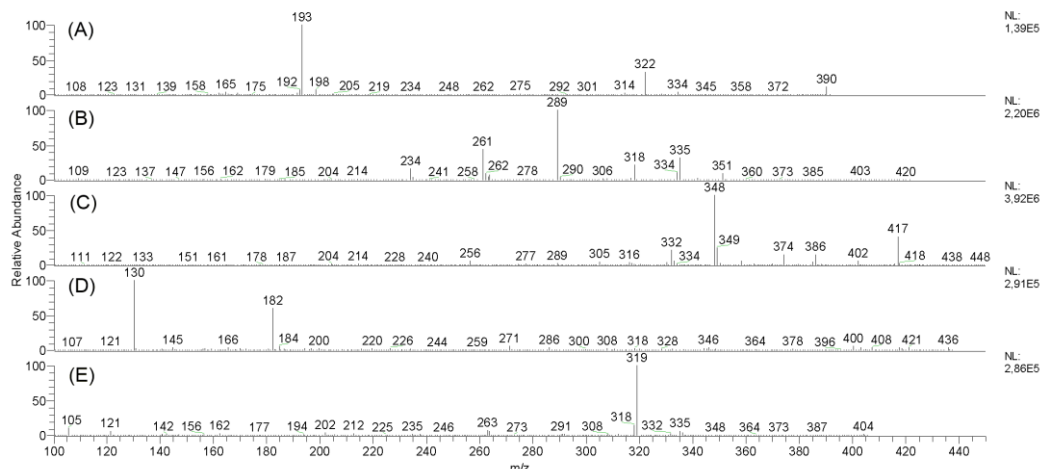


**Figure 2.** ESI-MS/MS spectra (positive mode) of the ion at  $m/z$  390 (A), 420 (B), 448 (C), 436 (D), and 404 (E), present in the crude extracts of *Penicillium* strains.

Besides, after a manual inspection of the MS spectra from group III, a minor ion at  $m/z$  404 was tentatively identified as glandicoline A (**4**), the precursor of the glandicoline B. Thus, the MS/MS spectrum of **4** (Figure 2E) presented a loss of prenyl group (-69 Da,  $m/z$  404  $\rightarrow$  335) as well as the base peak at  $m/z$  319, in coherence with the structure of glandicoline A.<sup>26</sup>

Since the alkaloids **1-5** were tentatively identified between strains from the groups I (**H**, **O**, and **X**), III (**B**, **N**, and **V**), and IV (**G**, **L**, **M**, and **T**), these organisms were assigned as alkaloid-producing strains and identified by molecular approach (Table 2). Using the BLASTn it was possible to identify the strains **H**, **O**, and **X** of the Group I as *P. paxilli*, a fungus known to produce indole diterpene alkaloids, such as paspaline, paxilline (**1**) and derivates.<sup>29,30</sup> Likewise, the strain **B**, from the group III, was identified as *P. chrysogenum*, while the strains **N** and **V** were identified as *P. rubens*. These two fungal species are genetically and chemically close, and has been described as promising sources of diketopiperazine alkaloids, such as roquefortines (**2-4**) and other alkaloids with biotechnological potential.<sup>31</sup> By its turn, the strains **G**, **L**, **M**, and **T** of the group IV were identified as *P. oxalicum*, which is also known to produce roquefortine alkaloids, however towards the end of the pathway such as meleagrin and oxaline (**5**).<sup>39</sup> These observations suggest a close biosynthetic relationship between the strains from the groups III and IV. Surprisingly, all species from the group IV were isolated from the same host (*V. amazonica*), suggesting that the host can play a role in the metabolites production or the selection of its fungi community.

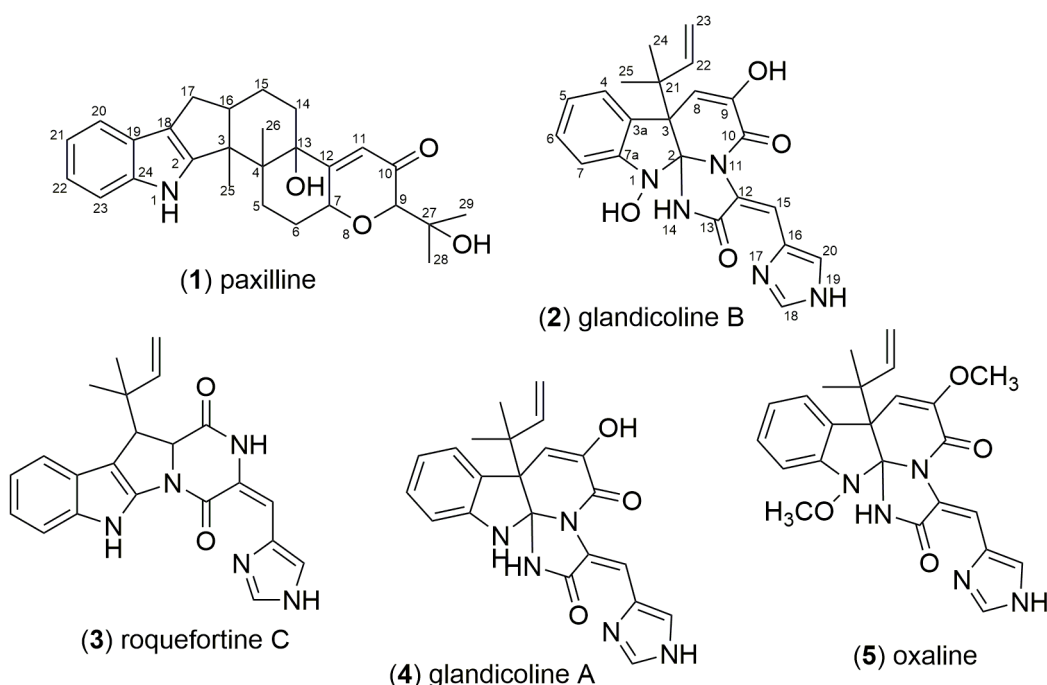


**Figure 3.** Isolated and identified compounds from the *Penicillium* strains present in groups I (**1**), III (**2-4**) and IV (**5**).

**Table 2.** Species identification of nine *Penicillium* endophytic strains by molecular approach with NCBI's BLASTn information.

Strains	Group	Description	Max score	Total score	Query cover	E value	Percent identity
<b>H</b>	I	<i>P. paxilli</i>	990	1165	99%	0	100.00%
<b>O</b>	I	<i>P. paxilli</i>	979	979	100%	0	100.00%
<b>X</b>	I	<i>P. paxilli</i>	924	924	98%	0	99.22%
<b>B</b>	III	<i>P. chrysogenum</i>	977	1082	100%	0	100.00%
<b>V</b>	III	<i>P. rubens</i>	1195	1517	100%	0	98.12%
<b>N</b>	III	<i>P. rubens</i>	1042	1042	99%	0	100.00%
<b>G</b>	IV	<i>P. oxalicum</i>	761	761	100%	0	98.61%
<b>L</b>	IV	<i>P. oxalicum</i>	911	911	99%	0	99.80%
<b>M</b>	IV	<i>P. oxalicum</i>	979	979	100%	0	100.00%
<b>T</b>	IV	<i>P. oxalicum</i>	952	952	98%	0	99.81%

Paxilline is a indole diterpene alkaloid firstly described in *P. paxilli*,<sup>30</sup> and also found in *P. tularensis*, *Acremonium lorii*, *Emericella desertorum*, *E. foveolata*, and *E. striata*.<sup>33,34</sup> It is known to have tremorgenic, anticonvulsant and antiinsectan activity.<sup>35-37</sup> Paxilline is also a calcium-activated K<sup>+</sup> channel blocker (BK), that has showed to attenuate thalidomide-caused synaptic and cognitive dysfunctions in mice.<sup>38</sup> On the other hand, glandicoline B is an important intermediate of the roquefortine-oxaline biosynthetic pathway.<sup>39</sup> Glandicoline B is a precursor of the diasteromeric pair oxaline (**5**) and neoxaline, both with anticancer activities against leukemic Jurkat cells through the inhibition of cell proliferation and arrest the cell cycle at the G2/M phase.<sup>40</sup> Glandicoline B was first described in *P. glandicola*<sup>41</sup> and was later reported in *P. hirsutum*, *P. alli*, *P. radiicolor*, *P. tulipae*, and *P. chrysogenum*.<sup>42,43</sup> On the other hand, roquefortine C (**3**) is

a relatively common fungal metabolite and has been reported in at least 30 fungal strains, being first reported in a strain of *P. roquefortii*.<sup>44-46</sup> It is considered as one of the most common fungal contaminants of cheese, beverages and meats.<sup>47</sup> Although it is considered a toxin, at low concentrations it was found to be safe for human consumption.<sup>48</sup> Moreover, roquefortine C possesses neurotoxic and antimicrobial activities, most likely through inactivation of cytochrome P450s.<sup>49,50</sup> The isolated compounds were characterized by <sup>1</sup>H and <sup>13</sup>C NMR and the data are presented in the supplementary material (Figures S32 to S39), including the NMR assignments (Tables 1S and 2S).

## Conclusions

The present work demonstrated the potential of several endophytic *Penicillium* strains from Amazon medicinal plants as alkaloid producers, including *P. chrysogenum*, *P. paxilli*, *P. rubens*, and *P. oxalicum*. Moreover, the proposed approach based on the chemical profile by ESI-MS in combination with PCA analysis provided a simple and effective strategy for discriminate *Penicillium* strains able to produce different types of alkaloids with biotechnological potential.

## Supplementary Information

Supplementary Information, including the <sup>1</sup>H and <sup>13</sup>C NMR data for the isolated compounds (MS and NMR data - Figure S1 to S39, NMR assignments - Table S1 and S2) is available free of charge at <http://jbcs.sbj.org.br>.

## Acknowledgements

The authors are grateful to Central Analítica (UFAM) for MS and NMR analysis, and Coordenação de Aperfeiçoamento de Pessoal de Nível Superior (CAPES), Conselho Nacional de Desenvolvimento Científico e Tecnológico (CNPQ), Financiadora de Estudos e Projetos (FINEP) and, Fundação de Amparo à Pesquisa do Estado do

Amazonas (FAPEAM) for financial support.

## Author Contributions

Francinaldo Araujo da Silva-Filho was responsible for the Conceptualization, Data curation, Formal analysis, and Writing original draft; Felipe Moura Araujo da Silva for the Formal analysis, Writing original draft and Writing-review & editing; Marjory Michely Martins de Souza, Gabriel de Oliveira Rezende, Jeferson Chagas da Cruz, and Gilvan Ferreira da Silva for the Formal analysis; Antonia Queiroz Lima de Souza and Afonso Duarte Leão de Souza were responsible for the Conceptualization, Formal analysis, Funding acquisition, Writing original draft, and Writing-review & editing.

## References

1. Branco, S.; *Fungal Biology Reviews* **2019**, *33*, 225.
2. Hawksworth, D. L.; Lucking, R.; *Microbiology Spectrum* **2017**, *5*, 1.
3. Borges, W.; Borges, K.; Bonato, P.; Said, S.; Pupo, M.; *Curr. Org. Chem.* **2009**, *13*, 1137.
4. Mane, R. S.; Vedamurthy, A. B.; *International Journal of Secondary Metabolites* **2018**, *5*, 288.
5. Suryanarayanan, T.; *Kavaka* **2017**, *48*, 1.
6. Newman, D. J.; Cragg, G. M.; *J. Nat. Prod.* **2016**, *79*, 629.
7. Aly, A. H.; Debbab, A.; Kjer, J.; Proksch, P.; *Fungal Diversity* **2010**, *41*, 1.
8. Du, L.; Feng, T.; Zhao, B.; Li, D.; Cai, S.; Zhu, T.; Wang, F.; Xiao, X.; Gu, Q.; *The Journal of Antibiotics* **2010**, *63*, 165.
9. Gunatilaka, A. A. A. L.; *J. Nat. Prod.* **2006**, *69*, 509.

10. Visagie, C. M.; Houbraken, J.; Frisvad, J. C.; Hong, S. B.; Klaassen, C. H. W.; Perrone, G.; Seifert, K. A.; Varga, J.; Yaguchi, T.; Samson, R.; *Studies in Mycology* **2014**, *78*, 343.
11. Lu, Z.; Zhu, H.; Fu, P.; Wang, Y.; Zhang, Z.; Lin, H.; Liu, P.; Zhuang, Y.; Hong, K.; Zhu, W.; J. *Nat. Prod.* **2010**, *73*, 911.
12. Marinho, A. M. R.; Rodrigues-Filho, E.; Moitinho, M. D. L. R.; Santos, L. S.; *J. Braz. Chem. Soc.* **2005**, *16*, 280.
13. Bringmann, G.; Lang, G.; Gulder, T. A. M.; Tsuruta, H.; Muhlbacher, J.; Maksimenka, K.; Steffens, S.; Schaumann, K.; Stohr, R.; Wiese, J.; Imhoff, J. F.; Perovic-Ottstadt, S.; Boreiko, O.; Muller, W. E. G.; *Tetrahedron* **2005**, *61*, 7252.
14. Hawas, W. U.; Lamia, T. A.; El-Kassem.; *Lett. Org. Chem.* **2019**, *16*, 409.
15. Hayashi, H.; Takiuchi, K.; Murao, S.; Arai, M.; *Agricultural and Biological Chemistry* **1989**, *53*, 461.
16. Kusano, M.; Koshino, H.; Uzawa, S.; Kawano, T.; Kimura, Y.; *Bioscience Biotechnology Biochemistry* **2000**, *64*, 2559.
17. Koolen, H. H. F.; Soares, E. R.; Silva, F. M. A.; Almeida, R. A.; Souza, A. D. L.; Medeiros, L. S.; Rodrigues-Filho, E.; Souza, A. Q. L.; *Quim. Nova* **2012**, *35*, 771.
18. Kozlovsky, A. G.; Zhelifonova, V. P.; Antipova, T. V.; *Journal of Organic and Biomolecular Chemistry* **2013**, *1*, 11.
19. Nielsen, K. F.; Smedsgaard, J.; *J. Chromatogr. A* **2003**, *1002*, 111.
20. Castrillo, J. I.; Hayes, A.; Mohammed, S.; Gaskell, S. J.; Oliver, S. G.; *Phytochemistry* **2003**, *62*, 929.
21. Bastos, L. M.; Silva, F. M. A.; Souza, L. R. S.; Sá, I. S.; Silva, R. M.; Souza, A. D. L.; Nunomura, R. C. S.; *J. Braz. Chem. Soc.* **2020**, *31*, 351.
22. Silva, F. M. A.; Silva-Filho, F. A.; Lima, B. R.; Almeida, R. A.; Soares, E. R.; Koolen, H. H. F.; Souza, A. D. L.; Pinheiro, M. L. B.; *J. Braz. Chem. Soc.* **2016**, *27*, 599.
23. Kim, H. Y.; Park, H. M.; Lee, C. H.; *Journal of Microbiological Methods* **2012**, *90*, 327.

24. Smedsgaard, J.; *J. Chromatogr. A* **1997**, *760*, 264.
25. Souza, A. Q. L.; Souza, A. D. L.; Filho, A. S.; Pinheiro, M. L. B.; Sarquis, M. I. M.; Pereira, J. O.; *Acta Amazonica* **2004**, *34*, 185.
26. Tata, A.; Perez, C.; Campos, M. L.; Bayfield, M. A.; Eberlin, M. N.; Ifa, D. R.; *Anal. Chem.* **2015**, *87*, 12298.
27. Kim, H. Y.; Park, H. M.; Lee, C. H.; *Journal of Microbiological Methods* **2012**, *90*, 327.
28. Bauer, J. I.; Gross, M.; Cramer, B.; Wegner, S.; Hausmann, H.; Hamscher, G.; Usleber, E.; *Anal. Bioanal. Chem.* **2017**, *409*, 5101.
29. Munday-Finch, S. C.; Wilkins, A. L.; Miles, C. O.; *Phytochemistry* **1996**, *41*, 327.
30. Springer, J. P.; Clardy, J.; Wells, J. M.; Cole, R. J.; Kirksey, J. W.; *Tetrahedron Lett.* **1975**, *30*, 2531.
31. Houbraken, J.; Frisvad, J. C.; Samson, R.; *IMA Fungus* **2011**, *2*, 87.
32. Matsui, C.; Ikeda, Y.; Linuma, H.; Kushida, N.; Kunisada, T.; Simizu, S.; Umezawa, K.; *The Journal of Antibiotics* **2014**, *67*, 787.
33. Alburae, N. A.; Mohammed, A. E.; Alorfi, H. S.; Turki, A. J.; Asfour, H. Z.; Alarif, W. M.; Abdell-Lateff, A.; *Metabolites* **2020**, *10*, 73.
34. Andersen, B.; Frisvad, J. C.; *J. Agric. Food. Chem.* **2004**, *52*, 7507.
35. Reddy, P.; Guthridge, K.; Vassiliadis, S.; Hemsworth, J.; Hettiarachchige, I.; Spangenberg, G.; Rochfort, S.; *Toxins* **2019**, *11*, 302.
36. Sheehan, J. J.; Benedetti, B. L.; Barth, A. L.; *Epilepsia* **2009**, *50*, 711.
37. Belofsky, G. N.; Gloer, J. B.; Wicklow, D. T.; Dowd, P. F.; *Tetrahedron* **1995**, *51*, 3959.
38. Choi, T. Y.; Lee, S. H.; Kim, S. J.; Jo, Y.; Park, C. S.; Choi, S. Y.; *Sci. Rep.* **2018**, *8*, 17653.
39. Overy, D. P.; Nielsen, K. F.; Smedsgaard, J.; *J. Chem. Ecol.* **2005**, *31*, 2373.
40. Koizumi, Y.; Arai, M.; Tomoda, H.; *Biochim. Biophys. Acta, Mol. Cell Res.* **2004**, *1693*, 47.

41. Kozlovsky, A. G.; Marfenina, O. G.; Vinokurova, N. G.; Zhelifonova, V. P.; Adanin, V. M.; *Mycotoxins* **1998**, *48*, 37.
42. Martín, J. F.; Liras, P.; García-Estrada, C. In *Biosynthesis and molecular genetics of fungal secondary metabolites*, Martín, J. F.; García-Estrada, C.; Zeilinger, S., eds.; Fungal Biology Springer: New York, United states of America, 2014, ch. 111.
43. Ali, H.; Ries, M. I.; Nijland, J. G.; Lankhorst, P. P.; Hankemeier, T.; Bovenberg, R. A. L.; Vreeken, R. J.; Driesssen, A. J. M.; *PLoS One* **2013**, *8*, 65328.
44. Polonsky, J.; Merrien, M. A.; Scott, P. M.; *Annales de la Nutrition et de l'Alimentation* **1977**, *31*, 963.
45. Ohmomo, S.; Sato, T.; Utagawa, T.; Abe, M.; *Agricultural and Biological Chemistry* **1975**, *39*, 1333.
46. Kokkonen, M.; Jestoi, M.; Rizzo, A.; *International Journal of Food Microbiology* **2005**, *99*, 207.
47. Borthwick, A. D.; Costa, N. C.; *Critical Reviews in Food Science and Nutrition* **2017**, *57*, 718.
48. Finoli, C.; Vecchio, A.; Galli, A.; Dragoni, I.; *Journal of Food Protection* **2001**, *64*, 246.
49. Kopp-Holtwiesche, B.; Rehm, H. J.; *Journal of Environmental Pathology* **1989**, *10*, 41.
50. Aninat, C.; André, F.; Delaforge, M.; *Food Additives & Contaminants* **2005**, *22*, 361.

## Supplementary Information

### Screening of Alkaloid-Producing Endophytic *Penicillium* strains from Amazon Medicinal Plants by Electrospray Ionization Mass Spectrometry (ESI-MS) and Principal Component Analysis (PCA)

**Francinaldo Araujo da Silva-Filho,<sup>a</sup> Marjory Michely Martins de Souza,<sup>b</sup> Gabriel de Oliveira Rezende,<sup>b</sup> Felipe Moura Araujo da Silva,<sup>c</sup> Jeferson Chagas da Cruz,<sup>d</sup> Gilvan Ferreira da Silva,<sup>d</sup> Afonso Duarte Leão de Souza,<sup>a,c,e</sup> and Antonia Queiroz Lima de Souza<sup>a,b,c,f,\*</sup>**

<sup>a</sup>Programa de Pós-Graduação da Rede Bionorte, Universidade Federal do Amazonas (UFAM), 69077-000, Manaus, AM, Brazil

<sup>b</sup>Programa de Pós-Graduação Em Biotecnologia e Recursos Naturais, Escola Superior de Ciências da Saúde, Universidade do Estado do Amazonas (UEA), 69.000-000, Manaus, AM, Brazil

<sup>c</sup>Central Analítica - Centro de Apoio Multidisciplinar (CAM), Universidade Federal do Amazonas (UFAM), 69077-000, Manaus, AM, Brazil

<sup>d</sup>Embrapa Amazônia Ocidental, Empresa Brasileira de Pesquisa Agropecuária (EMBRAPA) Manaus, AM, Brazil

<sup>e</sup>Departamento de Química (ICE), Universidade Federal do Amazonas (UFAM), 69077-000, Manaus, AM, Brazil

<sup>f</sup>Faculdade de Ciências Agrárias (FCA), Universidade Federal do Amazonas (UFAM), 69077-000, Manaus, AM, Brazil

---

\*e-mail: antoniaqueiroz@ufam.edu.br

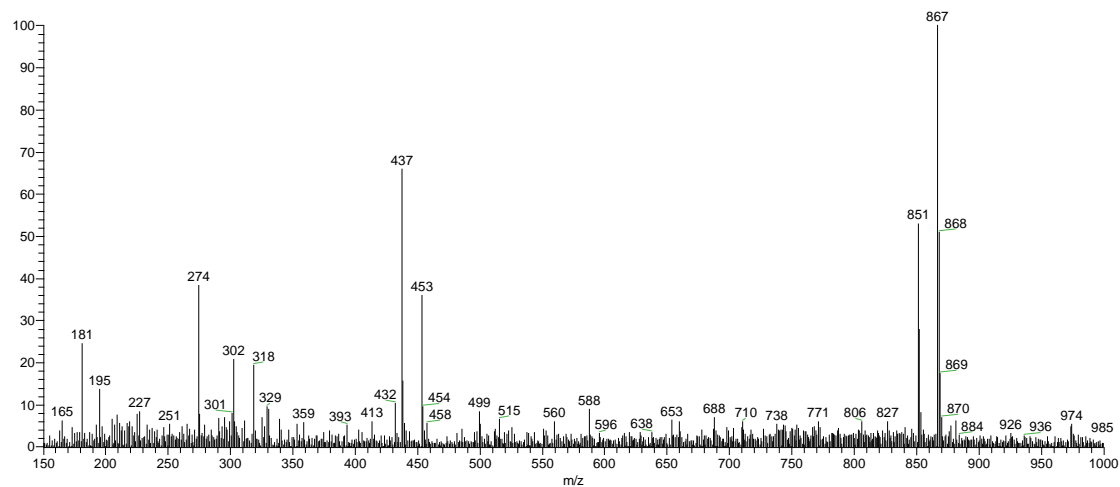


**Figure S1.** ESI-MS spectrum (positive mode) of the crude extract from *GhcR3* 2.2 (A).

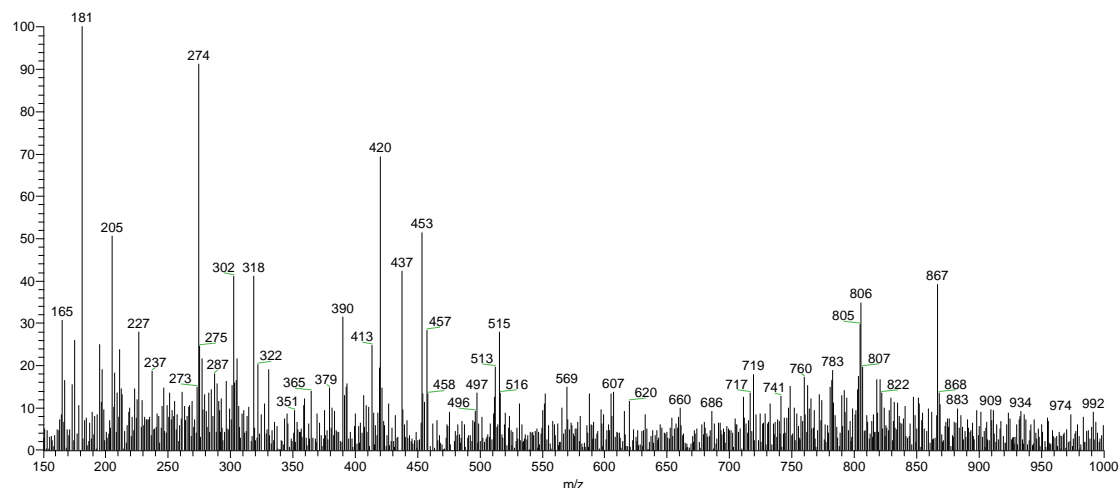


**Figure S2.** ESI-MS spectrum (positive mode) of the crude extract from *PbR2* 2.2 (B).

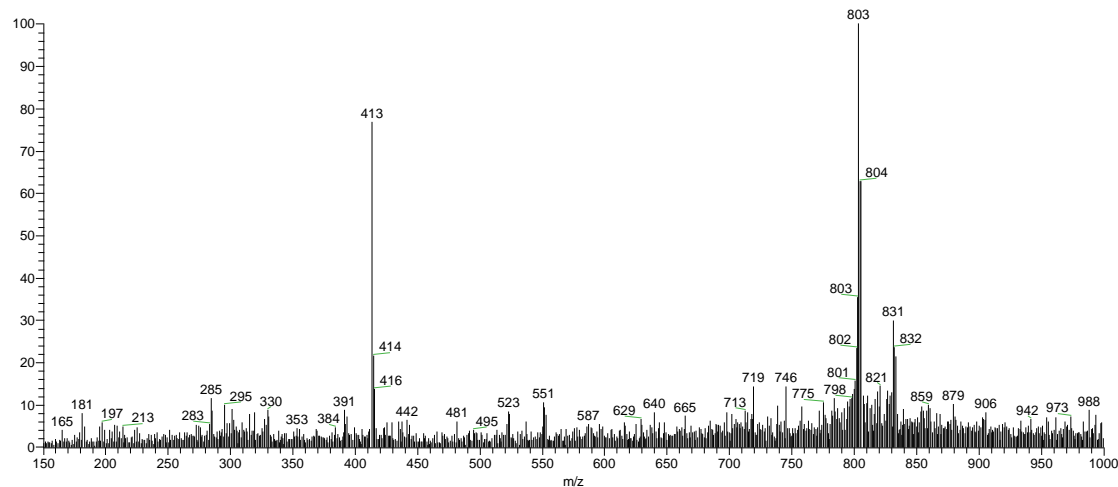


**Figure S3.** ESI-MS spectrum (positive mode) of the crude extract from GhcR1 1.1a (C).

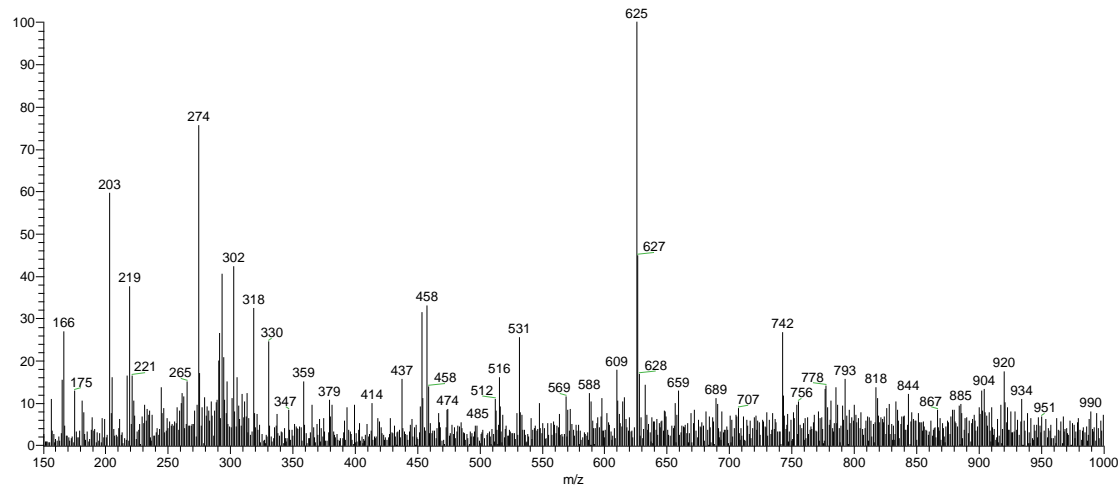


**Figure S4.** ESI-MS spectrum (positive mode) of the crude extract from GhcC1 1.2c (D).

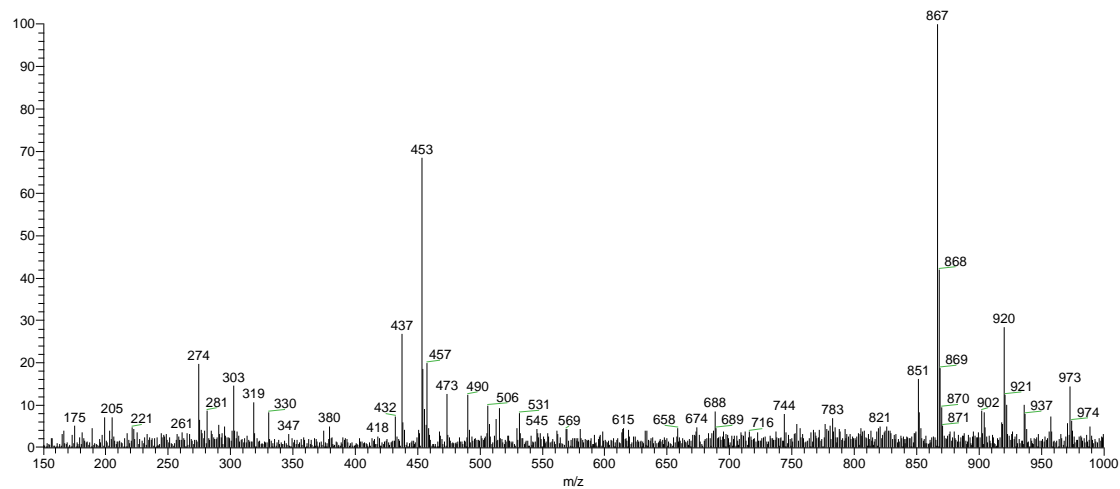


**Figure S5.** ESI-MS spectrum (positive mode) of the crude extract from *StspC2 1.2c* (E).

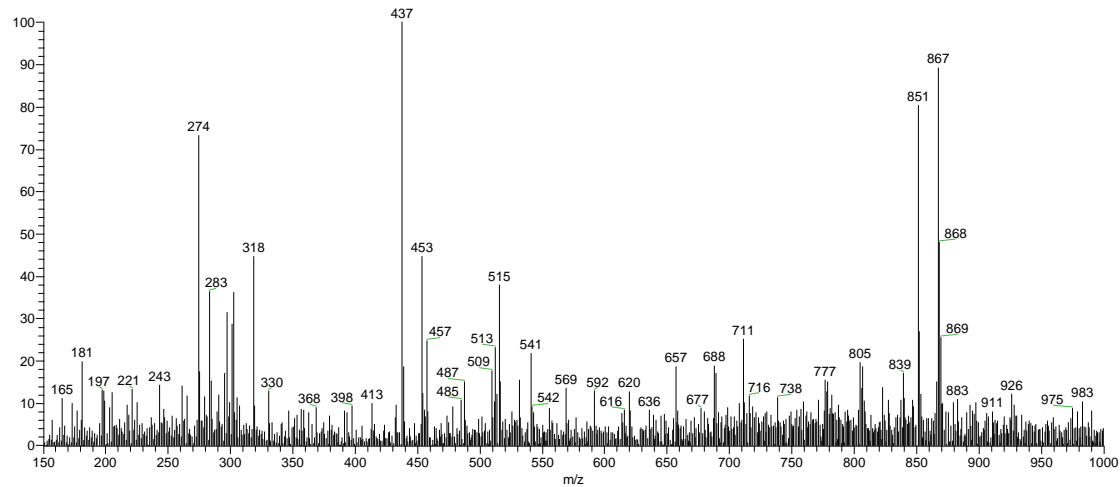


**Figure S6.** ESI-MS spectrum (positive mode) of the crude extract from *GhR1 2.1* (F).

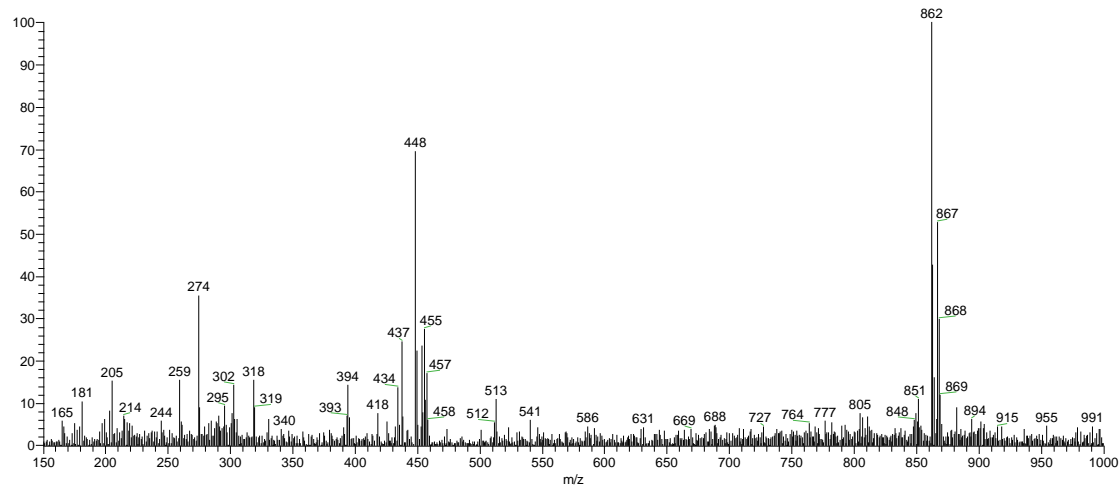


**Figure S7.** ESI-MS spectrum (positive mode) of the crude extract from *VrF1* 2.2(G).

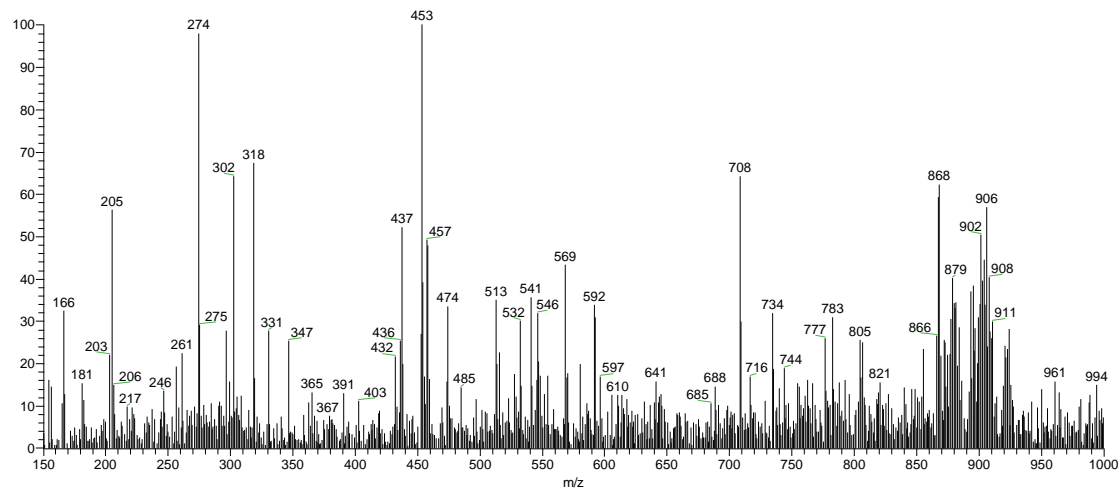


**Figure S8.** ESI-MS spectrum (positive mode) of the crude extract from *AspC2* 2.2 (H).

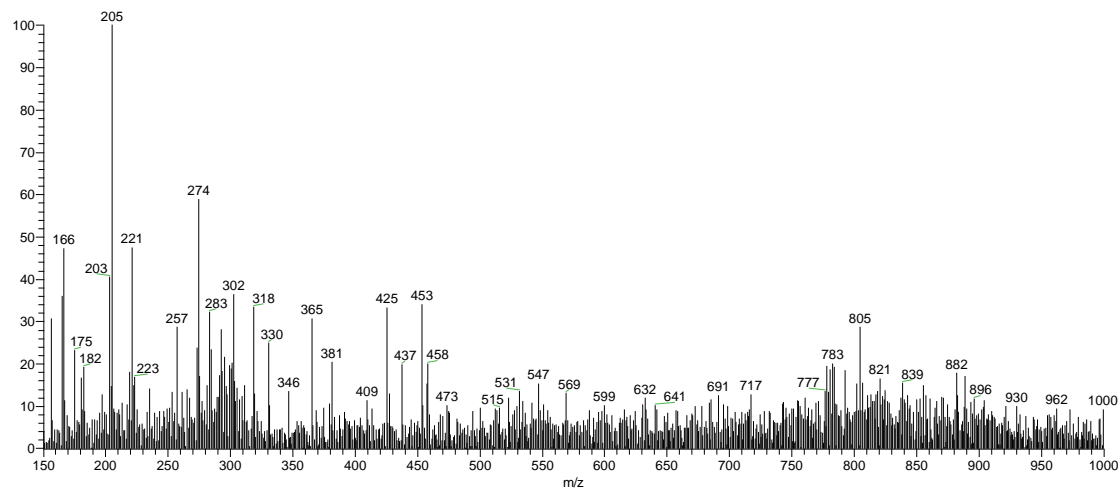


**Figure S9.** ESI-MS spectrum (positive mode) of the crude extract from *AnspG1* 2.2 (I).

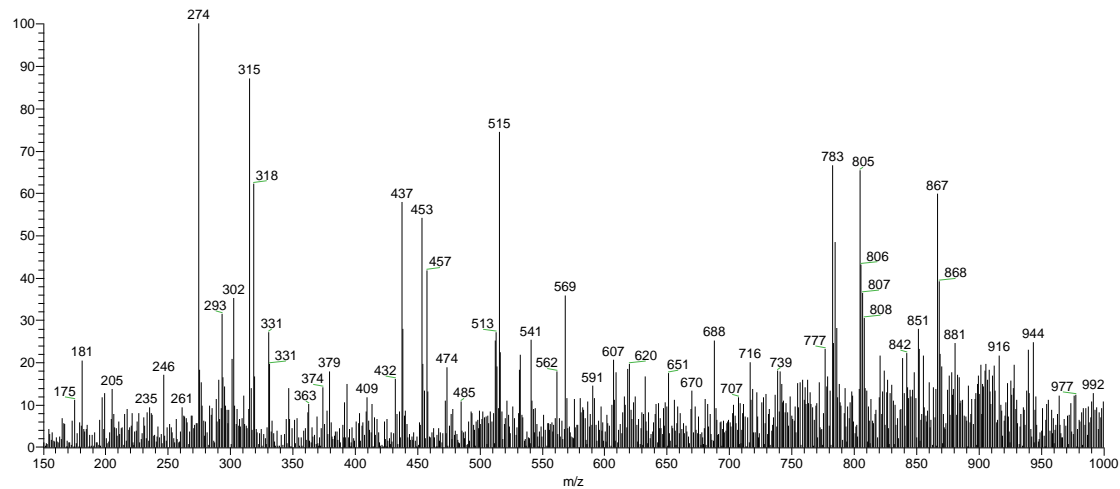


**Figure S10.** ESI-MS spectrum (positive mode) of the crude extract from *GhcR1 1.1b* (J).

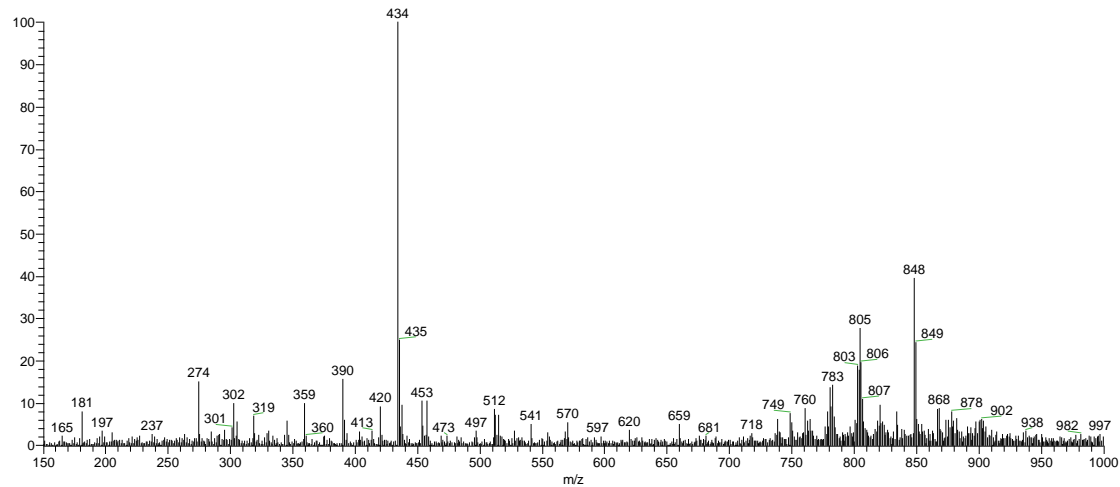


**Figure S11.** ESI-MS spectrum (positive mode) of the crude extract from *AnspG1 2.3b* (K).

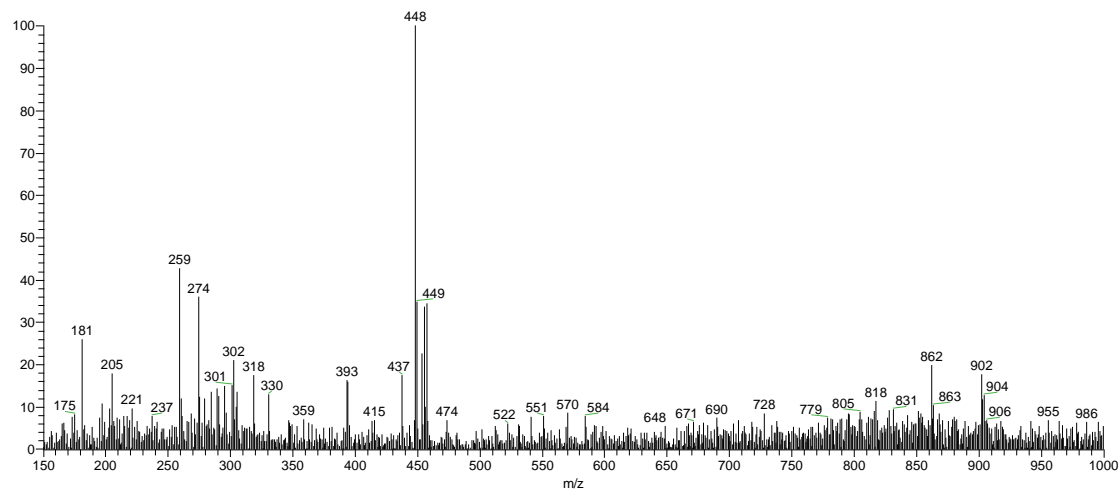


**Figure S12.** ESI-MS spectrum (positive mode) of the crude extract from VrF2 2.3 (L).

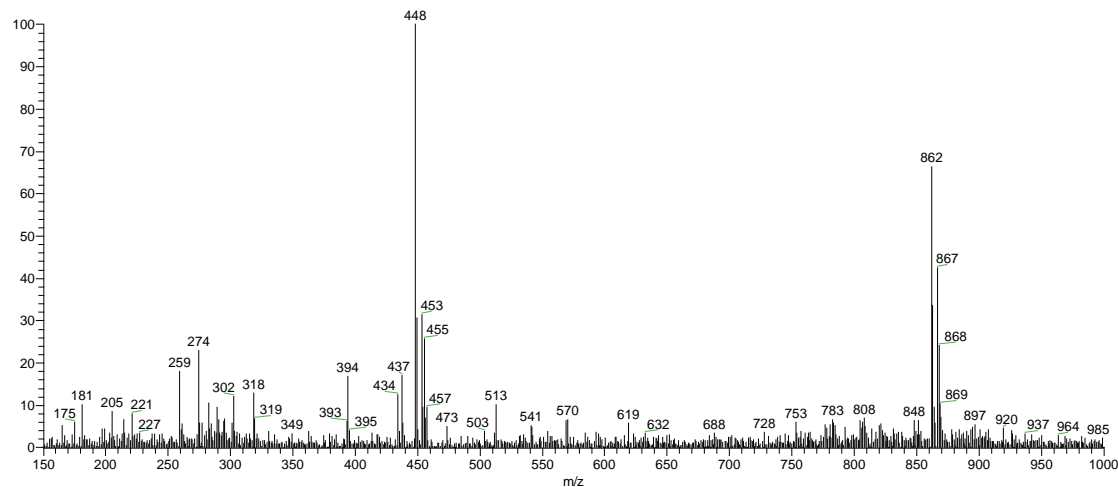


**Figure S13.** ESI-MS spectrum (positive mode) of the crude extract from VrC2 2.1c (M).

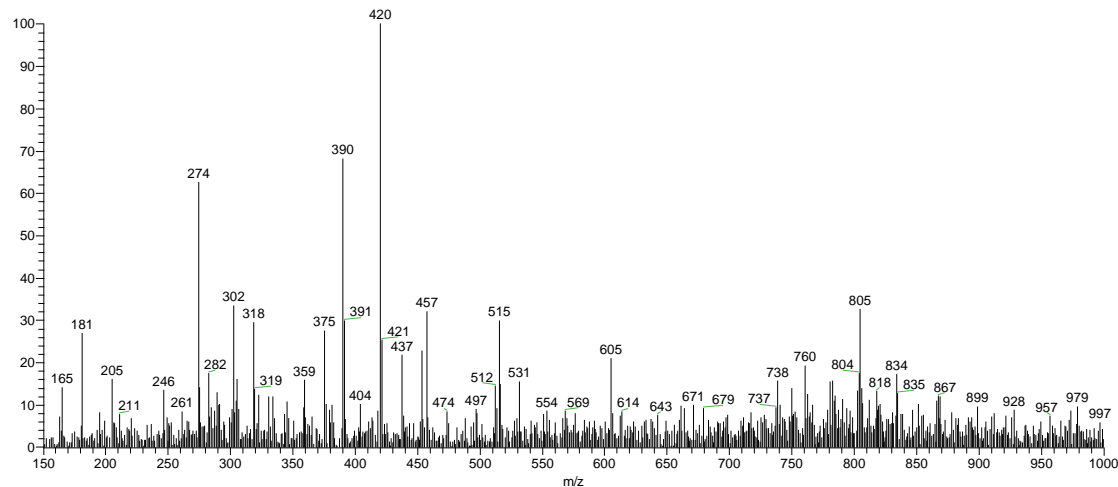


**Figure S14.** ESI-MS spectrum (positive mode) of the crude extract from GhG2 2.1 (N).

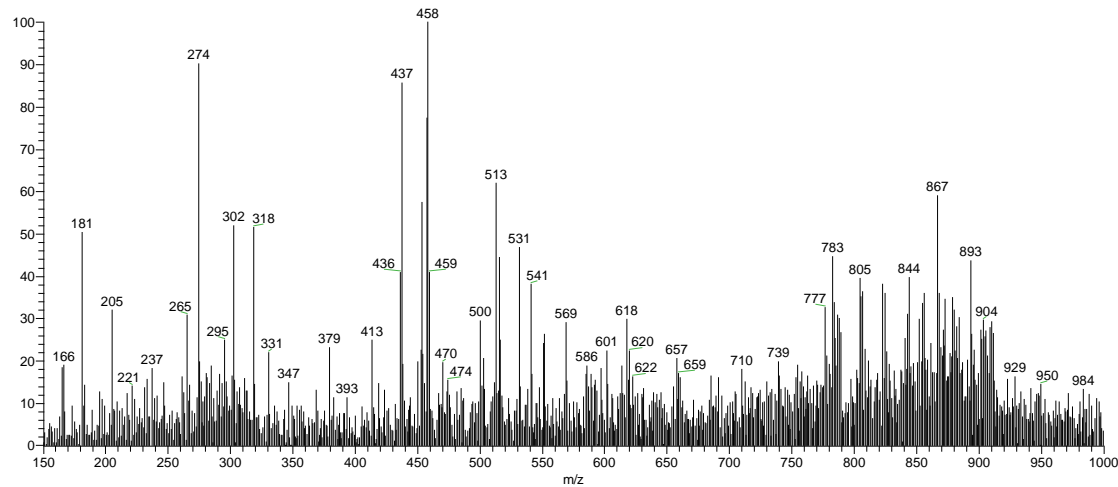


**Figure S15.** ESI-MS spectrum (positive mode) of the crude extract from AnspG1 2.3a (O).

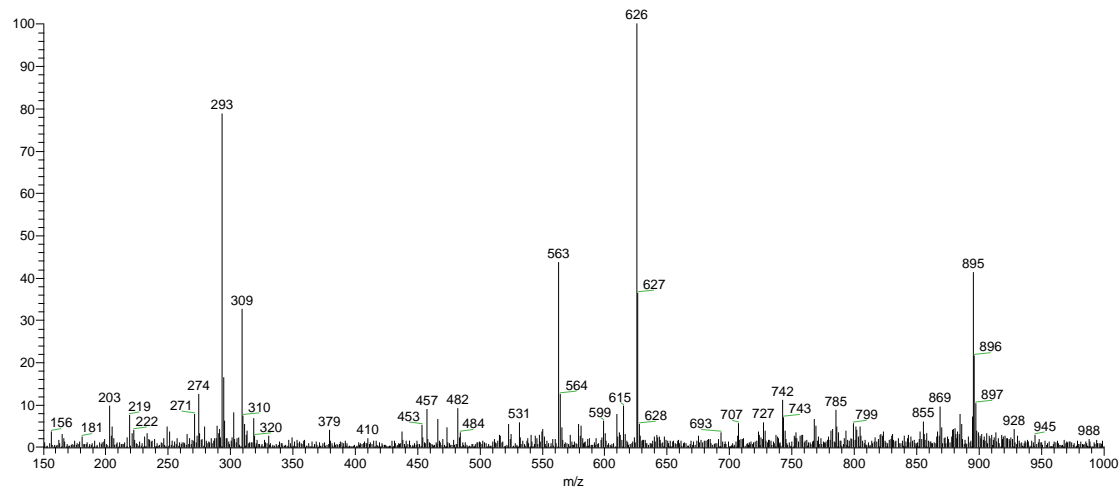


**Figure S16.** ESI-MS spectrum (positive mode) of the crude extract from AnspC2 3.1 (P).

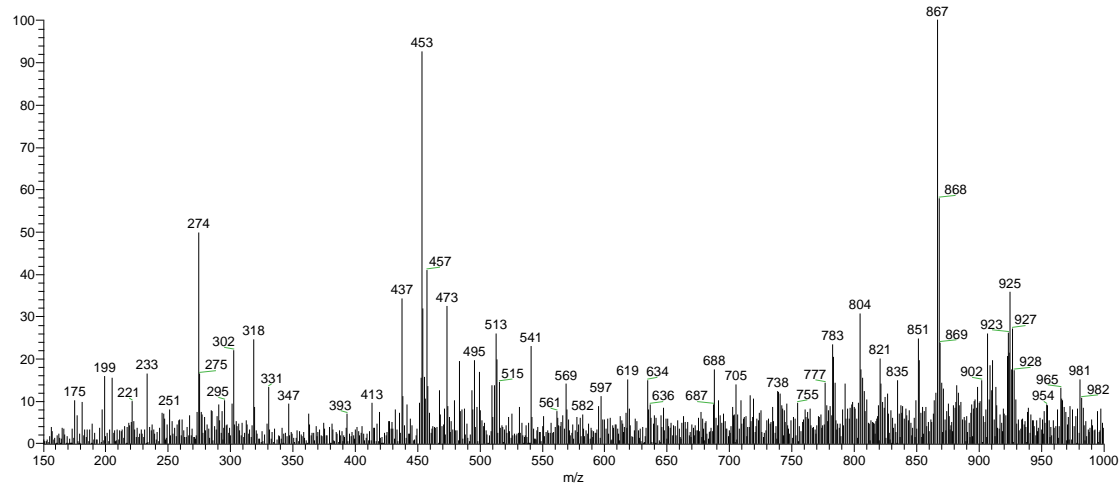


**Figure S17.** ESI-MS spectrum (positive mode) of the crude extract from GhR1 2.1a (Q).

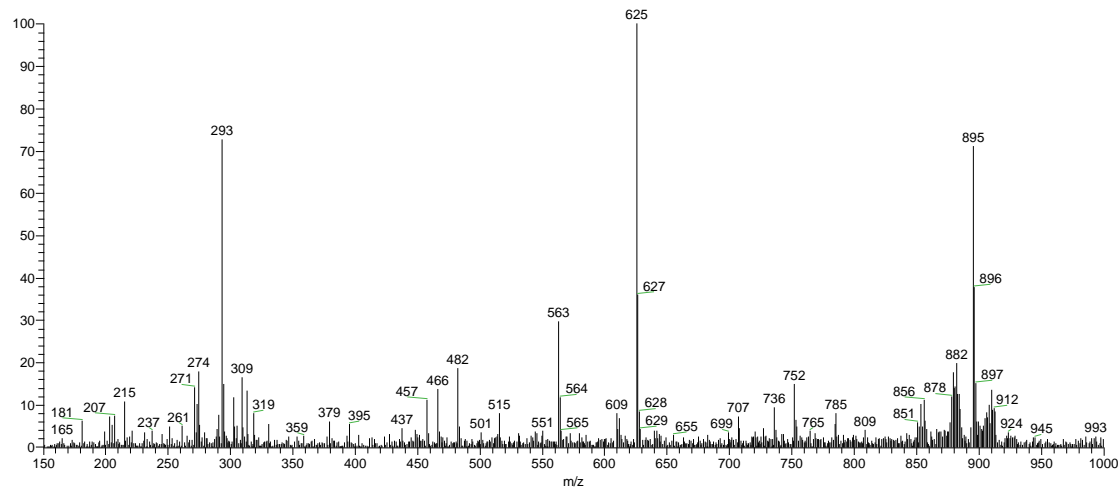


**Figure S18.** ESI-MS spectrum (positive mode) of the crude extract from GhcG3 2.2 (R).

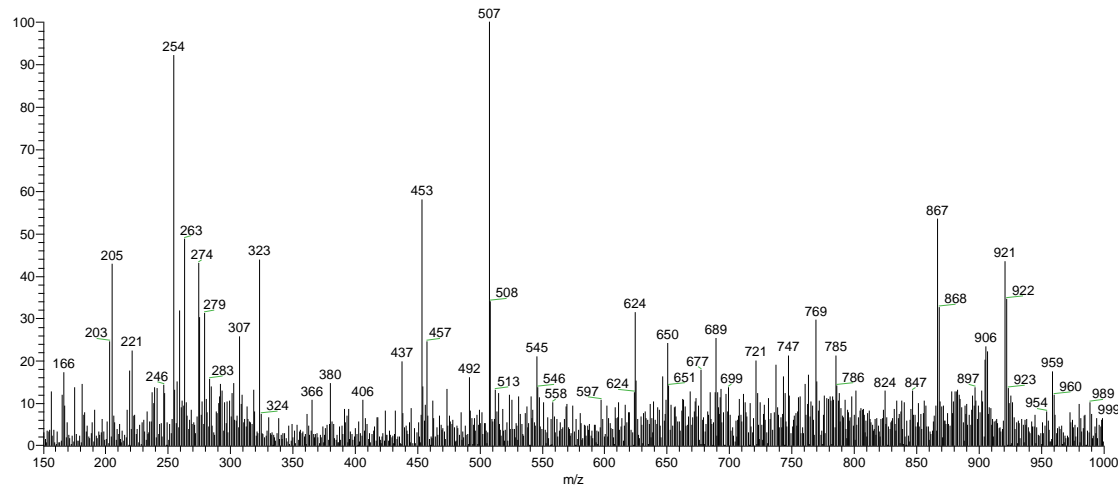


**Figure S19.** ESI-MS spectrum (positive mode) of the crude extract from GhR2 1.2b (S).

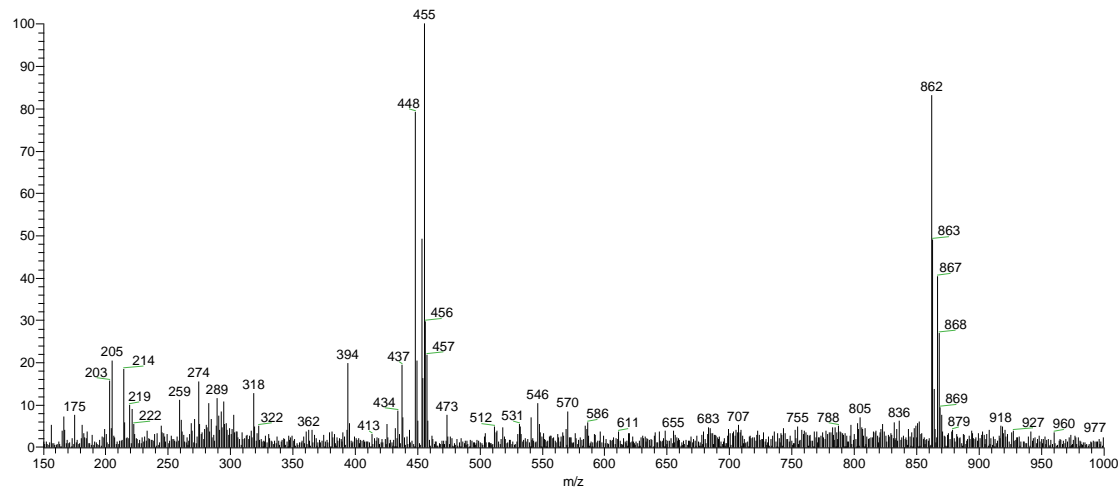


**Figure S20.** ESI-MS spectrum (positive mode) of the crude extract from *VrC2 1.2 (T)*.

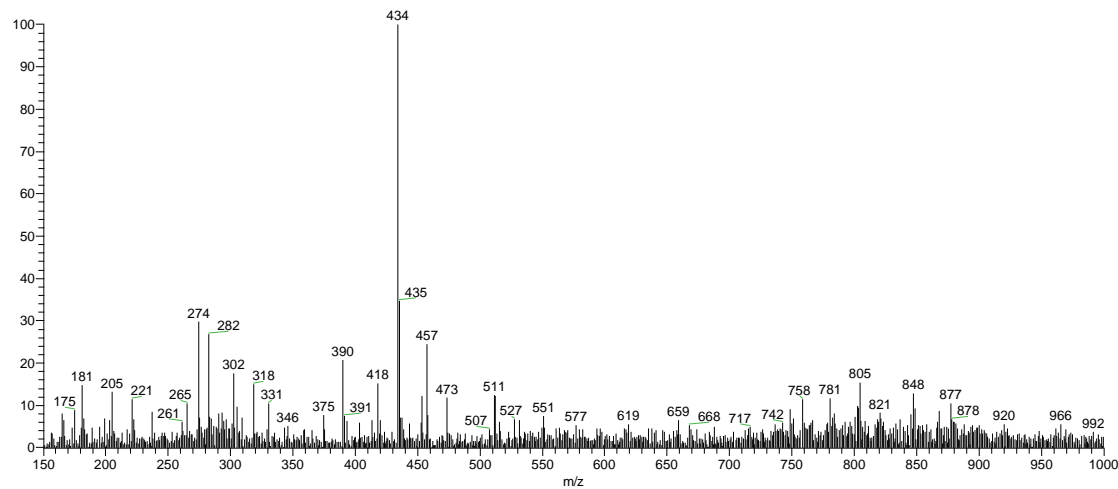


**Figure S21.** ESI-MS spectrum (positive mode) of the crude extract from *AnspcG1 3.3 (U)*.

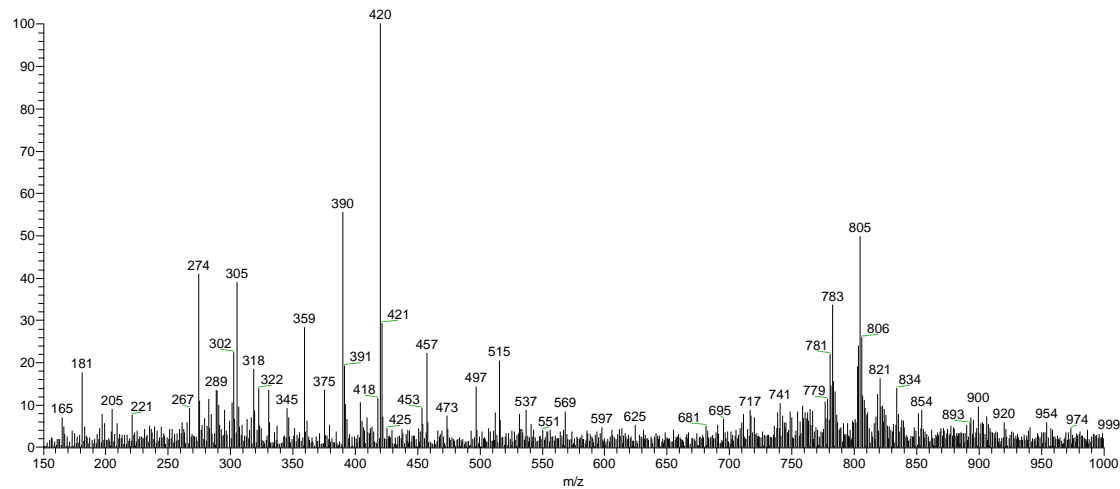


**Figure S22.** ESI-MS spectrum (positive mode) of the crude extract from GhcR3 2.2 (V).

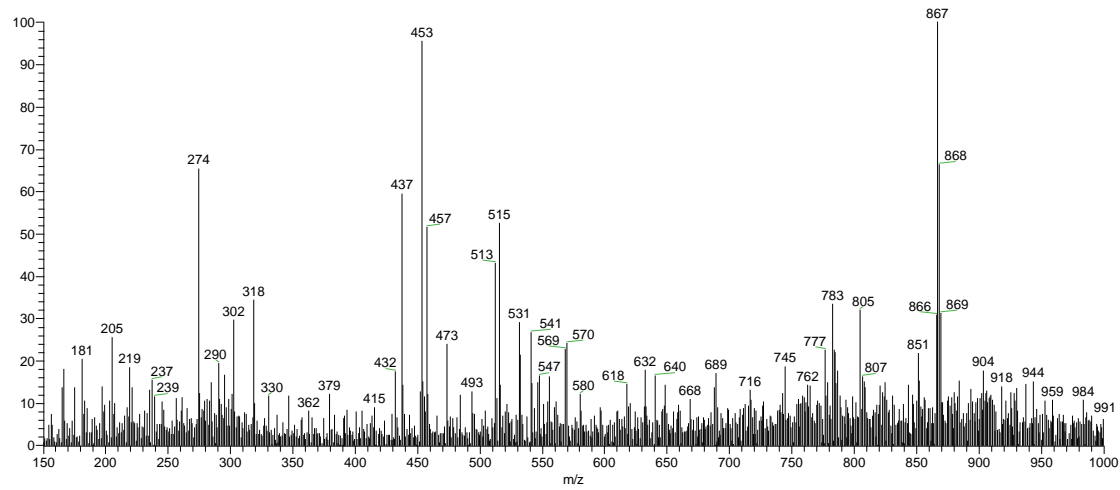


**Figure S23.** ESI-MS spectrum (positive mode) of the crude extract from GhG3 2.2c (W).

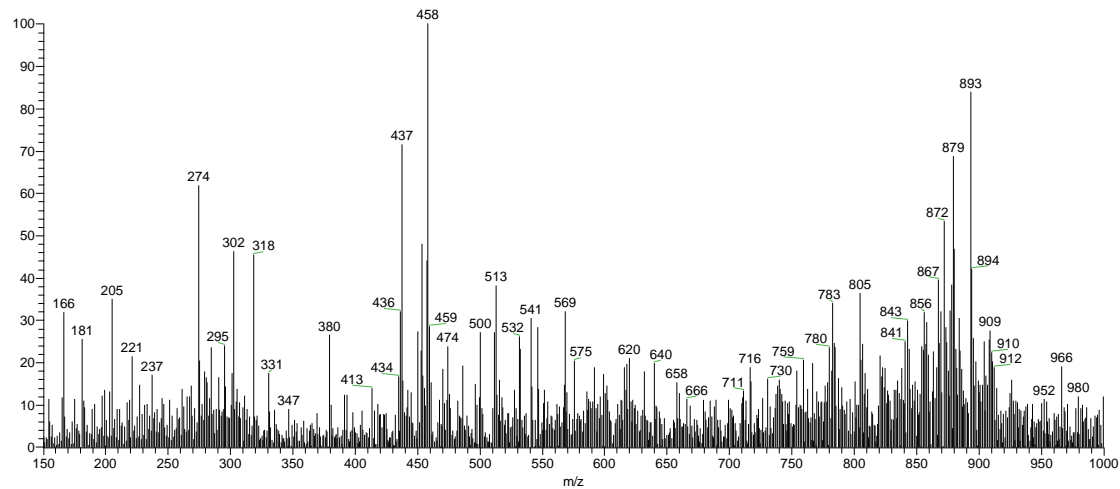


**Figure S24.** ESI-MS spectrum (positive mode) of the crude extract from EjC3 2.1a (X).

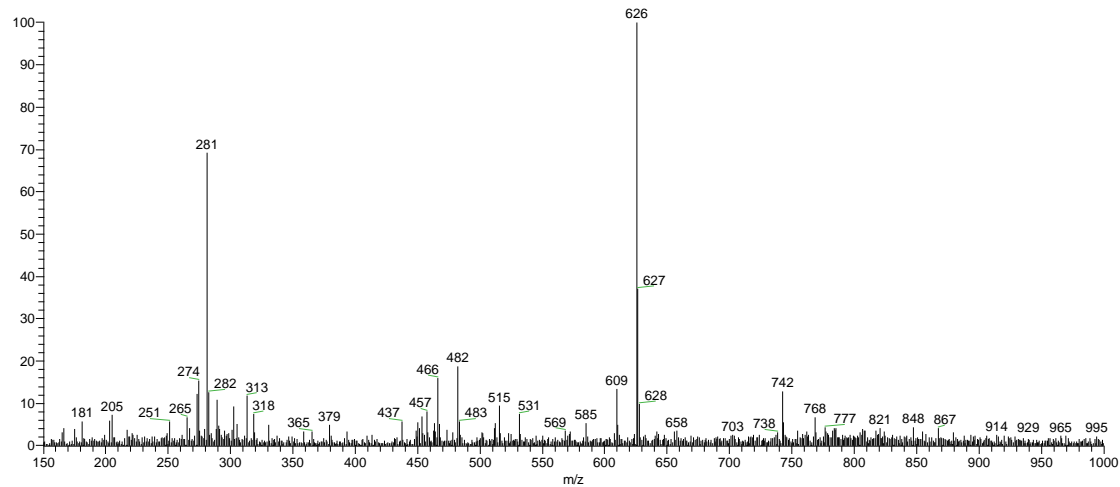


**Figure S25.** ESI-MS spectrum (positive mode) of the crude extract from GhcC2 2.2a (Y).

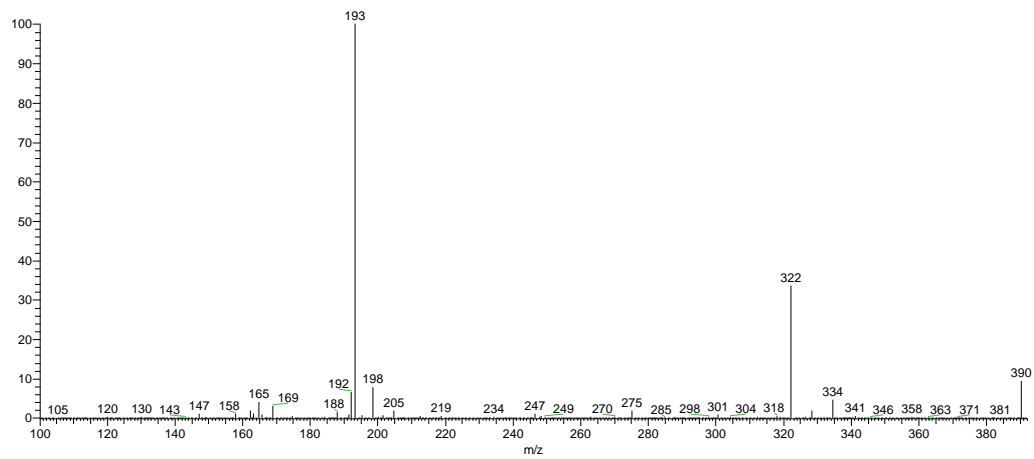


**Figure S26.** ESI-MS/MS spectrum (positive mode) of the ion at  $m/z$  390 present in the crude extract of GhcR3 2.2 (V).

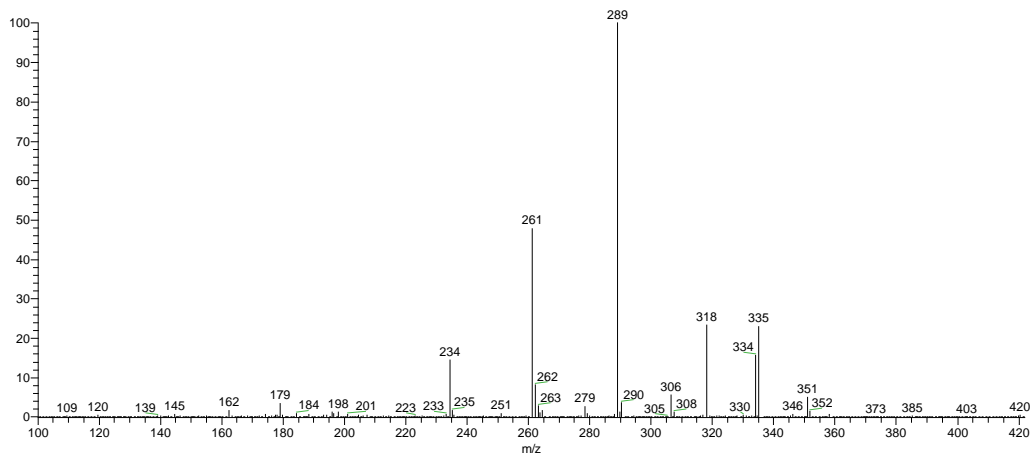


**Figure S27.** ESI-MS/MS spectrum (positive mode) of the ion at  $m/z$  420 present in the crude extract of GhcR3 2.2 (V).

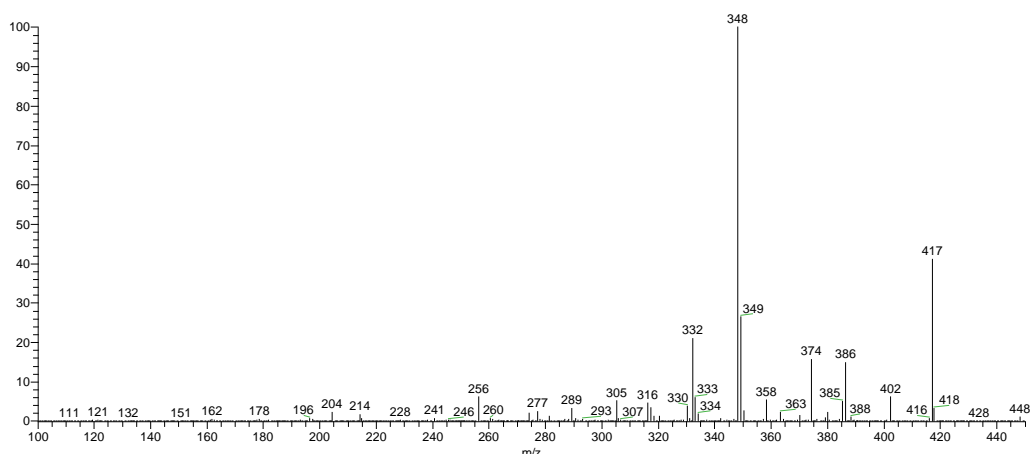


**Figure S28.** ESI-MS/MS spectrum (positive mode) of the ion at  $m/z$  448 present in the crude extract of VrC2 2.1c (M).

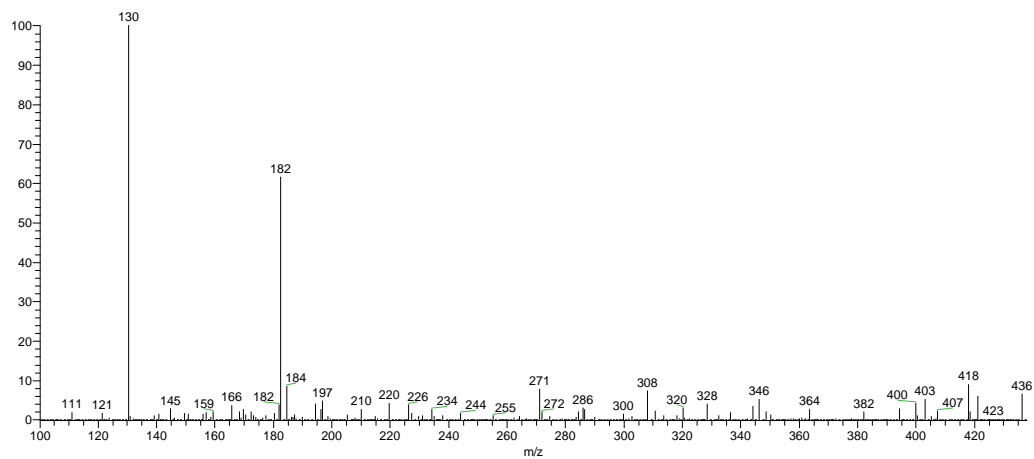


**Figure S29.** ESI-MS/MS spectrum (positive mode) of the ion at  $m/z$  436 present in the crude extract of AnspG1 2.3a (O).

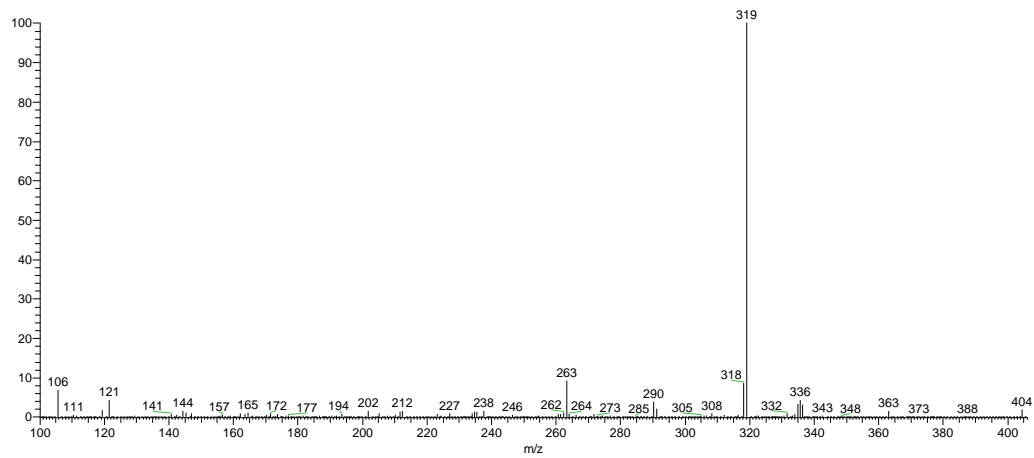


**Figure S30.** ESI-MS/MS spectrum (positive mode) of the ion at  $m/z$  404 present in the crude extract of GhcR3 2.2 (V).

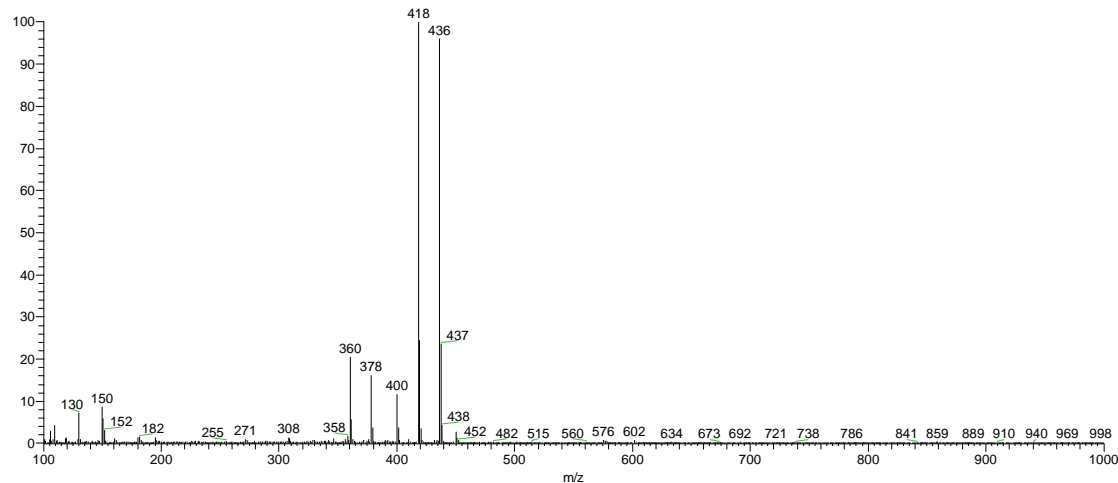


**Figure S31.** APCI-MS spectrum (positive mode) of the paxillin (**1**).

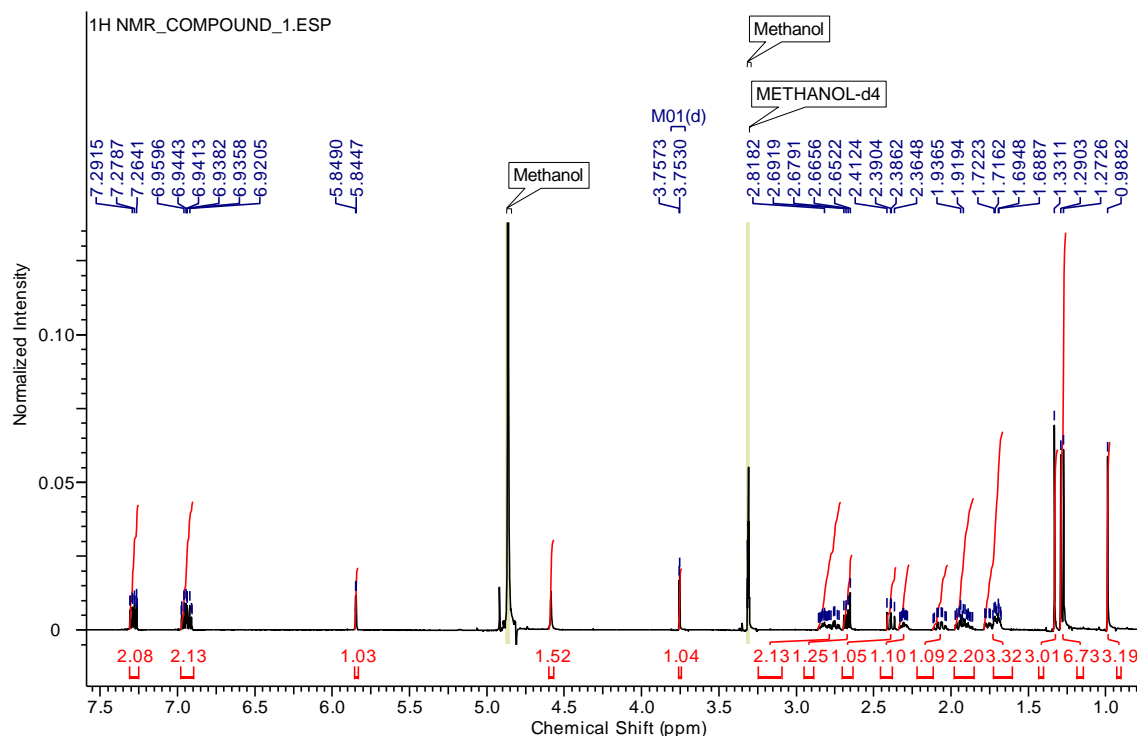


**Figure S32.**  $^1\text{H}$  NMR spectrum (500 MHz, MeOD) of the paxilline (**1**).

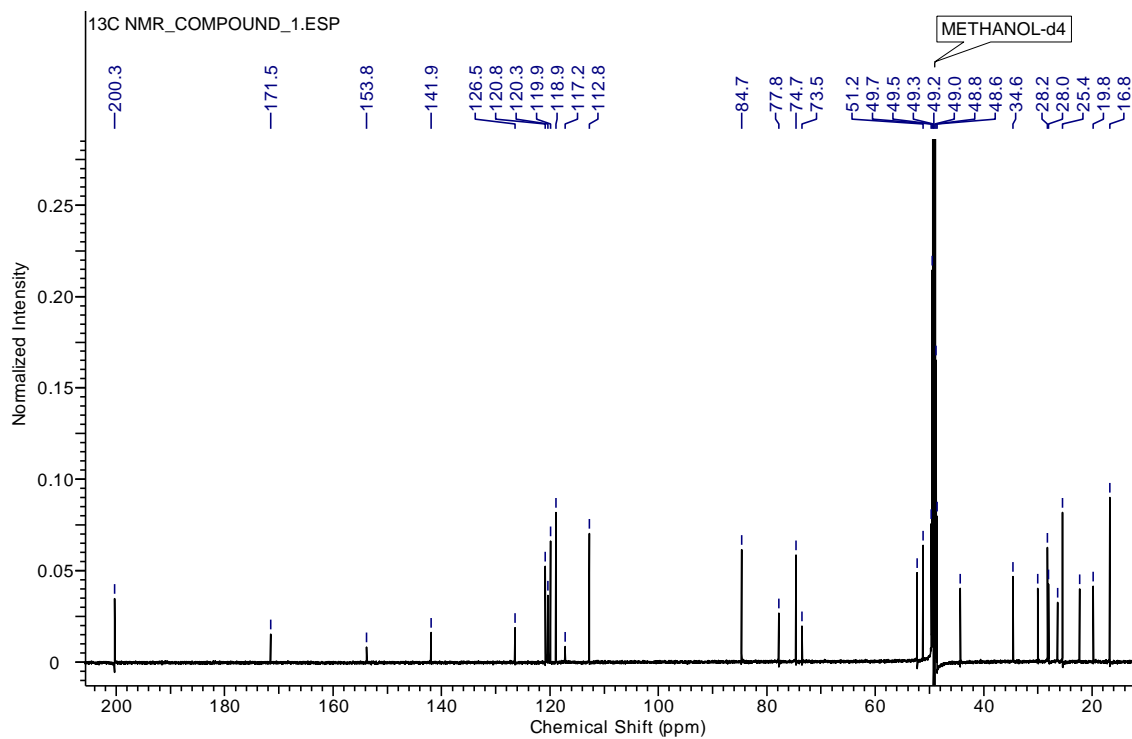


**Figure S33.**  $^{13}\text{C}$  NMR spectrum (125 MHz, MeOD) of the paxilline (**1**).

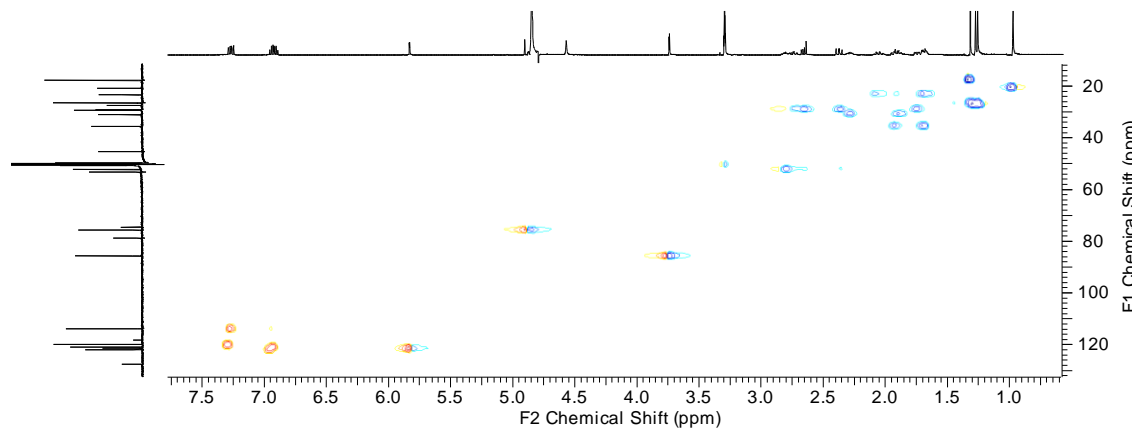


**Figure S34.**  $^1\text{H}$ - $^{13}\text{C}$  correlations observed by HSQC for the paxilline (**1**).

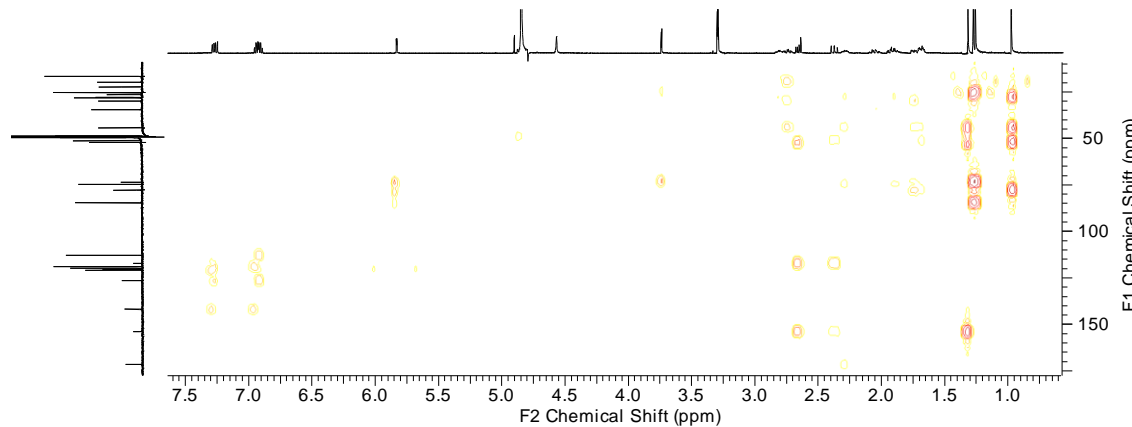


**Figure S35.**  $^1\text{H}$ - $^{13}\text{C}$  correlations observed by HMBC for the paxilline (**1**).

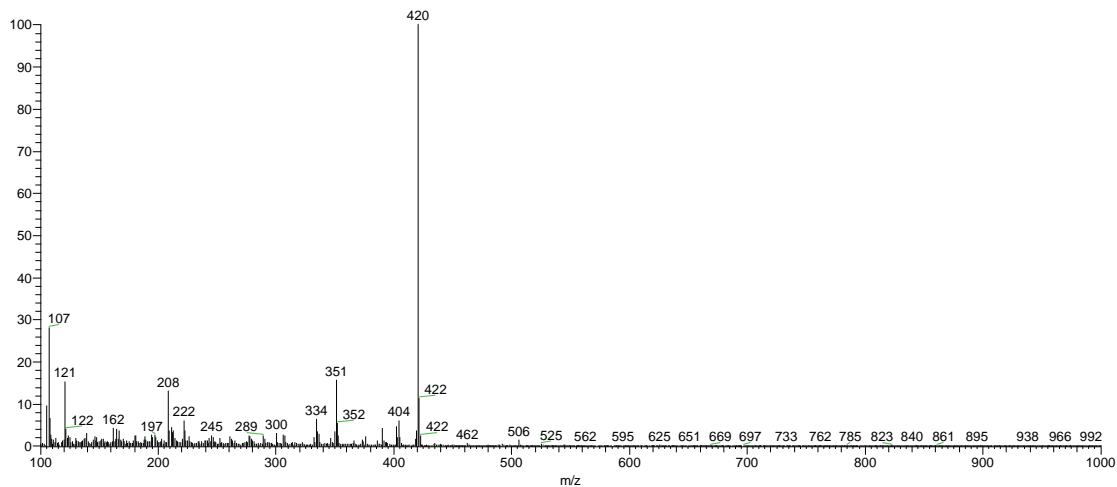


**Figure S36.** APCI-MS spectrum (positive mode) of the glandicoline B (**2**).

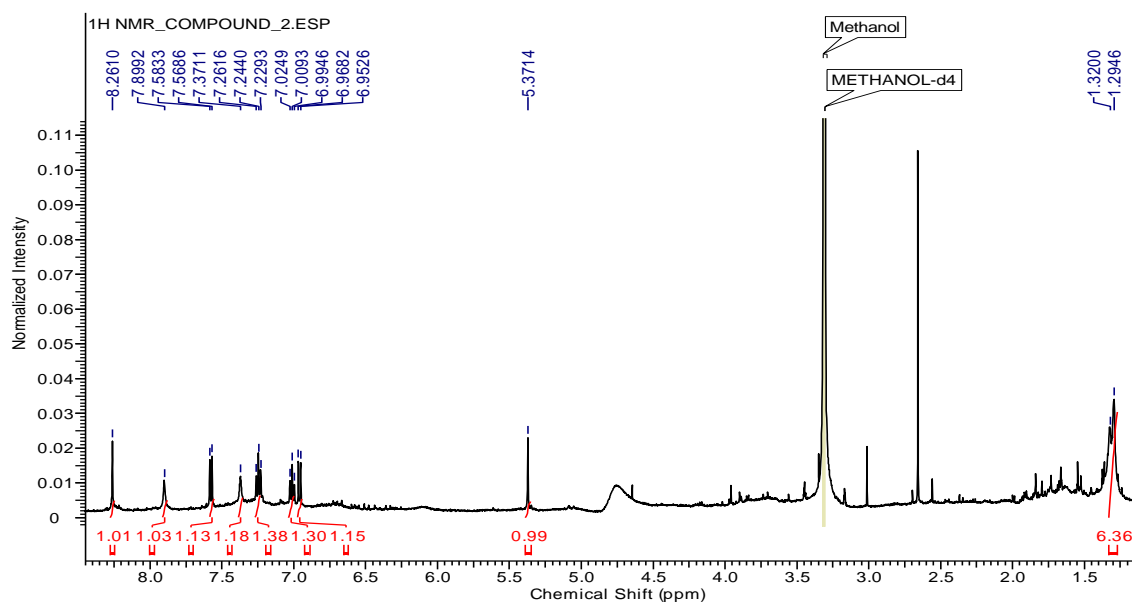


**Figure S37.**  $^1\text{H}$  NMR spectrum (500 MHz, MeOD) of the glandicoline B (**2**).

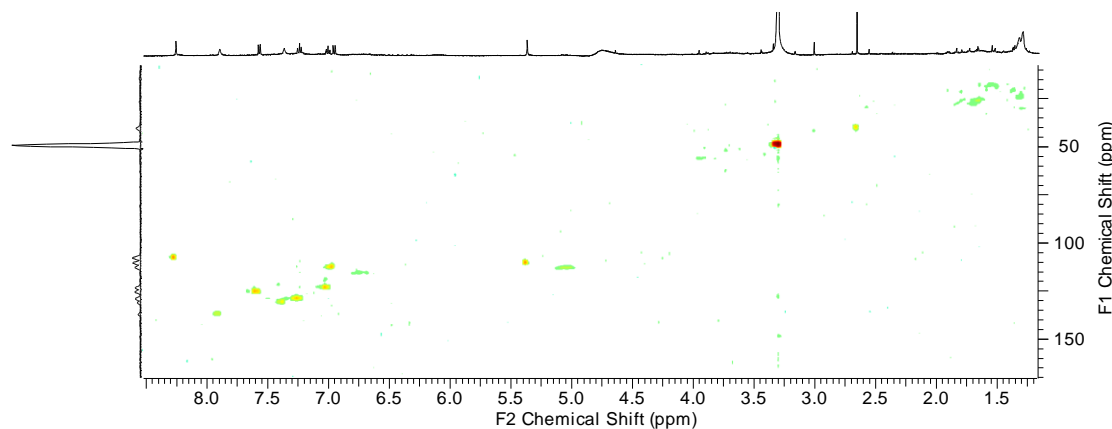


**Figure S38.** <sup>1</sup>H-<sup>13</sup>C correlations observed by HSQC for glandicoline B (**2**).

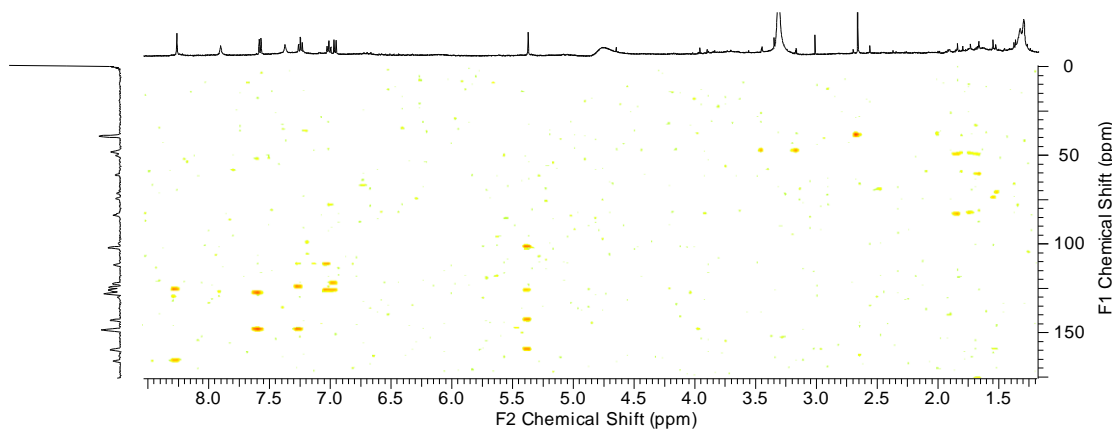


**Figure S39.** <sup>1</sup>H-<sup>13</sup>C correlations observed by HMBC for glandicoline B (**2**).

**Table 1S.** Assignment of <sup>1</sup>H and <sup>13</sup>C NMR data for the paxilline (**1**).

<b>paxilline (1)</b>		
<b>Position</b>	<sup>1</sup> H δ (mult., J in Hz) <sup>a</sup>	<sup>13</sup> C <sup>b</sup>
<b>1</b>	-	-
<b>2</b>	-	153.8
<b>3</b>	-	52.2
<b>4</b>	-	44.2
<b>5a</b>	1.76 (m)	28.03
<b>5b</b>	2.76 (dt, J = 13.6 and 5.2 Hz)	28.03
<b>6a</b>	1.89 (m)	29.9
<b>6b</b>	2.31 (m)	29.9
<b>7</b>	4.90 (m)	74.6
<b>8</b>	-	-
<b>9</b>	3.76 (d, J = 2.1 Hz)	84.6
<b>10</b>	-	200.2
<b>11</b>	5.85 (d, J = 2.1 Hz)	120.3
<b>12</b>	-	171.5
<b>13</b>	-	77.7

<b>14a</b>	1.69 ( <i>m</i> )	34.5
<b>14b</b>	1.94 ( <i>m</i> )	34.5
<b>15a</b>	1.71 ( <i>m</i> )	22.3
<b>15b</b>	2.07 ( <i>m</i> )	22.3
<b>16</b>	2.82 ( <i>m</i> )	51.2
<b>17a</b>	2.39 ( <i>dd</i> , <i>J</i> = 13.0 and 10.8 Hz)	28.2
<b>17b</b>	2.67 ( <i>m</i> )	28.2
<b>18</b>	-	117.2
<b>19</b>	-	126.4
<b>20</b>	7.30 ( <i>m</i> )	118.9
<b>21</b>	6.92 ( <i>m</i> )	119.8
<b>22</b>	6.96 ( <i>m</i> )	120.8
<b>23</b>	7.27 ( <i>m</i> )	112.7
<b>24</b>	-	141.9
<b>25</b>	1.33 ( <i>s</i> )	16.7
<b>26</b>	0.99 ( <i>s</i> )	19.7
<b>27</b>	-	73.4
<b>28</b>	1.27 ( <i>s</i> )	26.3
<b>29</b>	1.29 ( <i>s</i> )	25.4

<sup>a</sup>MeOD, 500 MHz; <sup>b</sup>MeOD, 125 MHz.**Table 2S.** Assignment of <sup>1</sup>H and <sup>13</sup>C NMR data for the glandicoline B (2).

Position	glandicoline B (1)	
	<sup>1</sup> H $\delta$ (mult., <i>J</i> in Hz) <sup>a</sup>	<sup>13</sup> C <sup>b</sup>
<b>1</b>	-	-
<b>2</b>	-	-
<b>3</b>	-	-
<b>3a</b>	-	-
<b>4</b>	7.57, ( <i>d</i> , <i>J</i> = 7.3 Hz)	125.4
<b>5</b>	7.01 ( <i>t</i> , <i>J</i> = 7.6 Hz)	123.3
<b>6</b>	7.24 ( <i>t</i> , <i>J</i> = 8.1 Hz)	129.1
<b>7</b>	6.96 ( <i>d</i> , <i>J</i> = 7.8 Hz)	112.7
<b>7a</b>	-	-
<b>8</b>	5.37 ( <i>s</i> )	110.4
<b>9</b>	-	-
<b>10</b>	-	-
<b>11</b>	-	-
<b>12</b>	-	-
<b>13</b>	-	-
<b>14</b>	-	-
<b>15</b>	8.26 ( <i>s</i> )	107.8
<b>16</b>	-	-
<b>17</b>	-	-
<b>18</b>	7.90 ( <i>s</i> )	137.2
<b>19</b>	-	-
<b>20</b>	7.37 ( <i>s</i> )	131.1
<b>21</b>	-	-
<b>22</b>	-	-
<b>23</b>	-	-
<b>24</b>	1.32 ( <i>s</i> )	-
<b>25</b>	1.29 ( <i>s</i> )	-

## 7. CAPÍTULO IV

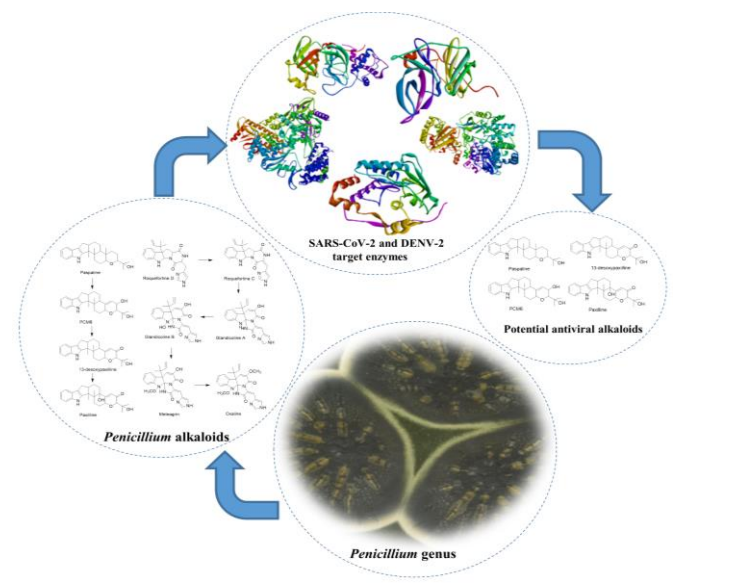
### **Alcalóides de linhagens de *Penicillium* da Amazônia como potenciais inibidores das enzimas alvo de SARS-CoV-2 e DENV-2<sup>4</sup>**

Francinaldo Araujo da Silva Filho, Felipe Moura Araujo da Silva, Gilvan Ferreira da Silva, Maria Lucia Belém Pinheiro, Sarah Raquel Silveira da Silva, Afonso Duarte Leão de Souza, Antonia Queiroz Lima de Souza

Este capítulo apresenta o estudo de docking molecular realizado com as moléculas isoladas anteriormente na parte química, sendo elas: paxillina, derivados da paxillina, glandicolina b e outros derivados da roquefortina. O trabalho se trata do teste dessas moléculas frente ao vírus da dengue tipo 2 e Sars-CoV-2, dois vírus que causam doenças que vem sendo pauta mundial recentemente. O presente trabalho demonstrou o potencial da paxillina e derivados como antiviral, enquanto a glandicolina e derivados da roquefortina, apesar de não terem apresentado atividade tão forte, apresentaram atividades moderadas. Esse capítulo ajuda a ressaltar o potencial dos alcalóides indólicos isolados de *Penicillium* endofíticos como antivirais, realçando a necessidade de conhecer a fundo a biodiversidade amazonica. Este capítulo abre espaço pra novas pesquisas *in silico* com essa classe de moléculas e também estudos *in vitro* para melhor entender a atividade das moléculas aqui estudadas e seus modos de ações, se confirmada *in vitro*.

---

<sup>4</sup>Este capítulo está na forma de artigo, formatado no modelo da revista e será submetido para publicação na *Journal of Brazilian Chemical Society* (ISSN 0887-2333)

**Graphical Abstract (GA)****GA Figure:**

**GA Text:** Molecular docking was used to investigate alkaloids previously reported from Amazon *Penicillium* strains, along with their related compounds, as potential inhibitors of SARS-CoV-2 and DENV-2 target enzymes.

## Alkaloids from Amazon *Penicillium* Strains as Potential Inhibitors of SARS-CoV-2 and DENV-2 Target Enzymes

***Francinaldo Araujo da Silva-Filho,<sup>a</sup> Felipe Moura Araujo da Silva,<sup>b</sup> Gilvan Ferreira da Silva<sup>f</sup>, Maria Lúcia Belém Pinheiro<sup>b</sup>, Sarah Raquel Silveira da Silva<sup>a</sup>, Afonso Duarte Leão de Souza,<sup>a,b,c</sup>and Antonia Queiroz Lima de Souza<sup>a,b,e,\*</sup>***

*<sup>a</sup>Programa de Pós-Graduação da Rede Bionorte, Universidade Federal do Amazonas (UFAM), 69077-000, Manaus, AM, Brazil*

*<sup>b</sup>Central Analítica - Centro de Apoio Multidisciplinar (CAM), Universidade Federal do Amazonas (UFAM), 69077-000, Manaus, AM, Brazil*

*<sup>c</sup>Departamento de Química (ICE), Universidade Federal do Amazonas (UFAM), 69077-000, Manaus, AM, Brazil*

*<sup>e</sup>Faculdade de Ciências Agrárias (FCA), Universidade Federal do Amazonas (UFAM), 69077-000, Manaus, AM, Brazil*

*<sup>f</sup>Embrapa Amazônia Ocidental, Empresa Brasileira de Pesquisa Agropecuária (EMBRAPA) Manaus, AM, Brazil*

\*e-mail: [antoniaqueiroz@ufam.edu.br](mailto:antoniaqueiroz@ufam.edu.br)

ORCID ID <http://orcid.org/0000-0001-5602-8617>

**Abstract**

COVID-19 and dengue fever are critical diseases caused by RNA viruses that led to thousands of deaths around the world. The co-infection of SARS-CoV-2 and dengue virus has been alerted as a dangerous combination for the health system in Brazil. On the other hand, the protease and RNA-dependent RNA polymerase (RdRp) enzymes from both viruses, and methyltransferase (Mtase) from dengue, have been identified as critical target for antiviral drug design due to its importance in the viral replication stages. Therefore, we performed a docking study to investigate several alkaloids previously reported from Amazon *Penicillium* strains, such as paxilline, roquefortine C, glandicoline A and B, oxaline, and their related compounds, as potential inhibitors of SARS-CoV-2 and DENV-2 target enzymes. The docking analysis indicated paxilline and their related compounds as potential inhibitors for target enzymes of SARS-CoV-2 and dengue virus, based on binding affinity and interactions in the presumed active sites. Overall, these results are in agreement with previously reported data about the antiviral potential of paxilline and reinforce the hypothesis that *Penicillium* alkaloid can play a key role as inhibitors of the SARS-CoV-2 and dengue virus target enzymes.

**Keywords:** co-infection, COVID-19, dengue, molecular docking, paxilline

## Introduction

The coronavirus disease 2019 (COVID-19) pandemic, caused by the emerging severe acute respiratory syndrome coronavirus 2 (SARS-CoV-2), is currently a major worldwide health crisis.<sup>1</sup> According to the World Health Organization (WHO),<sup>2</sup> by early May 2021, there had been about 153 million cases and more than 3,2 million deaths worldwide since late 2019, causing among other things massive economic consequences and social disruption.<sup>1</sup> While this global crisis rightly demands the world's attention, many other diseases are still on the rise and the risk increasing further. This is the case of dengue virus (DENV) fever, a disease transmitted by *Aedes* mosquitoes, whose symptoms are really close to COVID-19 and its incidence has increased over the past years.<sup>3-5</sup> In Brazil, the largest ever dengue epidemic was in 2020, with more than 1.4 million cases and 554 deaths and has already more than 200,000 cases and 43 deaths from January to May in 2021, according to Health Information Platform for the Americas (PLISA).<sup>6</sup> More recently, the possibility of co-infection between SARS-CoV-2 and dengue viruses has been alerted as a dangerous combination for the health system,<sup>7,8</sup> especially regarding the co-infection with dengue virus serotype 2, one of the most aggressive and the responsible for the most cases of severe hemorrhagic dengue diseases.<sup>9</sup>

Nowadays, a great effort has been made to identify antiviral agents with potential to inhibit important nonstructural proteins (nsp) for SARS-CoV-2 and dengue viruses, such as proteases, polymerases and methyltransferases, which are of great importance in the viral replication stages.<sup>10,11</sup> While proteases are responsible to cleave the junctions between the genome to facilitate the translation in the host ribosome, the polymerases are responsible to replicate the RNA genome.<sup>12</sup> On the other hand, the methyltransferases are involved in the regulation of several cellular processes, including DNA replication and repair.<sup>11</sup>

For SARS-CoV-2, a 3-chymotrypsin-like cysteine protease, named main protease (Mpro), along with the RNA-dependent RNA polymerase (RdRp) have been highlighted as important targets in computational strategies, such as molecular docking (MD).<sup>13,14</sup> On the other hand, a typical serine protease, named NS2B-NS3 protease, along with RdRp and methyltransferase (MTase), both belong to NS5 protein, are also important target enzymes for DENV-2 in MD approaches.<sup>15-17</sup> MD is a key tool in structural molecular biology and computer-assisted drug design and represents a powerful, rational and low-cost tool.<sup>18</sup> MD can be used to perform virtual screening on several types of compounds, and propose structural hypotheses of how the ligands interacts with the active site of the target, thus supporting the design and screening of new antiviral agents against COVID-19 and dengue fever.<sup>13,16</sup>

There are several kinds of natural products already described as antiviral, such as terpenes, flavonoids and alkaloids.<sup>19</sup> Regarding alkaloids, the indole-type showed great potential against several types of viruses, such as Coxsackie virus B3, influenza virus A/Hanfang/359/95(H3N2), human immunodeficiency virus (HIV) and hepatitis C virus (HCV).<sup>20,21</sup> This type of alkaloid can be found not only in plants, but also in fungi genera, such as *Aspergillus* and *Penicillium*.<sup>19,22,23</sup> Regarding *Penicillium*, a recent study showed the potential of several Amazon strains, including *P. paxilli*, *P. rubens*, *P. chrysogenum*, and *P. oxalicum*, to produce several indole alkaloids.<sup>24</sup>

Thus, in the present study, we screened some indole alkaloids previously reported in Amazon *Penicillium* strains, along with their related compounds, using molecular docking, in order to test them as potential inhibitors of the SARS-CoV-2 Mpro and RdRp as well as DENV-2 protease, RdRp and MTase.

## Experimental

### Ligand preparation

Initially, the three-dimensional (3D) structures of paxilline, glandicoline A and B, roquefortine C, and oxaline, all previously reported from Amazon *Penicillium* strains,<sup>24</sup> and their related compounds<sup>25,26</sup> (Figure 1), were downloaded from PubChem database (<https://pubchem.ncbi.nlm.nih.gov/>) in spatial data file (SDF) format. The ligand preparation was according to a previously reported methodology<sup>13</sup> All the structures were subjected to geometry optimization by the semi-empirical method PM7 using MOPAC2016 software,<sup>27</sup> being the results saved in protein data bank (PDB) format. Finally, the ligands were prepared for molecular docking using AutoDock Tools.<sup>28</sup> Briefly, Gasteiger charges were added for each compound and non-polar hydrogens were merged, being the results saved in protein data bank, partial charge (Q), & Atom Type (T) (PDBQT) format.

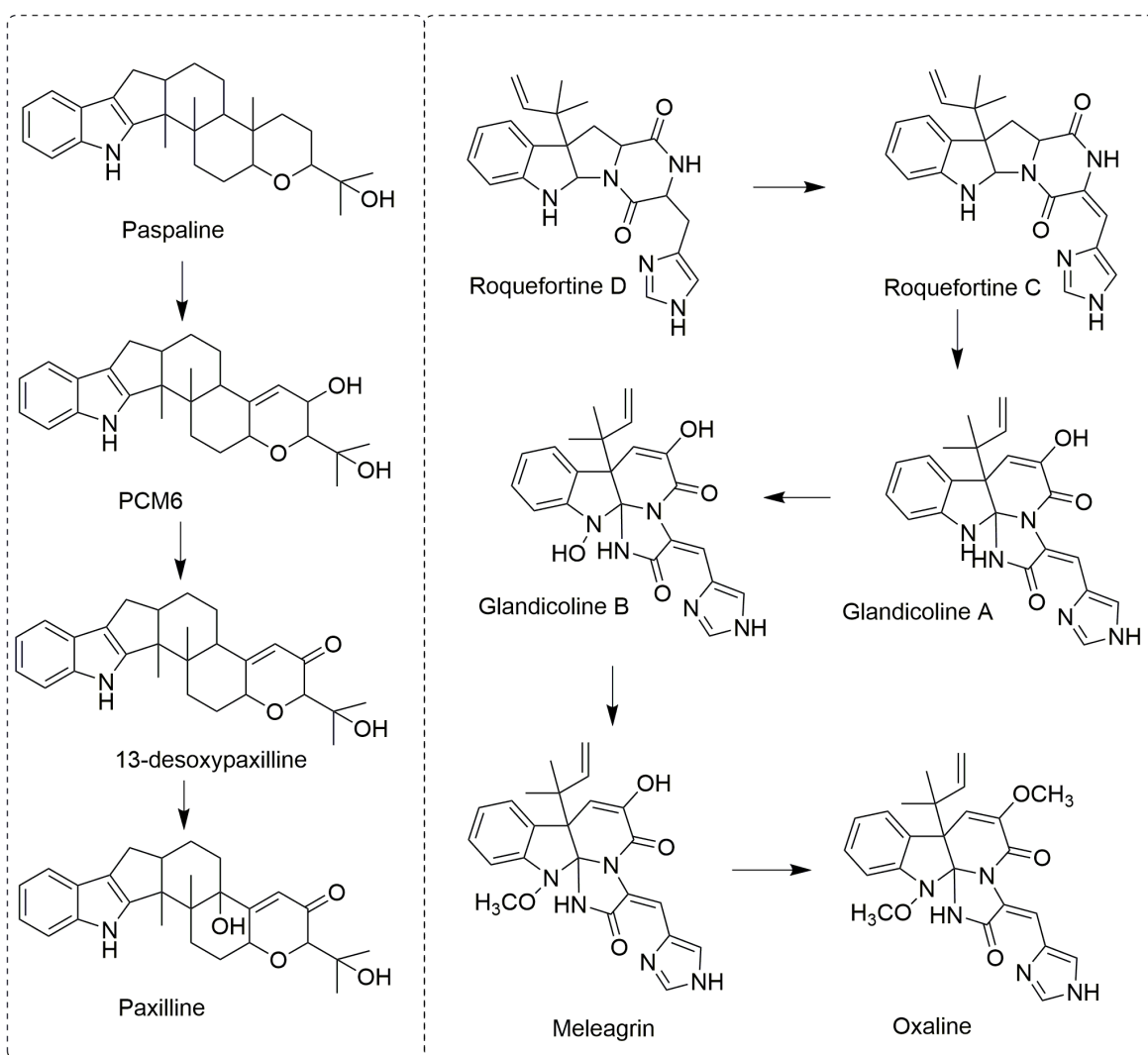


**Figure 1.** Chemical structures of alkaloids previously reported in Amazon *Penicillium* strains and their related compounds.

#### Protein preparation

The 3D crystal structures of the SARS-CoV-2 Mpro (PDB ID: 6W63) and RdRp (PDB ID: 6M71), along with DENV-2 protease (PDB ID: 2FOM), RdRp and MTase (PDB ID: 4V0Q), were retrieved from Research Collaboratory for Structural Bioinformatics Protein Data Bank (RCSB PDB) (<http://www.rcsb.org>) in PDB format. These receptors were prepared using AutoDock Tools.<sup>28</sup> Briefly, water molecules and bound ligands were removed, polar hydrogens and Kollman charges were added, and the

non-polar hydrogens were merged. For all proteins, the protonation states of the amino acid residues were automatically generated by Autodock tools based on the protonation states of the original 3D crystal structures. Finally, the results were saved as PDBQT format.

### Docking simulations

The docking simulations were as previously reported for SARS-CoV-2 Mpro and RdRp.<sup>13</sup> On the other hand, the grid box was centered at the presumed active sites for DENV-2 protease, RdRp and MTase.<sup>29</sup> For DENV-2 protease, the grid box was centered at the coordinate of x = -4.186, y = -10.090, and z = 15.204, with x = 25 Å, y = 25 Å, and z = 25 Å size. The DENV-2 RdRp grid box was centered at the coordinate of x = 33.355, y = 166.152, and z = 23.044, with x = 27 Å, y = 27 Å, and z = 27 Å size. Finally, the DENV-2 MTase grid box was centered at the coordinate of x = 21.223, y = 130.043, and z = 23.907, with x = 27 Å, y = 27 Å, and z = 27 Å size. The interactions and the binding affinity of the protein-ligand complex were predicted via a docking process using Autodock Vina.<sup>30</sup> The results were viewed with the Discovery Studio software.<sup>31</sup>

## Results and Discussion

Docking analysis with SARS-CoV Mpro revealed that paxilline (-8.5 kcal/mol), PCM6 (-8.5 kcal/mol), 13-desoxypaxilline (-8.5 kcal/mol), and paspalline (-8.4 kcal/mol), the top-scored inhibitors (Table 1), have close binding free energies to the previously described inhibitor X77 (redocking binding free energy = -8.4 kcal/mol, RMSD = 0.8909 Å), which suggests the establishment of favorable interactions for these ligand-Mpro complexes. On the other hand, the alkaloids from the roquefortine/oxaline pathway presented binding free energies ranging -7.2 to 7.8 kcal/mol, with glandicoline

B presenting the worse binding free energy. Docking analysis also revealed key interactions, such as hydrogen bonds and  $\pi$ -based interactions, between these compounds and the Mpro active site (Figure 2). For x77, hydrogen bonds were observed with Gly143, Cys145, His163, and Glu166, along with  $\pi$ -sulfur interactions with Met49 and Cys145,  $\pi$ -alkyl interaction with Cys145,  $\pi$ -amide interaction with Leu141, and  $\pi$ - $\pi$  interaction with His41 (Supplementary data). On the other hand, for top-scored inhibitors, several  $\pi$ -based interactions, such as  $\pi$ -alkyl,  $\pi$ - $\pi$ , and  $\pi$ -cation were observed with His41 from the catalytic dyad.<sup>13</sup> Moreover alkyl interactions were observed between paxilline, PCM6, and 13-desoxypaxilline and Cys145 also from the catalytic dyad.<sup>13</sup> All top-scored inhibitors presented  $\pi$ -sulphur interactions with Met165. On the other hand, PCM6, 13-desoxypaxilline and paspaline presented hydrogen bonds with Thr26, Thr24, and Asn142, respectively. The main observed interactions between all tested compounds and SARS-CoV-2 Mpro are summarized in Table 1.

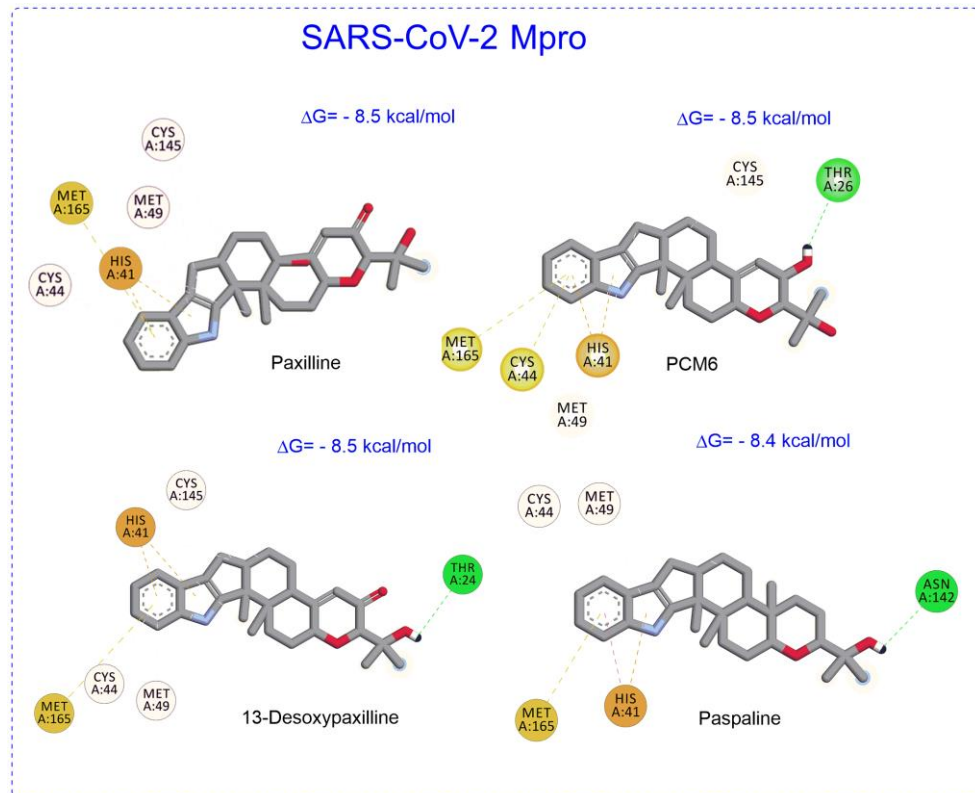


**Figure 2.** Main interactions observed for the top-scored inhibitors of SARS-CoV-2 Mpro by docking analysis.

**Table 1.** Docking analysis data for previously reported Amazon *Penicillium* alkaloids and their related compounds.

Compounds	Protein (PDB ID)	Binding energy (kcal/mol)	Main interactions
Paxilline	SARS-CoV-2 Mpro (6W63)	-8.5	PS (Met165), PAI (His41, Cys44, Met49), PP (His41), PC (His41), AI (Cys145)
PCM6	SARS-CoV-2 Mpro (6W63)	-8.5	HB (Thr26), PS (Cys44, Met165), PAI (His41, Met49), PP (His41), PC (His41), AI (Cys145)
13-desoxypaxilline	SARS-CoV-2 Mpro (6W63)	-8.5	HB (Thr24), PS (Met165), PAI (His41, Cys44, Met49), PP (His41), PC (His41), AI (Cys145)
Paspaline	SARS-CoV-2 Mpro (6W63)	-8.4	HB (Asn142), PS (Met165), PAI (Met49), PP (His41), PC (His41), AI (Cys44)
Roquefortine C	SARS-CoV-2 Mpro (6W63)	-7.8	HB (Glu166, Gln189), PS (Cys145), PAI (Met49), PP (His41), PC (His41), PA (Glu166), PSi (His41), AI (Cys44, Met49, Met165)
Roquefortine D	SARS-CoV-2 Mpro (6W63)	-7.5	HB (Gln189, Gln192), PS (Cys44), PAI (Met49, Pro168), AI (Pro 168)
Oxaline	SARS-CoV-2 Mpro (6W63)	-7.5	PAI (Cys145), AI (Met49)
Glandicoline A	SARS-CoV-2 Mpro (6W63)	-7.4	HB (His164, Glu166, Gln189), PS (Met49), PAI (His41, Pro168), AI (Met49, Met165)
Meleagrin	SARS-CoV-2 Mpro (6W63)	-7.3	PAI (Met49), AI (Met49), PDH (His41)
Glandicoline B	SARS-CoV-2 Mpro (6W63)	-7.2	PAI (Met165), PP (His41), AI (Met49)
Paspaline	SARS-CoV-2 RdRp (7M71)	-8.4	HB (Trp800), PAI (Lys621), AI (Lys798), PDH (Lys621)
13-desoxypaxilline	SARS-CoV-2 RdRp (7M71)	-8.3	HB (Asp623), PA (Glu811)
Paxilline	SARS-CoV-2 RdRp (7M71)	-8.2	HB (Glu796, Cys799), PAI (Phe766), AI (Ala771)
PCM6	SARS-CoV-2 RdRp (7M71)	-7.8	HB (Asp760, Asp761), PA (Asp760)
Roquefortine C	SARS-CoV-2 RdRp (7M71)	-7.6	HB (Arg553, Tyr619, Lys621, Asp623), PAI (Arg624), PC (Arg553), AI (Lys798)
Glandicoline A	SARS-CoV-2 RdRp (7M71)	-7.5	HB (Arg553, Lys621, Cys622, Asp623, Asp760), PAI (Lys621, Arg624), PC (Arg553), PA (Asp760)
Roquefortine D	SARS-CoV-2 RdRp (7M71)	-7.3	HB (Lys621, Cys622, Asp623, Arg 624), PC (Arg553), PA (Asp618), AI (Pro620, Lys798)
Meleagrin	SARS-CoV-2 RdRp (7M71)	-7.2	HB (Asp760), PAI (Lys798), PA (Glu811)
Glandicoline B	SARS-CoV-2 RdRp (7M71)	-7.1	HB (Lys621, Asp623), PAI (Arg624), PC (Arg553)
Oxaline	SARS-CoV-2 RdRp (7M71)	-6.7	HB (Arg553, Asp623, Asn691), AI (Lys621), PDH (Lys621)
PCM6	DENV2 protease (2FOM)	-9.5	HB (Asp75, Gly151, Asn152, Gly153), PAI (His51), PSi (Leu128), AI (Leu128, Pro132)
13-desoxypaxilline	DENV2 protease (2FOM)	-9.4	HB (His51, Gly153), PSi (Leu128), AI (Leu128, Pro132)
Paxilline	DENV2 protease (2FOM)	-9.4	HB (Gly 153), PSi (Leu128), AI (Leu128, Pro132), PDH (Tyr161)
Paspaline	DENV2 protease (2FOM)	-9.3	HB (Asp75), PAI (His41, Pro132), PSi (Leu128), AI (Leu128, Tyr161)
Glandicoline B	DENV2 protease (2FOM)	-8.8	HB (Asp75, Ser125, Gly153), PAI (Pro132), PC (Arg54), PSi (Leu128), AI (Leu128, Tyr161)
Roquefortine C	DENV2 protease (2FOM)	-8.7	HB (His51, Val52), PAI (Ile36, Val52, Arg54), AI (Ala49, Ala56)
Glandicoline A	DENV2 protease (2FOM)	-8.5	HB (Asp75, Gly153), PAI (Pro132), PP (His51), PC (Arg54), PSi (Leu128), AI (Leu128, Tyr161)
Roquefortine D	DENV2 protease (2FOM)	-8.2	HB (His51, Val52), PAI (Ile36, Val52, Arg54), AI (Ala49)
Meleagrin	DENV2 protease (2FOM)	-7.8	HB (Asp75, Gly153), PAI (His51, Leu128, Tyr150), AI (Leu128, Pro132)
Oxaline	DENV2 protease (2FOM)	-7.8	HB (Gly153), PAI (His41, Tyr150), PP (His51), PC (Arg54), PSi (Leu128), AI (Leu128, Pro132)
13-desoxypaxilline	DENV2 RdRp (4V0Q)	-8.7	PAI (Ile691), PA (Asp532), AI (Pro707)
Paxilline	DENV2 RdRp (4V0Q)	-8.6	PAI (Ile691), PA (Asp532), AI (Pro707)
Paspaline	DENV2 RdRp (4V0Q)	-8.3	HB (Gln602, Tyr606), PAI (His798, Tyr606), PA (Asp663), AI (Cys709, Ile797)
Glandicoline B	DENV2 RdRp (4V0Q)	-7.9	HB (Ser661, Asp663, Cys709, His798), PP (Tyr606), PA (Asp664)
Roquefortine D	DENV2 RdRp (4V0Q)	-7.8	HB (Ser661, Cys709, His798), PAI (Tyr606, Ile797)
PCM6	DENV2 RdRp (4V0Q)	-7.8	HB (Ser710), PAI (Ile691), PA (Asp532), AI (Pro707)
Roquefortine C	DENV2 RdRp (4V0Q)	-7.8	HB (Asp538, Asn609, Asp663), PAI (Tyr606, Ile797, His798), AI (Cys709)
Glandicoline A	DENV2 RdRp (4V0Q)	-7.8	HB (Ser661, Asp663, Cys709, His798), PP (Tyr606), PA (Asp664)
	DENV2 RdRp (4V0Q)	-7.3	

Meleagrin	DENV2 RdRp (4VOQ)	-7.0	HB (Asp532, Asp690, Lys698), PAI (Ile691, Pro707), PP (Trp700), AI (Lys689, Ile691), PDH (Gln695)
Oxaline	DENV2 MTase (4VOQ)	-11.0	HB (Cys709, Ser710), PAI (Cys709), PA (Asp663)
13-Desoxypaxilline	DENV2 MTase (4VOQ)	-11.0	HB (Asp146), PP (His110), PSi (Ile147), PAI (Lys105, His110, Val132)
Paxilline	DENV2 MTase (4VOQ)	-10.5	HB (Glu111), PP (His110), PSi (Ile147), PAI (Lys105, His110, Val132)
PCM6	DENV2 MTase (4VOQ)	-10.5	HB (Asp146), PSi (Ile147), PAI (Lys105, His110, Val132)
Paspaline	DENV2 MTase (4VOQ)	-8.6	HB (Ser56), PP (His110), PSi (Ile147), PAI (Lys105, His110, Val132)
Roquefortine C	DENV2 MTase (4VOQ)	-8.4	HB (Arg57, Lys61, Asp146)
Glandicoline B	DENV2 MTase (4VOQ)	-8.3	HB (Gly109, Asp146, Gly148, Lys180), PP (His110), PC (Lys180), PAI (Lys105, Ile 147)
Glandicoline A	DENV2 MTase (4VOQ)	-7.9	HB (Asp146, Gly 148, Lys180), PP (His110), PC (Lys180), PAI (Lys105, Ile 147)
Roquefortine D	DENV2 MTase (4VOQ)	-7.8	HB (His110, Val132, Gly1148), PSi (Lys105, Ile147)
Meleagrine	DENV2 MTase (4VOQ)	7.2	HB (Cys82, Glu111, Gly148, Lys180), PA (Glu111), PAI (His110)
Oxaline	DENV2 MTase (4VOQ)		PA (Glu111), PC (Lys61), PAI (Arg211)

<sup>a</sup>HB – hydrogen bond, PS – π-sulfur, PAI – π-alkyl, PP – π-π, PC – π-cation, PA – π-anion, PSi – π-sigma, AI – alkyl, PDH – π donor hydrogen bond

Docking analysis with SARS-CoV-2 RdRp revealed paspaline (-8.4 kcal/mol), 13-desoxypaxilline (-8.3 kcal/mol), paxilline (-8.2 kcal/mol), and PCM6 (-7.8 kcal/mol) as top-scored inhibitors (Table 1). Similarly to the Mpro molecular docking, alkaloids from the roquefortine/oxaline pathway presented minor binding free energies (-6.7 to -7.6 kcal/mol), with oxaline presenting the worse binding free energy. For top-scored inhibitors, the hydrogen bonds interactions were dominant to these compounds (Figure 3). However, just PCM6 presented interactions with the catalytic residues Asp760 and Asp761 from motif C.<sup>13</sup> The main observed interactions between all tested compounds and SARS-CoV-2 RdRp are summarized in Table 1.

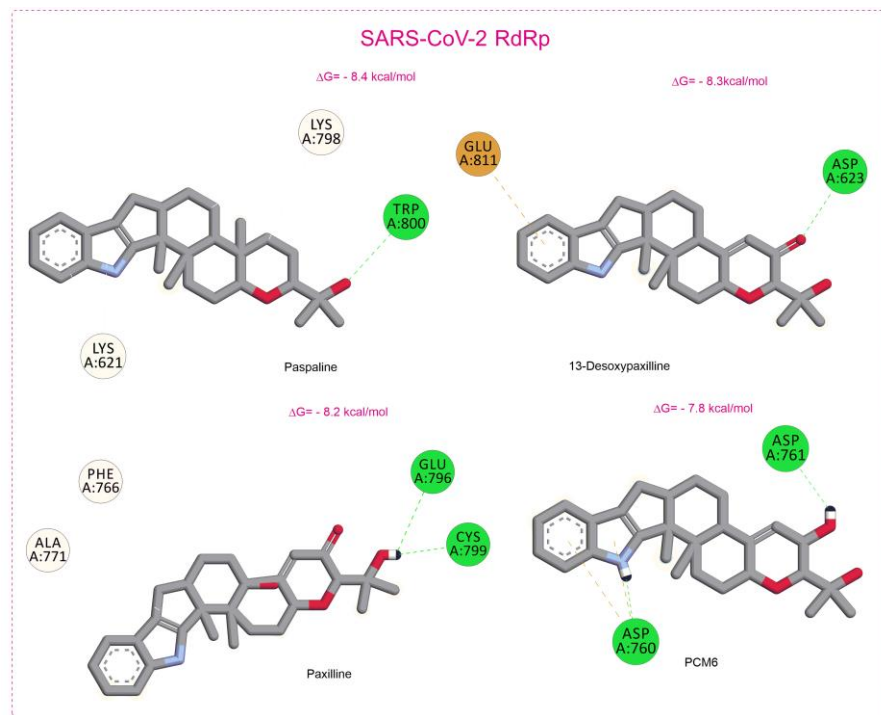


**Figure 3.** Main interactions observed for the top-scored inhibitors of SARS-CoV-2 RdRp by docking analysis.

Docking analysis with DENV-2 protease revealed that PCM6 (-9.5 kcal/mol), 13-desoxypaxilline (-9.4 kcal/mol), paxilline (-9.4 kcal/mol), and paspaline (-9.3 kcal/mol), the top-scored inhibitors, have close binding free energies (Table 1). Similarly to the SARS-CoV-2 Mpro molecular docking, alkaloids from the roquefortine/oxaline pathway presented minor binding free energies (-7.8 to -8.8 kcal/mol). Regarding to the observed interactions in the presumed active site of DENV-2 protease, hydrogen bonds,  $\pi$ -sigma, and  $\pi$ -alkyl interactions were dominant to the top-scored inhibitors (Figure 4). For PCM6 and paspaline, hydrogen bond with Asp75 and  $\pi$ -alkyl interaction with His51, both from the catalytic tryad,<sup>29</sup> were observed. On the other hand, 13-desoxypaspaline presented hydrogen bond with His51 from the catalytic tryad. The main observed interactions between all tested compounds and DENV-2 protease are summarized in Table 1.

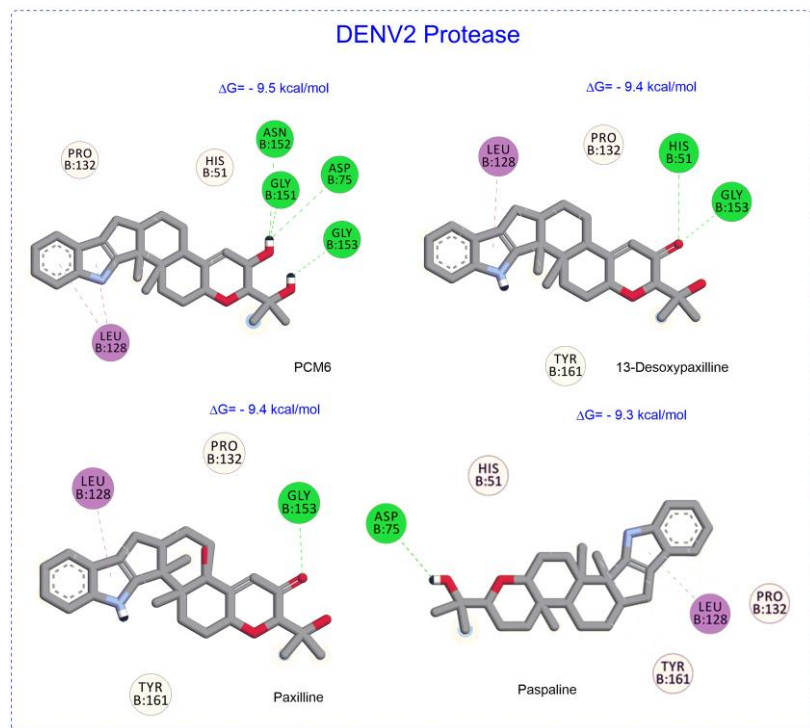


**Figure 4.** Main interactions observed for the top-scored inhibitors of DENV-2 protease by docking analysis.

Docking analysis with DENV-2 RdRp (redocking performed with S-adenosyl-L-homocysteine at MTase active site, RMSD = 0.7881) revealed that 13-desoxypaxilline (-8.7 kcal/mol), paxilline (-8.6 kcal/mol), paspalline (-8.3 kcal/mol), and glandicolin B (-7.9 kcal/mol) were the top-scored inhibitors (Table 1). Surprisingly, PCM6 (-7.8 kcal/mol) presented binding free energy close to glandicoline A (-7.8 kcal/mol), roquefortine C (-8.7 kcal/mol), and roquefortine D (-7.9 kcal/mol). Similarly to docking with SARS-CoV-2 RdRp and DENV-2 protease, oxaline presented the worse binding free energy (-7.0 kcal/mol).

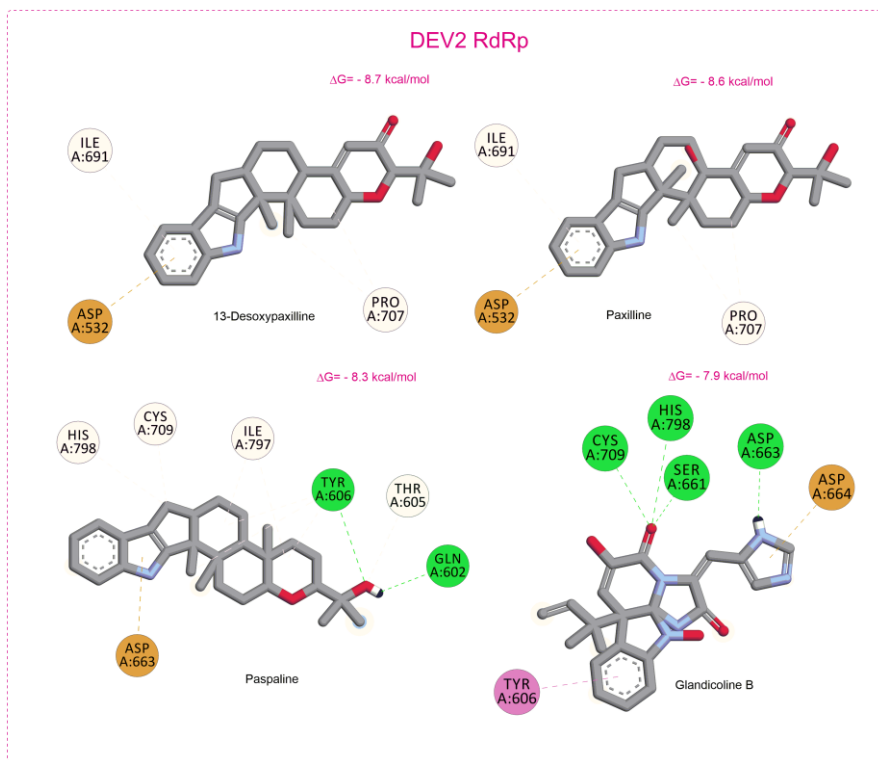


**Figure 5.** Main interactions observed for the top-scored inhibitors of DENV-2 RdRp by docking analysis.

Regarding to the interactions in the presumed active site of DENV-2 RdRp,  $\pi$ -alkyl (Ile691) and  $\pi$ -anion (Asp532), and alkyl (Pro707) interactions were observed to 13-desoxypaxilline and paxilline (Figure 5). For paspaline and glandicoline B, key interaction with residues from motif C (Asp663 and Asp664) from the subdomain contains the active site were observed.<sup>29</sup> The main observed interactions between all tested compounds and DENV2 RdRp are summarized in Table 1.

Finally, the docking analysis with DENV2 MTase also pointed paxilline and their related compounds [13-desoxypaxilline (-11.0 kcal/mol), paxilline (-11.0 kcal/mol), PCM6 (-10.5 kcal/mol), and paspaline (-10.5 kcal/mol)] as top-scored inhibitors (Table 1). These compounds presented binding free energies higher than the previously described inhibitor *S*-adenosyl-L-homocysteine (SAH) (redocking binding free energy = -8.0 kcal/mol, RMSD = 0.7881). On the other hand, the alkaloids from the roquefortine/oxaline pathway presented binding free energies ranging -7.2 to 8.6

kcal/mol. Oxaline presented the worse binding free energy. Docking analysis also revealed key interactions, such as hydrogen bonds and  $\pi$ -based interactions, for the top-scored inhibitors (Figure 6), similarly to that observed to SAH (Supplementary data). For SAH, hydrogen bonds were observed with Ser56, Trp87, Gly86, His110, Glu111, Asp131, Val132, Asp146, and Glu166, along with  $\pi$ -sigma interactions with Ile147 and  $\pi$ - $\pi$  interaction with Lys105. On the other hand, for 13-desoxypaxilline and paxilline, hydrogen bonds were observed with Asp146 and Glu111, respectively. In addition,  $\pi$ - $\pi$  interaction with His110,  $\pi$ -sigma interaction with Ile147, and  $\pi$ -alkyl interaction with Lys105, His110, and Val132 were observed to both compounds. The main observed interactions between all tested compounds and DENV2 MTase are summarized in Table 1.

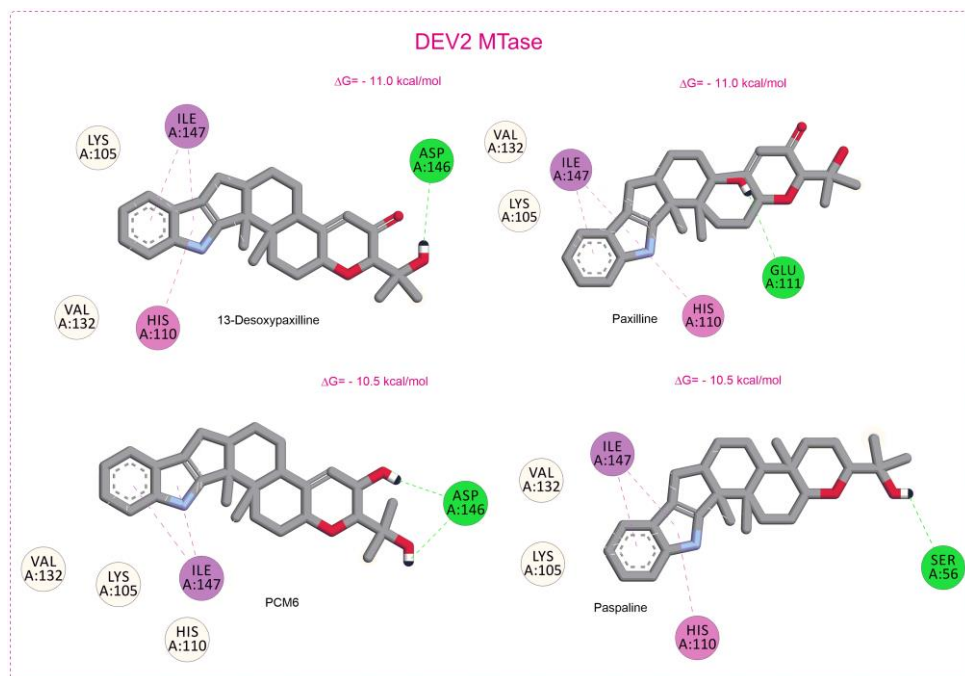


**Figure 6.** Main interactions observed for the top-scored inhibitors of DENV-2 MTase by docking analysis.

Natural products from Fungi belonging to the order Eurotiales, which includes *Penicillium*, have previously showed great antiviral potential against Enterovirus 71

(EV71), DENV, H1N1, HIV-1, H3N2, Japanese Encephalitis Virus (JEV) and Zika Virus (ZV).<sup>32</sup> This activity is related to small molecular weight compounds produced by the fungus of this order, such as polyketides (PKS), and indole alkaloids.<sup>33-35</sup> The indole core, present in indole alkaloids, is well known as one of the most important scaffolds for drug discovery, which are capable of serving as ligand for a diverse array of receptors.<sup>36</sup> Indole derivatives have the unique property of mimicking the structure of peptides and to bind reversibly to enzymes, which provide tremendous opportunities to discover novel drugs with different modes of action.<sup>37</sup> Previous studies with molecules containing an indole core such as umifenovir and derivates, which is used in Russia and China as a antiviral drug against HCV, can maintain its anti-HCV efficacy even with the removal of the 6-bromo and 5-hydroxy groups, as well as the phenylsufonil moiety from the indole ring, implying that the indole core rather than these groups might be the antiviral pharmacophore.<sup>35</sup> Therefore, the inhibitory potential observed for paxilline and related compounds in this study can be related, in part, to its indole core. This observation is in agreement with a previous report that demonstrated for paxilline significant antiviral activity against the H1N1 virus.<sup>38</sup>

## Conclusions

The docking analysis suggested that paxilline and their related compounds can play a key role as inhibitors of important nonstructural proteins (nsp) for SARS-CoV-2 and dengue viruses. These observations, which are in agreement with previous reports about the biological potential of indole alkaloids, reinforce the potential of *Penicillium* alkaloids as antiviral agents. Obviously, further researches are necessary to certify the docking results reported here, as well as the adequate application of these substances against COVID-19 and dengue fever.

## **Supplementary Information**

Supplementary Information, is available free of charge at <http://jbc.sbj.org.br>.

## **Acknowledgements**

The authors are grateful to Coordenação de Aperfeiçoamento de Pessoal de Nível Superior (CAPES) (Finance code 001), Conselho Nacional de Desenvolvimento Científico e Tecnológico (CNPQ), Financiadora de Estudos e Projetos (FINEP) and, Fundação de Amparo à Pesquisa do Estado do Amazonas (FAPEAM) for financial support.

## **Author Contributions**

Francinaldo Araujo da Silva-Filho was responsible for the Conceptualization, Data curation, Formal analysis, Methodology, and Writing original draft; Felipe Moura Araujo da Silva for the Conceptualization Formal analysis, Methodology, Writing original draft; Antonia Queiroz Lima de Souza and Afonso Duarte Leão de Souza were responsible for the Conceptualization, Formal analysis, Funding acquisition, Methodology, Supervision, Writing original draft.

## **References**

### **References**

1. Di Gennaro, F., Pizzol, D., Marotta, C., Antunes, M., Racalbuto, V., Veronese, N., Smith, L.; Coronavirus diseases (COVID-19) current status and future perspectives: a narrative review. *International Journal of Environmental Research and Public Health* **2020**, *17*, 2690.
2. <https://covid19.who.int/>, accessed 05 may 2021.

3. Nacher, M., Douine, M., Gaillet, M., Flamand, C., Rousset, D., Rousseau, C., Mahdaoui, C., Carroll, S., Valdes, A., Passard, N., Carles, G., Djossou, F., Demar, M., Epelboin, L.; Simultaneous dengue and COVID-19 epidemics: Difficult days ahead?. *PLoS Negl Trop Dis* **2020**, *14*, e0008426.
4. Ridwan, R.; COVID-19 and dengue: a deadly duo. *Tropical Doctor* **2020**, *50*, 270.
5. Cardona-Ospina, J. A., Arteaga-Livias, K., Villamil-Gómez, W. E., Pérez-Díaz, C. E., Bonilla-Aldana, D. K., Mondragon-Cardona, Á., Solarte-Portilla, M., Martinez, E., Millan-Oñate, J., López-Medina, E., López, P., Navarro, J. C., Perez-Garcia, L., Mogollon-Rodriguez, E., Rodríguez-Morales, A. J., Paniz-Mondolfi, A.; Dengue and COVID-19, overlapping epidemics? An analysis from Colombia. *Journal of Medical Virology* **2020**, *93*, 522-527.
6. <https://www.paho.org/data/index.php/en/mnu-topics/indicadores-dengue-en/dengue-nacional-en/252-dengue-pais-ano-en.html>, accessed 05 may 2021.
7. Verduyn, M., Allou, N., Gazaille, V., Andre, M., Desroche, T., Jaffar, M. C., Traversier, N., Levin, C., Lagrange-Xelot, M., Moiton, M. P., Hoang, S.; Co-infection of dengue and COVID-19: A case report. *PLoS Negl Trop Dis* **2020**, *14*, e0008476.
8. Lorenz, C., Azevedo, T. S., Chiaravalloti-Neto, F.; COVID-19 and dengue fever: A dangerous combination for the health system in Brazil. *Travel Medicine and Infectious Disease* **2020**, *35*, 101659.
9. Messina, J. P., Brady, O. J., Scott, T. W., Zou, C., Pigott, D. M., Duda, K. A., Bhatt, S., Katzelnick, L., Howes, R. E., Battle, K. E., Simmons, C. P., Hay, S. I.; Global spread of dengue virus types: mapping the 70 year history. *Trends in microbiology* **2014**, *22*, 138-146.

10. Cannalire, R., Cerchia, C., Beccari, A. R., Di Leva, F. S., Summa, V.; Targeting SARS-CoV-2 Proteases and Polymerase for COVID-19 Treatment: State of the Art and Future Opportunities. *Journal of Medicinal Chemistry* **2020**, doi.org/10.1021/acs.jmedchem.0c01140.
11. Yokokawa, F.; Recent progress on phenotype-based discovery of dengue inhibitors. *RSC Medicinal Chemistry* **2020**, *11*, 541-551.
12. Morse, J. S., Lalonde, T., Xu, S., Liu, W. R.; Learning from the past: possible urgent prevention and treatment options for severe acute respiratory infections caused by 2019-nCoV. *ChemBioChem* **2020**, *21*, 730.
13. Silva, F. M. A., Silva, K. P. A., Oliveira, L. P. M., Costa, E. V., Koolen, H. H., Pinheiro, M. L. B., Souza, A. Q. L., Souza, A. D. L. Flavonoid glycosides and their putative human metabolites as potential inhibitors of the SARS-CoV-2 main protease (Mpro) and RNA-dependent RNA polymerase (RdRp). *Memórias do Instituto Oswaldo Cruz* **2020**, *115*, e200207.
14. Indu, P., Rameshkumar, M. R., Arunagirinathan, N., Al-Dhabi, N. A., Arasu, M. V., & Ignacimuthu, S.; Raltegravir, Indinavir, Tipranavir, Dolutegravir, and Etravirine against main protease and RNA-dependent RNA polymerase of SARS-CoV-2: A molecular docking and drug repurposing approach. *Journal of Infection and Public Health* **2020**, *13*, 1856.
15. Sousa, L. R. F., Wu, H., Nebo, L., Fernandes, J. B., Silva, M. F. G. F., Kiefer, W., Kanitz, M., Bodem, J., Diederich, W. E., Schirmeister, T., Vieira, P. C.; Flavonoids as noncompetitive inhibitors of Dengue virus NS2B-NS3 protease: inhibition kinetics and docking studies. *Bioorganic & Medicinal Chemistry* **2015**, *23*, 466.

16. Galiano, V., Garcia-Valtanen, P., Micol, V., Encinar, J. A.; Looking for inhibitors of the dengue virus NS5 RNA-dependent RNA-polymerase using a molecular docking approach. *Drug Design, Development and Therapy* **2016**, *10*, 3163.
17. Vora, J., Patel, S., Athar, M., Sinha, S., Chhabria, M. T., Jha, P. C., Shrivastava, N.; Pharmacophore modeling, molecular docking and molecular dynamics simulation for screening and identifying anti-dengue phytocompounds. *Journal of Biomolecular Structure and Dynamics* **2019**, *38*, 1726.
18. Lin, X., Li, X., Lin, X.; A review on applications of computational methods in drug screening and design. *Molecules* **2020**, *25*, 1375.
19. El Sayed, K. A.; Natural products as antiviral agents. *Studies in Natural Products Chemistry* **2000**, *24*, 473.
20. Meng, L., Guo, Q., Liu, Y., Chen, M., Li, Y., Jiang, J., Shi, J.; Indole alkaloid sulfonic acids from an aqueous extract of *Isatis indigotica* roots and their antiviral activity. *Acta Pharmaceutica Sinica B*, **2017**, *7*, 334.
21. Singh, T. P., Singh, O. M.; Recent progress in biological activities of indole and indole alkaloids. *Mini Reviews in Medicinal Chemistry*, **2018**, *18*, 9.
22. Ali, T., Pham, T. M., Ju, K. S., Rakotondraibe, H. L. Ent-homocyclopamine B, a prenylated indole alkaloid of biogenetic interest from the endophytic fungus *Penicillium concentricum*. *Molecules* **2019**, *24*, 218.
23. Chen, M., Wang, R., Zhao, W., Yu, L., Zhang, C., Chang, S., Li, Y., Zhang, T., Xing, J., Gan, M., Feng, F., Si, S. Isocoumarindole A, a chlorinated isocoumarin and indole alkaloid hybrid metabolite from an endolichenic fungus *Aspergillus* sp. *Organic letters* **2019**, *21*, 1530
24. Silva-Filho, F. A., Souza, M. M. M., Rezende, G. O., Silva, F. M. A., Cruz, J. C., Silva, J. F., Souza, A. D. L., Souza, A. Q. L.; Screening of Alkaloid-Producing

- Endophytic Penicillium Strains from Amazon Medicinal Plants by Electrospray Ionization Mass Spectrometry (ESI-MS) and Principal Component Analysis (PCA). *J Braz Chem Soc* **2021**, *32*, 1832.
25. Saikia, S., Parker, E. J., Koulman, A., Scott, B.; Defining paxilline biosynthesis in *Penicillium paxilli*: functional characterization of two cytochrome P450 monooxygenases. *Journal of Biological Chemistry* **2007**, *282*, 16829-16837.
26. Overy, D. P., Nielsen, K. F., Smedsgaard, J.; Roquefortine/oxaline biosynthesis pathway metabolites in *Penicillium* ser. *Corymbifera*: in planta production and implications for competitive fitness. *Journal of Chemical Ecology* **2005**, *31*, 2373.
27. Stewart, J. J. (2016). Stewart Computational Chemistry, Colorado Springs, CO, USA. <http://OpenMOPAC.net>.
28. Morris, G. M., Huey, R., Lindstrom, W., Sanner, M. F., Belew, R. K., Goodsell, D. S., Olson, A. J.; AutoDock4 and AutoDockTools4: Automated Docking with Selective Receptor Flexibility. *J Comput Chem* **2009**, *30*, 2785.
29. Noble, C. G., Shi, P. Y.; Structural biology of dengue virus enzymes: towards rational design of therapeutics. *Antiviral Research* **2012**, *96*, 115.
30. Trott, O., Olson, A. J.; AutoDockVina: improving the speed and accuracy of docking with a new scoring function, efficient optimization, and multithreading. *J Comput Chem* **2010**, *31*, 455.
31. Discovery Studio Visualizer, v16.1.0.15350, Dassault Systemes Biovia Corp, 2015.
32. Linnakoski, R., Reshamwala, D., Veteli, P., Cortina-Escribano, M., Vanhanen, H., & Marjomäki, V.; Antiviral agents from fungi: Diversity, mechanisms and potential applications. *Frontiers in Microbiology* **2018**, *9*, 2325.

33. Pang, X., Lin, X., Tian, Y., Liang, R., Wang, J., Yang, B., Zhou, X., Kaliyaperumal, K., Luo, X., Tu, Z., Liu, Y.; Three new polyketides from the marine sponge-derived fungus *Trichoderma* sp. SCSIO41004. *Natural Product Research* **2018**, *32*, 10.
34. Peng, J., Lin, T., Wang, W., Xin, Z., Zhu, T., Gu, Q., Li, D.; Antiviral alkaloids produced by the mangrove-derived fungus *Cladosporium* sp. PJX-41. *Journal of Natural Products* **2013**, *76*, 1133.
35. Zhang, M. Z., Chen, Q., Yang, G. F.; A review on recent developments of indole-containing antiviral agents. *European Journal of Medicinal Chemistry* **2015**, *89*, 421.
36. Sa Alves, F. R., Barreiro, E. J., Manssour Fraga, C. A.; From nature to drug discovery: the indole scaffold as a ‘privileged structure’. *Mini Reviews in Medicinal Chemistry* **2009**, *9*, 782.
37. Kaushik, N. K., Kaushik, N., Attri, P., Kumar, N., Kim, C. H., Verma, A. K., Choi, E. H.; Biomedical importance of indoles. *Molecules* **2013**, *18*, 6620.
38. Fan, Y., Wang, Y., Liu, P., Fu, P., Zhu, T., Wang, W., Zhu, W.; Indole-diterpenoids with anti-H1N1 activity from the aciduric fungus *Penicillium camemberti* OUCMDZ-1492. *Journal of Natural Products* **20**

## Supplementary Information

### **Alkaloids from Amazon *Penicillium* Strains as Potential Inhibitors of SARS-CoV-2 and DENV-2 Target Enzymes**

*Francinaldo Araujo da Silva-Filho,<sup>a</sup> Felipe Moura Araujo da Silva,<sup>b</sup> Gilvan Ferreira*

*da Silva<sup>f</sup>, Maria Lúcia Belém Pinheiro<sup>b</sup>, Sarah Raquel Silveira da Silva<sup>a</sup>, Afonso*

*Duarte Leão de Souza,<sup>a,b,c</sup>and Antonia Queiroz Lima de Souza<sup>a,b,e,\*</sup>*

*<sup>a</sup>Programa de Pós-Graduação da Rede Bionorte, Universidade Federal do Amazonas*

*(UFAM), 69077-000, Manaus, AM, Brazil*

*<sup>b</sup>Central Analítica - Centro de Apoio Multidisciplinar (CAM), Universidade Federal do*

*Amazonas (UFAM), 69077-000, Manaus, AM, Brazil*

*<sup>c</sup>Departamento de Química (ICE), Universidade Federal do Amazonas (UFAM), 69077-*

*000, Manaus, AM, Brazil*

*<sup>e</sup>Faculdade de Ciências Agrárias (FCA), Universidade Federal do Amazonas (UFAM),*

*69077-000, Manaus, AM, Brazil*

*<sup>f</sup>Embrapa Amazônia Ocidental, Empresa Brasileira de Pesquisa Agropecuária*

*(EMBRAPA) Manaus, AM, Brazil*

\*e-mail: [antoniaqueiroz@ufam.edu.br](mailto:antoniaqueiroz@ufam.edu.br)

ORCID ID <http://orcid.org/0000-0001-5602-8617>

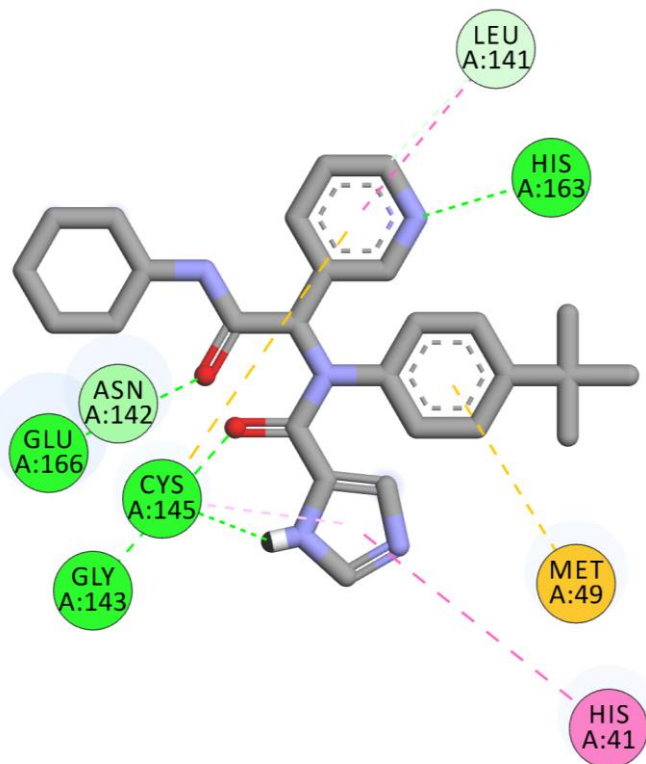


**Figure S1.** Main interactions observed between X77 and SARS-CoV-2 Mpro by docking analysis.

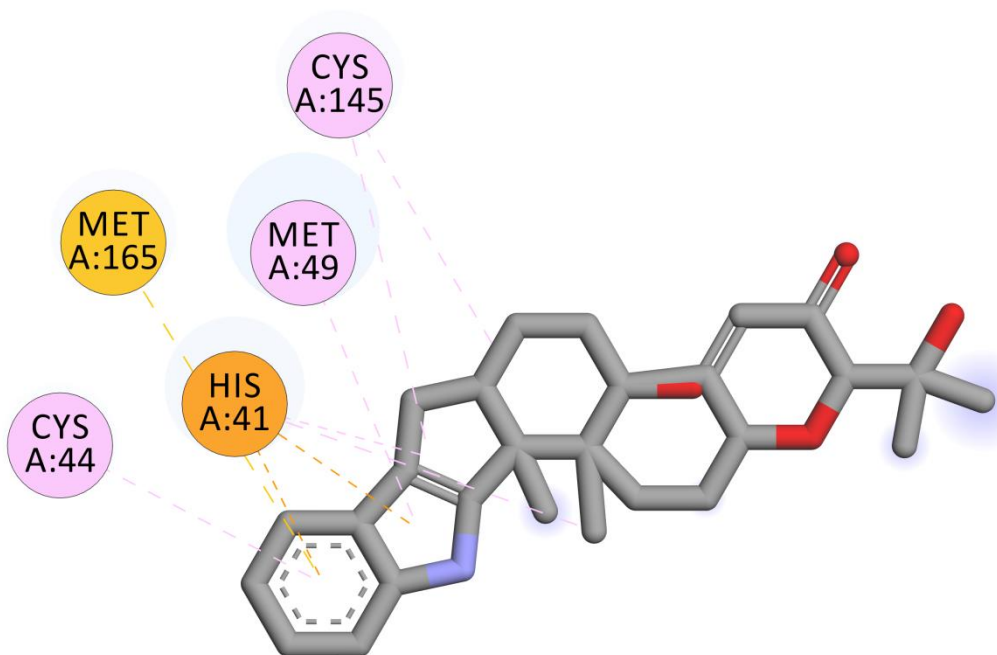


**Figure S2.** Main interactions observed between paxiline and SARS-CoV-2 Mpro by docking analysis.

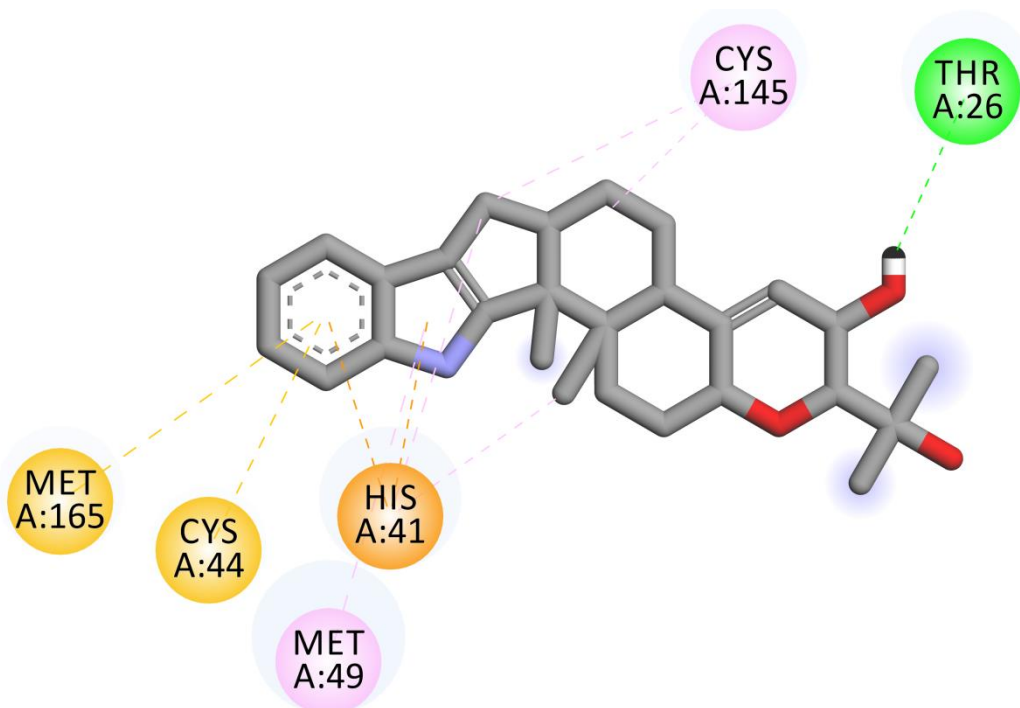


**Figure S3.** Main interactions observed between PCM6 and SARS-CoV-2 Mpro by docking analysis.

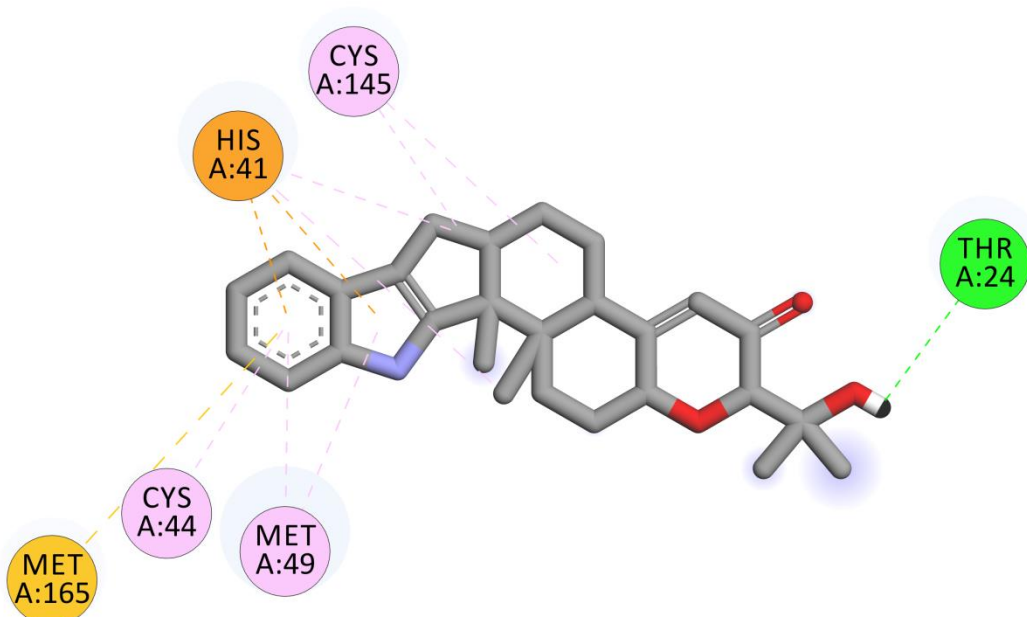


**Figure S4.** Main interactions observed between 13-desoxy-paxilline and SARS-CoV-2 Mpro by docking analysis.

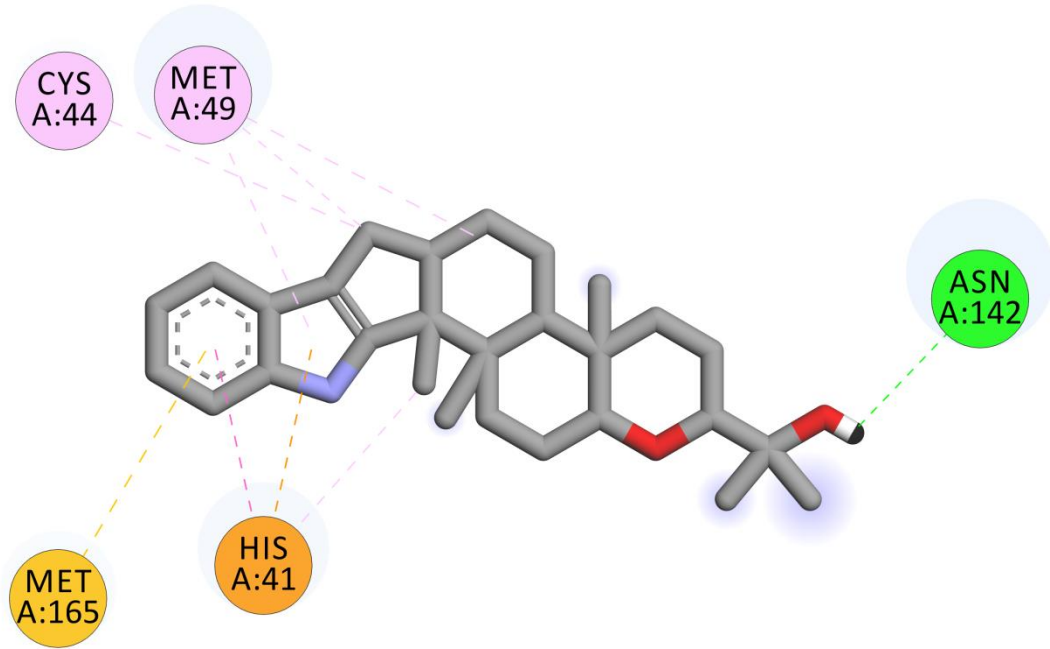


**Figure S5.** Main interactions observed between paspaline and SARS-CoV-2 Mpro by docking analysis.

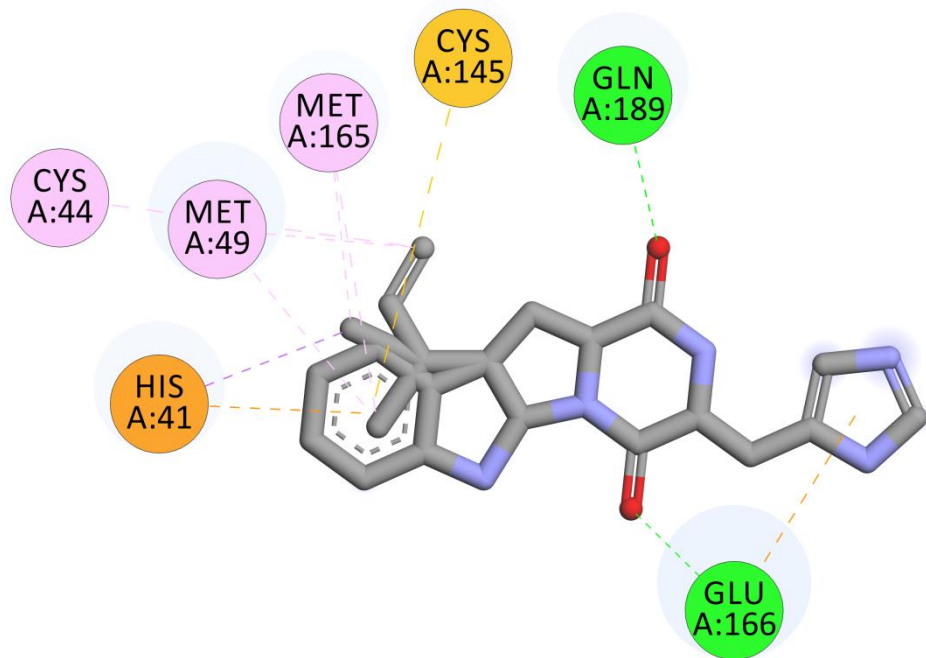


**Figure S6.** Main interactions observed between roquefortine C and SARS-CoV-2 Mpro by docking analysis.

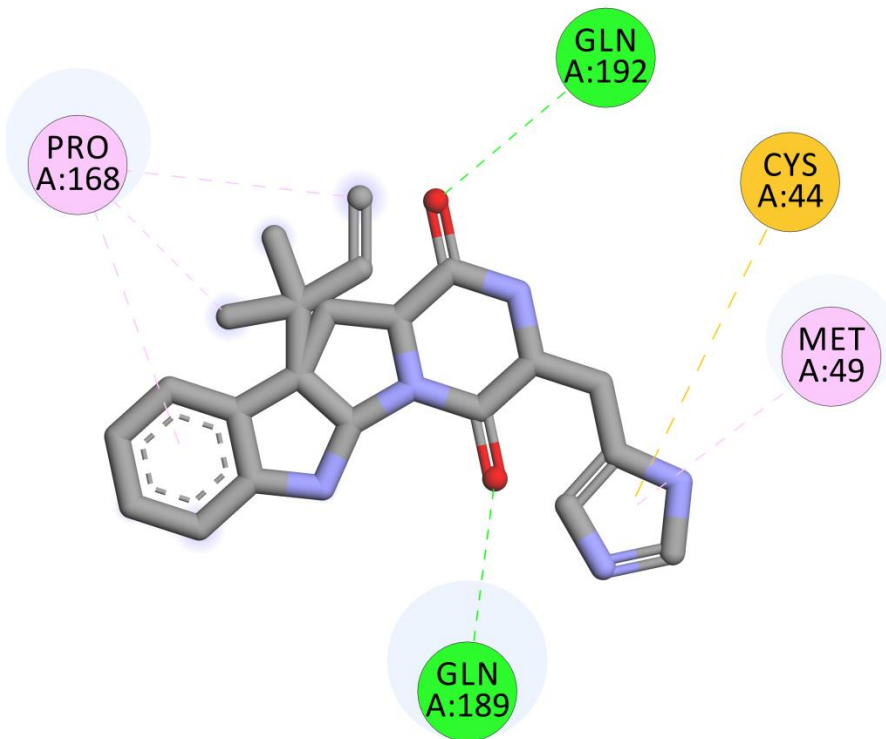


**Figure S7.** Main interactions observed between roquefortine D and SARS-CoV-2 Mpro by docking analysis.

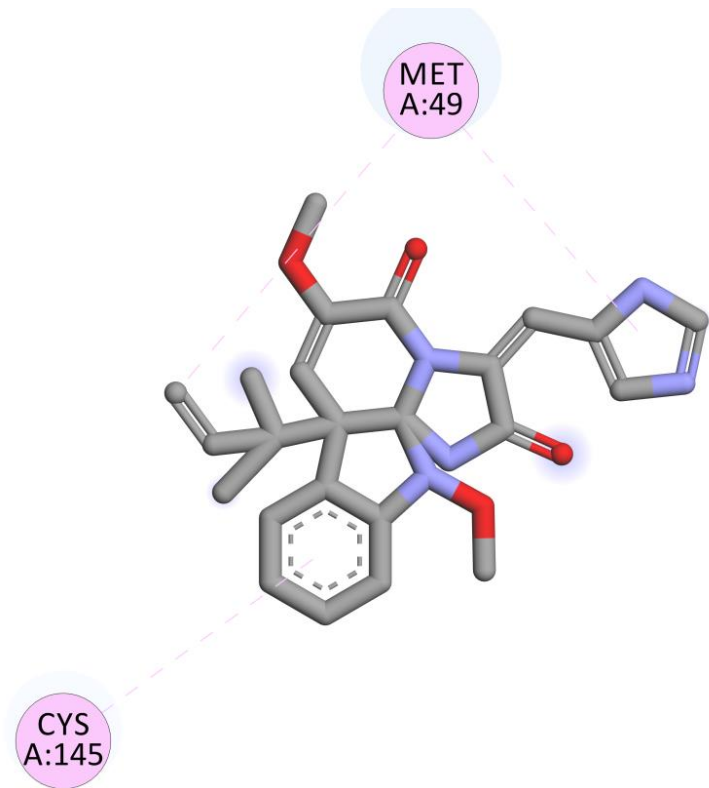


**Figure S8.** Main interactions observed between oxaline and SARS-CoV-2 Mpro by docking analysis.

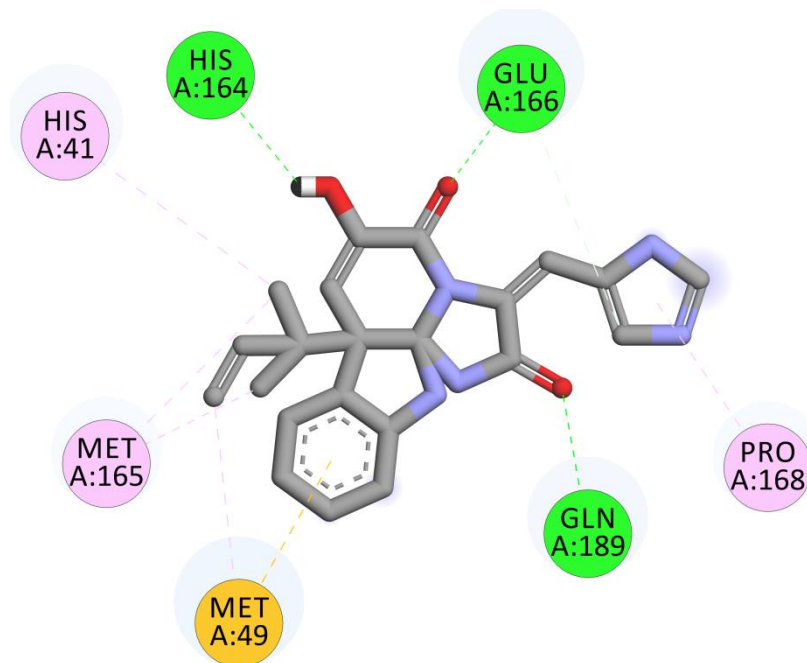


**Figure S9.** Main interactions observed between glandicoline A and SARS-CoV-2 Mpro by docking analysis.

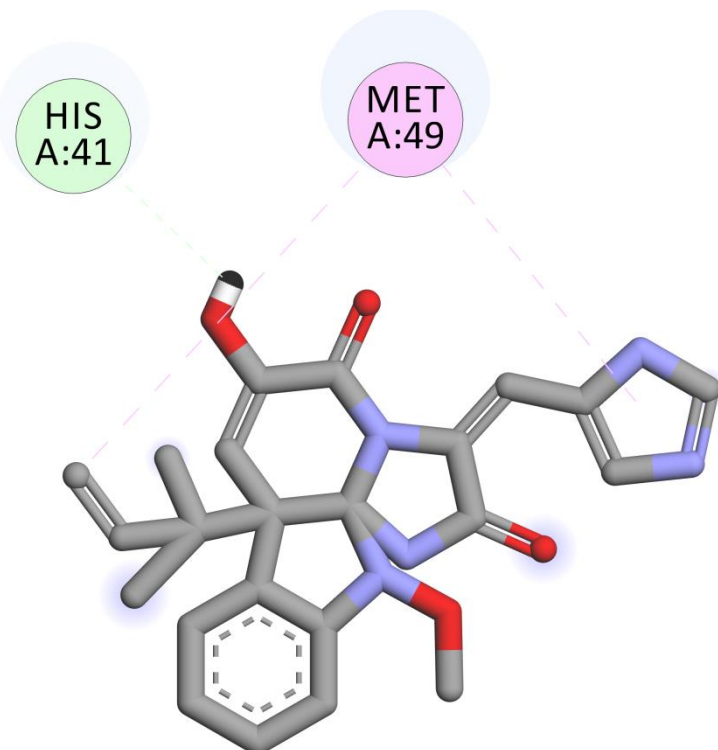


**Figure S10.** Main interactions observed between meleagrine and SARS-CoV-2 Mpro by docking analysis.

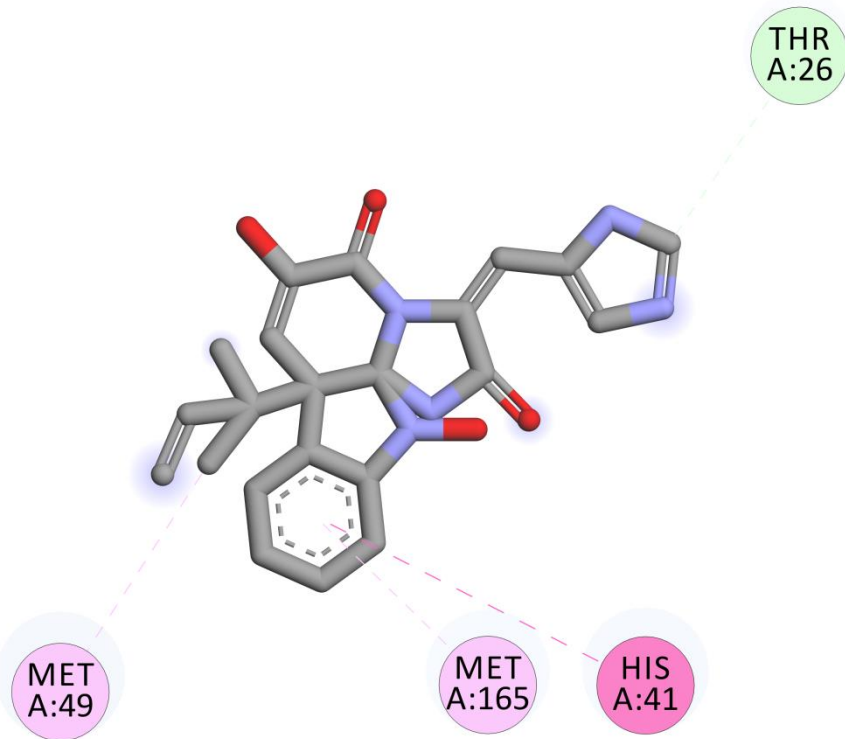


**Figure S11.** Main interactions observed between glandicoline B and SARS-CoV-2 Mpro by docking analysis.

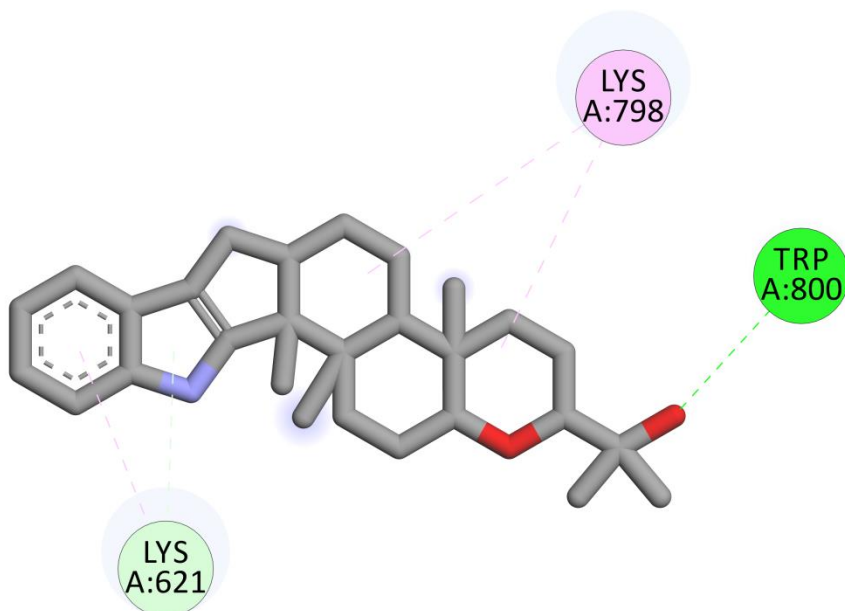


**Figure S12.** Main interactions observed between paspaline and SARS-CoV-2 RdRp by docking analysis.

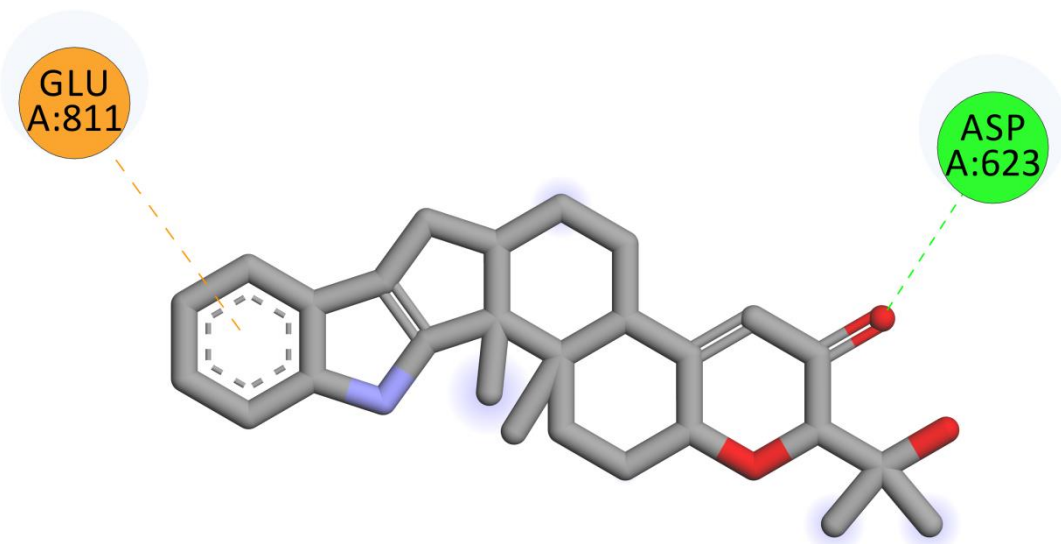


**Figure S13.** Main interactions observed between 13-desoxy-paxilline and SARS-CoV-2 RdRp by docking analysis.

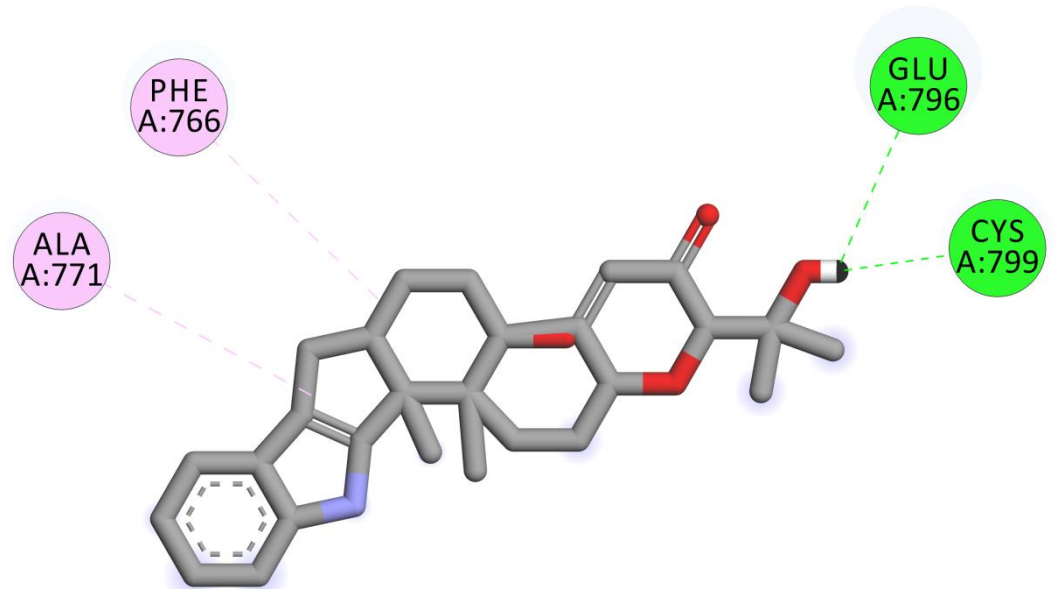


**Figure S14.** Main interactions observed between paxilline and SARS-CoV-2 RdRp by docking analysis.

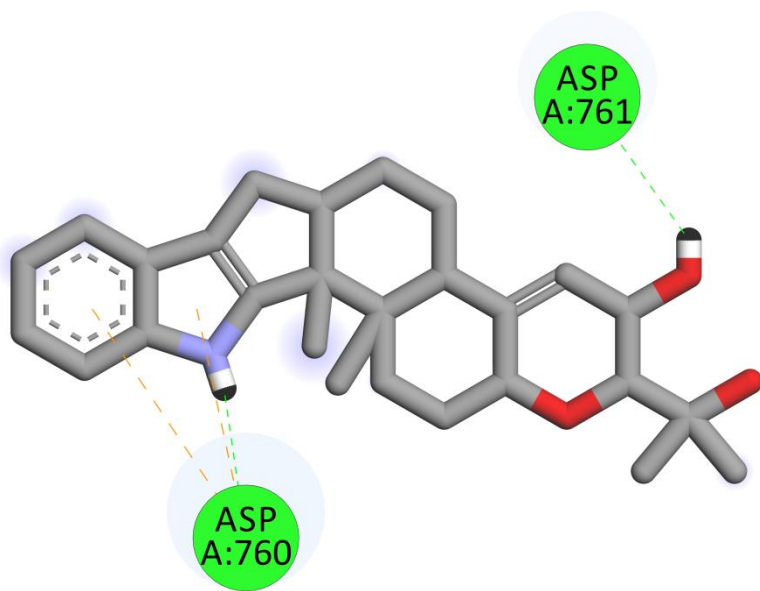


**Figure S15.** Main interactions observed between PCM6 and SARS-CoV-2 RdRp by docking analysis.

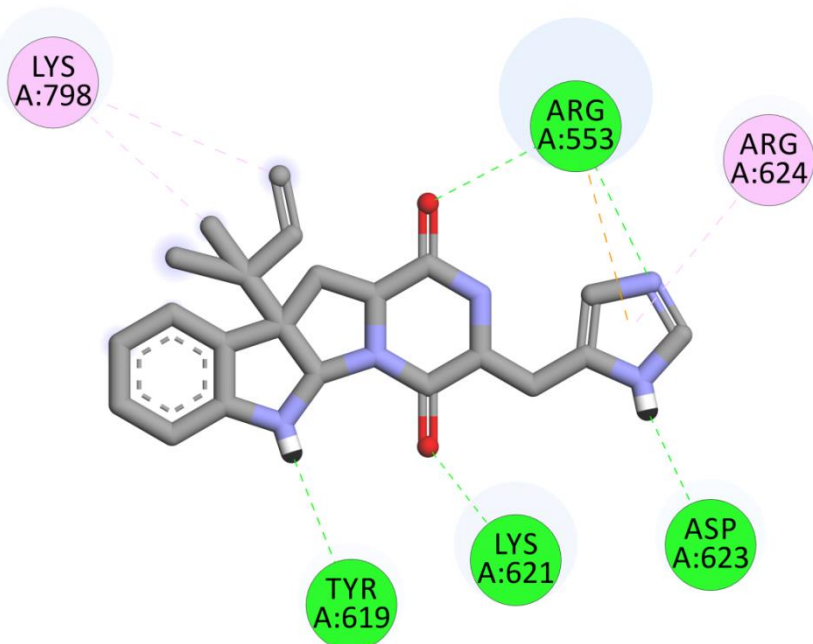


**Figure S16.** Main interactions observed between roquefortine C and SARS-CoV-2 RdRp by docking analysis.

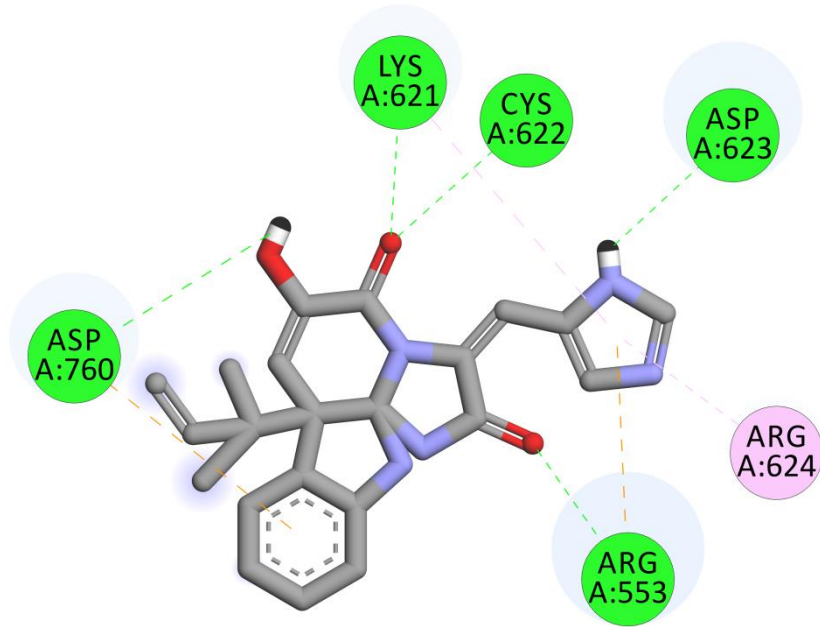


**Figure S17.** Main interactions observed between glandicoline A and SARS-CoV-2 RdRp by docking analysis.

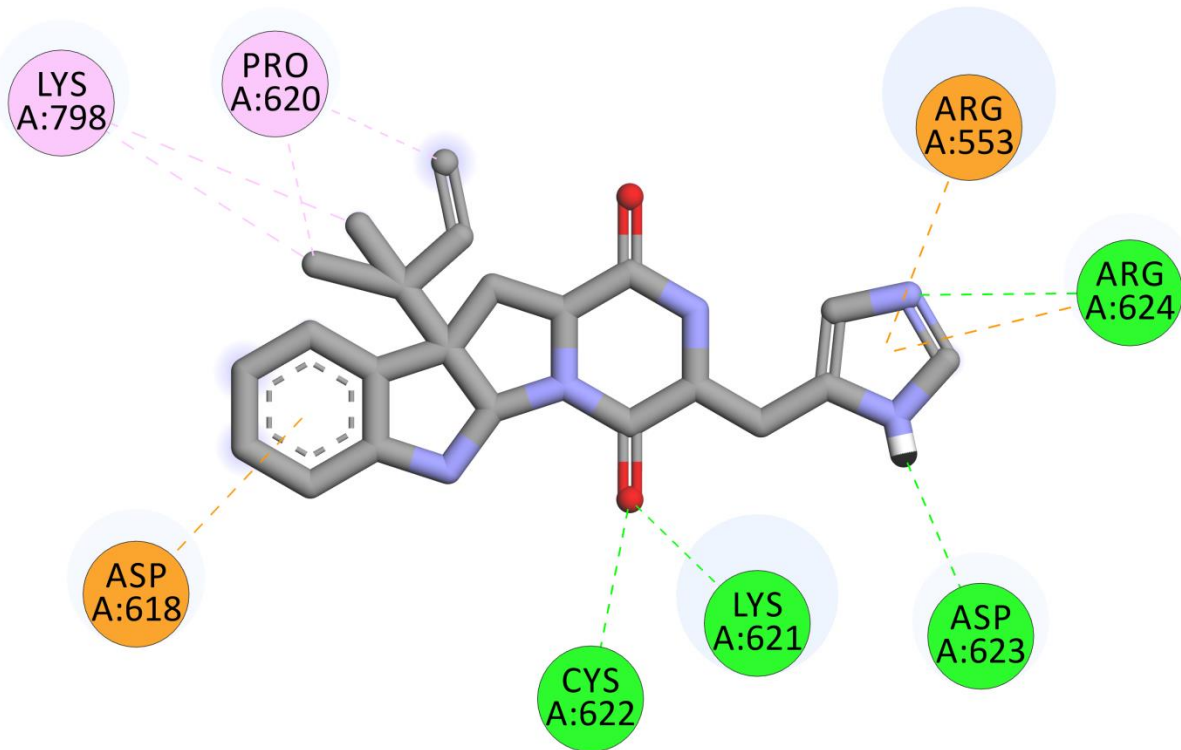


**Figure S18.** Main interactions observed between roquefortine D and SARS-CoV-2 RdRp by docking analysis.

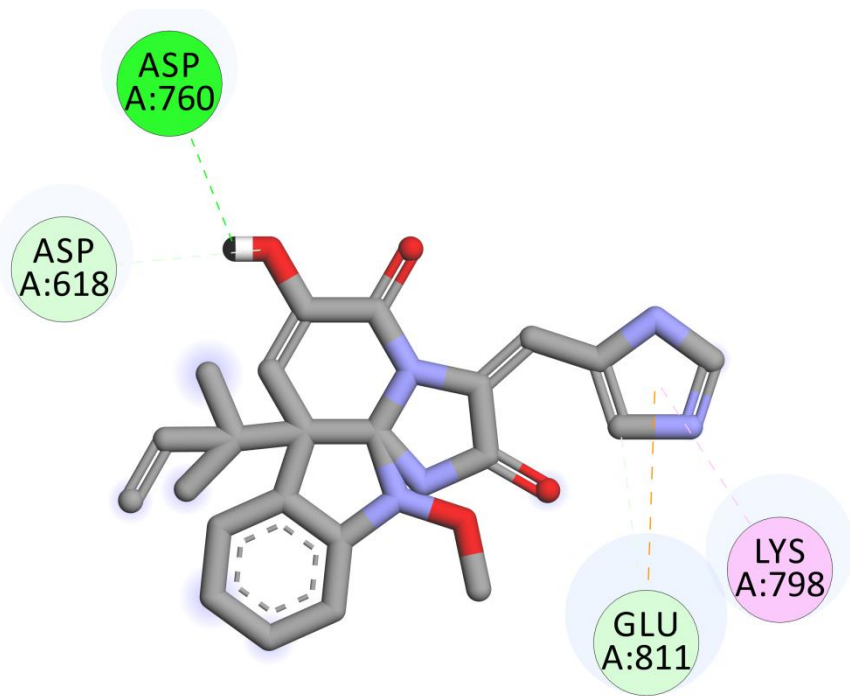


**Figure S19.** Main interactions observed between meleagrine and SARS-CoV-2 RdRp by docking analysis.

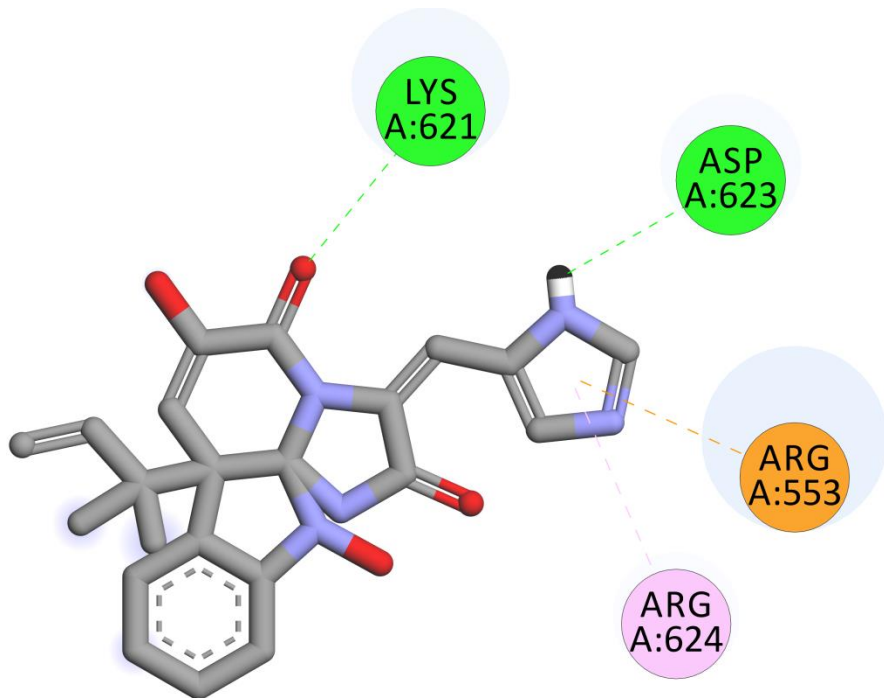


**Figure S20.** Main interactions observed between glandicoline B and SARS-CoV-2 RdRp by docking analysis.

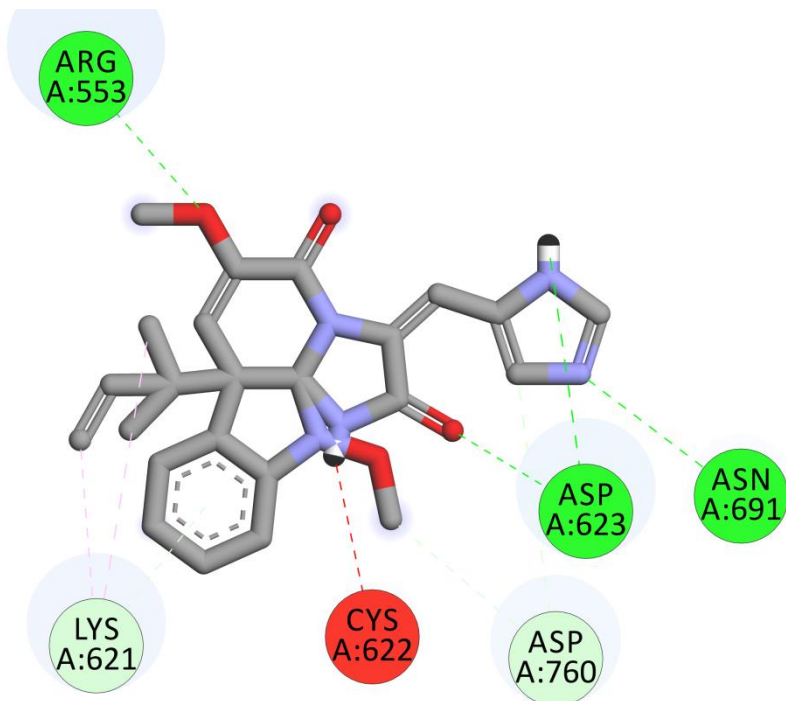


**Figure S21.** Main interactions observed between oxaline and SARS-CoV-2 RdRp by docking analysis.

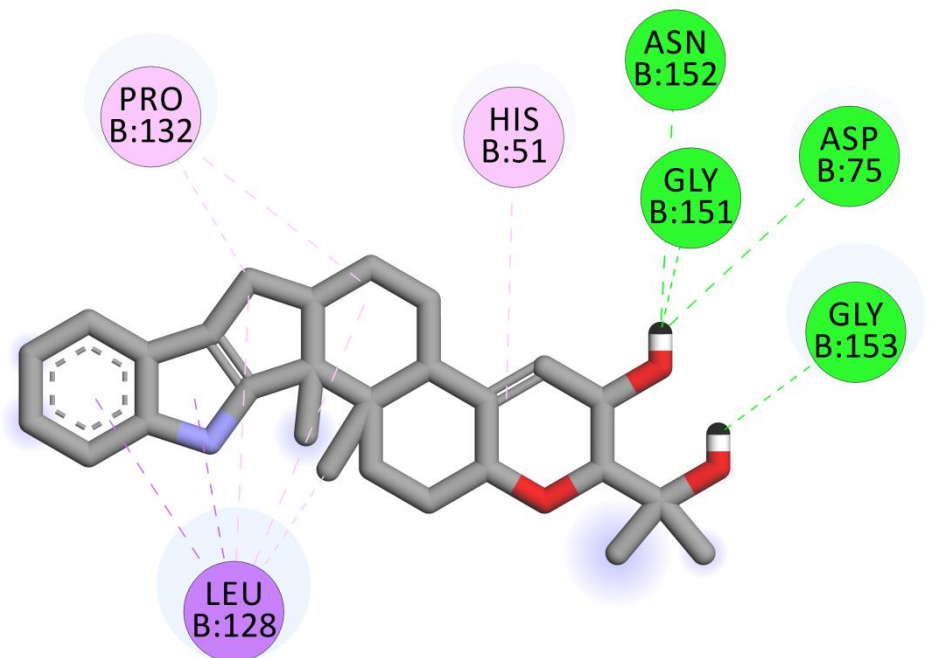


**Figure S22.** Main interactions observed between PCM6 and DENV2 NS2B-NS3 protease by docking analysis.

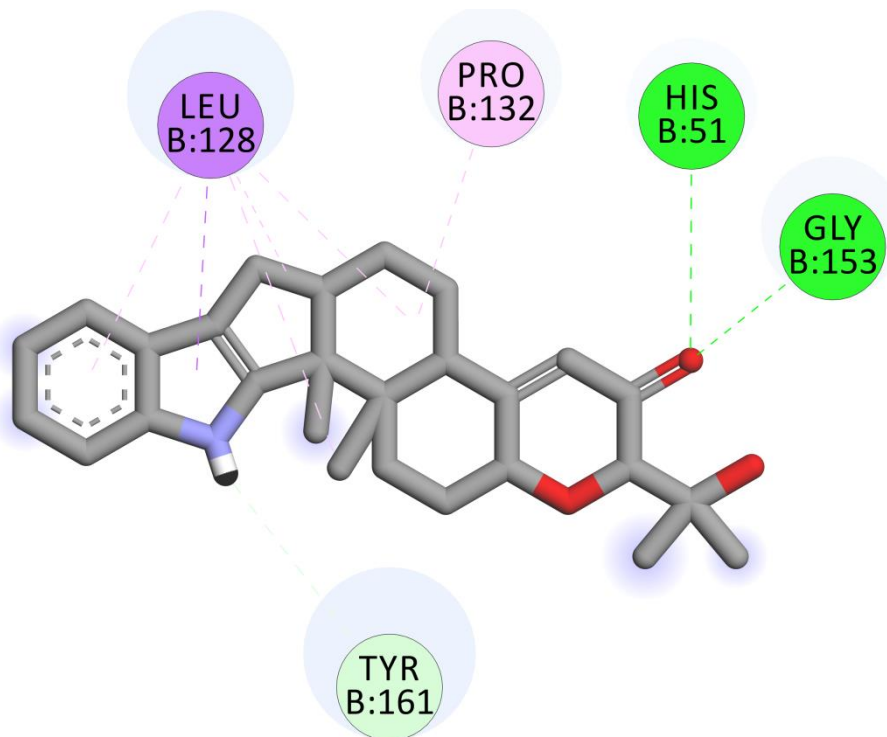


**Figure S23.** Main interactions observed between 13-desoxy-paxilline and DENV2 NS2B-NS3 protease by docking analysis.

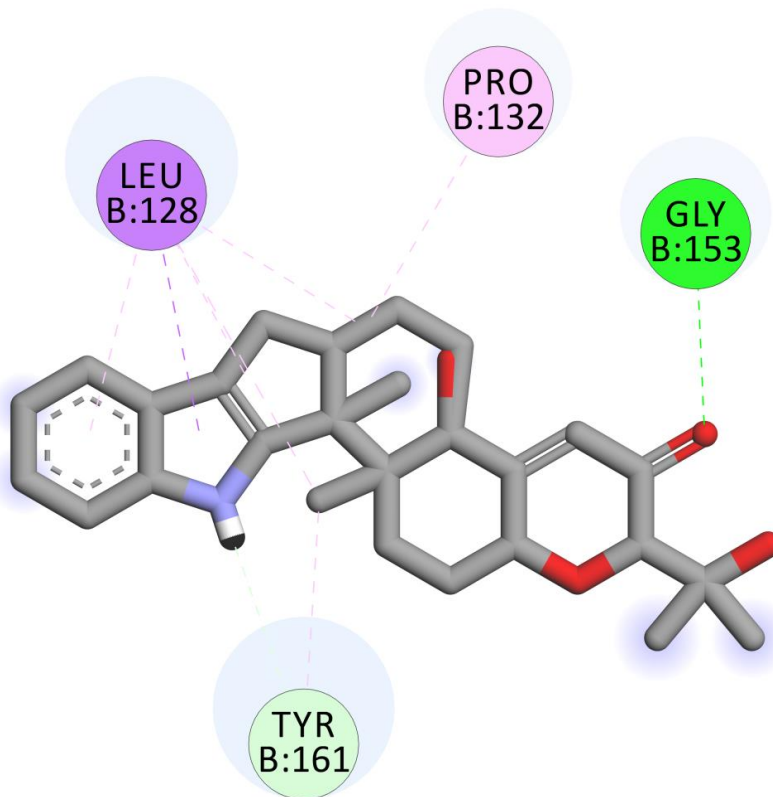


**Figure S24.** Main interactions observed between paxilline and DENV2 NS2B-NS3 protease by docking analysis.

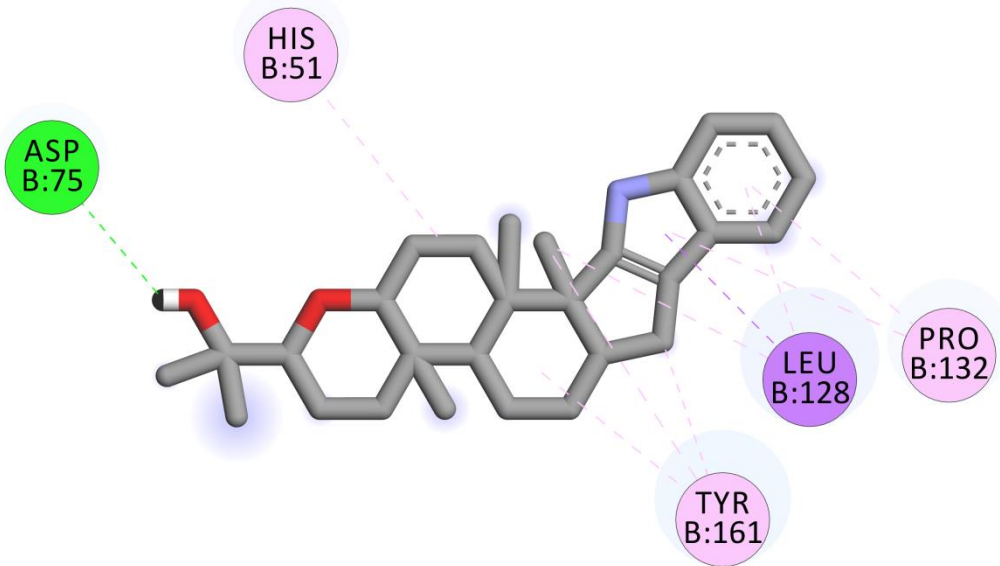


**Figure S25.** Main interactions observed between paspaline and DENV2 NS2B-NS3 protease by docking analysis.

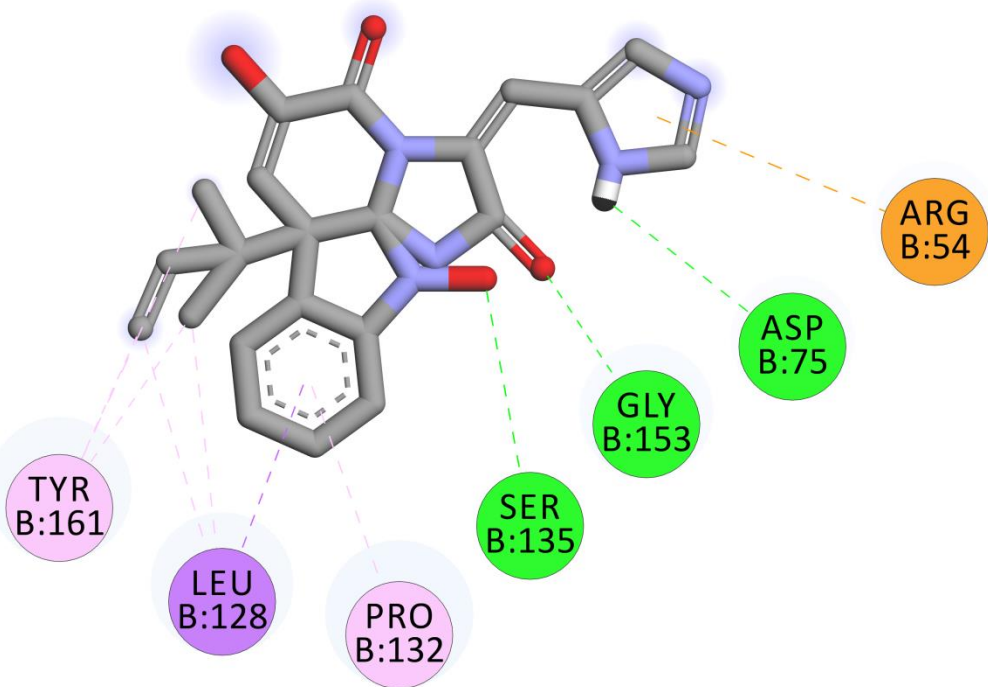


**Figure S26.** Main interactions observed between glandicoline B and DENV2 NS2B-NS3 protease by docking analysis.

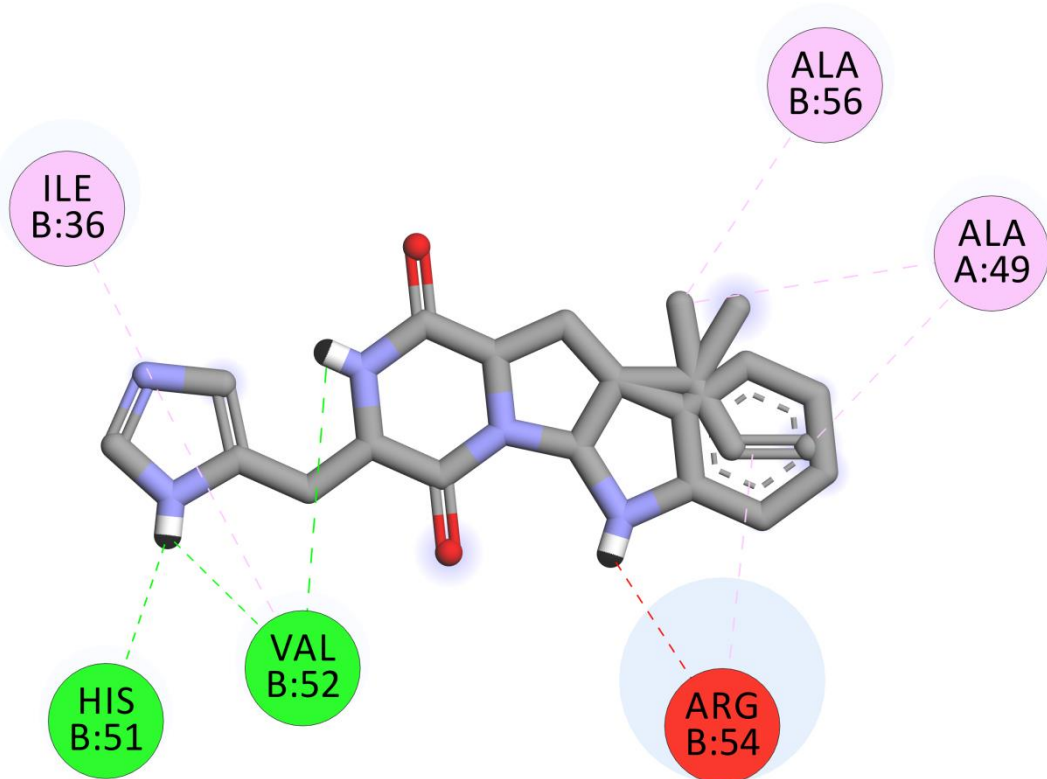


**Figure S27.** Main interactions observed between roquefortine C and DENV2 NS2B-NS3 protease by docking analysis.

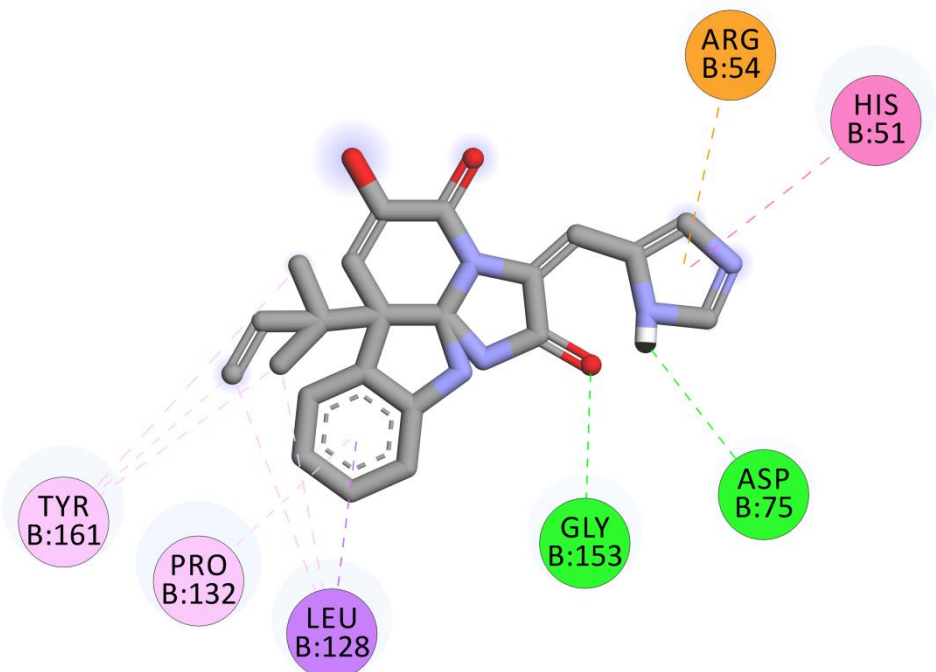


**Figure S28.** Main interactions observed between glandicoline A and DENV2 NS2B-NS3 protease by docking analysis.

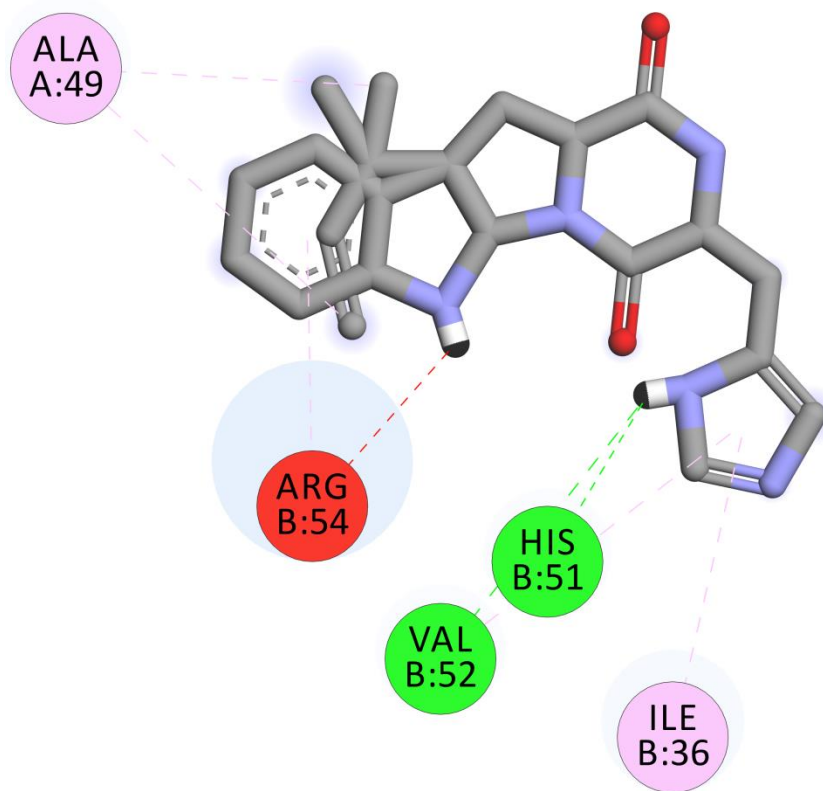


**Figure S29.** Main interactions observed between roquefortine D and DENV2 NS2B-NS3 protease by docking analysis.

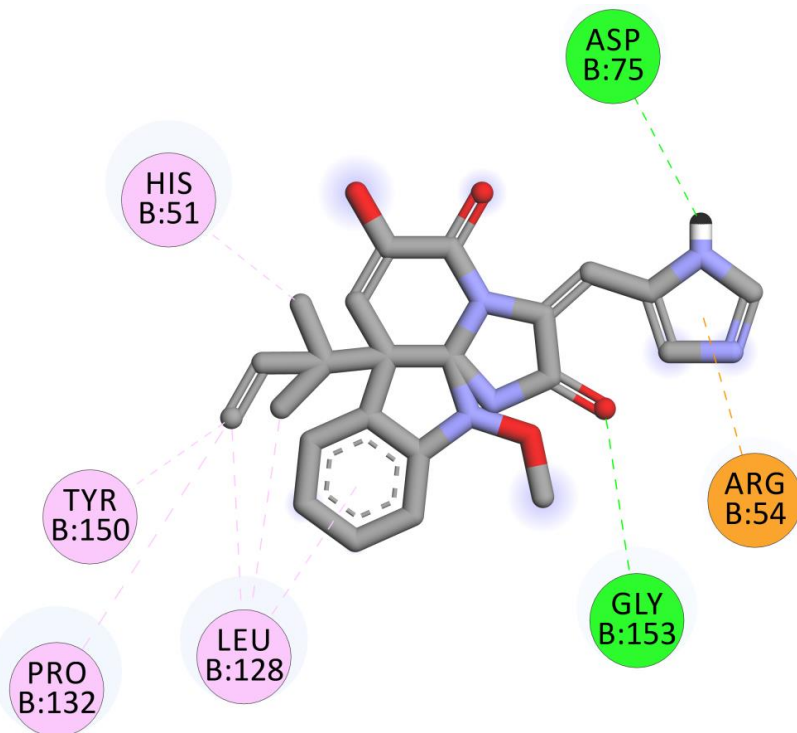


**Figure S30.** Main interactions observed between meleagrine and DENV2 NS2B-NS3 protease by docking analysis.

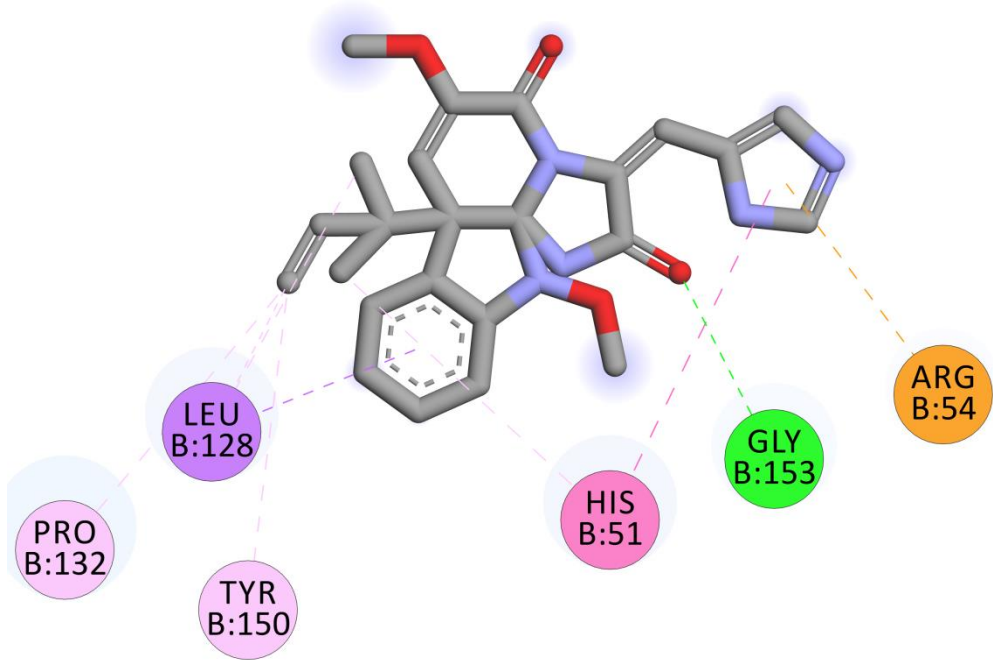


**Figure S31.** Main interactions observed between oxaline and DENV2 NS2B-NS3 protease by docking analysis.

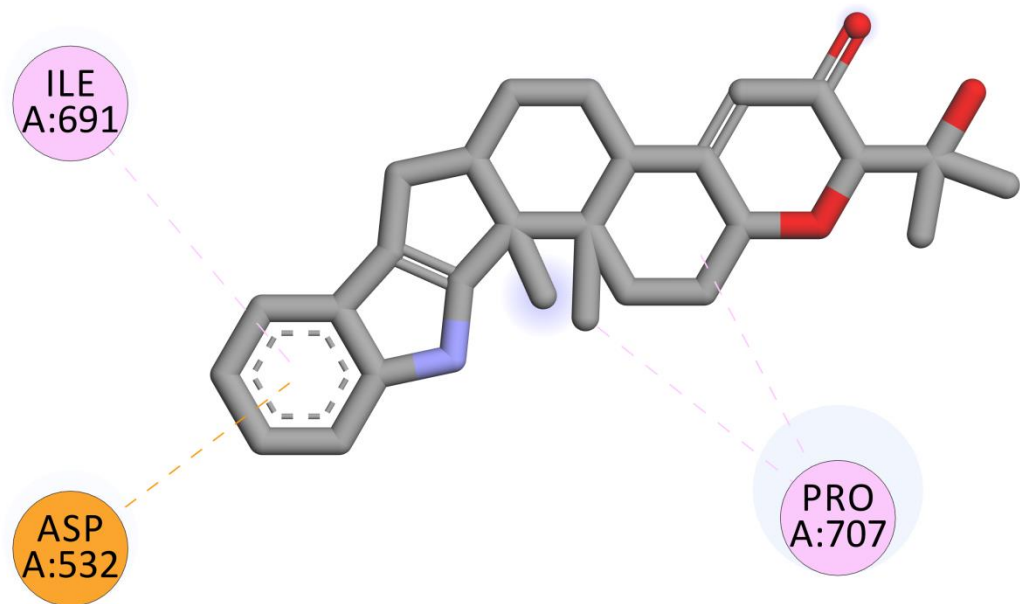


**Figure S32.** Main interactions observed between 13-desoxy-paxilline and DENV2 RdRp by docking analysis.

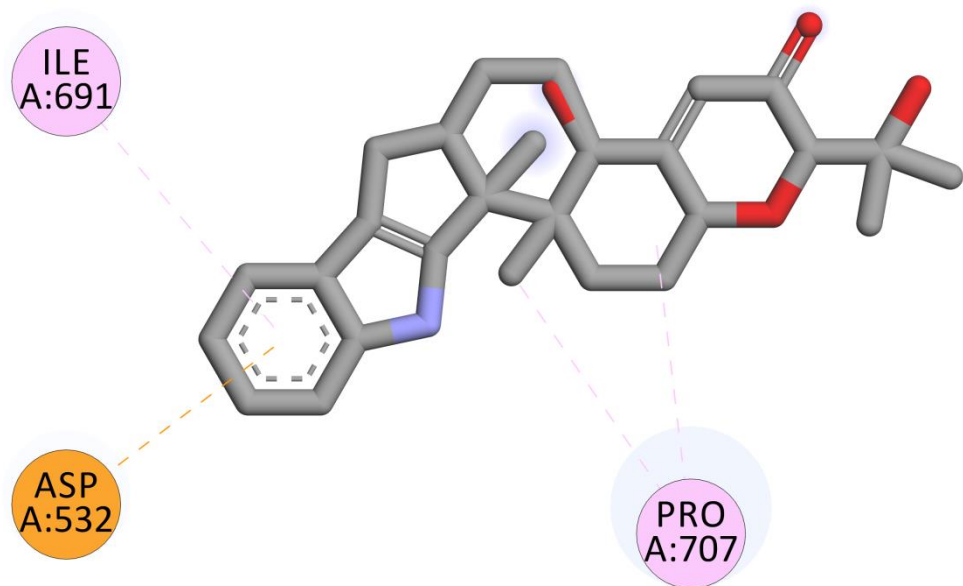


**Figure S33.** Main interactions observed between paxilline and DENV2 RdRp by docking analysis.

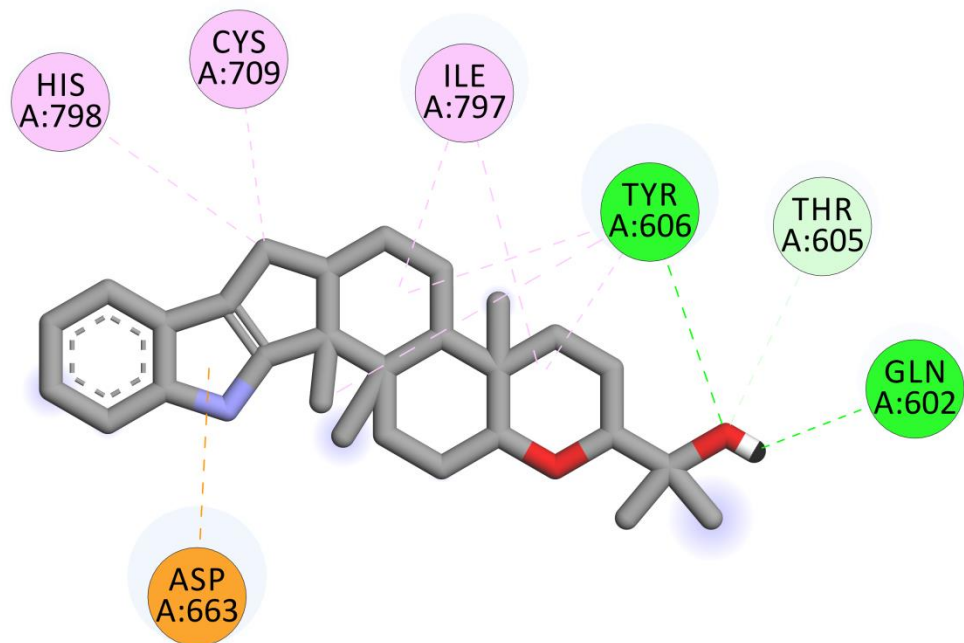


**Figure S34.** Main interactions observed between paspaline and DENV2 RdRp by docking analysis.

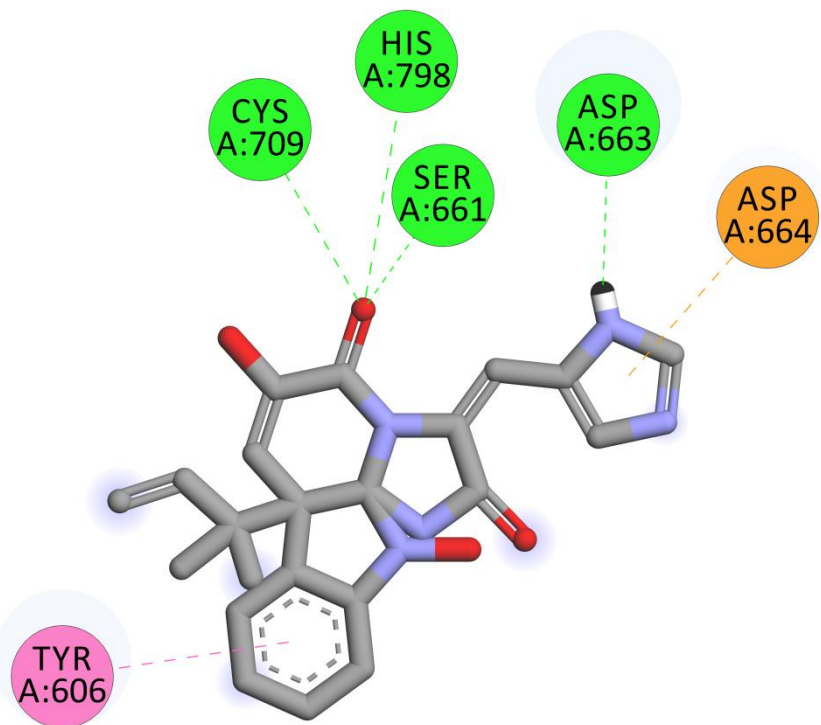


**Figure S35.** Main interactions observed between glandicoline B and DENV2 RdRp by docking analysis.

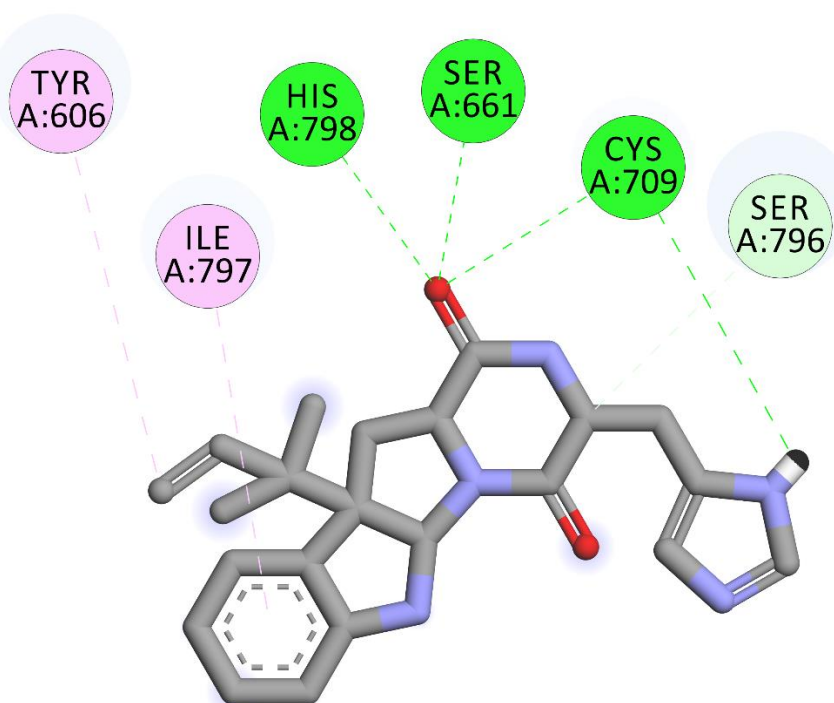


**Figure S36.** Main interactions observed between roquefortine D and DENV2 RdRp by docking analysis.

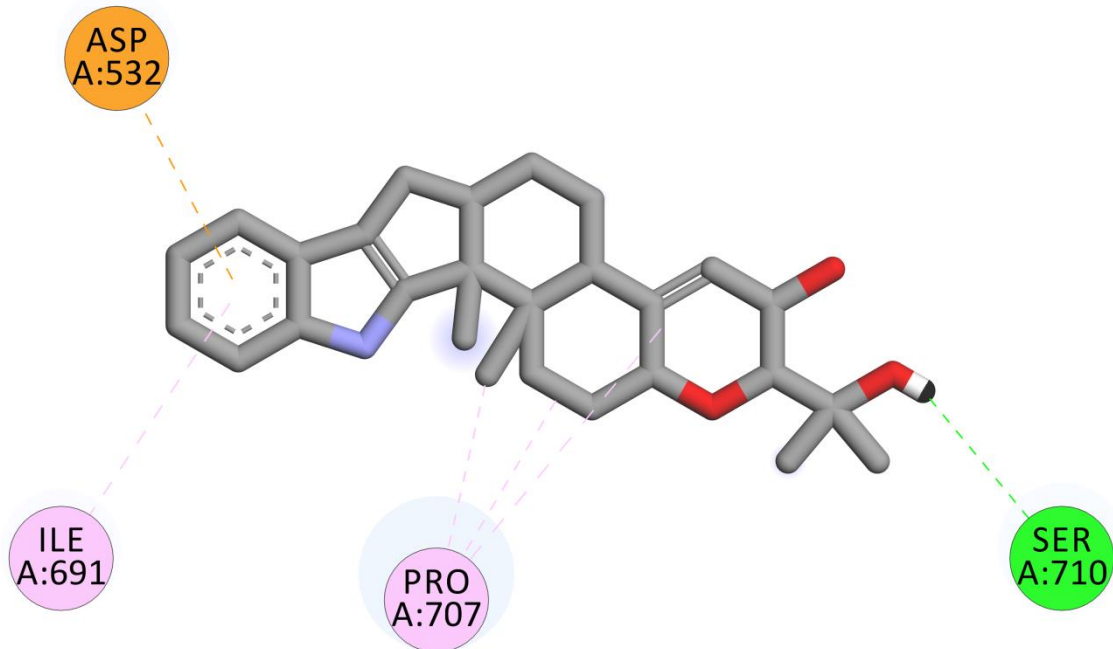


**Figure S37.** Main interactions observed between PCM6 and DENV2 RdRp by docking analysis.

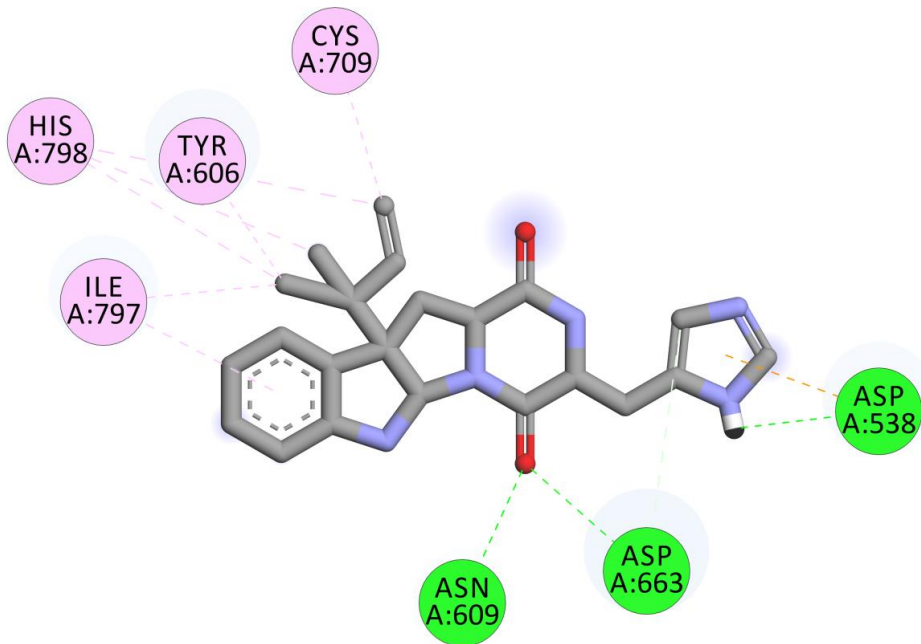


**Figure S38.** Main interactions observed between roquefortine C and DENV2 RdRp by docking analysis.

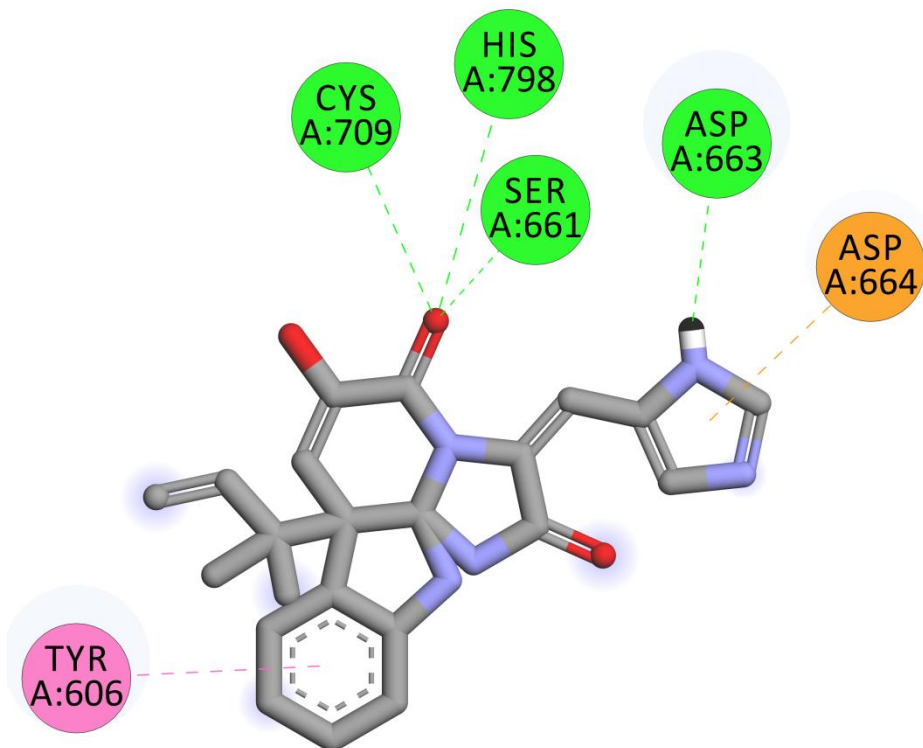


**Figure S39.** Main interactions observed between glandicoline A and DENV2 RdRp by docking analysis.

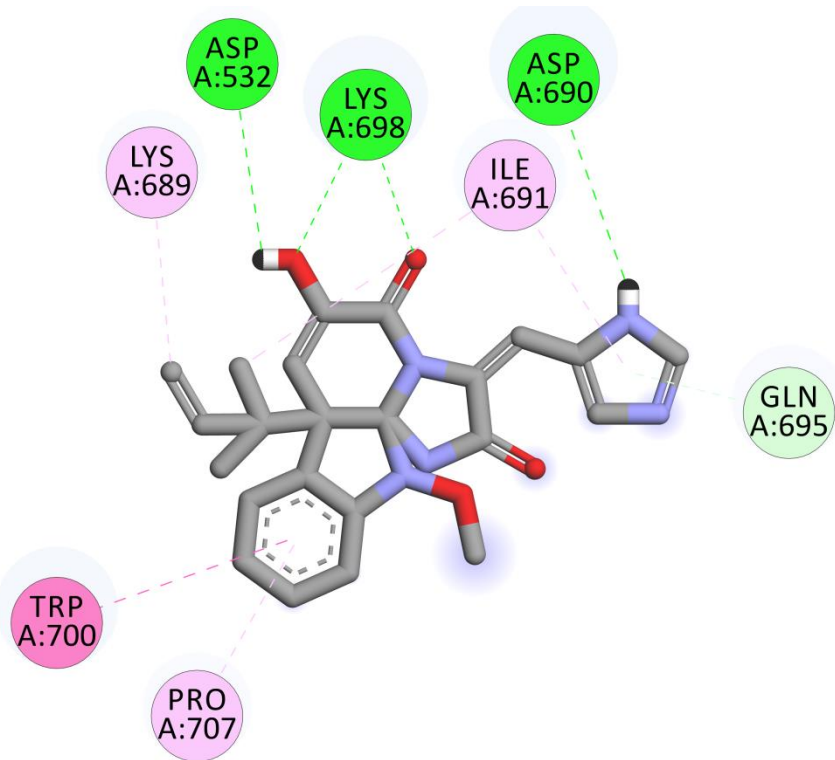


**Figure S40.** Main interactions observed between meleagrine and DENV2 RdRp by docking analysis.

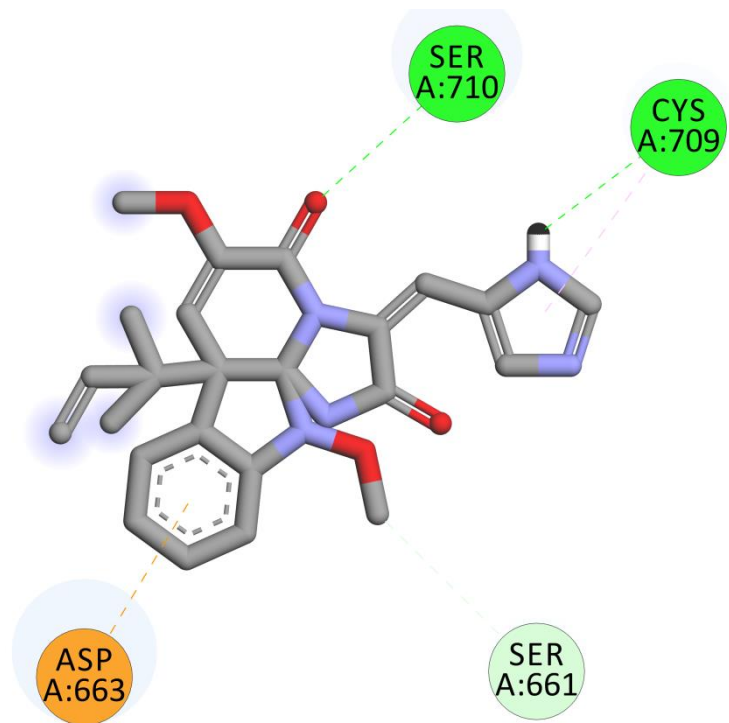


**Figure S41.** Main interactions observed between oxaline and DENV2 RdRp by docking analysis.

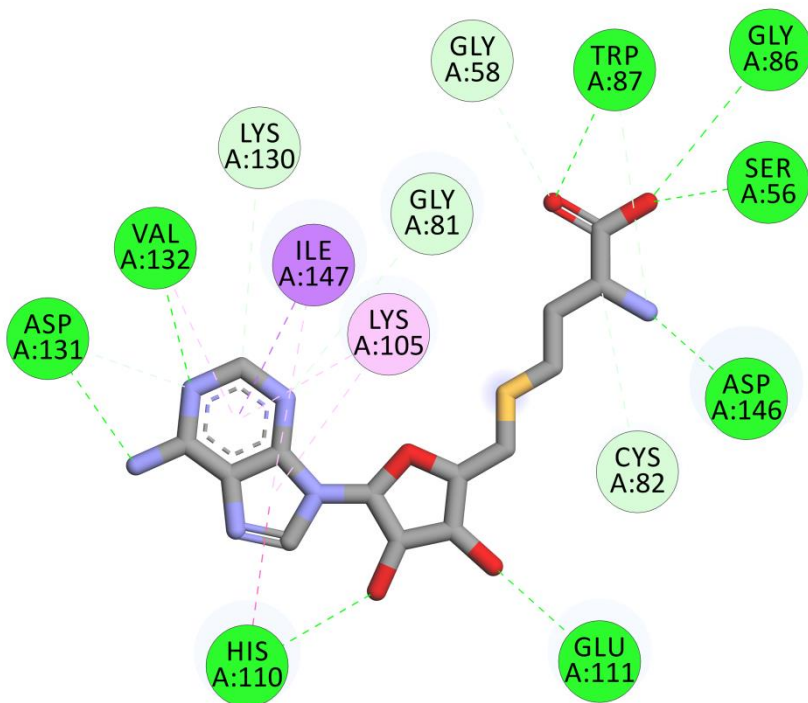


**Figure S42.** Main interactions observed between SAH and DENV2 MTase by docking analysis.

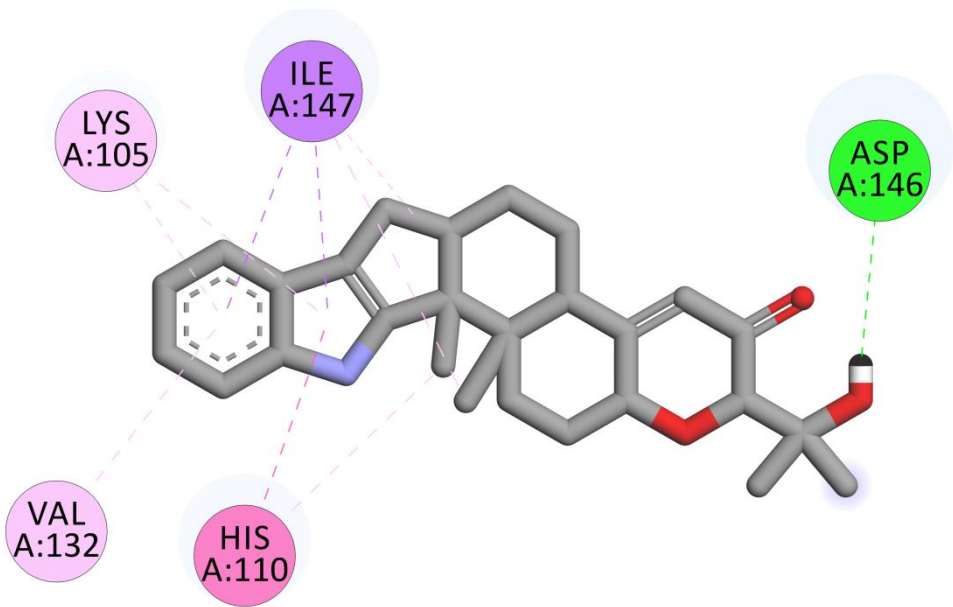


**Figure S43.** Main interactions observed between 13-desoxy-paxilline and DENV2 MTase by docking analysis.

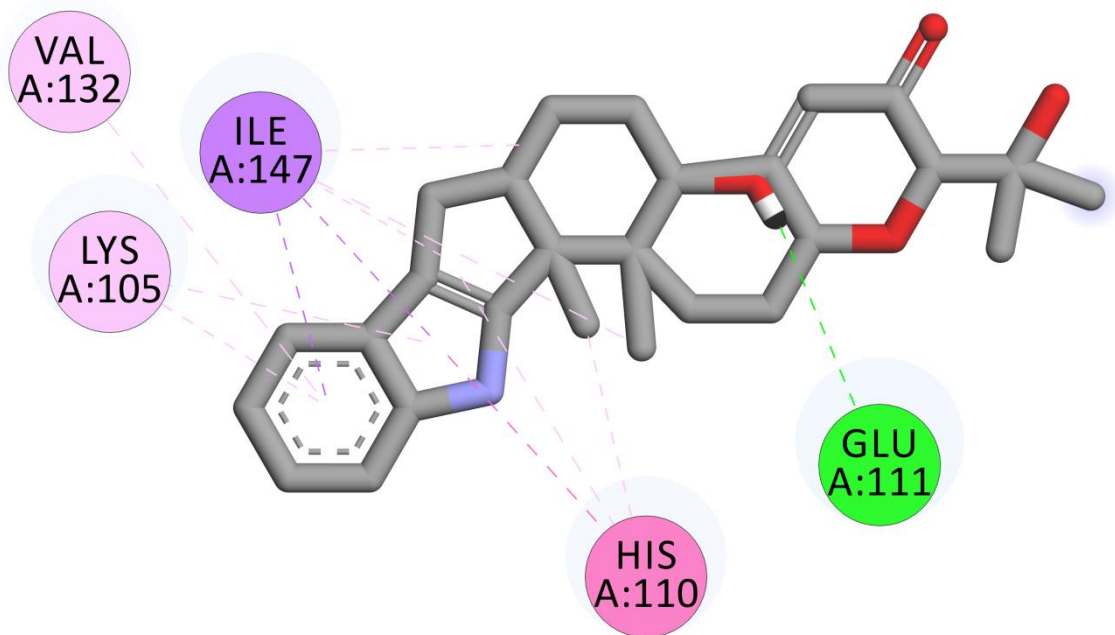


**Figure S44.** Main interactions observed between paxilline and DENV2 MTase by docking analysis.

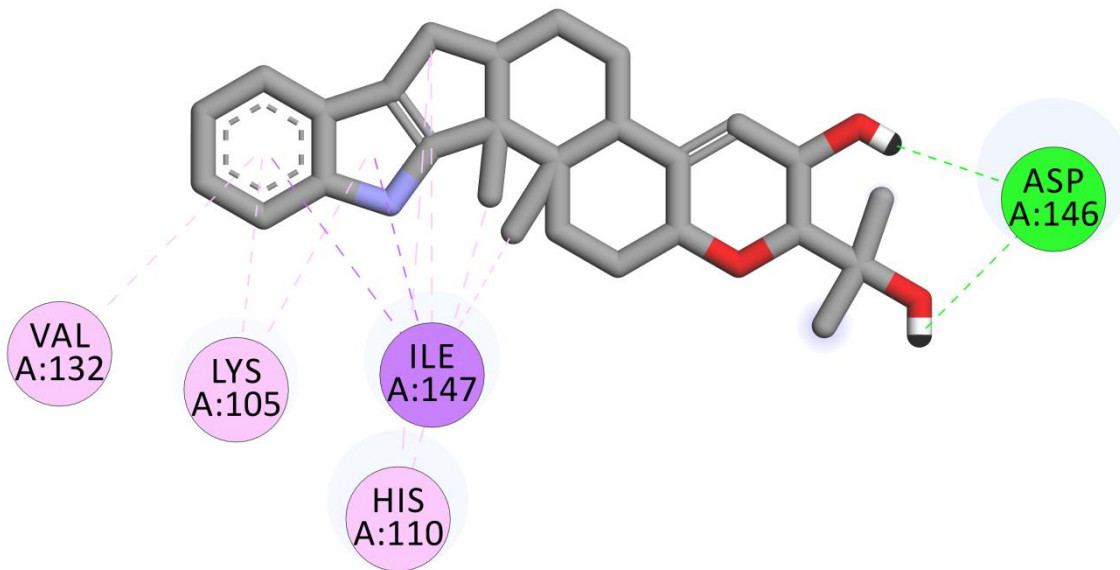


**Figure S45.** Main interactions observed between PCM6 and DENV2 MTase by docking analysis.

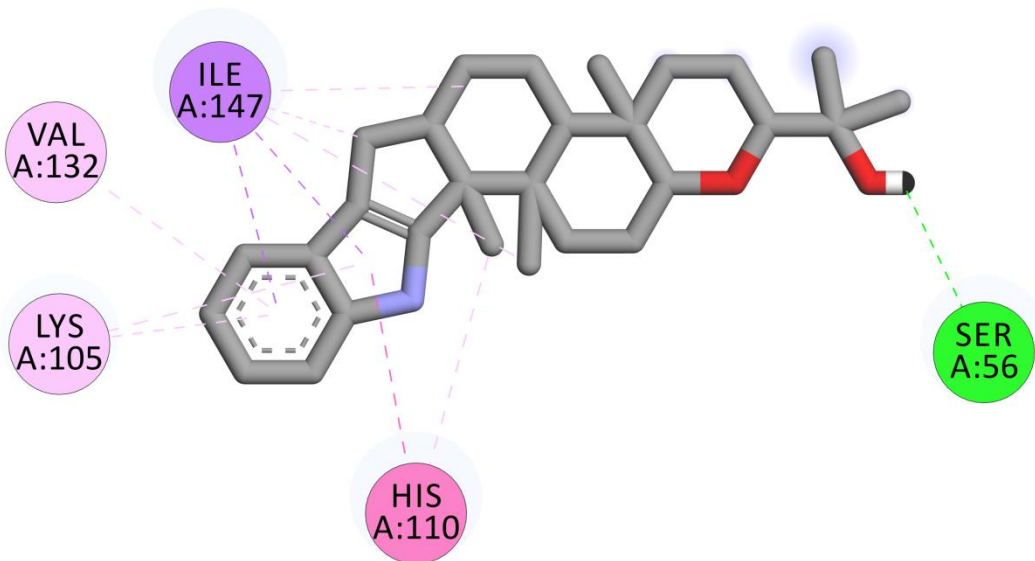


**Figure S46.** Main interactions observed between paspaline and DENV2 MTase by docking analysis.

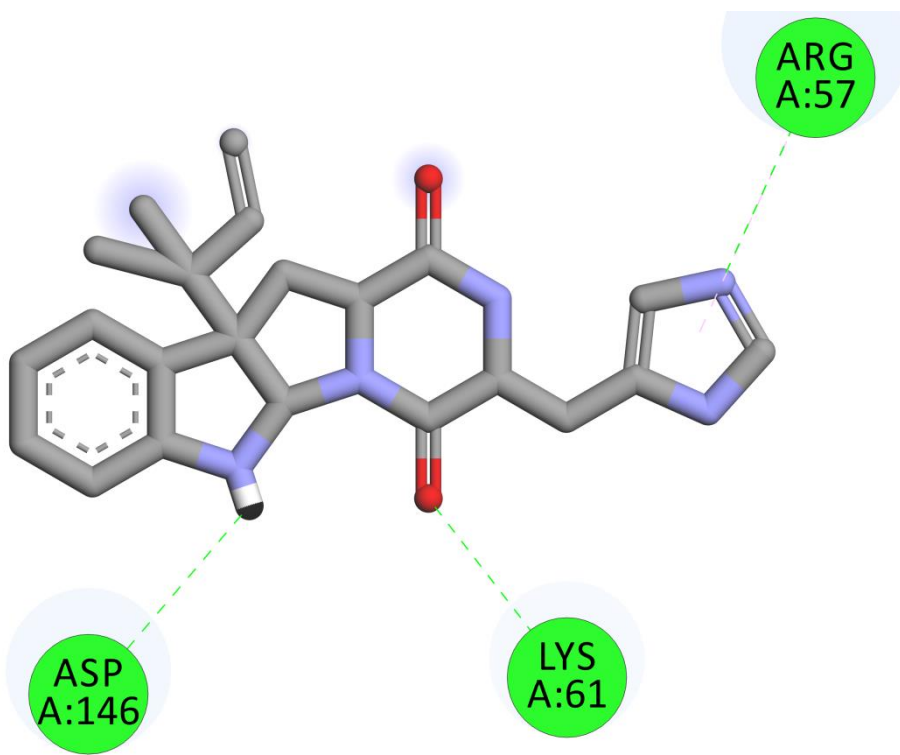


**Figure S47.** Main interactions observed between roquefortine C and DENV2 MTase by docking analysis.

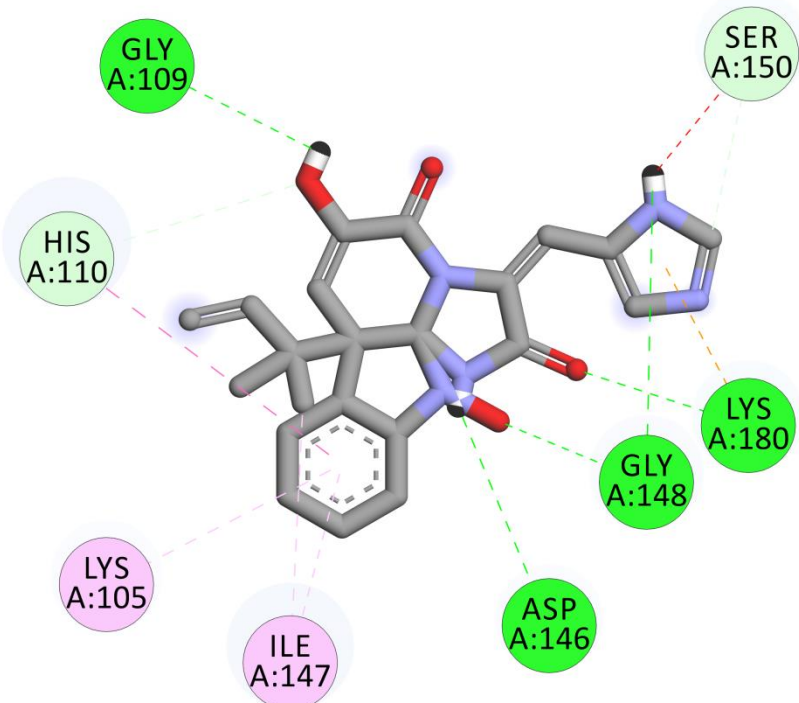


**Figure S48.** Main interactions observed between glandicoline B and DENV2 MTase by docking analysis.

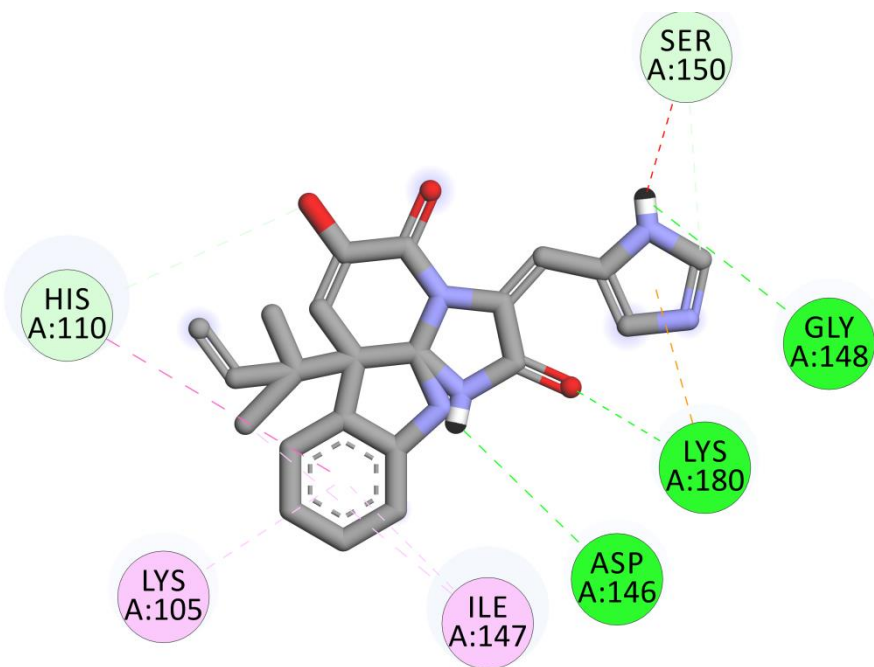


**Figure S49.** Main interactions observed between glandicoline A and DENV2 MTase by docking analysis.

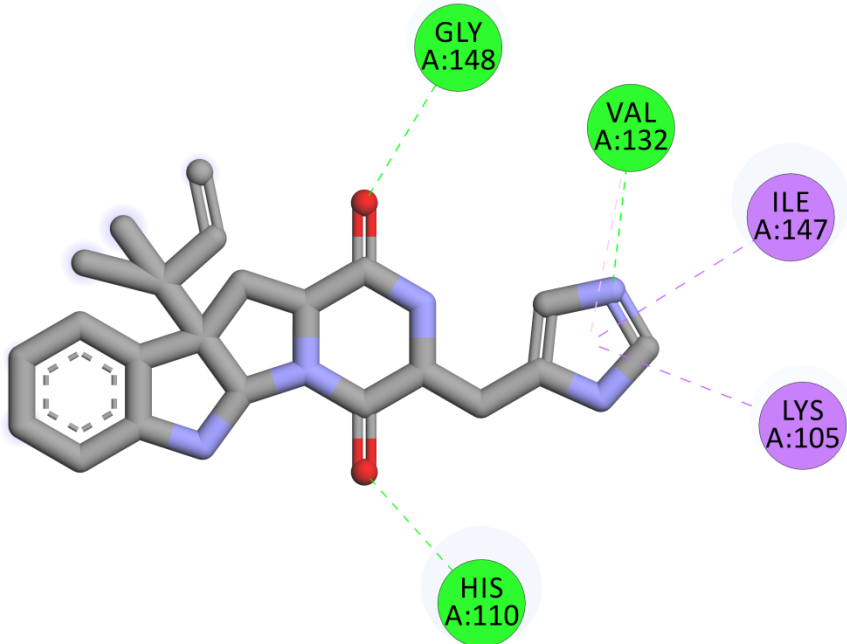


**Figure S50.** Main interactions observed between roquefortine D and DENV2 MTase by docking analysis

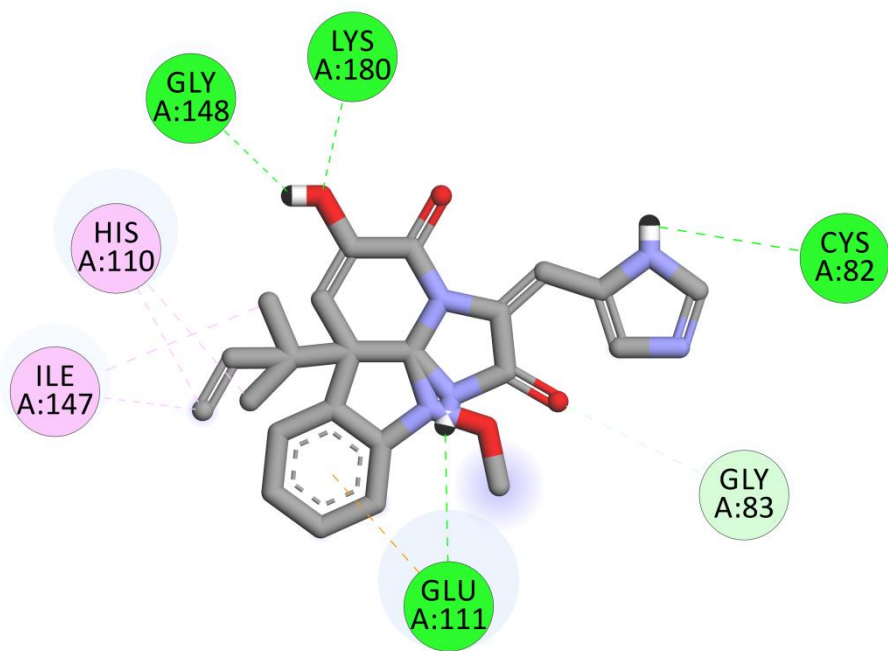


**Figure S51.** Main interactions observed between meleagrine and DENV2 MTase by docking analysis.

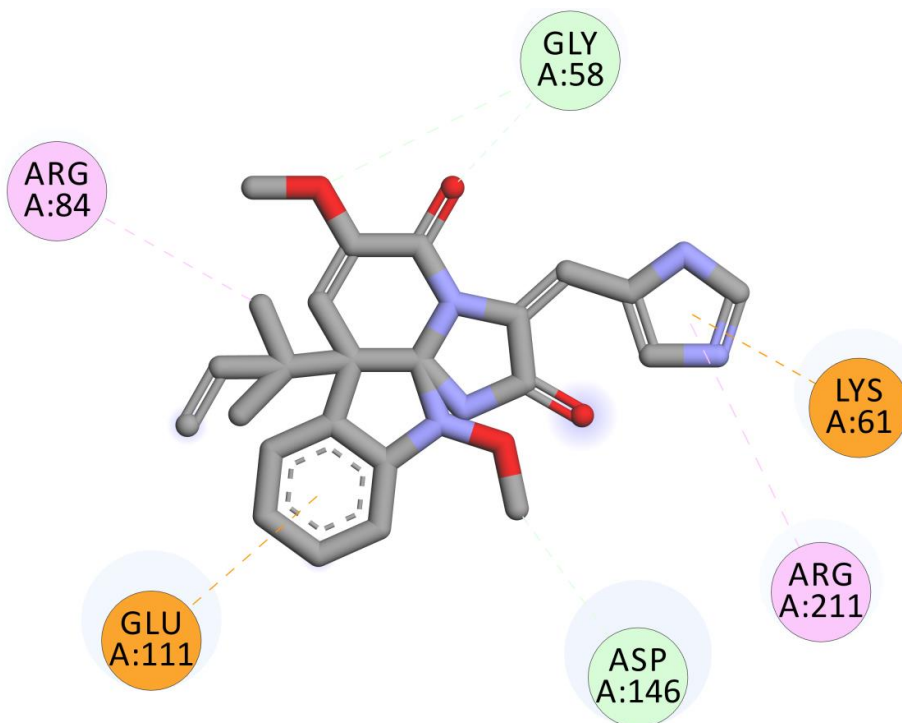


**Figure S52.** Main interactions observed between oxaline and DENV2 MTase by docking analysis.

## 8. Conclusões Gerais

Foi demonstrado que linhagens endofíticas de *Penicillium* isolados de plantas medicinais Amazonicas são excelentes produtores de metabólitos secundários, principalmente alcalóides. Onde conseguimos isolar a paxillina e glandicolina B, além de observar diversos outros alcalóides por meio da técnica de espectrometria de massas.

A utilização da abordagem polifásica (análises morfológicas, molecular e química) para taxonomia e identificação do gênero *Penicillium* se mostrou eficaz até para espécies cripticas.

As moléculas isoladas de *P. paxillini* mostraram um significativo potencial antiviral contra enzimas alvos da dengue tipo 2 e do *Sars-CoV-2*, por meio de análises de Docking Molecular, onde especialmente a paxillina e derivados mostraram atividade interessante. Porém, mais estudos, principalmente quanto a toxicidade da molécula são necessários.

Por fim, este trabalho contribui significativamente para o conhecimento de espécies endofíticas do gênero *Penicillium* na região Amazônica, tanto molecularmente, quimicamente, quanto para a compreensão desta biodiversidade, abrindo um leque de oportunidades para futuros estudos com as linhagens acessadas nesta pesquisa, as quais já demonstraram que possuem um interessante potencial biotecnológico.